PEDIATRIC CANCER IMMUNOTHERAPY

EDITED BY: Pouya Faridi, Nicholas Vitanza and Orazio Vittorio
PUBLISHED IN: Frontiers in Immunology and Frontiers in Oncology

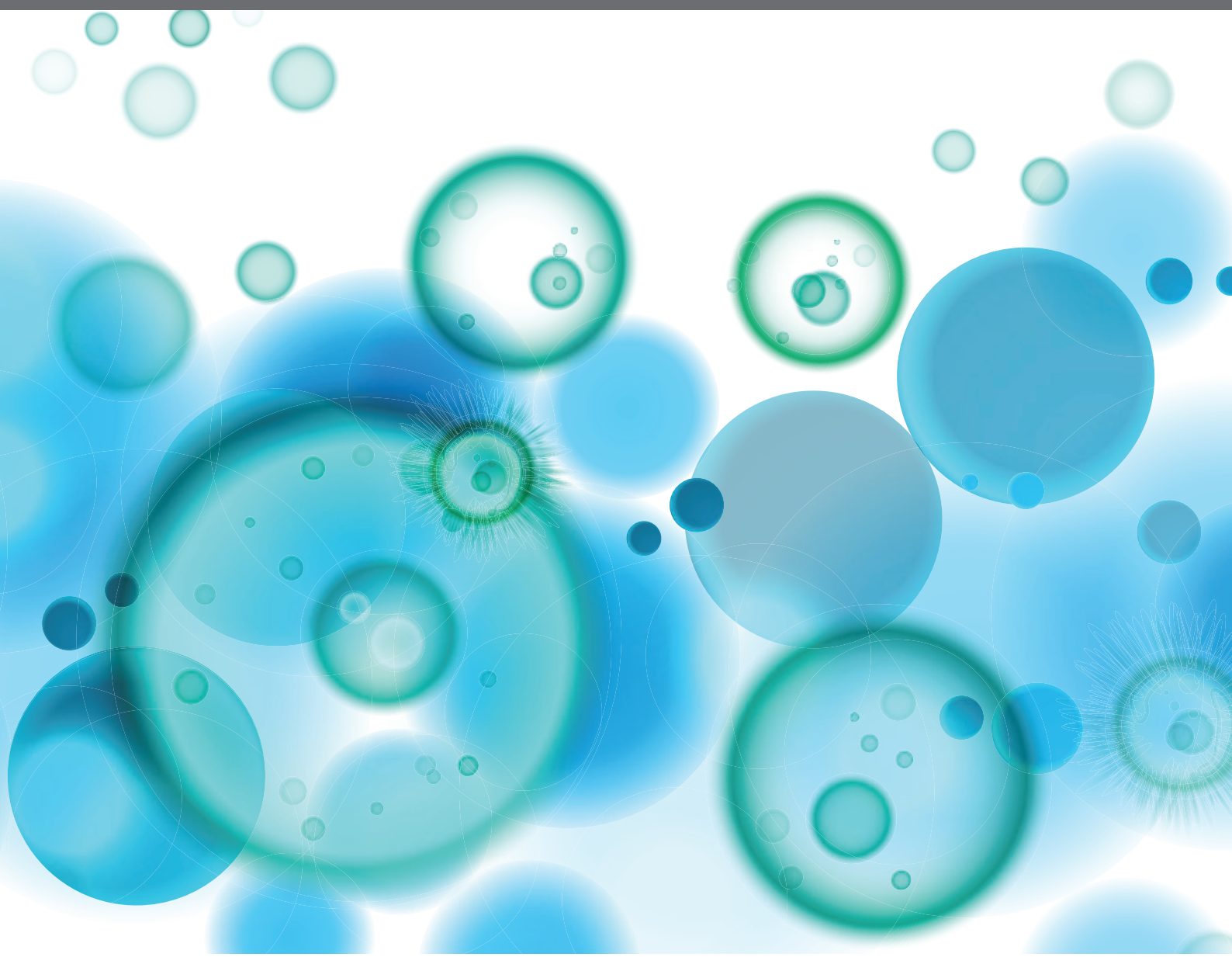

frontiers Research Topics

frontiers

ISSN 1664-8714
ISBN 978-2-83250-036-1
DOI 10.3389/978-2-83250-036-1

About Frontiers

Frontiers is more than just an open-access publisher of scholarly articles: it is a pioneering approach to the world of academia, radically improving the way scholarly research is managed. The grand vision of Frontiers is a world where all people have an equal opportunity to seek, share and generate knowledge. Frontiers provides immediate and permanent online open access to all its publications, but this alone is not enough to realize our grand goals.

Frontiers Journal Series

The Frontiers Journal Series is a multi-tier and interdisciplinary set of open-access, online journals, promising a paradigm shift from the current review, selection and dissemination processes in academic publishing. All Frontiers journals are driven by researchers for researchers; therefore, they constitute a service to the scholarly community. At the same time, the Frontiers Journal Series operates on a revolutionary invention, the tiered publishing system, initially addressing specific communities of scholars, and gradually climbing up to broader public understanding, thus serving the interests of the lay society, too.

Dedication to Quality

Each Frontiers article is a landmark of the highest quality, thanks to genuinely collaborative interactions between authors and review editors, who include some of the world's best academicians. Research must be certified by peers before entering a stream of knowledge that may eventually reach the public - and shape society; therefore, Frontiers only applies the most rigorous and unbiased reviews.
Frontiers revolutionizes research publishing by freely delivering the most outstanding research, evaluated with no bias from both the academic and social point of view. By applying the most advanced information technologies, Frontiers is catapulting scholarly publishing into a new generation.

What are Frontiers Research Topics?

Frontiers Research Topics are very popular trademarks of the Frontiers Journals Series: they are collections of at least ten articles, all centered on a particular subject. With their unique mix of varied contributions from Original Research to Review Articles, Frontiers Research Topics unify the most influential researchers, the latest key findings and historical advances in a hot research area! Find out more on how to host your own Frontiers Research Topic or contribute to one as an author by contacting the Frontiers Editorial Office: frontiersin.org/about/contact

PEDIATRIC CANCER IMMUNOTHERAPY

Topic Editors:
Pouya Faridi, Monash University, Australia
Nicholas Vitanza, Seattle Children's Hospital, United States
Orazio Vittorio, University of New South Wales, Australia

Citation: Faridi, P., Vitanza, N., Vittorio, O., eds. (2022). Pediatric Cancer Immunotherapy. Lausanne: Frontiers Media SA. doi: 10.3389/978-2-83250-036-1

Table of Contents

frontiers in Immunology

SYSTEMATIC REVIEW
published: 27 September 2021
doi: 10.3389/fimmu.2021.746171

Effects of Exercise Interventions on Immune Function in Children and Adolescents With Cancer and HSCT Recipients - A Systematic Review

Ronja Beller[1†], Sabrina Bianca Bennstein[2†] and Miriam Götte[1]*

[1] Department of Pediatric Hematology/Oncology, Center for Child and Adolescent Medicine, Clinic for Pediatrics III, West German Cancer Centre, University Hospital Essen, Essen, Germany, [2] Institute for Transplantation Diagnostics and Cell Therapeutics, Medical Faculty, Heinrich-Heine University Düsseldorf, Düsseldorf, Germany

Background: Pediatric cancer patients are at high risk for life-threatening infections, therapy associated complications and cancer-related side effects. Exercise is a promising tool to support the immune system and reduce inflammation. The primary objective of this systematic review was to evaluate the effects of exercise interventions in pediatric cancer patients and survivors on the immune system.

Methods: For this systematic review (PROSPERO ID: CRD42021194282) we searched four databases (MEDLINE, Cochrane Library, ClinicalTrials.gov, SPORTDiscus) in June 2021. Studies with pediatric patients with oncological disease were included as main criterion. Two authors independently performed data extraction, risk of bias assessment, descriptive analysis and a direction ratio was calculated for all immune cell parameters.

Findings: Of the 1448 detected articles, eight studies with overall n = 400 children and adolescents with cancer and n = 17 healthy children as controls aged 4-19 years met the inclusion criteria. Three randomized, four non-randomized controlled trials and one case series were analyzed descriptively. The exercise interventions had no negative adverse effects on the immune system. Statistically significant results indicated enhanced cytotoxicity through exercise, while changes in immune cell numbers did not differ significantly. Interventions further reduced days of in-hospitalization and reduced the risk of infections. Several beneficial direction ratios in immune parameters were identified favoring the intervention group.

Interpretation: Exercise interventions for pediatric cancer patients and survivors had no negative but promising beneficial effects on the immune system, especially regarding cytotoxicity, but data is very limited. Further research should be conducted on the immunological effects of different training modalities and intensities, during various treatment phases, and for different pediatric cancer types. The direction ratio parameters given here may provide useful guidance for future clinical trials.

Systemic Review Registration: https://www.crd.york.ac.uk/prospero/display_record.php?ID=CRD42021194282, Prospero ID: CRD42021194282.

Keywords: pediatric oncology, childhood cancer, exercise intervention, immune system, inflammation, natural killer cells, physical performance, physical activity

OPEN ACCESS

Edited by:
Orazio Vittorio, University of New South Wales, Australia

Reviewed by:
Carmen Fiuza-Luces, Research Institute Hospital 12 de Octubre, Spain
David Mizrahi, The Daffodil Centre, Australia

***Correspondence:**
Ronja Beller
ronja.beller@uk-essen.de

[†]These authors have contributed equally to this work

Specialty section:
This article was submitted to Cancer Immunity and Immunotherapy, a section of the journal Frontiers in Immunology

Received: *23 July 2021*
Accepted: *10 September 2021*
Published: *27 September 2021*

Citation:
Beller R, Bennstein SB and Götte M (2021) Effects of Exercise Interventions on Immune Function in Children and Adolescents With Cancer and HSCT Recipients - A Systematic Review. Front. Immunol. 12:746171. doi: 10.3389/fimmu.2021.746171

INTRODUCTION

Children and adolescents with cancer are at high risk for life-threatening infections and therapy associated complications. They further have a risk for disease recurrence or development of secondary malignancies (1, 2). Thus, interventions are needed to decrease the probability of cancer-related side effects and increase the patients' quality of life. Studies suggest that enhanced immunosurveillance by cytotoxic natural killer (NK) cells and T-cells after moderate exercise might be beneficial for anti-cancer surveillance, as both are highly activated during acute aerobic exercise (3–6). Especially exercise-induced NK cells were recognized to have an anti-tumor effect (7). Furthermore, phagocytosis and oxidative burst in granulocytes are also increased by exercise (8) suggesting that regular exercise strengthens the immune system. Exercise induced effects, like increased NK cell cytotoxicity, lymphocyte proliferation and increased frequencies of granulocytes, have been reported in adult cancer patients (9, 10). Thus, performing moderate exercise interventions regularly might result in fewer infections and better clinical outcome in cancer patients. Growing evidence summarized in systematic reviews suggests positive effects of exercise therapy in pediatric oncology on cardiopulmonary capacity, functional mobility, muscle strength, quality of life and fatigue (11–13). Even though research is still limited, the current studies underline that exercise programs are safe and feasible in children with oncological diseases, while not increasing the risk of mortality, cancer recurrence or side effects (14). Moreover, an in-hospital exercise program seems to reduce days of hospitalization and treatment costs (15). Of note, evidence from experimental murine studies have shown beneficial effects of exercise intervention on graft versus host disease (GvHD) after hematopoietic stem cell transplantation (HSCT) (16, 17).

Studies in adult cancer patients already suggest beneficial effects of exercise on the immune system (9, 10). However, as the immune system undergoes systematic changes from pre- to post-birth (18, 19) and during aging (20, 21), the knowledge taken from the immune response of adult cancer patients after exercise may not be directly transferable to pediatric cancer patients. The type, frequency, duration, and intensity of exercise could also affect the immune system in different ways (22). Therefore, research studies focusing on how exercise affects the pediatric immune system of cancer patients is a relevant research question. The most recent systematic review focusing on general exercise and the immune system including studies with children and adults with cancer has been published in 2013 (10). Thus, this systematic review aims at analyzing the current knowledge on this topic. The primary objective of the review is to determine the effects of exercise interventions in pediatric oncology on the immune system. As secondary objectives the effects on physical and functional performance, body composition, and hematopoietic stem cell transplantation (HSCT) outcome will be discussed.

Abbreviations: A, Adherence; ALC, Absolute lymphocyte count; ALL, Acute lymphoblastic leukemia; ANC, Absolute neutrophil count; CCT, Controlled clinical trial; CG, Control group; D, Duration; DC, Dendritic cell; EM, Effector memory; F, Frequency; GvHD, Graft-versus-host disease; GvL, Graft-versus-leukemia; HSCT, Hematopoietic stem cell transplantation; I, Intensity; KIR, Killer-cell immunoglobulin-like receptors; IG, Intervention group; MVPA, Moderate-vigorous physical activity; NCT, Non-randomized controlled trials; NK cells, Natural killer cells; NKCC, Natural killer cytotoxicity; NKT, Natural killer T cell; OD, Other designs; RCT, Randomized controlled trials; T, Time; WBC, Whole blood cell.

METHODS

Search Strategy and Selection Criteria

This systematic review was conducted according to the PRISMA recommendations (23). A comprehensive search by two authors (RB, MG) of four databases (MEDLINE, Cochrane Library, ClinicalTrials.gov, SPORTDiscus) was conducted in June 2021. Search terms were based on PICO (24) for children or adolescents with cancer and/or recipients of stem cell transplantation during and after acute cancer therapy (Patient Population), exercise (Intervention), usual care/healthy control group (Comparator group), and immune function (Outcome). A combination of MeSH terms and search terms in title/abstract and relevant headings, keywords and synonyms for the search focuses was used. There were no restrictions in terms of publication date. The exact search terms are listed in **Supplement 1** and inclusion and exclusion criteria are shown in **Supplement 2**. The protocol of this review was registered in PROSPERO https://www.crd.york.ac.uk/prospero/display_record.php?ID=CRD42021194282.

After removing duplicates, two authors (RB, SBB) independently reviewed all identified studies by reviewing titles and abstracts. Remaining studies were checked accordingly for eligibility in full text (**Supplement 5**). Disagreements between the reviewers were discussed between the two researchers. If no consensus was reached, a third researcher (MG) was contacted. Eligible studies as well as identified systematic reviews were further screened for potentially missed relevant studies (**Figure 1**).

Data Analyses

Two authors (RB, SBB) assessed the risk of bias of included studies according to the PEDro scale (26). The PEDro scale is based on the Delphi list and was made for assessment of internal validity and sufficient statistical information (27). This tool is applicable for randomized clinic trials like randomized controlled trials (RCTs) and controlled clinical trial (CCT). The risk of bias was rated on a scale of 0-10 points (**Supplement 3**) and any disagreements were resolved by consensus. Two authors (RB, SBB) independently reviewed all identified studies and extracted relevant information for each study into standardized tables (see **Supplement 4** for details on data extraction and **Table 1** for results). A third researcher (MG) collected this information for each study.

For clarity only p-values for significant values are shown in **Table 1**. Due to the limited numbers of studies, different study designs and heterogeneous immunological parameters analyzed, no meta-analysis was conducted. We calculated a direction ratio for each immunological parameter analyzed within the different studies between the start and end point: Direction arrows were given if the ratio of an immunological parameters within the

intervention group (IG) differs more than 30% (value IG > 30% control group (CG)/healthy controls) compared to the CG or healthy controls. Calculation and results are shown in **Supplement 4** and **Table 1**.

RESULTS

In total, 1448 articles were identified in the systematic search, where eight studies were included within this review (**Figure 1**, exclusion criteria listed in **Supplement 2**). Of those, three studies were RCTs (29, 31, 32), four were NCTs (15, 28, 30, 34) and one case series (33). Seven of these studies focused on chronic effects (15, 28–33) of regular exercise and one of them on acute effects after exercise (34). Immune parameters were primary outcomes in five studies (28, 29, 32–34) and secondary outcomes in three studies (15, 30, 31). A total of 400 children within an age range of four to 19 years with different cancer types, such as solid tumor, leukemia, and neoplasms, and 17 children as healthy controls participated in the included studies. 246 boys and 154 girls took

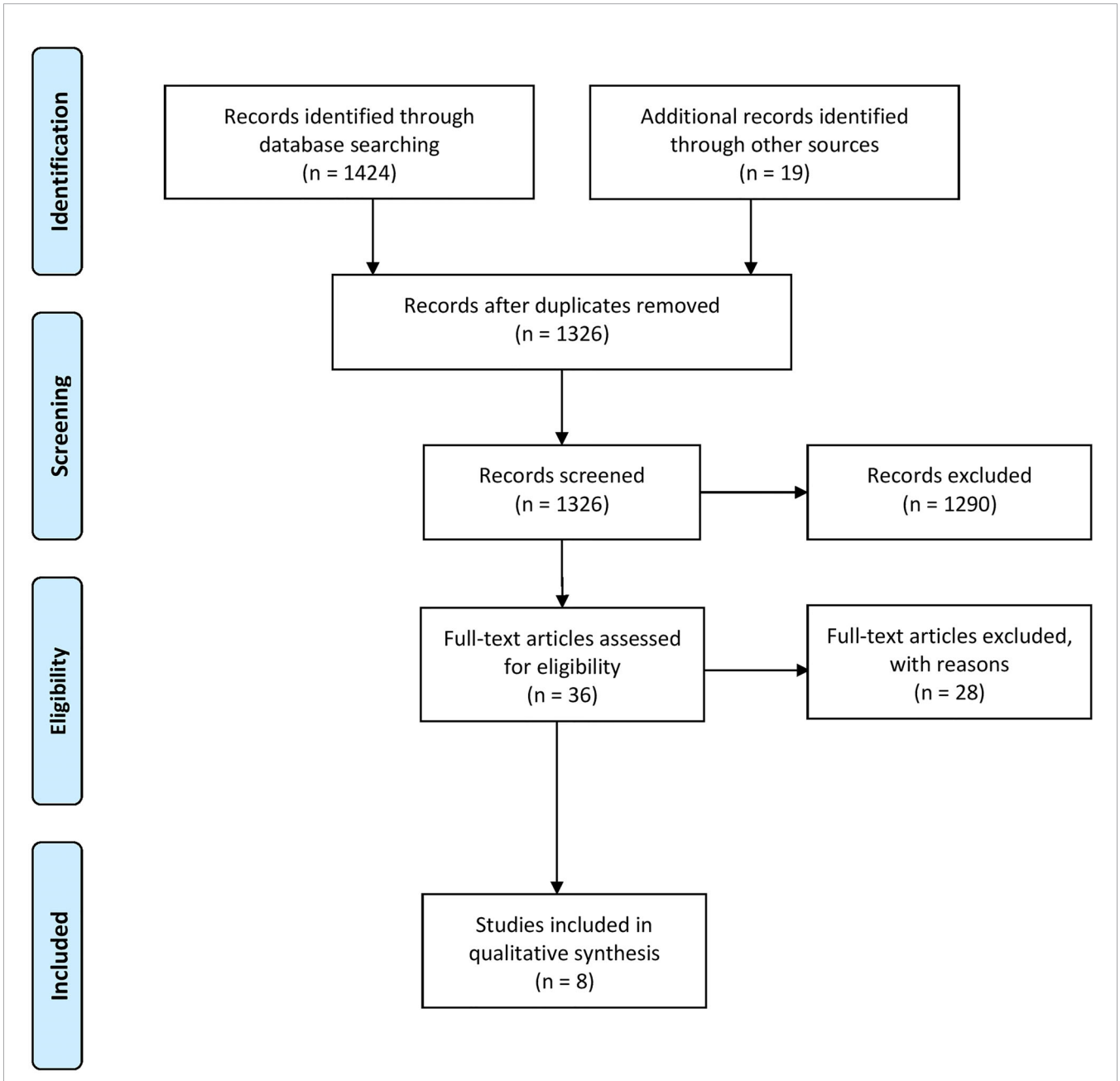

FIGURE 1 | Flow diagram according to Prisma guidelines (25).

TABLE 1 | Characteristics and Results of Included Studies.

Reference number, Registration number and name of register	Study design	Participant characterization	N (IG/ CG/HC)	Intervention Description	Frequency (F)/Intensity(I)/Time (T)/ Duration (D)/Adherence (A)	Outcome Between-Group Differences (Group)	Outcome Within-Group Differences (Time)	Outcome interaction (group x time)	Direction ratio [Intervention (IG) *vs.* Control (CG) group or healthy control group (HC)]
Effects of exercise intervention in context of HSCT on immune parameter									
28	Historically controlled study – NCT	Age IG: 8 ± 4 yr (5-16 yr); CG: 7 ± 3 yr (4-13 yr) Cancer entities Mixed high-risk cancer needing allo-HSCT Treatment-phase On-treatment during allo-HSCT	20 (7/ 13/0)	IG: Supervised in-hospital strength & aerobic exercises CG: Usual care (no training)	F: 5x/wk (3 x aerobic, 2 x aerobic & strength) I: 50 % - 70 % of age predicted max. HR, hypertrophy training T: ~50 min D: mean ~3 wks (until discharge) A: 92 ± 8% of planned sessions	No significant differences	Not significant after multiple correction: T-lymphocytes (p = .040); $CD4^+$ (p = .032); DC`s (p = .001)	Not significant after multiple correction: DC's (p = .045)	**30d *vs* 15d post-HSCT**: Leukocytes IG: 4.1 *vs.* CG: 2.5 ↑ Lymphocytes IG: 2.5 *vs.* CG: 5.1 ↓ Monocytes IG: 1.4 *vs.* CG: 1.4 → T-cells IG: 3.3 *vs.* CG: 5.2 ↓ NKs IG: 1.7 *vs.* CG: 3.5 ↓ NKT IG: 1.9 *vs.* CG: 4.1 ↓ $CD4^+$ IG: 1.9 *vs.* CG: 3.8 ↓ $CD8^+$ IG: 3.2 *vs.* CG: 7.4 ↓ DC`s IG: 1.3 *vs.* CG: 1.2 →
29	RCT	Age IG: 12.7 ± 4.0 yr (9-17 yr); CG: 13.3 ± 5.5 yr (8-19 yr) Treatment-phase On-treatment after discharge of allo-HSCT	6 (3/3/0)	IG: Supervised in-hospital & home-based strength & aerobic exercises CG: Usual care (no training) Cancer entities Mixed cancer types after allo-HSCT	F: 3x/wk (1x supervised, 2x home-based) I: N/A T: 60 min D: 10 wks A: 80.3 ± 1.4%	N/A	N/A	Not significant after multiple correction: : Mean ratio $CD56^{dim}$ (p = .03) % Ratio: NKCC (p <.05) pg/ml:	**Pre *vs.* post exercise program** NKs: IG: 2.2 *vs.* CG: 2.7 → NKs IG: 5.1 *vs.* CG: 2.1 ↑ $CD56^{dim}$ IG: 1.3 *vs.* CG: 1.0 → $CD56^{bright}$ IG: 0.5 *vs.* CG: 1.0 ↓ NKG2D IG: 1.0 *vs.* CG: 0.9 → NK_p30 IG: 1.2 *vs.* CG: 0.5 ↑ NK_p44 IG: 0.4 *vs.* CG: 2.0 ↓ IL-2 IG: 2.0 *vs.* CG: 1.0 ↑ IL-4 IG: 2.6 *vs.* CG: 0.8 ↑ IL-6 IG: 3.5 *vs.* CG: 2.3 ↑ IL-8 IG: 4.8 *vs.* CG: 4.1 → IL-10 IG: 2.2 *vs.* CG: 1.1 ↑ IFNγ IG: 2.8 *vs.* CG: 0.8 ↑ TNFα IG: 2.5 *vs.* CG: 0.9 ↑ GM-CSF IG: 1.8 *vs.* CG: 0.5 ↑
30	NCT	Age IG: 11 ± 5 yr (5-18 yr);	118 (66/54/0)	IG: Supervised in-hospital strength & aerobic exercises	F: 5x/wk I: 65-80% of age predicted max. HR	Not significant after multiple corrections:	Not significant after multiple corrections:	Not significant after multiple corrections:	**30d *vs* 15d post-HSCT** allo-HSCT :

(Continued)

TABLE 1 | Continued

Reference number, Registration number and name of register	Study design	Participant characterization	N (IG/ CG/HC)	Intervention Description	Frequency (F)/Intensity(I)/Time (T)/ Duration (D)/Adherence (A)	Outcome Between-Group Differences (Group)		Outcome Within-Group Differences (Time)		Outcome interaction (group x time)		Direction ratio [Intervention (IG) *vs.* Control (CG) group or healthy control group (HC)]		
		CG: 10 ± 4 yr (4-18yr)			T: ~60 min	allo- HSCT		allo- HSCT		allo- HSCT		Neutrophils	IG: 3.8 *vs.* CG: 3.6	→
			allo-HSCT			#:		#:		#:		Lymphocytes	IG: 1.9 *vs.* CG: 2.4	→
					D: ~3 wks	Lymphocytes				EM CD4$^+$	(p = .005)	Monocytes	IG: 0.9 *vs.* CG: 1.6	↓
							(p = .045)	Leukocytes	(p <.001)	Naïve CD4$^+$	(p = .005)	T-cells	IG: 5.6 *vs.* CG: 1.4	↑
			IG: n = 47	CG:	A: 80.3 ± 1.4%	T-cells	(p = .006)	Neutrophils	(p <.001)	Treg	(p = .003)	actCD4$^+$	IG: 1.3 *vs.* CG: 2.8	↓
						actCD4$^+$	(p = .004)	Lymphocytes		CD56^{bright}	(p = .003)	CM CD4$^+$	IG: 1.3 *vs.* CG: 1.7	→
		Cancer entities		Usual care (no training)		CM CD4$^+$	(p = .011)		(p = .001)			EM CD4$^+$	IG: 1.6 *vs.* CG: 2.0	→
			CG: n= 39			CD56^{bright}	(p = .011)	T-cells	(p <.001)			naive CD4$^+$	IG: 1.5 *vs.* CG: 2.6	↓
		Mixed high risk cancer types needing allo- or auto-HSCT				CD8$^+$	(p = .024)	actCD4$^+$	(p <.001)			Treg	IG: 1.0 *vs.* CG: 1.1	→
								CM CD4$^+$	(p = .007)	auto-HSCT:		CM CD8$^+$	IG: 1.7 *vs.* CG: 1.8	→
						auto-HSCT:		EM CD4$^+$	(p <.001)			EM CD8$^+$	IG: 11.6 *vs.* CG: 26.3	↓
								Naïve CD4$^+$	(p <.001)			Naive CD8$^+$	IG: 4.0 *vs.* CG: 1.7	↑
			auto-HSCT									NKs	IG: 3.3 *vs.* CG: 2.4	↑
						:		Treg	(p <.001)	:		CD56^{bright}	IG: 4.0 *vs.* CG: 2.0	↑
						Leukocytes	(p = .001)	Naïve CD8$^+$	(p <.001)	Naïve CD4$^+$	(p = .001)	CD56^{dim}	IG: 3.0 *vs.* CG: 3.0	→
						Neutrophils	(p = .048)	NKs	(p = .001)	CD4$^+$	(p = .048)	mB-cells	IG: 2.3 *vs.* CG: 0.4	↑
			IG: n = 18			Monocytes	(p = .005)	CD56^{bright}	(p <.001)	CD8$^+$	(p = .041)	CD4$^+$	IG: 1.4 *vs.* CG: 2.0	↓
						T-cells	(p = .037)	CD56^{dim}	(p <.001)			CD8$^+$	IG: 4.2 *vs.* CG: 3.9	→
		Treatment-phase				Naïve CD4$^+$	(p <.001)	mB-cells	(p<.001)			DCs	IG: 0.8 *vs.* CG: 1.2	↓
			CG: n = 14			CD4$^+$	(p = .008)	DCs	(p = .034)					
						DCs	(p = .019)							
		On-treatment during allo- or auto-HSCT						Auto-HSCT: : Lymphocytes				auto-HSCT :		
									(p = .027)			Leukocytes	IG: 1.0 *vs.* CG: 1.5	→
												Neutrophils	IG: 1.2 *vs.* CG: 1.7	
								CM CD4$^+$	(p = .040)			Lymphocytes	IG: 0.9 *vs.* CG: 1.5	↓
								EM CD4$^+$	(p <.001)			Monocytes	IG: 1.7 *vs.* CG: 1.4	→
								Naïve CD4$^+$	(p <.001)			T-cells	IG: 1.3 *vs.* CG: 1.8	→
								Treg	(p = .027)			actCD4$^+$	IG: 1.0 *vs.* CG: 1.6	↓
								CD4$^+$	(p = .019)			CM CD4$^+$	IG: 0.8 *vs.* CG: 1.5	↓
								CD8$^+$	(p = .008)			EM CD4$^+$	IG: 1.3 *vs.* CG: 0.9	↑
												naive CD4$^+$	IG: 1.6 *vs.* CG: 0.9	↑
												Treg		↓

(Continued)

TABLE 1 | Continued

Reference number, Registration number and name of register	Study design	Participant characterization	N (IG/ CG/HC)	Intervention Description	Frequency (F)/Intensity(I)/Time (T)/ Duration (D)/Adherence (A)	Outcome Between-Group Differences (Group)	Outcome Within-Group Differences (Time)	Outcome interaction (group x time)	Direction ratio [Intervention (IG) *vs.* Control (CG) group or healthy control group (HC)]		
										IG: 1.3 *vs.* CG: 2.2	
									CM $CD8^+$	IG: 1.3 *vs.* CG: 0.4	↑
									EM $CD8^+$	IG: 1.3 *vs.* CG: 2.7	↓
									Naive $CD8^+$	IG: 2.1 *vs.* CG: 1.5	↑
									NKs	IG: 1.3 *vs.* CG: 1.8	→
									$CD56^{bright}$	IG: 2.6 *vs.* CG: 2.0	→
									$CD56^{dim}$	IG: 0.9 *vs.* CG: 1.6	↓
									mB-cells	IG: 0.8 *vs.* CG: 0.8	→
									$CD4^+$	IG: 1.2 *vs.* CG: 1.4	↓
									$CD8^+$	IG: 1.5 *vs.* CG: 1.2	→
									DCs	IG: 0.9 *vs.* CG: 0.8	→
31; **ClinicalTrials.gov ID: NCT01575704**	RCT	Age IG: 11 yr (5-17 yr) CG: 12 yr (6-18 yr) Cancer entities Mixed high risk cancer needing allo- or auto-HSCT Treatment-phase On-treatment during allo- or auto-HSCT	57 (28/ 29/0) allo-HSCT IG: n = 31 CG: n = 30 auto-HSCT IG: n = 4 CG: n = 5	IG: Supervised in-hospital strength & aerobic exercises CG: Mental & relaxation training (no training)	F: 5x/wk I: IG: moderate training targeted with RPE (12–14) T: 30-60 min D: ~6 wks (until discharge) A: IG: 94.4 (63.3-100) %, CG: 68.2 (5.8–100) %	No significant differences	No significant differences	No significant differences	**Post exercise program** N/A ‡		
Effects of regular exercise intervention in context of chemotherapy on immune parameter											
32; **ClinicalTrials.gov ID: NCT01645436**	RCT	Age IG: 11 ± 4 yr CG: 12 ± 4 yr Cancer entities Solid tumors (sarcoma, lymphoma, blastoma)	20 (9/11/0)	IG: Supervised in-hospital (patient`s room or hospital gym) strength & aerobic exercises	F: 3x/wk I: 60%–70% of measured max HR, 8-15 rep (hypertrophy training) T: 60-70 min D: 17 wks ± 5 A: 70%	Not significant after multiple corrections: %: NK 69 (p = .013) NKp44 (p = .021) NKCC (ratio): Ratio 8:1 (p= .038)	**%:** NKT^* (p <.001) Not significant after multiple corrections: %: $CD56^{bright}$ (p = .017) NKp44 (p= .004)	Not significant after multiple corrections: %: KIR2DS4 (p = .028) NKp46 (p = .037) pg/ml: PDGF (p = .023)	**Pre *vs.* Post exercise program** #: Leukocytes T-cells B-cells NKs NKT $CD56^{dim}$ $CD56^{bright}$ KIR2DL1 KIR2DL2/3 KIR3DL1	IG: 0.7 *vs.* CG: 0.7 IG: 0.6 *vs.* CG: 0.7 IG: 0.8 *vs.* CG: 0.3 IG: 2.2 *vs.* CG: 1.0 IG: 1.5 *vs.* CG: 1.3 IG: 1.8 *vs.* CG: 0.9 IG: 20.0 *vs.* CG: 3.0 IG: 0.5 *vs.* CG: 0.8 IG: 1.0 *vs.* CG: 1.0	→ → ↑ ↑ → ↑ ↑ ↓ → ↑

(Continued)

TABLE 1 | Continued

Reference number, Registration number and name of register	Study design	Participant characterization	N (IG/ CG/HC)	Intervention Description	Frequency (F)/Intensity(I)/Time (T)/ Duration (D)/Adherence (A)	Outcome Between-Group Differences (Group)	Outcome Within-Group Differences (Time)	Outcome interaction (group x time)	Direction ratio [Intervention (IG) *vs.* Control (CG) group or healthy control group (HC)]		
										IG: 0.5 *vs.* CG: 0.3	
									NK 25	IG: 2.0 *vs.* CG: 2.0	→
				CG:					NK 69	IG: 2.0 *vs.* CG: 1.5	↑
									KIR2DS4	IG: 1.7 *vs.* CG: 1.3	↑
									NKG2D	IG: 1.6 *vs.* CG: 1.0	↑
				Usual care (no training)					NKp44	IG: 2.0 *vs.* CG: 1.0	↑
									NKp46	IG: 1.5 *vs.* CG: 1.0	↑
		Treatment-phase							NKp30	IG: 1.7 *vs.* CG: 1.0	↑
		On-treatment during neoadjuvant therapy							DNAM	IG: 2.3 *vs.* CG: 1.3	↑
									NKG2A	IG: 2.0 *vs.* CG: 1.2	↑
									CXCR6	IG: 0.3 *vs.* CG: 1.0	↓
									%:		
									T-cells	IG: 0.8 *vs.* CG: 1.1	→
									B-cells	IG: 0.5 *vs.* CG: 0.3	↑
									NKs	IG: 2.4 *vs.* CG: 1.3	↑
									NKT	IG: 1.0 *vs.* CG: 1.7	↓
									$CD56^{dim}$	IG: 0.9 *vs.* CG: 1.1	→
									$CD56^{bright}$	IG: 2.5 *vs.* CG: 1.8	↑
									KIR2DL1	IG: 0.4 *vs.* CG: 0.6	↓
									KIR2DL2/3	IG: 0.8 *vs.* CG: 1.2	↓
									KIR3DL1	IG: 0.3 *vs.* CG: 0.4	→
									NK 25	IG: 1.1 *vs.* CG: 1.8	↓
									NK 69	IG: 1.3 *vs.* CG: 1.1	→
									KIR2DS4	IG: 1.0 *vs.* CG: 1.8	↓
									NKG2D	IG: 1.0 *vs.* CG: 1.2	→
									NKp44	IG: 1.0 *vs.* CG: 1.7	↓
									NKp46	IG: 1.2 *vs.* CG: 2.9	↓
									NKp30	IG: 1.1 *vs.* CG: 1.3	→
									DNAM	IG: 0.9 *vs.* CG: 1.5	↓
									NKG2A	IG: 1.0 *vs.* CG: 1.3	→
									CXCR6	IG: 1.0 *vs.* CG: 1.8	↓
									NKCC (ratio):		

(Continued)

TABLE 1 | Continued

Reference number, Registration number and name of register	Study design	Participant characterization	N (IG/ CG/HC)	Intervention Description	Frequency (F)/Intensity(I)/Time (T)/ Duration (D)/Adherence (A)	Outcome Between-Group Differences (Group)	Outcome Within-Group Differences (Time)	Outcome interaction (group x time)	Direction ratio [Intervention (IG) *vs.* Control (CG) group or healthy control group (HC)]		
									4:1	IG: 0.8 *vs.* CG: 0.9	→
									8:1	IG: 0.3 *vs.* CG: 0.9	↑
									2:1	IG: 0.8 *vs.* CG: 0.9	→
									1:1	IG: 0.7 *vs.* CG: 1.0	↓
									pg/ml:		
									CTACK	IG: 1.1 *vs.* CG: 0.9	→
									Eotaxin	IG: 1.0 *vs.* CG: 1.5	↓
									FGF	IG: 1.1 *vs.* CG: 1.3	→
									GSCF	IG: 1.1 *vs.* CG: 0.7	↑
									GRO-α	IG: 1.4 *vs.* CG: 0.7	↑
									HGF	IG: 1.4 *vs.* CG: 1.0	↑
									ICAM	IG: 1.0 *vs.* CG: 0.9	→
									IFNγ	IG: 1.1 *vs.* CG: 1.0	→
									IL-1α	IG: 0.9 *vs.* CG: 0.9	→
									IL-2	IG: 1.1 *vs.* CG: 1.1	→
									IL-3	IG: 0.7 *vs.* CG: 2.0	↓
									IL-4	IG: 0.9 *vs.* CG: 1.0	→
									IL-6	IG: 1.0 *vs.* CG: 0.8	→
									IL-7	IG: 1.3 *vs.* CG: 0.5	↑
									IL-8	IG: 0.5 *vs.* CG: 0.8	↓
									IL-9	IG: 1.0 *vs.* CG: 1.1	→
									IL-10	IG: 0.5 *vs.* CG: 0.6	→
									IL-16	IG: 0.9 *vs.* CG: 0.6	↑
									IL-18	IG: 1.3 *vs.* CG: 0.9	↑
									IP10/ CXCL10	IG: 1.9 *vs.* CG: 0.6	↑
									MCP1/CCL2	IG: 1.4 *vs.* CG: 1.0	↑
									MCP3/CCL7	IG: 3.6 *vs.* CG: 0.5	↑
									MIG/CXCL9	IG: 1.6 *vs.* CG: 0.9	↑
									MIF	IG: 1.4 *vs.* CG: 0.5	↑
									MIP-1 α/ CCL3	IG: 0.6 *vs.* CG: 0.9	↓
									MSCF	IG: 0.8 *vs.* CG: 1.5	↓
									PDGF	IG: 1.4 *vs.* CG: 0.8	↑
									TNF-β	IG: 0.6 *vs.* CG: 0.8	→

(Continued)

TABLE 1 | Continued

Reference number, Registration number and name of register	Study design	Participant characterization	N (IG/ CG/HC)	Intervention Description	Frequency (F)/Intensity(I)/Time (T)/ Duration (D)/Adherence (A)	Outcome Between-Group Differences (Group)	Outcome Within-Group Differences (Time)	Outcome interaction (group x time)	Direction ratio [Intervention (IG) *vs.* Control (CG) group or healthy control group (HC)]
									TRAIL IG: 1.2 *vs.* CG: 0.8 ↑
									VCAM1 IG: 1.1 *vs.* CG: 1.2 →
									VEGF IG: 0.7 *vs.* CG: 0.8 →
15	NCT	Age IG: 11 ± 3 yr (4-17 yr); CG: 11 ± 4 yr (4-18yr) Cancer entities Solid tumor & leukemia	169 (68/101/ 0)	IG: Supervised in-hospital strength & aerobic exercises CG: Usual care (no training)	F: 2-3x/wk I: 65-80% of age predicted max. HR T: ~60-70 min D: ~22 wks A: N/A	No significant differences	# Leukocytes* (p <.0001)	No significant differences	**Pre *vs.* Post exercise program** Leukocytes IG: 0.6 *vs.* CG: 0.8 ↓
33	CS	Age IG: 14 ± 0.6 yr; CG: 13.0 ± 3.1 yr; HC: N/A Cancer entities IG & CG: ALL & neoplasms HC: healthy controls Treatment-phase On Treatment after induction therapy	17 (3/3/ 11)	IG & HC: Supervised of fitness instructor or parents aerobic exercise CG: Usual care (no training)	F: 3x/wk I: 70%–85% of measured max HR, T: 30 min D: 12 wks A: N/A	**Initial resting immune function (IG *vs.* HC):** Leukocytes* Lymphocytes* CD3+* CD4+* CD8+* CD19+* CD25+* PHA-induced lymphocyte proliferation*	No significant differences in IG Significant changes in HC: Leukocytes* CD3+* CD25+*	N/A	**Pre *vs.* Post exercise program** Leukocytes IG: 0.9 *vs.* HC: 0.8 → Lymphocytes IG: 0.6 *vs.* HC: 1.3 → Monocytes IG: 0.7 *vs.* HC: 1.3 ↓ Granulocytes IG: 0.6 *vs.* HC: 0.8 → T-cells IG: 0.6 *vs.* HC: 0.8 → CD4+ IG: 0.4 *vs.* HC: 1.1 ↓ CD8+ IG: 0.7 *vs.* HC: 0.9 → B-cells IG: 7.0 *vs.* HC: 1.1 ↑ NKs IG: 0.8 *vs.* HC: 0.9 → CD25+ IG: 0.3 *vs.* HC: 0.6 ↓ CD122+ IG: 1.3 *vs.* HC: 0.8 ↑ Ratio: CD4+/CD8+ IG: 0.8 *vs.* HC: 1.1 → Cytolytic activity: Spontaneous IG: 2.3 *vs.* HC: 0.6 ↑ IL-2-induced IG: 1.3 *vs.* HC: 0.7 ↑ Proliferation: PHA-induced IG: 0.5 *vs.* HC: 1.1 ↓ PWM-induced IG: 0.6 *vs.* HC: 1.0 ↓
Effects of acute exercise intervention on immune parameter									
34	NCT	Age IG: 11.3 ± 5.3 yr HC: 10.8 ± 4.6 yr	10 (4/0/6)	IG & HC: Supervised in-hospital moderate to vigorous intermittent aerobic exercise	F: N/A I: 70-85% of measured VO2 peak	#: ALC* (p = .000) Eosinophils* (p = .006)	#: WBC* (p = .023) ALC* (p = .008) Monocytes	Ratio of active neutrophils compared to unstimulated neutrophils at time 0:	**Pre *vs.* Post exercise intervention**: WBC IG: 1.3 *vs.* HC: 1.4 → ALC IG: 1.5 *vs.* HC: 1.3 → Monocytes →

(Continued)

TABLE 1 | Continued

Reference number, Registration number and name of register	Study design	Participant characterization	N (IG/ CG/HC)	Intervention Description	Frequency (F)/Intensity(I)/Time (T)/ Duration (D)/Adherence (A)	Outcome Between-Group Differences (Group)	Outcome Within-Group Differences (Time)	Outcome interaction (group x time)	Direction ratio [Intervention (IG) *vs.* Control (CG) group or healthy control group (HC)]
							(p = .059)		IG: 1.5 *vs.* HC: 1.5
					T: 30 min (10 min walk, 10 min run, 10 min walk)		Eosinophils*	Ratio time15* (p = .006)	Eosinophils IG: 1.0 *vs.* HC: 1.1 →
						Ratio of active neutrophils compared to unstimulated neutrophils at time 0:	(p = .042)		Basophils IG: 1.6 *vs.* HC: 1.9 →
		Cancer entities			D: N/A→ acute effects				
		IG: Pre B-ALL							Ratio of active neutrophils compared to unstimulated neutrophils at time 0 (Post *vs.* Pre exercise):
					A: N/A	Ratio time5*	Ratio of active neutrophils:		
		HC: healthy controls				(p = .048)			
							pre-post exercise		Ratio time5 IG: 0.8 *vs.* HC: 0.7 →
						Ratio time10◊			Ratio time10 IG: 0.6 *vs.* HC: 0.4 →
		Treatment-phase				(p = .074)	(p = .011)		Ratio time15 IG: 0.8 *vs.* HC: 0.6 →
						Ratio time15*	post to 1-h post exercise (p = .045)		**Pre- *vs.* 2-h post exercise intervention** :
						(p = .050)			
							1-h to 2-h post exercise		WBC IG: 1.1 *vs.* HC: 1.2 →
									ALC IG: 1.1 *vs.* HC: 1.1 →
		On maintenance treatment				Neutrophil oxidative burst:	(p = .052)		Monocytes IG: 1.3 *vs.* HC: 1.2 →
									Eosinophils IG: 0.7 *vs.* HC: 0.9 →
						time 0 (p = .029)			Basophils IG: 1.0 *vs.* HC: 1.6 ↓
									Ratio of active neutrophils compared to unstimulated neutrophils at time 0 (2-h post *vs.* Pre exercise):
									Ratio time 5 min IG: 0.6 *vs.* HC: 1.2 ↓
									Ratio time 10 min IG: 0.4 *vs.* HC: 1.2 ↓
									Ratio time 15 min IG: 0.5 *vs.* HC: 1.7 ↓

Characteristics, exercise descriptions and results from the included studies are summarized. P-values are shown within the columns: Outcome Between-Group Differences (Group), Outcome Within-Group Differences (Time), and Outcome interaction (group x time). A trend ratio was calculated by dividing values 30d post-HSCT by 15d post- HSCT (28, 30), post-HSCT by pre-HSCT (29), posttreatment by baseline (15, 32), final by initial (33), and post- exercise or 2-h post exercise by pre-exercise (34)., significant (p-values are shown if reported), ◊, significant with p <.1 due to the small sample size of the study; ‡, no calculation of change possible, because only data for one time point is available even after further inquiry; #, cell count, %, percent, ↓↑→, Direction of trend or difference if the ratio of the intervention group differs >30% compared to the ratio of the control/healthy group, ALC, absolute lymphocyte count; ANC, absolute neutrophil count, B, B cells; CD, cluster of differentiation; CG, Control group; CS, case series; DC, dendritic cells; ex., exercise; HC, Healthy controls; HSCT, Hematopoetic stem cell transplantation; IG, Intervention group; IL, Interleukin; KIR, killer cell immunoglobulin-like receptors; min, minute(s); N/A, data not available; NCT, Non-randomized controlled trial; NK, natural killer cells; NK T, natural killer T cells; RCT, Randomized controlled trial; T, T cells; WBC, whole blood cells; wks, weeks; yr, years; h, hour(s); actCD4$^+$, activated CD4$^+$ T cells; CM CD4$^+$, central memory CD4$^+$ T cells; EM CD4$^+$, effector memory CD4$^+$ T cells; Treg, regulatory CD4$^+$ T cell; mB-cells, mature B-cells.*

part in the included studies, whereas sex is not mentioned in one study (n = 17) (33). Treatment phases and cancer treatment differed within the studies. Detailed study characterizations are available in **Table 1**. Risk of bias assessment could be performed for the three RCTs and studies scored with 4 out of 10 (32), 6 out of 10 (29), and 5 out of 10 (31) possible points (see **Supplement 3**).

Most studies focused on mixed interventions with strength and aerobic exercises. In the study of Chamorro-Vina et al. (28), Morales et al. (30) and Senn-Malashonak et al. (31) participants attended a supervised in-hospital exercise program five times per week for about three weeks until discharge during HSCT. In Chamorro-Vina et al. (29) children performed three times per week a supervised in-hospital & home-based training after discharge of HSCT for ten weeks. In Fiuza-Luces et al. (32) children participated at the supervised in-hospital exercise program three times per week for about 17 weeks on-treatment during neoadjuvant therapy. In Morales et al. (15) participants trained supervised in-hospital two to three times per week for about 22 weeks.

Only in two studies (33, 34) exercise programs consisted of aerobic exercises alone. In Shore and Shepard (33) children participated three times per week for 12 weeks in a supervised aerobic exercise training. In Ladha et al. (34) children attended a supervised in-hospital moderate to vigorous intermittent aerobic exercise test for 30 minutes. Detailed exercise modalities are described in **Table 1**.

Effects of Regular Exercise Intervention in the Context of HSCT on Immune Parameters

Four studies focused on the immunological changes in the context of HSCT (28–31). Significant effects of the intervention (group x time) were seen for DC counts (p= .045) (28) and following T cell subset counts: effector memory (EM) $CD4^+$ (p = .005), regulatory $CD4^+$ T cells (Tregs, p = .003), and naïve $CD4^+$ T cells (p= .005) during allo-HSCT as well as $CD8^+$ T cells (p = .041), naïve $CD4^+$ T cells (p= .048), and total $CD4^+$ T cell counts (p = .048) during auto-HSCT (30). A significant intervention induced effect (group x time) was noticed for $CD56^{bright}$ NK cell counts in patients receiving allo-HSCT and $CD56^{dim}$ NK cells (mean ratio) showing a significant increase in the IG compared to the CG (p= .003; p = .03) (29, 30). Detected time (within-group) effects within various immune cell subset counts were dominantly seen in patient receiving allo-HSCT, whereas patients receiving auto-HSCT showed more differences in immune cell counts between IG and CG (between- group) (30). All reported significances became non-significant after adjustment for multiple comparison (**Supplement 4**). No further significant intervention induced effect has been noticed for NK cell specific cell surface receptors, such as NKG2D, NKp30, and NKp44.

The NK cells were analyzed for their cytotoxic potential against the target cell line K562 from both groups. A ratio of observed natural killer cytotoxicity (NKCC) pre-training and post-training for groups was calculated. The NKCC was significantly higher in the IG compared to the CG (8 times higher, p <.05) (29). In line with slightly higher cytotoxic NK cell potential, a decreased risk of infections was reported within the IG (30).

Serum cytokines levels were measured for eight different cytokines (**Table 1**). No significant intervention effect was found between the two groups. However, a slight increase of IL-2, IL-4, IFNγ, TNFα, and GM-CSF was observed within the IG, while no change was seen within the CG for the first four cytokines, but a decrease for GM-CSF (29).

Effects of Regular Exercise Intervention in Context of Chemotherapy on Immune Parameters

Three studies examined changes within the immune system in patients with solid tumors and leukemia receiving chemotherapy (15, 32, 33). No significant interaction (group x time) effect for leukocytes or lymphocyte subset counts was reported. Different dynamics in leukocyte counts were seen for IG and CG during follow-ups unto 5-years after posttreatment (15). From posttreatment and within the 1-year follow-up both groups showed significant decreased leukocyte counts compared to baseline (within-group, all p-values <.001). Within the 2-year follow-up, leukocyte counts in IG differed non-significantly compared to baseline (p = .192), while leukocyte counts remained significantly decreased in CG (p = .011). A slight decrease was also seen within the 3-year follow up in CG (p = .061), but not seen within the 4- and 5-year follow-up (15). The study further reported significantly decreased days of in-hospitalization for the IG compared to CG (p = .031) resulting in reduced treatment costs.

When analyzing various NK cell receptors needed for recognition of HLA-class I molecules and other important NK cell receptors, most receptors showed no intervention effect (group x time), but a trend towards an interaction effect was seen for the KIR2DS4 which remained stable in the IG but increased in the CG (p = .028).

In two studies the cytotoxic potential of the cells were analyzed either by the spontaneous or IL-2-induced cytolytic activity of all mononuclear cells (33) or target-induced NKCC (32), however no significant intervention effect (group x time) was reported. Shore and Shepard (33) showed higher baseline levels of spontaneous as well as IL-2-induced cytolytic activity in the healthy controls compared to the IG (pediatric cancer patients). After exercise, a decrease of spontaneous as well as IL-2-induced cytolytic activity was observed within the healthy controls, while both activities increased in the IG to comparable levels as the healthy controls (33). Fiuza-Luces et al. (2017) reported (32) higher baseline levels of NKCC for all four dilutions in the IG (8:1 – 1:1), which was stable for the next two time points after intervention as well. No significant intervention effect (group x time) was reported for NKCC (32). No significant intervention effect (group x time) was seen for the 31 analyzed inflammatory cytokines after testing for multiple corrections (p = .0016) (32).

Effects of Acute Exercise Intervention on Immune Parameters

One study focused on the effects on neutrophil count and function after an acute 30-minute exercise intervention (34). IG values were compared to age- and sex-matched healthy controls. Both groups received an acute bout of aerobic exercise and neutrophil counts and

function were analyzed pre-exercise, post-exercise, 1h, and 2h post-exercise. Neutrophil oxidative burst was monitored at 0min, 5min, 10min, and 15min (34). The authors observed a significant increase in whole blood cell (WBC, p = .002), absolute neutrophil count (ANC, p = .006), and absolute lymphocyte count (ALC, p = .003) as well as a significant decrease in eosinophils (p = .003) in both groups from pre-exercise to post-exercise. The effects on absolute lymphocyte counts and eosinophils were also significant within the group analyses (ALC, p = .000, eosinophils p = .003). When comparing the oxidative burst capacity of the neutrophils between IG and healthy controls, the study showed a significant higher capacity at 0min within the healthy controls compared to IG (main effect for group, p = .029). After 5min, 10min, and 15min the IG showed a significant higher oxidative burst compared to the healthy controls (p = .048,.078,.050, the study set the significant p-value to p <.1 due to low number of participants).

Direction Ratios of the immunological Changes

Direction ratios in the context of HSCT with regular exercise intervention showed different immune cell reconstitution dynamics between allo-HSCT and auto-HSCT. In IG compared to CG 30d post-HSCT to 15d post-HSCT either no change or an increase in leukocytes counts were observed. An increase in mature immune cell subsets regarding total NK cell, $CD56^{bright}$ NK cell, total T cell, effector memory (EM) $CD8^+$ T cell, and memory B cell counts in patients receiving allo-HSCT was detected, compared to patients with auto-HSCT. Patients with auto-HSCT showed an increase in naïve $CD4^+$ and EM $CD4^+$ T cells. Both patients' cohorts showed increased naïve $CD8^+$ T cell counts (**Table 1**).

NK cell and $NKp30^+$ NK cell frequencies as well as serum cytokine levels of IL-2, IL-4, IL-6, IFNγ, IL-10, TNFα, and GM-CSF were higher in the IG compared to the CG post-exercise intervention compared to pre-exercise intervention after discharge of HSCT.

Total cell counts of NK cells and expression of certain NK cell specific molecules (3DL1, CD69, 2DS4, NKG2A, NKG2D, NKp44, NKp46, NKp30, DNAM) were increased in the IG receiving neoadjuvant therapy compared to the CG after usual care. This was also seen for NK cell frequencies, due to $CD56^{bright}$ NK cells, but not for frequencies of NK-specific molecules which decreased. Furthermore, 13 out of 30 inflammatory serum cytokines levels were increased and five out of 30 decreased (**Table 1**). Two studies showed a direction ratio increase of the IG compared to CG or healthy controls in B cell counts and cytotoxicity (8:1 NKCC or spontaneous cytolytic activity). Besides increase in total lymphocyte counts, monocytes, $CD4^+$ T cells, $CD25^+$, and $CD122^+$ cell counts as well as PHA- and PWM-induced proliferation were decreased between the IG and healthy controls.

For acute exercise intervention effects, a decrease in basophil counts as well as in neutrophil activity ratio time 5, 10, and 15 minutes was detected 2-h post exercise compared to pre-exercise within the IG compared to healthy controls.

Secondary Outcomes

In children undergoing a HSCT no significant differences in transplantation outcomes such as duration of myelosuppression, neutropenic phase or duration of hospitalization were found between IG and CG (28). In Morales et al., 2020b (30) a trend towards between-group differences in the duration of hospitalization was noted (p = .052) with less days for IG. Same result was reported for children during neoadjuvant or intense chemotherapy treatment period in IG according to Morales et al., 2020a (p = .031) (15). Morales et al., 2020b (30) showed a lower number of infections after allo-HSCT in the exercise group (p = .023 and p = .083 for total and viral infections). Senn-Malashonak et al. (31) and Morales et al., 2020b (30) reported no differences in transplantation outcomes such as complications or GvHD for children undergoing HSCT. The effects on physical and/or functional performance as well as body composition have been reviewed in other studies in depth (13, 14, 35). Hence, this study focused on effects directly related to the immune system.

DISCUSSION

This systemic review included eight studies evaluating the changes in immune cell parameters after acute and chronic exercise in pediatric cancer patients, survivors, and HSCT recipients. In summary, no negative effects of exercise on the immune system, but positive effects on immune cell functionality, especially cytotoxicity, were noted, whereas immune cell counts, and inflammatory serum cytokine levels showed no significant intervention effect. Notably, some studies reported an exercise induced effect on slightly decreased infection rates and significant decreased days of in-hospitalization resulting in decreased treatment costs.

After acute aerobic exercise, patients with acute lymphoblastic leukemia showed a significant higher oxidative burst in neutrophils compared to healthy controls. This is of particular interest, as neutrophils belong to the innate immune system and are therefore responsible for the first line of defense. Neutrophils are able to migrate into tissues in order to eliminate invading pathogens by reactive oxygen species production, cytokine secretion, and phagocytosis (36). Thus, abnormal low frequencies of neutrophils, called neutropenia, can increase the chance of life-threatening infections and is a common side effect during cancer therapy (37–39). This finding by Ladha et al. (34) is in line with published data from adult cancer patients, where an increase in neutrophil function was observed after acute exercise (40). Studies in adult cancer patients and experimental mouse models further suggest that regular exercise intervention sustains enhanced neutrophil function and migratory capacity (40, 41). Furthermore, exercise can reduce chemotherapy related neutropenia in cancer patients (40) which might decrease the risk of infections in cancer patients. This is in line to a lower number of total and viral infections that could be observed (15).

Regular exercise interventions, comprising of combined aerobic and strength training, in pediatric patients post-HSCT led to significant higher mean ratio of $CD56^{dim}$ NK cells and in patients receiving allo-HSCT also increased T cell, B cell, and NK cell counts. This is in line with current literature, as NK cells are one of the first immune cell subsets to reconstitute after HSCT

(42, 43). Besides cytotoxic $CD8^+$ T cells, $CD56^{dim}$ NK cells are the only other immune cell subset having cytotoxic potential. Indeed, NKCC was significantly higher (8-fold) within the IG compared to the CG suggesting that exercise increases the functionality of NK cells in pediatric cancer patients, which is comparable with literature in healthy adults (44–46) and adults with cancer (47). This is of major importance post-HSCT, as the reconstituted NK cells have been described to promote a graft-versus-leukemia effect, where the donor derived NK cells prevent a potential relapse (48). High NK cell counts (above a median of 120 per µl blood) at day 32 post-HSCT have been described to predict a higher cumulative event-free survival rate, reduced transplant-related mortality and reduced cumulative relapse incidence (49). Hence, regular exercise in pediatric patients may increase NK cell functionality providing a natural defense against life threatening infections. Of note, within the study by Shore and Shepard (33) which focused on aerobic exercises IG showed a similar cytolytic activity compared to healthy children after exercise, although their initial levels of cytolytic activity were lower. Thus, this exercise induced effect of enhanced cytotoxicity is not only seen in patients receiving HSCT, but also in pediatric cancer patients without HSCT. It has to be mentioned that the type of exercise and exercise intensity also seems to influence NKCC (47). No study conducted in pediatric cancer patients so far focused on NK cell phenotyping and function after acute exercise.

Unfortunately, there is still too little data in pediatric cancer patients to define what exercise type and intensity is most beneficial for this population. Especially as most studies used a combination of aerobic and strength exercise programs. Of note, in healthy adults a recent systematic review highlights that aerobic/endurance training has a greater influence on NK cell cytotoxicity compared to strength training (45). Nevertheless, exercise programs during cancer therapy seem to be a useful and safe tool for children to keep their level of physical or functional performance or to improve muscle strength, physical fitness, body composition and functionality (12, 13, 35, 50). In this regard, guidelines regarding physical activity of pediatric cancer patients have recently been published (51) or are currently under development (52).

In summary, this systematic review suggests that no adverse effects on immunological parameters occurred during or after exercise intervention with pediatric cancer patients. Most studies reported an enhanced functional immune cell capacity after exercise indicating that exercise induces a boost to the immune system within pediatric cancer patients. This is in line with the reported reduced risks of infections and reduced days of in-hospitalization in the IG, which in turn decreases treatment costs. Interestingly, within an up to 5-year follow up, the IG was able to regain a comparable leukocyte count compared to baseline one year earlier compared to the CG, suggesting that exercise induced effects might have long lasting effects. Overall, both acute and chronic exercise interventions seem to enhance immune cell functionality in pediatric cancer patients, however data is limited to one immune cell subset in acute exercise intervention.

Some limitations of this review should be acknowledged. All studies included very limited or very heterogeneous populations. Furthermore, varying exercise interventions, differently composed control groups, and a broad variety of immune parameters made accurate comparison of the studies difficult. Therefore, meta-analyses were not possible and descriptive analyses were used instead. We addressed this issue by including a direction ratio. Finally, assessment of quality was only possible for three RCTs, which have a middle and low-quality rating. This is mainly due to lack of participant blinding, missing intention-to-treat analysis and inadequate follow up. However, most of these difficulties are common in exercise intervention studies. Despite these limitations, the strengths of this review are the systematic and thorough search of several databases and the independent quality assessment by two reviewers. This review provides initial information for the planning and implementation of exercise interventions from an immunological point of view in pediatric oncology, as the included studies indicate that exercise is beneficial for the patients. It further highlights the need of further studies to evaluate and understand the mechanistic effects of different exercise modalities on the immune system in pediatric cancer patients and survivors, especially in the context of allo- and auto-HSCT.

DATA AVAILABILITY STATEMENT

All data collected for this article, including data extraction tables and the statistical analysis, will be made available. Requests to access these data should be made to the corresponding author.

AUTHOR CONTRIBUTIONS

RB: study design, search of four data bases, review of studies, risk of bias assessment, data extraction, data analyses, writing the manuscript. SB: review of studies, risk of bias assessment, data extraction, data analyses, writing the manuscript. MG: study design, search of four data bases, final decision on study inclusion, data collection, writing the manuscript. All authors contributed to the article and approved the submitted version.

FUNDING

We acknowledge support by the Open Access Publication Fund of the University of Duisburg-Essen.

ACKNOWLEDGMENTS

The authors would like to thank Sandra Goertz for data extraction and all researchers who provided information about their research studies.

SUPPLEMENTARY MATERIAL

The Supplementary Material for this article can be found online at: https://www.frontiersin.org/articles/10.3389/fimmu.2021.746171/full#supplementary-material

REFERENCES

1. Berendsen AJ, Groot Nibbelink A, Blaauwbroek R, Berger MY, Tissing WJE. Second Cancers After Childhood Cancer–GPs Beware! *Scand J Prim Health Care* (2013) 31(3):147–52. doi: 10.3109/02813432.2013.824152
2. Schrappe M, Bleckmann K, Zimmermann M, Biondi A, Möricke A, Locatelli F, et al. Reduced-Intensity Delayed Intensification in Standard-Risk Pediatric Acute Lymphoblastic Leukemia Defined by Undetectable Minimal Residual Disease: Results of an International Randomized Trial (AIEOP-BFM ALL 2000). *J Clin Oncol* (2018) 36(3):244–53. doi: 10.1200/JCO.2017.74.4946
3. Bigley AB, Rezvani K, Chew C, Sekine T, Pistillo M, Crucian B, et al. Acute Exercise Preferentially Redeploys NK-Cells With a Highly-Differentiated Phenotype and Augments Cytotoxicity Against Lymphoma and Multiple Myeloma Target Cells. *Brain Behav Immun* (2014) 39:160–71. doi: 10.1016/j.bbi.2013.10.030
4. LaVoy EC, Bollard CM, Hanley PJ, Blaney JW, O'Connor DP, Bosch JA, et al. A Single Bout of Dynamic Exercise Enhances the Expansion of MAGE-A4 and PRAME-Specific Cytotoxic T-Cells From Healthy Adults. *Exercise Immunol Rev* (2015) 21:144–53.
5. Campbell JP, Riddell NE, Burns VE, Turner M, van Zanten JJ, Drayson MT, et al. Acute Exercise Mobilises CD8+ T Lymphocytes Exhibiting an Effector-Memory Phenotype. *Brain Behav Immun* (2009) 23(6):767–75. doi: 10.1016/j.bbi.2009.02.011
6. Fiuza-Luces C, Valenzuela PL, Castillo-García A, Lucia A. Exercise Benefits Meet Cancer Immunosurveillance: Implications for Immunotherapy. *Trends Cancer* (2021) 7(2):91–3. doi: 10.1016/j.trecan.2020.12.003
7. Idorn M, Hojman P. Exercise-Dependent Regulation of NK Cells in Cancer Protection. *Trends Mol Med* (2016) 22(7):565–77. doi: 10.1016/j.molmed.2016.05.007
8. Pedersen BK, Hoffman-Goetz L. Exercise and the Immune System: Regulation, Integration, and Adaptation. *Physiol Rev* (2000) 80(3):1055–81. doi: 10.1152/physrev.2000.80.3.1055
9. Bigley AB, Simpson RJ. NK Cells and Exercise: Implications for Cancer Immunotherapy and Survivorship. *Discovery Med* (2015) 19(107):433–45.
10. Kruijsen-Jaarsma M, Révész D, Bierings MB, Buffart LM, Takken T. Effects of Exercise on Immune Function in Patients With Cancer: A Systematic Review. *Exercise Immunol Rev* (2013) 19:120–43.
11. Stössel S, Neu MA, Wingerter A, Bloch W, Zimmer P, Paret C, et al. Benefits of Exercise Training for Children and Adolescents Undergoing Cancer Treatment: Results From the Randomized Controlled MUCKI Trial. *Front Pediatr* (2020) 8:243. doi: 10.3389/fped.2020.00243
12. Braam KI, van der Torre P, Takken T, Veening MA, van Dulmen-den Broeder E, Kaspers GJ. Physical Exercise Training Interventions for Children and Young Adults During and After Treatment for Childhood Cancer. *Cochrane Database Syst Rev* (2016) 3(3):Cd008796. doi: 10.1002/14651858.CD008796.pub3
13. Coombs A, Schilperoort H, Sargent B. The Effect of Exercise and Motor Interventions on Physical Activity and Motor Outcomes During and After Medical Intervention for Children and Adolescents With Acute Lymphoblastic Leukemia: A Systematic Review. *Crit Rev Oncol Hematol* (2020) 152:103004. doi: 10.1016/j.critrevonc.2020.103004
14. Morales JS, Valenzuela PL, Rincón-Castanedo C, Takken T, Fiuza-Luces C, Santos-Lozano A, et al. Exercise Training in Childhood Cancer: A Systematic Review and Meta-Analysis of Randomized Controlled Trials. *Cancer Treat Rev* (2018) 70:154–67. doi: 10.1016/j.ctrv.2018.08.012
15. Morales JS, Santana-Sosa E, Santos-Lozano A, Baño-Rodrigo A, Valenzuela PL, Rincón-Castanedo C, et al. Inhospital Exercise Benefits in Childhood Cancer: A Prospective Cohort Study. *Scand J Med Sci Sports* (2020) 30(1):126–34. doi: 10.1111/sms.13545
16. Fiuza-Luces C, González-Murillo A, Soares-Miranda L, Martínez Palacio J, Colmenero I, Casco F, et al. Effects of Exercise Interventions in Graft-Versus-Host Disease Models. *Cell Transplant* (2013) 22(12):2409–20. doi: 10.3727/096368912X658746
17. Fiuza-Luces C, Soares-Miranda L, González-Murillo A, Palacio JM, Colmenero I, Casco F, et al. Exercise Benefits in Chronic Graft Versus Host Disease: A Murine Model Study. *Med Sci Sports Exerc* (2013) 45(9):1703–11. doi: 10.1249/MSS.0b013e31828fa004
18. Olin A, Henckel E, Chen Y, Lakshmikanth T, Pou C, Mikes J, et al. Stereotypic Immune System Development in Newborn Children. *Cell* (2018) 174(5):1277–92.e14. doi: 10.1016/j.cell.2018.06.045
19. Bennstein SB, Scherenschlich N, Weinhold S, Manser AR, Noll A, Raba K, et al. Transcriptional and Functional Characterization of Neonatal Circulating ILCs. *Stem Cells Trans Med* (2021) N/A:1–16. doi: 10.1002/sctm.20-0300
20. Valiathan R, Ashman M, Asthana D. Effects of Ageing on the Immune System: Infants to Elderly. *Scand J Immunol* (2016) 83(4):255–66. doi: 10.1111/sji.12413
21. Bennstein SB, Weinhold S, Manser AR, Scherenschlich N, Noll A, Raba K, et al. Umbilical Cord Blood-Derived ILC1-Like Cells Constitute a Novel Precursor for Mature KIR+NKG2A- NK Cells. *eLife* (2020) 9:e55232. doi: 10.1101/2020.01.24.918318
22. Schauer T, Mazzoni AS, Henriksson A, Demmelmaier I, Berntsen S, Raastad T, et al. Exercise Intensity and Markers of Inflammation During and After (Neo-) Adjuvant Cancer Treatment. *Endocr Relat Cancer* (2021) 28(3):191–201. doi: 10.1530/ERC-20-0507
23. Moher D, Liberati A, Tetzlaff J, Altman DG. Preferred Reporting Items for Systematic Reviews and Meta-Analyses: The PRISMA Statement. *PloS Med* (2009) 6(7):e1000097. doi: 10.1371/journal.pmed.1000097
24. Schardt C, Adams MB, Owens T, Keitz S, Fontelo P. Utilization of the PICO Framework to Improve Searching PubMed for Clinical Questions. *BMC Med Inf Decision Making* (2007) 7(1):16. doi: 10.1186/1472-6947-7-16
25. Page MJ, McKenzie JE, Bossuyt PM, Boutron I, Hoffmann TC, Mulrow CD, et al. The PRISMA 2020 Statement: An Updated Guideline for Reporting Systematic Reviews. *BMJ* (2021) 372:n71. doi: 10.1136/bmj.n71
26. Herbert R, Moseley A, Sherrington C. PEDro: A Database of Randomised Controlled Trials in Physiotherapy. *Health Inf Manage* (1998) 28(4):186–8. doi: 10.1177/183335839902800410
27. Verhagen AP, de Vet HC, de Bie RA, Kessels AG, Boers M, Bouter LM, et al. The Delphi List: A Criteria List for Quality Assessment of Randomized Clinical Trials for Conducting Systematic Reviews Developed by Delphi Consensus. *J Clin Epidemiol* (1998) 51(12):1235–41. doi: 10.1016/S0895-4356(98)00131-0
28. Chamorro-Viña C, Ruiz JR, Santana-Sosa E, González Vicent M, Madero L, Pérez M, et al. Exercise During Hematopoietic Stem Cell Transplant Hospitalization in Children. *Med Sci Sports Exerc* (2010) 42(6):1045–53. doi: 10.1249/MSS.0b013e3181c4dac1
29. Chamorro-Viña C, Valentín J, Fernández L, González-Vicent M, Pérez-Ruiz M, Lucía A, et al. Influence of a Moderate-Intensity Exercise Program on Early NK Cell Immune Recovery in Pediatric Patients After Reduced-Intensity Hematopoietic Stem Cell Transplantation. *Integr Cancer Ther* (2017) 16(4):464–72. doi: 10.1177/1534735416679515
30. Morales JS, González Vicent M, Valenzuela PL, Castillo-García A, Santana-Sosa E, Lassaletta A, et al. Tailored Exercise During Hematopoietic Stem Cell Transplantation Hospitalization in Children With Cancer: A Prospective Cohort Study. *Cancers* (2020) 12(10):3020. doi: 10.3390/cancers12103020
31. Senn-Malashonak A, Wallek S, Schmidt K, Rosenhagen A, Vogt L, Bader P, et al. Psychophysical Effects of an Exercise Therapy During Pediatric Stem Cell Transplantation: A Randomized Controlled Trial. *Bone Marrow Transplant* (2019) 54(11):1827–35. doi: 10.1038/s41409-019-0535-z
32. Fiuza-Luces C, Padilla JR, Valentín J, Santana-Sosa E, Santos-Lozano A, Sanchis-Gomar F, et al. Effects of Exercise on the Immune Function of Pediatric Patients With Solid Tumors: Insights From the PAPEC Randomized Trial. *Am J Phys Med Rehabil* (2017) 96(11):831–7. doi: 10.1097/PHM.0000000000000757
33. Shore S, Shepard RJ. Immune Responses to Exercise in Children Treated for Cancer. *J Sports Med Phys Fitness* (1999) 39(3):240–3.
34. Ladha A, Courneya K, Bell G, Field C, Grundy P. Effects of Acute Exercise on Neutrophils in Pediatric Acute Lymphoblastic Leukemia Survivors: A Pilot Study. *J Pediatr Hematol/Oncol* (2006) 28:671–7. doi: 10.1097/01.mph.0000243644.20993.54
35. Wurz A, McLaughlin E, Lategan C, Ellis K, Culos-Reed SN. Synthesizing the Literature on Physical Activity Among Children and Adolescents Affected by Cancer: Evidence for the International Pediatric Oncology Exercise Guidelines (iPOEG). *Trans Behav Med* (2021) 11(3):699–708. doi: 10.1093/tbm/ibaa136
36. Malech HL, Deleo FR, Quinn MT. The Role of Neutrophils in the Immune System: An Overview. *Methods Mol Biol (Clifton NJ)* (2014) 1124:3–10. doi: 10.1007/978-1-62703-845-4_1

37. Celkan T, Ozkan A, Apak H, Diren S, Can G, Yuksel L, et al. Bacteremia in Childhood Cancer. *J Trop Pediatr* (2002) 48(6):373–7. doi: 10.1093/tropej/48.6.373
38. Goodman M. Managing the Side Effects of Chemotherapy. *Semin Oncol Nurs* (1989) 5(2 Suppl 1):29–52. doi: 10.1016/0749-2081(89)90080-6
39. Orudjev E, Lange BJ. Evolving Concepts of Management of Febrile Neutropenia in Children With Cancer. *Med Pediatr Oncol* (2002) 39(2):77–85. doi: 10.1002/mpo.10073
40. Schauer T, Hojman P, Gehl J, Christensen JF. Exercise Training as Prophylactic Strategy in the Management of Neutropenia During Chemotherapy. *Br J Pharmacol* (2020) 1–13. doi: 10.1111/bph.15141
41. Martín-Ruiz A, Fiuza-Luces C, Rincón-Castanedo C, Fernández-Moreno D, Gálvez BG, Martínez-Martínez E, et al. Benefits of Exercise and Immunotherapy in a Murine Model of Human Non-Small-Cell Lung Carcinoma. *Exercise Immunol Rev* (2020) 26:100–15.
42. Bosch M, Khan FM, Storek J. Immune Reconstitution After Hematopoietic Cell Transplantation. *Curr Opin Hematol* (2012) 19(4):324–35. doi: 10.1097/MOH.0b013e328353bc7d
43. Dulphy N, Haas P, Busson M, Belhadj S, Peffault de Latour R, Robin M, et al. An Unusual CD56bright/CD16low NK Cell Subset Dominates the Early Posttransplant Period Following HLA-Matched Hematopoietic Stem Cell Transplantation. *J Immunol* (2008) 181(3):2227–37. doi: 10.4049/jimmunol.181.3.2227
44. Moro-García MA, Fernández-García B, Echeverría A, Rodríguez-Alonso M, Suárez-García FM, Solano-Jaurrieta JJ, et al. Frequent Participation in High Volume Exercise Throughout Life Is Associated With a More Differentiated Adaptive Immune Response. *Brain Behav Immun* (2014) 39:61–74. doi: 10.1016/j.bbi.2013.12.014
45. Rumpf C, Proschinger S, Schenk A, Bloch W, Lampit A, Javelle F, et al. The Effect of Acute Physical Exercise on NK-Cell Cytolytic Activity: A Systematic Review and Meta-Analysis. *Sports Med* (2021) 51(3):519–30. doi: 10.1007/s40279-020-01402-9
46. Llavero F, Alejo LB, Fiuza-Luces C, López Soto A, Valenzuela PL, Castillo-García A, et al. Exercise Training Effects on Natural Killer Cells: A Preliminary Proteomics and Systems Biology Approach. *Exercise Immunol Rev* (2021) 27:125–41.
47. Zimmer P, Schenk A, Kieven M, Holthaus M, Lehmann J, Lövenich L, et al. Exercise Induced Alterations in NK-Cell Cytotoxicity - Methodological Issues and Future Perspectives. *Exercise Immunol Rev* (2017) 23:66–81.
48. Arvindam US, Aguilar EG, Felices M, Murphy W, Miller J. Chapter 16 - Natural Killer Cells in GvHD and GvL. In: G Socié, R Zeiser, BR Blazar, editors. *Immune Biology of Allogeneic Hematopoietic Stem Cell Transplantation, 2nd ed.* Academic Press (2019). p. 275–92.
49. Huttunen P, Taskinen M, Siitonen S, Saarinen-Pihkala UM. Impact of Very Early CD4+/CD8+ T Cell Counts on the Occurrence of Acute Graft-Versus-Host Disease and NK Cell Counts on Outcome After Pediatric Allogeneic Hematopoietic Stem Cell Transplantation. *Pediatr Blood Cancer* (2015) 62 (3):522–8. doi: 10.1002/pbc.25347
50. Santos SDS, Moussalle LD, Heinzmann-Filho JP. Effects of Physical Exercise During Hospitalization in Children and Adolescents With Cancer: A Systematic Review. *Rev Paul Pediatr* (2020) 39:e2019313. doi: 10.1590/1984-0462/2021/39/2019313
51. Wurz A, McLaughlin E, Lategan C, Chamorro Viña C, Grimshaw SL, Hamari L, et al. The International Pediatric Oncology Exercise Guidelines (iPOEG). *Trans Behav Med* (2021). doi: 10.1093/tbm/ibab028
52. Götte M, Gauß G. *Bewegungsförderung Und Bewegungstherapie in Der Pädiatrischen Onkologie*. Registriernummer 025-036.in preparation (2021).

Conflict of Interest: The authors declare that the research was conducted in the absence of any commercial or financial relationships that could be construed as a potential conflict of interest.

frontiers in Immunology

ORIGINAL RESEARCH
published: 06 October 2021
doi: 10.3389/fimmu.2021.758845

Low GNG12 Expression Predicts Adverse Outcomes: A Potential Therapeutic Target for Osteosarcoma

Jinghong Yuan[1†], Zhao Yuan[2†], Aifang Ye[3], Tianlong Wu[4], Jingyu Jia[5], Jia Guo[6], Jian Zhang[1], Tao Li[1] and Xigao Cheng[1,4,5]*

[1] Department of Orthopaedics, The Second Affiliated Hospital of Nanchang University, Nanchang, China, [2] Clinical Research Center, The Second Affiliated Hospital of Nanchang University, Nanchang, China, [3] Department of Otorhinolaryngology, Jiangxi Provincial Children's Hospital, Nanchang, China, [4] Institute of Orthopaedics of Jiangxi Province, Nanchang, China, [5] Institute of Minimally Invasive Orthopaedics of Nanchang University, Nanchang University, Nanchang, China, [6] Department of Orthopaedics, Jiangxi Provincial People's Hospital Affiliated to Nanchang University, Nanchang, China

OPEN ACCESS

Edited by:
Nicholas Vitanza, Seattle Children's Hospital, United States

Reviewed by:
Ashleigh Fordham, Children's Cancer Institute Australia, Australia
Xiaoling Zhang, Zhejiang University, China

***Correspondence:**
Xigao Cheng
228206846@qq.com

[†]These authors have contributed equally to this work

Specialty section:
This article was submitted to Cancer Immunity and Immunotherapy, a section of the journal Frontiers in Immunology

Received: *15 August 2021*
Accepted: *17 September 2021*
Published: *06 October 2021*

Citation:
Yuan J, Yuan Z, Ye A, Wu T, Jia J, Guo J, Zhang J, Li T and Cheng X (2021) Low GNG12 Expression Predicts Adverse Outcomes: A Potential Therapeutic Target for Osteosarcoma. Front. Immunol. 12:758845. doi: 10.3389/fimmu.2021.758845

Background: G protein subunit gamma 12 (GNG12) is observed in some types of cancer, but its role in osteosarcoma is unknown. This study hypothesized that GNG12 may be a potential biomarker and therapeutic target. We aimed to identify an association between GNG12 and osteosarcoma based on the Gene Expression Omnibus and the Therapeutically Applicable Research to Generate Effective Treatments (TARGET) databases.

Methods: Osteosarcoma samples in GSE42352 and TARGET database were selected as the test cohorts. As the external validation cohort, 78 osteosarcoma specimens from The Second Affiliated Hospital of Nanchang University were collected. Patients with osteosarcoma were divided into high and low GNG12 mRNA-expression groups; differentially expressed genes were identified as GNG12-related genes. The biological function of GNG12 was annotated using Gene Ontology, Kyoto Encyclopedia of Genes and Genomes, gene set enrichment analysis, and immune infiltration analysis. Gene expression correlation analysis and competing endogenous RNA regulatory network construction were used to determine potential biological regulatory relationships of GNG12. Overall survival, Kaplan–Meier analysis, and log-rank tests were calculated to determine GNG12 reliability in predicting survival prognosis.

Results: GNG12 expression decreased in osteosarcoma samples. GNG12 was a highly effective biomarker for osteosarcoma [area under the receiver operating characteristic (ROC) curve (AUC) = 0.920], and the results of our Kaplan–Meier analysis indicated that overall survival and progression-free survival differed significantly between low and high GNG-expression group ($p < 0.05$). Functional analyses indicated that GNG12 may promote osteosarcoma through regulating the endoplasmic reticulum. Expression correlation analysis and competing endogenous RNA network construction showed that HOTTIP/miR-27a-3p may regulate GNG12 expression. Furthermore, the subunit

suppresses adaptive immunity *via* inhibiting M1 and M2 macrophage infiltration. GNG12 was inhibited in metastatic osteosarcoma compared with non-metastatic osteosarcoma, and its expression predicted survival of patients (1, 3, and 5-year AUCs were 0.961, 0.826, and 0.808, respectively).

Conclusion: This study identified GNG12 as a potential biomarker for osteosarcoma prognosis, highlighting its potential as an immunotherapy target.

Keywords: osteosarcoma, GNG12, biomarker, therapeutic target, prognosis

1 INTRODUCTION

Osteosarcoma is among the most common primary solid malignant bone tumors in adolescents and young adults. Usually originating in the metaphyses of long bones, the cancer is characterized by heterogeneous presentation, high mortality, and an annual incidence of 8–11 million among 15–19-year-olds (1). After comprehensive treatment with methods such as radiotherapy and chemotherapy, the 5-year survival rate is 65%–70% (2, 3), but these improvements have been mainly limited to patients with non-metastatic disease. Moreover, the progress of research aiming to raise osteosarcoma survival has stalled over the past 30 years (4). Therefore, it is critical to determine reliable predictors related to osteosarcoma metastasis and prognosis and to make available novel targets for therapy and prognosis prediction. However, due to the complex molecular mechanisms of osteosarcoma, the predictive capability of traditional clinical information is limited. Thus, it is crucial to find novel prognostic biomarkers to predict survival and metastases more accurately in osteosarcoma. Although biomarkers such as FAT10 and MYC have been associated with osteosarcoma in recent studies, their reliability requires further investigation (5, 6).

G protein subunit gamma 12 (GNG12) is a protein-coding gene located on chromosome 1, first reported in 1995 (7). In the GeneCards database (www.genecards.org), related pathways include "Translation Translation regulation by Alpha-1 adrenergic receptors" and "Sweet Taste Signaling". Gene Ontology (GO) annotations related to this gene include obsolete signal transducer activity and phosphate ion binding. Previous research (8) suggested that GNG12 knockdown in BV-2 cells increased nitric oxide levels and tumor necrosis factor alpha (TNF-α) expression in response to lipopolysaccharide (LPS) stimulation, indicating that GNG12 was an essential negative regulator of inflammation. Transforming growth factor beta (TGF-β)-induced chondrogenic differentiation of mesenchymal stem cells is promoted when C-type natriuretic peptide/natriuretic peptide receptor-B reduces GNG12 expression (9). The first association of GNG12 with cancer was a study showing that low GNG12 expression increases the proliferation of endometrial cancer (10). Subsequently, HOXA13 upregulation was found to be a promoter of lung squamous cancer progression through reducing GNG12 expression (11). Although these studies suggest an important role for GNG12 in cancer progression, we currently know little about the underlying mechanisms and function of this protein in osteosarcoma progression and immunology.

This study thus aimed to determine the role of GNG12 in patients with osteosarcoma. We obtained two test cohort from the Gene Expression Omnibus (GEO) database and the Therapeutically Applicable Research to Generate Effective Treatments (TARGET) database. To clarify biological function, we compared expression matrices of high and low GNG12-expression groups to identify potential GNG12-related genes. These genes were screened using functional enrichment analyses, gene set enrichment analysis (GSEA) regulation networks, immune infiltration analysis, and pan-cancer analysis. We also collected osteosarcoma samples to evaluate GNG12 predictive ability on survival and prognosis, using immunohistochemistry, histochemistry score (H-Score) analysis, and receiver operating characteristic (ROC) analysis.

Our results demonstrated that low GNG12 expression is a potential biomarker of osteosarcoma, linked to poor prognosis. GSEA revealed that GNG12 expression was associated with "extracellular matrix organization", "core matrisome", "cytoplasmic ribosomal proteins", "cell adhesion molecules cams", "class A 1 rhodopsin-like receptors", "GPCR ligand binding", and "diseases of metabolism", and "Matrisome". Immune infiltration analysis demonstrated that GNG12 regulated the proportions of macrophages (M0, M1, and M2) and mast cells to influence the tumor microenvironment. Finally, we confirmed the feasibility of GNG12 as a biomarker in our collected osteosarcoma samples.

2 MATERIALS AND METHODS

2.1 Patients and Identification of Differentially Expressed Genes

The GEO (http://www.ncbi.nlm.nih.gov/geo) database is a free public gene-expression data repository containing microarray and high-throughput sequencing data. Gene-expression datasets from GSE42352 (12, 13), including 103 osteosarcoma cases and 15 normal controls, were collected from GEO as the test cohort. Using the median value of GNG12 expression as the cutoff, the 103 patients were divided into high (n = 52) and low (n = 51) GNG12 mRNA expression groups. Significant differentially expressed genes (DEGs) between high and low GNG12-expression groups were screened with the limma package (http://www.bioconductor.org/packages/release/bioc/html/

limma.html) in R version 3.6.3 (http://www.R-project.org/) (14). Genes were considered differentially expressed with an adjusted $p < 0.5$ and |log fold change| (|logFC|) ≥ 1. Heat maps were constructed using R package "pheatmap", version 1.0.12 (https://cran.rproject.org/web/packages/pheatmap/index.html), and volcano plots were generated with "ggplot2" version 3.3.3 (https://cran.r-project.org/web/packages/ggplot2/index.html). In addition, gene expression profiles and clinical data of osteosarcoma cases were collected from TARGET (https://ocg.cancer.gov/programs/target). The TARGET cohort (n = 101) were divided into high/low groups using the same cutoff as the GEO cohort (high, 51 cases; low, 50 cases). The same method as described above was used to determine DEGs between TARGET high/low groups. Common DEGs between the GSE42352 and TARGET datasets were represented with a Venn diagram made in ggplot2.

The Second Affiliated Hospital of Nanchang University provided 78 osteosarcoma specimens from January 2012 to December 2016 as an external validation cohort. Samples were provided as formalin fixed paraffin-embedded blocks.

This research was approved by the Ethics Committee of The Second Affiliated Hospital of Nanchang University [Review (2020) No. (086)]. All participants provided informed consent.

2.2 Functional Enrichment Analysis

Functional enrichment analyses (Gene Ontology, GO; https://www.geneontology.org and Kyoto Encyclopedia of Genes and Genomes, KEGG; https://www.genome.jp/kegg/) were performed on DEGs between high and low GNG12-expression groups in the test cohort, using clusterProfiler version 3.14.3 (http://www.bioconductor.org/packages/release/bioc/html/clusterProfiler.html). The results were visualized with the "ggplot2" package (https://cran.r-project.org/web/packages/ggplot2/index.html). Xiantao Academic online (https://www.xiantao.love) was used to generate a diagram of the functional enrichment network analysis.

Significant differences in function and pathways between high/low GNG12-expression groups were determined using GSEA in clusterProfiler and Xiantao Academic online. For each analysis, gene set permutations were performed 1,000 times to obtain a normalized enrichment score (NES). Enrichment was considered significant with adjusted $p < 0.05$, false discovery rate (FDR) $q < 0.25$, and $|NES| > 1$. The selected reference gene set was c2.cp.v7.2.symbols.gmt (Curated), and results were visualized in ggplot2.

2.3 Protein–Protein Interaction Network Construction and Hub-Gene Extraction

A protein–protein interaction (PPI) network of DEGs was constructed using Metascape online tools (https://metascape.org) with the following parameters: min network size = 3 and max network size = 500. Crucial proteins in this PPI network were screened using the Molecular Complex Detection (MCODE, http://apps.cytoscape.org/apps/mcode), a plug-in of Cytoscape version 3.7.2 (https://cytoscape.org/).

2.4 Immune Infiltration Analysis

CIBERSORT (https://cibersort.stanford.edu/) is an algorithm developed to characterize the cellular composition of complex tissues through gene expression profiles compared with a signature matrix (LM22). LM22 comprises 547 genes that define 22 immunization cell subtypes. This analysis was used to calculate infiltration abundance of 22 immune cells (T cells, B cells, plasma cells, natural killer cells, myeloid subgroups) in 103 osteosarcoma samples across high and low GNG12-expression groups. We also analyzed any correlations between the two GNG12 groups in terms of expression distribution among the 22 infiltrating immune cells; the correlation heat map was then plotted. Red represents a positive correlation, and blue represents a negative correlation, with darker colors and values closer to 1 indicating stronger correlations.

2.5 GNG12 Expression Analysis

The UCSC XENA platform (https://xenabrowser.net/datapages/) is a pan-cancer HTSeq-TPM database of TCGA and GTEx, processed uniformly by Toil. Based on XENA data, differential GNG12 mRNA expression between tumor and normal tissues was determined in R and visualized with ggplot2. Spearman's correlations were calculated between GNG12 expression in the TARGET cohort with the expression of nine DEGs (GREM1, CAV1, PTGDS, PRB2, PRB1, NDUFB9, AMBN, FAT3, and IBSP) common across GSE42352 and TARGET datasets. Again, the analysis was performed in R and the results visualized in ggplot2.

2.5.1 Construction of Competing Endogenous RNA Network

A differential long noncoding RNA (lncRNA) expression matrix was obtained from TARGET using the limma package. The miRcode database (http://www.mircode.org/) was used to predict a series of highly conserved microRNAs (miRNAs) linked to differentially expressed lncRNA. The miRNA target genes were predicted using miRDB (http://mirdb.org/), miRTarBase (http://miRTarBase.cuhk.edu.cn/), and TargetScan (http://www.targetscan.org/mamm_31/) databases. Predicted mRNAs were associated with the six GNG12-related genes (GREM1, CAV1, NDUFB9, AMBN, FAT3, and IBSP) to establish a competing endogenous RNA (ceRNA) network.

2.6 Survival Analysis

Kaplan–Meier (KM) analyses of the TARGET database were performed using R packages survival (https://www.rdocumentation.org/packages/survival/versions/2.42-3) and survminer (https://cran.rstudio.com/web/packages/survminer/index.html), to determine whether GNG12 expression accurately predicted overall survival time (OS) and progression-free survival (PFS). The timeROC package (https://cran.r-project.org/web/packages/timeROC/index.html) was used to analyze 1-, 3-, and 5-year survival prognosis of GNG12-related lncRNAs, miRNAs, and genes. All outcomes were visualized in ggplot2.

2.7 Assessing Diagnostic Performance

An ROC curve was generated using the pROC package (https://cran.r-project.org/web/packages/pROC/). The ordinate was drawn with the true positive rate (sensitivity), and the abscissa was the false positive rate (1 − specificity). This analysis determined whether GNG12 expression can distinguish between 15 standard samples and 103 osteosarcoma samples. Also determined was the cutoff value that produces the highest likelihood ratio for assessing the recognition threshold of GNG12 as a biomarker for distinguishing osteosarcoma from normal tissue.

2.8 Immunohistochemical Staining and Evaluation

To further verify the suitability of GNG12 expression for predicting survival, immunohistochemistry was performed on paraffin sections following the standard protocol (GNG12, Ab204757, 1:100). All slides were observed and photographed under a XSP-C204 microscope (CIC). GNG12 expression was assessed using the H-score.

2.9 Validation of GNG12 as a Prognostic Predictor of Osteosarcoma

Known survival outcomes of osteosarcoma patients with high and low H-scores were subjected to KM analysis using the R package "survival" and visualized in "surviminer". The accuracy of GNG12 expression in predicting survival prognosis (1, 3, and 5 years) was verified with timeROC and visualized in ggplot2. An AUC >0.5 directly reflects the prognostic value of the biomarker. Additionally, an AUC closer to 1 and to the (0, 1) point indicates greater authenticity of the prognostic prediction.

2.10 Statistical Analysis

Statistics were performed in Microsoft Excel and R version 3.6.3. The log-rank test was used to perform the KM survival analysis. Continuous variables that violated the normality assumption according to the Shapiro–Wilk normality test were analyzed with the Wilcoxon rank sum test. Categorical variables were analyzed with chi-square tests. Significance was set at $p < 0.05$ (ns, $p > 0.05$; $^{*}p < 0.05$; $^{**}p < 0.01$; $^{***}p < 0.001$).

3 RESULTS

3.1 Identification of DEGs

GNG12 expression was significantly different between the standard samples (n = 15) and osteosarcoma samples (n = 103) (**Figure 1A**). After screening for DEGs between high and low GNG12-expression groups (**Figure 1B**), we found 210 coexpressed genes (165 upregulated and 45 downregulated, **Supplementary Table 1**) that we have visualized in a volcano plot (**Figure 1D**) and a heat map (**Figure 1E**). Using the same method to divide the TARGET cohort (n = 101) into high/low GNG12-expression groups (**Figure 1C**), we obtained 347 DEGs (178 upregulated and 169 downregulated, **Supplementary Table 2** and **Figures 1F, G**). We then screened out nine common DEGs (six upregulated and three downregulated) across the two DEG sets (**Figures 1H, I**).

3.2 Functional Enrichment Analysis and GSEA

The GO and KEGG enrichment results for the GEO cohort (**Figures 2A, B**) indicated that the following terms were enriched: "protein targeting to endoplasmic reticulum (ER)", "establishment of protein localization to ER", "focal adhesion", and "cell adhesion molecule binding" (**Figure 2C**). For the TARGET cohort, enriched terms were "ossification", "cartilage development", "integrin binding", "PI3K-Akt signaling pathway", and "Focal adhesion" (**Figure 3**).

We selected msigdb.v7.0.entrez.gmt as the reference gene set for our GSEA. For the GEO cohort, DEGs were involved in "extracellular matrix organization" from the Reactome database, "core matrisome" from NABA, "cytoplasmic ribosomal proteins" from WP, and "cell adhesion molecules cams" from KEGG (**Figure 4A**). For the TARGET cohort, DEGs were involved in "class A 1 rhodopsin like receptors", "GPCR ligand binding", and "diseases of metabolism" from the Reactome database, and "Matrisome" from NABA (**Figure 4B**).

3.3 Construction of PPI Networks and Hub-Gene Screening

Based on the Metascape online tool, we constructed two PPI networks of DEGs from the GEO and TARGET cohorts (**Figures 5A, C**). We then screened hub-gene clusters using the MCODE clustering algorithm. In the GEO cohort, screened hub genes were linked in the following networks: MCODE_1 (cytoplasmic translation, cytosolic ribosome, and ribosome; EIF3A, RPL23, RPL14, RPL7, RPL27A, RPS28, RPLP1, RPS3A, RPL10A, and RPN2), MCODE_2 (NLS-bearing protein import into the nucleus, protein import into the nucleus, and import into the nucleus; KPNA2, RGPD6, RGPD3, RGPD8, SUMO2, ACTR3, WIPF1, ARPC5, and GMFG), and MCODE_3 (ER, growth factor activity, and extracellular matrix structural constituent; VCAN, CCN1, AMBN, CDH2, VGF, and IL6; **Figure 5B**). Hub genes of the TARGET cohort were involved in more networks. These were MCODE_1 (extracellular matrix structural constituent conferring tensile strength, collagen trimer, and protein digestion and absorption; COL8A2, COL9A1, COL11A1, COL11A2, COL15A1, COL22A1, COL24A1, P4HA3, COL14A1, COL27A1, COL2A1, COL3A1, COL6A1, and COL6A2), MCODE_2 (*in utero* embryonic development, peptidyl-tyrosine phosphorylation, and peptidyl-tyrosine modification; FGFR4, ISLR, FGF2, IGF2, TGFB3, CAV1, TP53, ACTA2, ALDH1A1, PYGM, GPI, GFPT2, and H2AW), MCODE_3 (G-protein beta-subunit binding, neuropeptide hormone activity, and heterotrimeric G-protein complex; GNG12, GAL, CORT, NPB, GNG4, GNGT2, HCRT, HRH1, PTGFR, ADRA1D, and TBXA2R), MCODE_4 (ER lumen, biomineral tissue development, and biomineralization; MELTF, PENK, MEPE, SPP2, MOTUM, DMP1, FBN1, AMBN, AMELX, and GPC3), MCODE_5 (anchored component of membrane; NTM, ALPL, NTNG1, CD109, and LY6K), MCODE_6 (lamellar

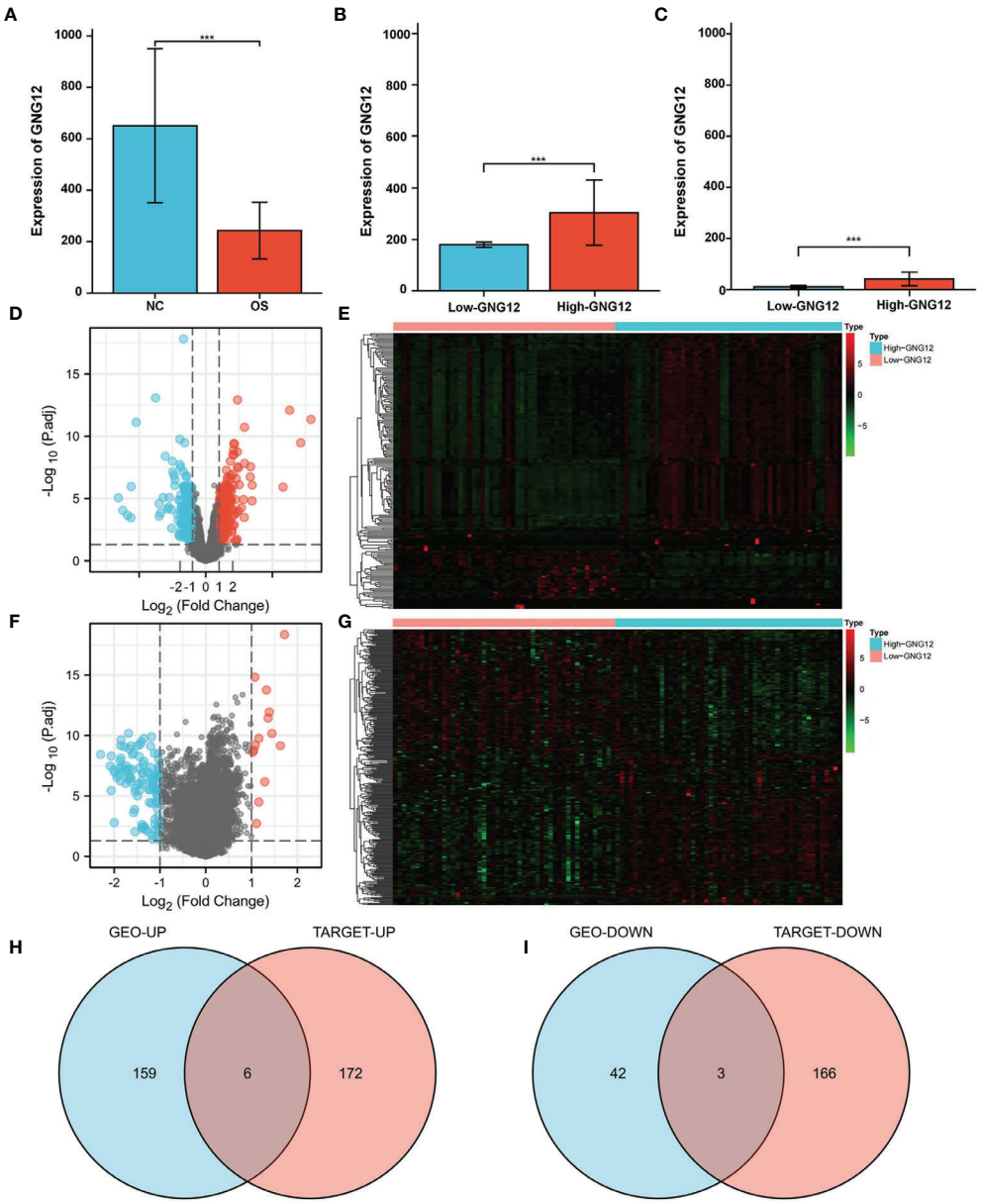

FIGURE 1 | GNG12 and coexpressed gene difference analysis. **(A)** Compared with normal tissues, GNG12 is significantly lower expressed in tumor tissues. **(B)** In GSE42352 cohort, the expression level of GNG12 in low/high GNG12-expression groups. **(C)** In TARGET cohort, the expression level of GNG12 in low/high GNG12 expression groups. **(D)** The median expression of GNG12 in 103 osteosarcoma samples in the GSE42352 data set was divided into high and low expression groups, and the significantly different genes between the two groups were displayed in the form of a volcano graph. **(E)** A heat map showing the significantly different genes between the two groups of the GSE42352 data set. **(F)** GNG12 was used in the median expression values of 101 osteosarcoma samples in the TARGET data set divided into high and low expression groups, showing the significant difference genes between the two groups in the form of volcano maps. **(G)** The TARGET data set shows the significant difference genes between the two groups in the form of a heat map. **(H)** Venn diagram of the intersection of upregulated DEGs in the GEO and TARGET cohort. **(I)** Venn diagram of the intersection of downregulated DEGs in the GEO and TARGET cohort. ***$p < 0.001$.

body, mutivesicular body and respiratory gaseous exchange by respiratory system; SFTPB, SFTPC, SFTPA1, and SFTPA2), and MCODE_7 (Wnt signaling pathway; CCND2, TCF7L2, and FOSL1; **Figure 5D**).

3.4 Correlation Between GNG12 Expression and Immune Infiltration

For further immune infiltration analysis, we used CIBERSORT package and LM22 algorithm to calculate the infiltration

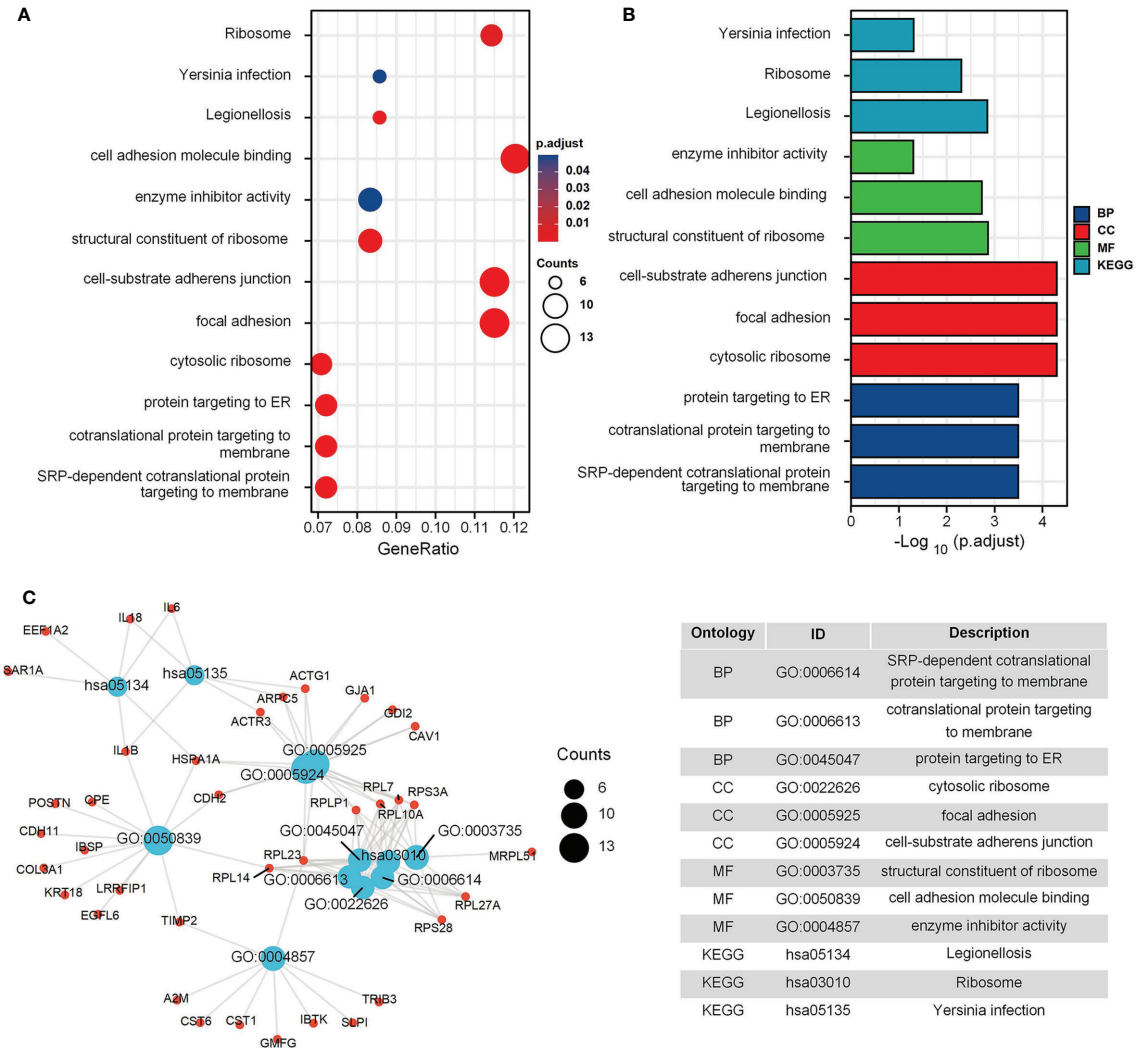

Ontology	ID	Description
BP	GO:0006614	SRP-dependent cotranslational protein targeting to membrane
BP	GO:0006613	cotranslational protein targeting to membrane
BP	GO:0045047	protein targeting to ER
CC	GO:0022626	cytosolic ribosome
CC	GO:0005925	focal adhesion
CC	GO:0005924	cell-substrate adherens junction
MF	GO:0003735	structural constituent of ribosome
MF	GO:0050839	cell adhesion molecule binding
MF	GO:0004857	enzyme inhibitor activity
KEGG	hsa05134	Legionellosis
KEGG	hsa03010	Ribosome
KEGG	hsa05135	Yersinia infection

FIGURE 2 | GO and KEGG enrichment analysis in GEO cohort. **(A)** The bubble graph of clusterProfiler package for GO and KEGG enrichment analysis; the bubble size represents the number of gene enrichment, and color represents significance in GSE42352 data set. **(B)** The bar graph of clusterProfiler package for GO and KEGG enrichment analysis; length represents significance in GSE42352 data set. **(C)** A function enrichment network in GSE42352 data set.

abundance of 22 kinds of immune cells between high/low expression level of GNG12 groups in test and validation cohort, including different B cells, T cells, natural killer cells, plasma cells, and different myeloid subsets. The results were visualized as two violin maps (**Figures 6A, B**) and two correlation heat maps (**Figures 6C, D**) to reveal the differences in the expression of immune cells between groups.

3.5 Expression Analysis of GNG12-Related Genes

Evaluation of differential GNG12 expression in pan-cancer revealed that GNG12 was downregulated in 12 tumor types (i.e., ACC, BLCA, BRCA, CESC, KIRC, LAML, OV, PCPG, PRAD, TGCT, UCEC, and UCS) and upregulated in 11 (CHOL, COAD, DLBC, ESCA, GBM, LGG, LIHC, PAAD, READ, STAD, and THYM; **Figure 7A**). When we used a gene-expression heat map to examine the nine common DEGs across GEO and TARGET cohorts, we found that GREM1 and CAV1 expression were positively correlated with GNG12 expression in the TARGET cohort. Additionally, NDUFB9, AMBN, FAT3, and IBSP expression were negatively correlated (**Figure 7B**). We then generated six scatterplots of correlations between the expression of these six genes and of GNG12 (**Figures 7C–H**).

3.6 Competitive Endogenous RNA Network

Using limma, we obtained 22 differentially expressed lncRNAs (DELs) from the TARGET database and visualized them on a

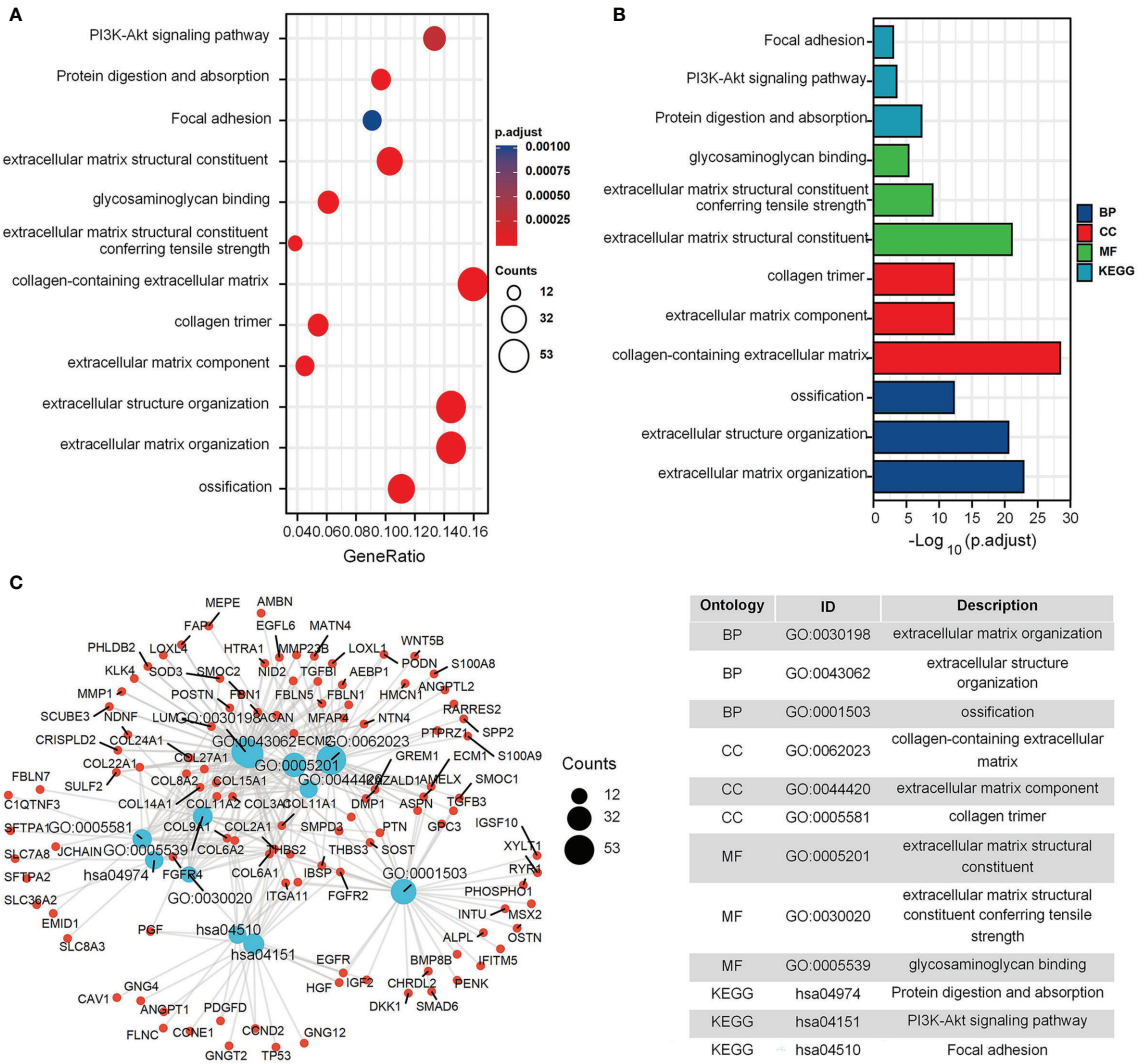

Ontology	ID	Description
BP	GO:0030198	extracellular matrix organization
BP	GO:0043062	extracellular structure organization
BP	GO:0001503	ossification
CC	GO:0062023	collagen-containing extracellular matrix
CC	GO:0044420	extracellular matrix component
CC	GO:0005581	collagen trimer
MF	GO:0005201	extracellular matrix structural constituent
MF	GO:0030020	extracellular matrix structural constituent conferring tensile strength
MF	GO:0005539	glycosaminoglycan binding
KEGG	hsa04974	Protein digestion and absorption
KEGG	hsa04151	PI3K-Akt signaling pathway
KEGG	hsa04510	Focal adhesion

FIGURE 3 | GO and KEGG enrichment analysis in TARGET cohort. **(A)** The bubble graph of clusterProfiler package for GO and KEGG enrichment analysis; the bubble size represents the number of gene enrichment, and color represents significance in TARGET data set. **(B)** The bar graph of clusterProfiler package for GO and KEGG enrichment analysis; length represents significance in TARGET data set. **(C)** A function enrichment network in TARGET data set.

heat map (**Figure 8A**). We then used the miRcode website to predict miRNAs that were highly conserved with DELs. Furthermore, we identified mRNAs targeted by the miRNAs through a series of databases and then constructed a ceRNA network with DEGs (**Figure 8B**).

3.7 Survival Analysis of GNG12 in TARGET Cohort

The results of our KM analysis indicated that OS and PFS differed significantly between low and high GNG-expression groups (**Figures 8C, F**). In addition, the ceRNA network revealed that low HOTTIP and GNG12 expression led to high risk. Elevated hsa-miR-27a-3p expression also resulted in high risk (**Figures 8D, E**). Through time-dependent ROC curves, we found that GNG12 was a reliable predictor of patient prognosis (**Figure 8G**).

We used an ROC curve to analyze whether GNG12 expression could distinguish between 15 normal samples and 103 tumor samples from the GEO dataset. We found an AUC of 0.920, indicating that GNG12 expression was an excellent biomarker for distinguishing osteosarcoma from normal tissue. (**Figure 8H**).

3.8 Validating Prognostic Value of GNG12 Expression in Osteosarcoma

We used 78 patients with osteosarcoma as a validation cohort to confirm the prognostic reliability of GNG12 (**Table 1** and **Supplementary Table S3**). GNG12 expression levels (high *vs.*

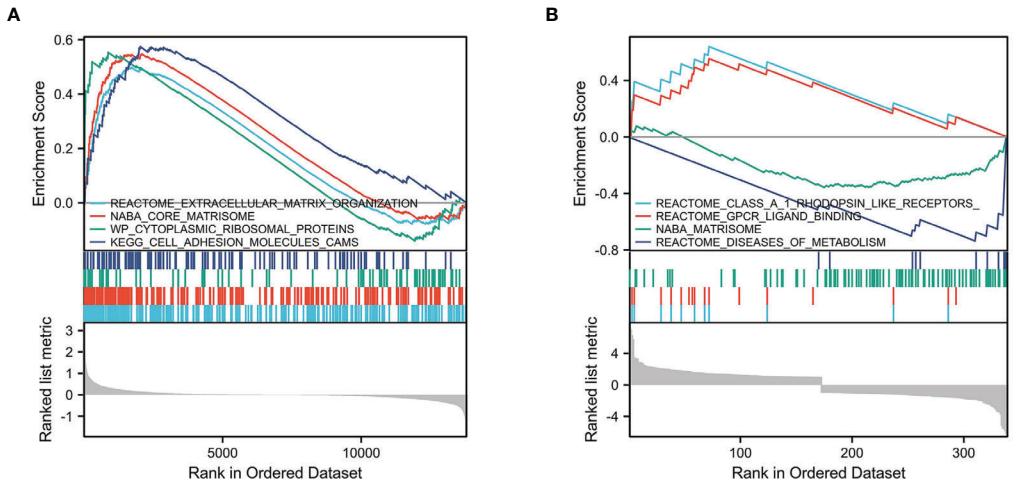

FIGURE 4 | GSEA enrichment analysis. **(A)** GSEA enrichment analysis in GEO cohort. **(B)** GSEA enrichment analysis in TARGET cohort.

low) of these patients were confirmed using immunohistochemistry (IHC) (**Figures 9A, B**). The results of KM analysis showed that patients with low GNG12 expression tend to have poor survival prognosis (**Figure 9C**). Analysis of time-dependent ROC curves revealed that 1-/3-/5-year AUCs were 0.961, 0.826, and 0.808 (**Figure 9F**). In addition, GNG12 expression was lower in metastatic than in non-metastatic osteosarcoma (**Figure 9D**); patients with metastatic osteosarcoma have a poor survival prognosis (**Figure 9E**).

4 DISCUSSION

The transducer and transmembrane-signal regulator GNG12 plays an important role in cancer progression through enhancing cell proliferation (15, 16). It is indispensable for guanosine triphosphatase (GTPase) activity, which functions in GTP-to-GDP catalysis (17). GTPase is associated with proliferation, invasion, and migration of tumors in multiple cancers, including osteosarcoma (18, 19). Despite this link, few studies have explored the role of GNG12 in osteosarcoma. Therefore, in this study, we hypothesized that GNG12 expression may influence osteosarcoma progression. Furthermore, GNG12 may have prognostic and therapeutic value for this cancer.

Analysis of data from GEO indicated that GNG12 expression was significantly downregulated in osteosarcoma tissues compared with normal samples. This reduced expression was positively correlated with poor prognosis in the TARGET cohort. Our functional analyses corroborated previous studies, showing that GNG12 was involved in ossification (20–22), protein targeting to ER (23, 24), extracellular-related terms (25, 26), focal adhesion (25, 27), PI3K-Akt signaling pathway (28, 29), GPCR ligand binding (30), and the matrisome. Through PPI networks, we identified the ER lumen as the location of hub gene clusters present in both GEO and TARGET cohorts. Regulating ER function plays a major role in the treatment of osteosarcoma (23, 31). Specifically, H_2S-releasing doxorubicins caused misfolding of ER-related proteins to enhance ER-dependent apoptosis, which is effective against doxorubicin-resistant osteosarcoma *in vitro* (23). Additionally, lexibulin induces autophagy and apoptosis of osteosarcoma *in vitro* through triggering mutually enhanced reactive oxygen species and ER stress, suggesting that it could be an effective drug for osteosarcoma therapy (31). Taken together, our research and previous studies provided insight on GNG12's role in cancer pathogenesis and demonstrated that the protein is a potential biomarker of osteosarcoma.

Integrated landscapes depicting the osteosarcoma microenvironment may help explain how the cancer responds to immunotherapy and help the development of new treatment strategies (32, 33). Our immune infiltration analysis of the GEO cohort showed that the high and low GNG12-expression groups differed significantly in macrophages (M0, M1, and M2), activated CD4+ memory T cells, mast cells, activated dendritic cells, and eosinophils. The same analysis on the TARGET cohort revealed that the three macrophage subtypes and mast cells were significantly different. Combining the two results indicated that macrophages and mast cells play a crucial role in the immune microenvironment of osteosarcoma. Moreover, osteosarcoma occurrence and development are probably related to inflammation and metabolic pathways. Thus, novel osteosarcoma therapy could potentially target macrophages and mast cells to improve their distribution in patients (34, 35). Findings from a mouse tail metastasis model indicated that M2 macrophages enhanced metastasis of osteosarcoma cells (K7M2 WT), thus identifying M2-polarized tumor-associated macrophages (TAMs) as a therapeutic target. The same study also found that all-trans retinoic acid (ATRA) inhibited M2 polarization of TAMs *via* downregulating MMP12 expression, thereby limiting osteosarcoma (36). Our study thus examined the correlation between GNG12

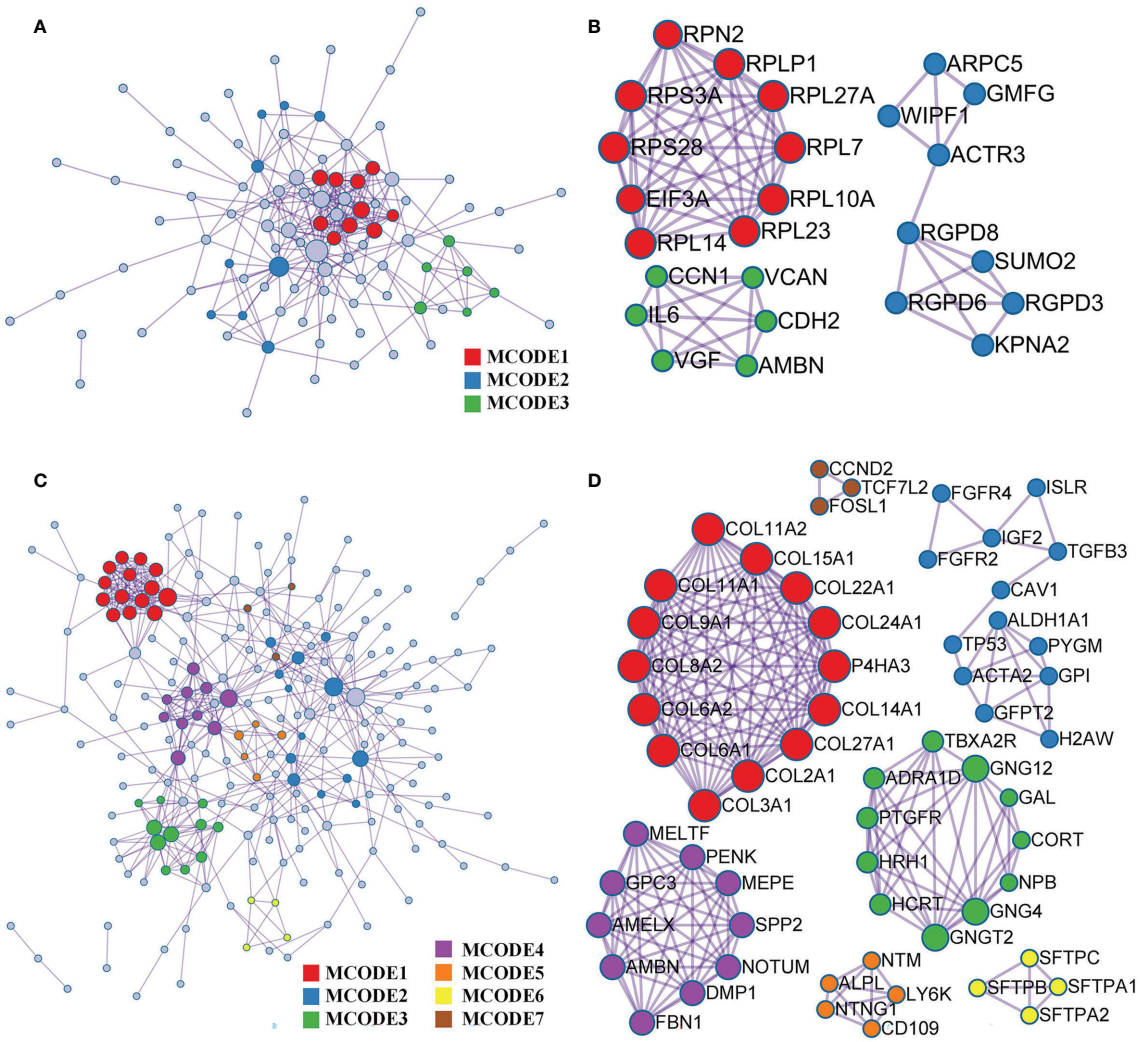

FIGURE 5 | PPI and hub gene clusters network construction. **(A)** A PPI network from GSE42352 data set. **(B)** Three hub gene clusters obtained by the MCODE clustering algorithm from GSE42352 data set. **(C)** A PPI network from TARGET data set. **(D)** Seven hub gene clusters obtained by the MCODE clustering algorithm from TARGET data set.

expression and MMP12. We found that MMP12 expression is negatively correlated with GNG12 expression, and high MMP12 expression can also predict poor osteosarcoma PFS (**Supplementary Figure S1A, B**). Therefore, GNG12 may inhibit M2 polarization of TAMs, which negatively regulates MMP12 expression and thus suppresses osteosarcoma metastasis.

Most studies have shown that ceRNA plays an important role in osteosarcoma occurrence and development (37, 38). We constructed a ceRNA network based on TARGET data and found that lncRNA HOTTIP (a low risk factor) can function as a ceRNA, decoying miR-27a-3p (a high risk factor) to promote GNG12-mediated metastasis. Targeting HOTTIP may therefore prove to be beneficial for osteosarcoma treatment (39). Liu et al. reported that miR-27a-3p were upregulated in osteosarcoma to promote the proliferation and invasion of osteosarcoma cells *via* inhibiting expression of TET1 (40). Although these results suggest that HOTTIP may regulate GNG12 through ceRNA and is involved in osteosarcoma progress, further experimental studies are needed to confirm these conclusions. Nevertheless, HOTTIP, miR-27a-3p, and GNG12 are all potential therapeutic targets for osteosarcoma.

This study has several limitations. First, the sample size of our healthy controls was much smaller than the sample size of patients with osteosarcoma. Future studies would benefit from balancing the number of participants in each group. Second, our outcomes were validated in a set of 78 patients with osteosarcoma, using an H-score to evaluate GNG12 expression in osteosarcoma tissue. Although the results confirmed that patients with low GNG12 expression had poor prognosis, this was a retrospective analysis. Thus, future research should employ

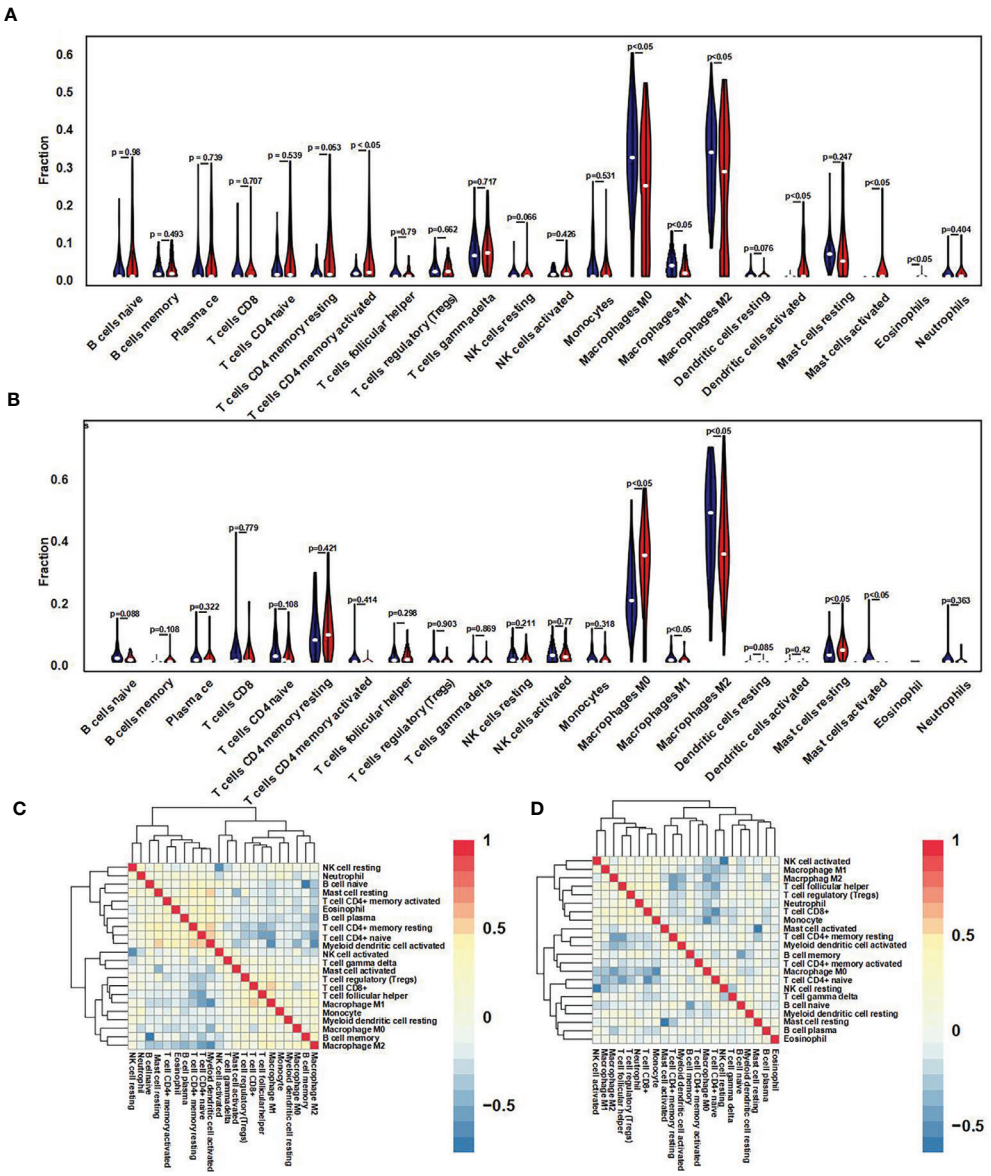

FIGURE 6 | Immune cell infiltration difference and correlation analysis. **(A)** Using the CIBERSORT package, the LM22 algorithm was used to calculate the difference in expression of 22 immune cells in the GNG12 high and low expression groups in the 103 osteosarcoma samples in the GEO set. Blue represents the low expression group, and red represents the high expression group. **(B)** Violin diagram of the difference in expression of 22 immune cells infiltration between the high and low expression groups of GNG12 in 101 osteosarcoma samples in the TARGET set. Blue represents the low expression group; red represents the high expression group. **(C)** Correlation heat map of 22 immune cells in the GEO set. **(D)** Correlation heat map of 22 immune cells in the TARGET set. The *p*-value represents the significance of the difference; $p < 0.05$ is considered a significant difference.

a prospective methodology to avoid analysis bias. Finally, we did not verify our findings using *in vitro* or *in vivo* experiments, meaning that the exact mechanisms of GNG12 involvement in osteosarcoma remain unclear. This is an important topic for further investigation. Therefore, we highlight several areas in which further work is needed to deepen our understanding. First, as the response of GNG12, it would be interesting to examine the basic expression of these predicted DEGs and hub genes with Western blot, quantitative PCR (qPCR), IHC, immunofluorescence (IF) assays, and so on. Second, to clarify the function of GNG12, DEGs, and hub genes in osteosarcoma, a clean loss-of-function and gain-on-function study with tissue- and cell-type specificities remains warranted.

In conclusion, GNG12 mRNA and protein expression were downregulated in osteosarcoma, a change that was related to poor prognosis. We found that GNG12 may promote

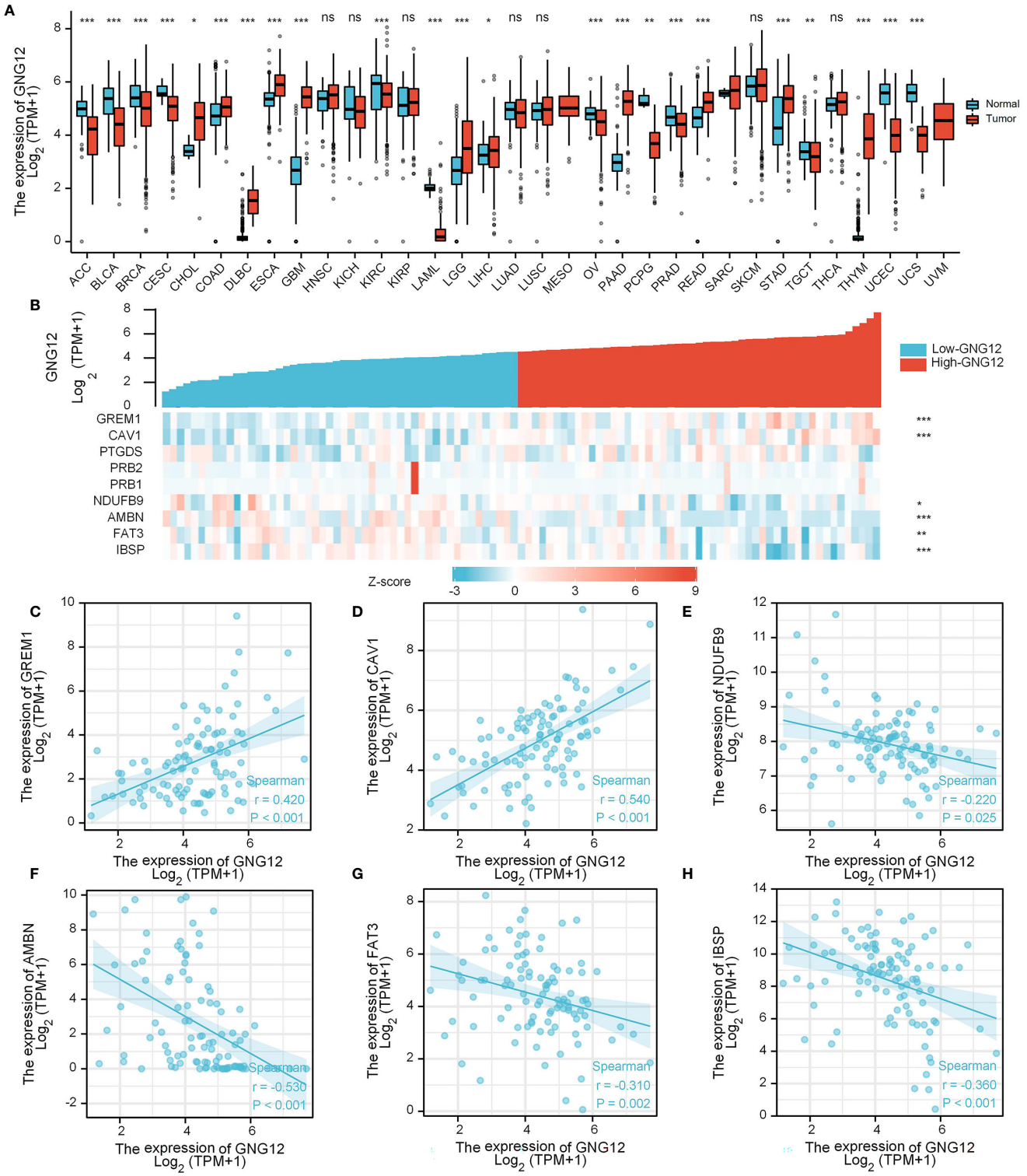

FIGURE 7 | Expression analysis of GNG12-related genes. **(A)** Differential expression of GNG12 in pan-cancer. **(B)** A gene expression-related heat map of the nine common DEGs between GEO and TARGET sets. **(C–H)** Scatter plots of the expression correlation between GREM1, CAV1, NDUFB9, AMBN, FAT3, and IBSP and GNG12. Significance was set at $p < 0.05$ (ns, $p < 0.05$; *$p < 0.05$; **$p < 0.01$; ***$p < 0.001$).

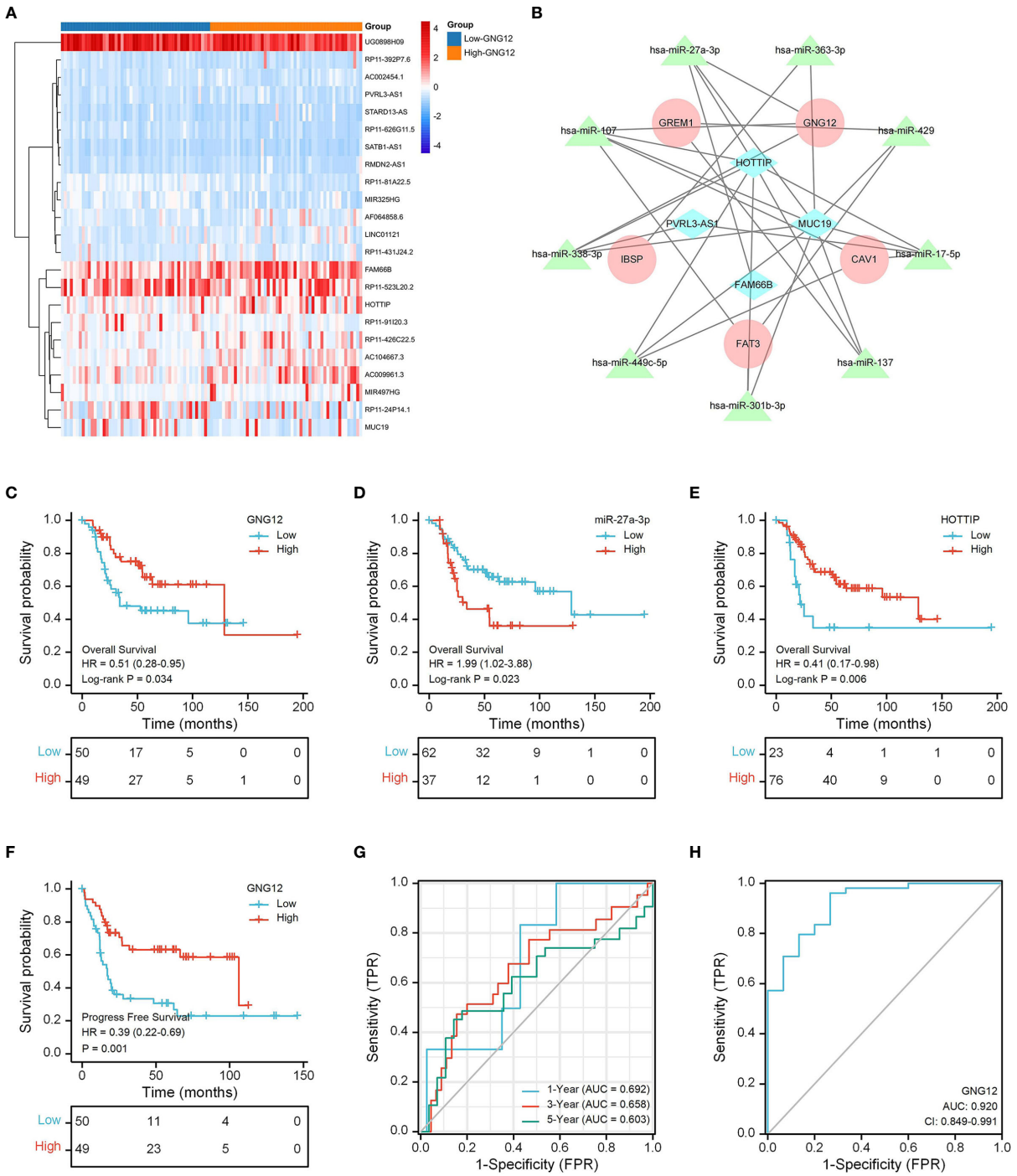

FIGURE 8 | GNG12-related ceRNA network construction and survival analysis. **(A)** The TARGET data set shows the significant difference lncRNAs between the two groups in the form of a heat map. **(B)** A ceRNA network: blue diamond, lncRNAs; green triangle, miRNAs; red round, mRNAs. **(C)** The effect of low GNG12 expression on the prognosis of osteosarcoma overall survival (OS) is statistically significant. **(D)** The effect of high miR-27a-3p expression on the prognosis of osteosarcoma overall survival (OS) is statistically significant. **(E)** The effect of low HOTTIP expression on the prognosis of osteosarcoma overall survival (OS) is statistically significant. **(F)** The effect of low GNG12 expression on the prognosis of osteosarcoma progress-free survival (PFS) is statistically significant. **(G)** Time-dependent ROC curves, 1 year (AUC = 0.692), 3 years (AUC = 0.658), and 5 years (AUC = 0.603). **(H)** The area under the ROC curve (AUC) in the GEO set assesses the performance for distinguishing osteosarcoma from normal tissue of GNG12 (AUC = 0.92).

TABLE 1 | Baseline clinical characteristics of validation cohort.

Characteristic	Low GNG12	High GNG12	*p*-value
N	39	39	
Gender, n (%)			0.425
Female	12 (15.6%)	16 (20.8%)	
Male	27 (35.1%)	22 (28.6%)	
M/NM, n (%)			0.036
Metastasis	20 (25.6%)	10 (12.8%)	
Non-Metastasis	19 (24.4%)	29 (37.2%)	
Recurrence/non-recurrence, n (%)			0.001
Non-recurrence	16 (20.5%)	31 (39.7%)	
Recurrence	23 (29.5%)	8 (10.3%)	
Survival status, n (%)			<0.001
Alive	15 (19.2%)	33 (42.3%)	
Dead	24 (30.8%)	6 (7.7%)	
Age, median (IQR)	25 (14.5, 32.5)	23 (17.5, 38.5)	0.545
Survival time, median (IQR)	767 (312.5, 2303)	2336 (1,639, 2,557)	<0.001

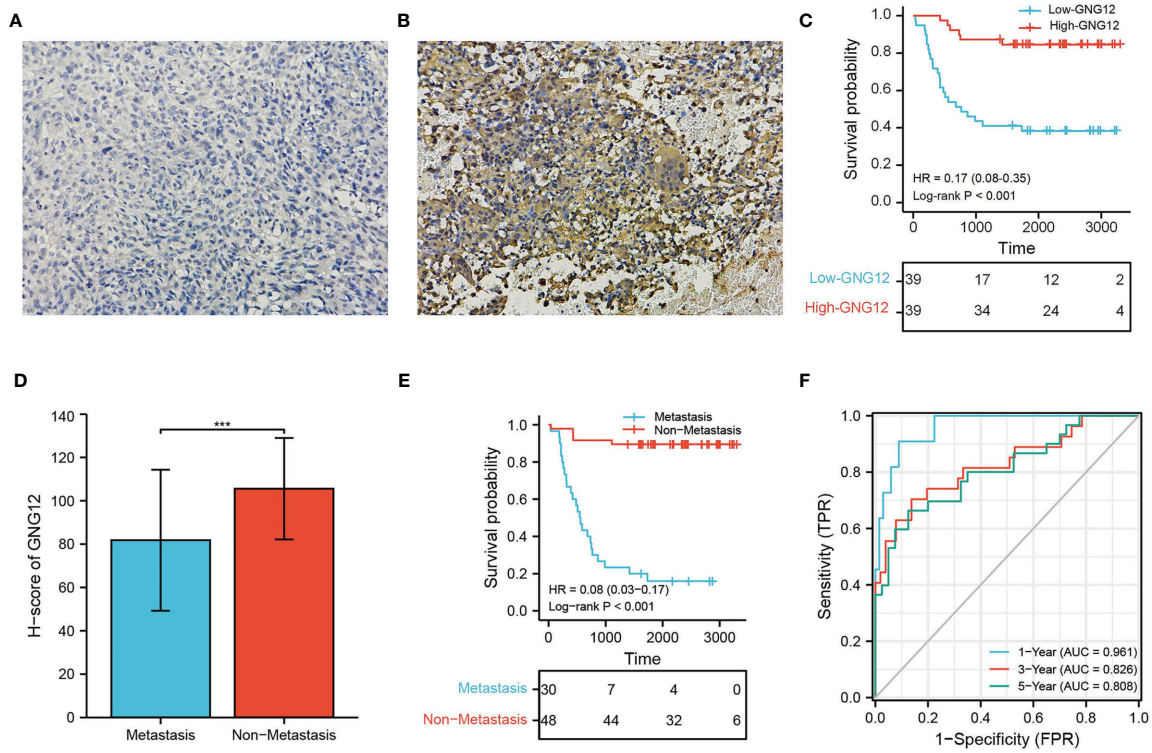

FIGURE 9 | Validation the GNG12 expression and prognostic value of GNG12. **(A, B)** Low/high H-score of GNG12 ICH images. **(C)** The effect of low GNG12 expression on the prognosis of osteosarcoma overall survival (OS) is statistically significant in the validation cohort. **(D)** In the validation cohort, the H-score level of GNG12 between metastasis and non-metastasis groups. **(E)** The effect of metastasis on the prognosis of osteosarcoma overall survival (OS) is statistically significant in the validation cohort. **(F)** Time-dependent ROC curves: 1 year (AUC = 0.961), 3 years (AUC = 0.826), and 5 years (AUC = 0.808). ***p < 0.001.

osteosarcoma through regulating ER function. HOTTIP/miR-27a-3p are candidates for regulating GNG12 expression to inhibit macrophage infiltration and suppress adaptive immunity. We provided important evidence supporting GNG12 as a biomarker for osteosarcoma prognosis and highlighting its potential as a target for immunotherapy.

DATA AVAILABILITY STATEMENT

The datasets analyzed for this study can be found in the TARGET repository (https://target-data.nci.nih.gov/Public/OS/mRNA-seq/) and Gene Expression Omnibus (GEO, https://ftp.ncbi.nlm.nih.gov/geo/series/GSE42nnn/GSE42352/matrix/).

In addition, the validation cohort presented in this study can be found in online repositories. The names of the repository/repositories and accession number(s) can be found in the article/**Supplementary Material**.

ETHICS STATEMENT

The studies involving human participants were reviewed and approved by Ethics Committee of The Second Affiliated Hospital of Nanchang University [Review (2020) No. (086)]. Written informed consent to participate in this study was provided by the participants' legal guardian/next of kin.

AUTHOR CONTRIBUTIONS

JY, ZY, and XC contributed to the conception and design of this study. JY and ZY collected the data sets from the database. JY, TW, JJ, JG, JZ, and TL performed the bioinformatics and statistical analysis. JY, ZY, and AY wrote the first draft of the manuscript. All authors contributed to the article and approved the submitted version.

FUNDING

The present study was supported by the National Natural Science Foundation of China (grant nos. 8166090137 and 8186090165), the National Natural Science Foundation of Jiangxi Province (No. 911084415069), and General Plan of Jiangxi Provincial Health Commission (No. 20195568).

SUPPLEMENTARY MATERIAL

The Supplementary Material for this article can be found online at: https://www.frontiersin.org/articles/10.3389/fimmu.2021.758845/full#supplementary-material

REFERENCES

1. Ritter J, Bielack SS. Osteosarcoma. *Ann Oncol* (2010) 21 Suppl 7:vii320–325. doi: 10.1093/annonc/mdq276
2. Isakoff MS, Bielack SS, Meltzer P, Gorlick R. Osteosarcoma: Current Treatment and a Collaborative Pathway to Success. *J Clin Oncol* (2015) 33 (27):3029–35. doi: 10.1200/JCO.2014.59.4895
3. Rickel K, Fang F, Tao J. Molecular Genetics of Osteosarcoma. *Bone* (2017) 102:69–79. doi: 10.1016/j.bone.2016.10.017
4. Bishop MW, Janeway KA, Gorlick R. Future Directions in the Treatment of Osteosarcoma. *Curr Opin Pediatr* (2016) 28(1):26–33. doi: 10.1097/MOP.0000000000000298
5. Yi X, Deng X, Zhao Y, Deng B, Deng J, Fan H, et al. Ubiquitin-Like Protein FAT10 Promotes Osteosarcoma Growth by Modifying the Ubiquitination and Degradation of YAP1. *Exp Cell Res* (2020) 387(2):111804. doi: 10.1016/j.yexcr.2019.111804
6. Feng W, Dean DC, Hornicek FJ, Spentzos D, Hoffman RM, Shi H, et al. Myc Is a Prognostic Biomarker and Potential Therapeutic Target in Osteosarcoma. *Ther Adv Med Oncol* (2020) 12:1758835920922055. doi: 10.1177/1758835920922055
7. Morishita R, Nakayama H, Isobe T, Matsuda T, Hashimoto Y, Okano T, et al. Primary Structure of a Gamma Subunit of G Protein, Gamma 12, and Its Phosphorylation by Protein Kinase C. *J Biol Chem* (1995) 270(49):29469–75. doi: 10.1074/jbc.270.49.29469
8. Larson KC, Lipko M, Dabrowski M, Draper MP. Gng12 Is a Novel Negative Regulator of LPS-Induced Inflammation in the Microglial Cell Line BV-2. *Inflammation Res* (2010) 59(1):15–22. doi: 10.1007/s00011-009-0062-2
9. Babadagli ME, Tezcan B, Yilmaz ST, Tufan AC. Matrilin-3 as a Putative Effector of C-Type Natriuretic Peptide Signaling During TGF-β Induced Chondrogenic Differentiation of Mesenchymal Stem Cells. *Mol Biol Rep* (2014) 41(9):5549–55. doi: 10.1007/s11033-014-3448-3
10. Orchel J, Witek L, Kimsa M, Strzalka-Mrozik B, Kimsa M, Olejek A, et al. Expression Patterns of Kinin-Dependent Genes in Endometrial Cancer. *Int J Gynecol Cancer* (2012) 22(6):937–44. doi: 10.1097/IGC.0b013e318259d8da
11. Zhang R, Deng Y, Zhang Y, Zhai GQ, He RQ, Hu XH, et al. Upregulation of HOXA13 as a Potential Tumorigenesis and Progression Promoter of LUSC Based on qRT-PCR and Bioinformatics. *Int J Clin Exp Pathol* (2017) 10 (10):10650–65.
12. Kuijjer ML, Peterse EF, van den Akker BE, Briaire-de Bruijn IH, Serra M, Meza-Zepeda LA, et al. IR/IGF1R Signaling as Potential Target for Treatment of High-Grade Osteosarcoma. *BMC Cancer* (2013) 13:245. doi: 10.1186/1471-2407-13-245
13. Kuijjer ML, van den Akker BE, Hilhorst R, Mommersteeg M, Buddingh EP, Serra M, et al. Kinome and mRNA Expression Profiling of High-Grade Osteosarcoma Cell Lines Implies Akt Signaling as Possible Target for Therapy. *BMC Med Genomics* (2014) 7:4. doi: 10.1186/1755-8794-7-4
14. Ritchie ME, Phipson B, Wu D, Hu Y, Law CW, Shi W, et al. Limma Powers Differential Expression Analyses for RNA-Sequencing and Microarray Studies. *Nucleic Acids Res* (2015) 43(7):e47. doi: 10.1093/nar/gkv007
15. Luo C, Zhao S, Dai W, Zheng N, Wang J. Proteomic Analyses Reveal GNG12 Regulates Cell Growth and Casein Synthesis by Activating the Leu-Mediated Mtorc1 Signaling Pathway. *Biochim Biophys Acta Proteins Proteom* (2018) 1866(11):1092–101. doi: 10.1016/j.bbapap.2018.08.013
16. Li J, Jin C, Zou C, Qiao X, Ma P, Hu D, et al. GNG12 Regulates PD-L1 Expression by Activating NF-κb Signaling in Pancreatic Ductal Adenocarcinoma. *FEBS Open Bio* (2020) 10(2):278–87. doi: 10.1002/2211-5463.12784
17. Cai YD, Zhang S, Zhang YH, Pan X, Feng K, Chen L, et al. Identification of the Gene Expression Rules That Define the Subtypes in Glioma. *J Clin Med* (2018) 7(10):350. doi: 10.3390/jcm7100350
18. Lopez-Guerrero AM, Espinosa-Bermejo N, Sanchez-Lopez I, Macartney T, Pascual-Caro C, Orantos-Aguilera Y, et al. RAC1-Dependent ORAI1 Translocation to the Leading Edge Supports Lamellipodia Formation and Directional Persistence. *Sci Rep* (2020) 10(1):6580. doi: 10.1038/s41598-020-63353-5
19. Marko TA, Shamsan GA, Edwards EN, Hazelton PE, Rathe SK, Cornax I, et al. Slit-Robo GTPase-Activating Protein 2 as a Metastasis Suppressor in Osteosarcoma. *Sci Rep* (2016) 6:39059. doi: 10.1038/srep39059
20. Eckardt JJ, Ivins JC, Perry HO, Unni KK. Osteosarcoma Arising in Heterotopic Ossification of Dermatomyositis: Case Report and Review of the Literature. *Cancer* (1981) 48(5):1256–61. doi: 10.1002/1097-0142(19810901)48:5<1256::AID-CNCR2820480534>3.0.CO;2-4
21. Iannaci G, Luise R, Sapere P, Costanzo RM, Rossiello R. Extraskeletal Osteosarcoma: A Very Rare Case Report of Primary Tumor of the Colon-Rectum and Review of the Literature. *Pathol Res Pract* (2013) 209(6):393–6. doi: 10.1016/j.prp.2013.03.010
22. Hoshi M, Takada J, Oebisu N, Nakamura H. Osteosarcoma Arising From the Parapharyngeal Space: A Case Report. *Oncol Lett* (2014) 8(3):1240–2. doi: 10.3892/ol.2014.2265
23. Buondonno I, Gazzano E, Tavanti E, Chegaev K, Kopecka J, Fanelli M, et al. Endoplasmic Reticulum-Targeting Doxorubicin: A New Tool Effective Against Doxorubicin-Resistant Osteosarcoma. *Cell Mol Life Sci* (2019) 76 (3):609–25. doi: 10.1007/s00018-018-2967-9

24. Ward BK, Rea SL, Magno AL, Pedersen B, Brown SJ, Mullin S, et al. The Endoplasmic Reticulum-Associated Protein, OS-9, Behaves as a Lectin in Targeting the Immature Calcium-Sensing Receptor. *J Cell Physiol* (2018) 233 (1):38–56. doi: 10.1002/jcp.25957
25. Chen Y, Pasapera AM, Koretsky AP, Waterman CM. Orientation-Specific Responses to Sustained Uniaxial Stretching in Focal Adhesion Growth and Turnover. *Proc Natl Acad Sci USA* (2013) 110(26):E2352–61. doi: 10.1073/pnas.1221637110
26. Cui J, Dean D, Hornicek FJ, Chen Z, Duan Z. The Role of Extracelluar Matrix in Osteosarcoma Progression and Metastasis. *J Exp Clin Cancer Res* (2020) 39 (1):178. doi: 10.1186/s13046-020-01685-w
27. Hu C, Chen X, Wen J, Gong L, Liu Z, Wang J, et al. Antitumor Effect of Focal Adhesion Kinase Inhibitor PF562271 Against Human Osteosarcoma In Vitro and In Vivo. *Cancer Sci* (2017) 108(7):1347–56. doi: 10.1111/cas.13256
28. Wang R, Liu W, Wang Q, Li G, Wan B, Sun Y, et al. Anti-Osteosarcoma Effect of Hydroxyapatite Nanoparticles Both *In Vitro* and *In Vivo* by Downregulating the FAK/PI3K/Akt Signaling Pathway. *Biomater Sci* (2020) 8(16):4426–37. doi: 10.1039/D0BM00898B
29. Ma Z, Yang J, Yang Y, Wang X, Chen G, Shi A, et al. Rosmarinic Acid Exerts an Anticancer Effect on Osteosarcoma Cells by Inhibiting DJ-1 *via* Regulation of the PTEN-PI3K-Akt Signaling Pathway. *Phytomedicine* (2020) 68:153186. doi: 10.1016/j.phymed.2020.153186
30. Luo J, Sun P, Siwko S, Liu M, Xiao J. The Role of GPCRs in Bone Diseases and Dysfunctions. *Bone Res* (2019) 7:19. doi: 10.1038/s41413-019-0059-6
31. Wang Z, Yin F, Xu J, Zhang T, Wang G, Mao M, et al. CYT997(Lexibulin) Induces Apoptosis and Autophagy Through the Activation of Mutually Reinforced ER Stress and ROS in Osteosarcoma. *J Exp Clin Cancer Res* (2019) 38(1):44. doi: 10.1186/s13046-019-1047-9
32. Zhou Y, Yang D, Yang Q, Lv X, Huang W, Zhou Z, et al. Single-Cell RNA Landscape of Intratumoral Heterogeneity and Immunosuppressive Microenvironment in Advanced Osteosarcoma. *Nat Commun* (2020) 11 (1):6322. doi: 10.1038/s41467-020-20059-6
33. Hong W, Yuan H, Gu Y, Liu M, Ji Y, Huang Z, et al. Immune-Related Prognosis Biomarkers Associated With Osteosarcoma Microenvironment. *Cancer Cell Int* (2020) 20:83. doi: 10.1186/s12935-020-1165-7
34. Zhang C, Zheng JH, Lin ZH, Lv HY, Ye ZM, Chen YP, et al. Profiles of Immune Cell Infiltration and Immune-Related Genes in the Tumor Microenvironment of Osteosarcoma. *Aging (Albany NY)* (2020) 12(4):3486–501. doi: 10.18632/aging.102824
35. Heymann MF, Lézot F, Heymann D. The Contribution of Immune Infiltrates and the Local Microenvironment in the Pathogenesis of Osteosarcoma. *Cell Immunol* (2019) 343:103711. doi: 10.1016/j.cellimm.2017.10.011
36. Zhou Q, Xian M, Xiang S, Xiang D, Shao X, Wang J, et al. All-Trans Retinoic Acid Prevents Osteosarcoma Metastasis by Inhibiting M2 Polarization of Tumor-Associated Macrophages. *Cancer Immunol Res* (2017) 5(7):547–59. doi: 10.1158/2326-6066.CIR-16-0259
37. Wang Y, Zeng X, Wang N, Zhao W, Zhang X, Teng S, et al. Long Noncoding RNA DANCR, Working as a Competitive Endogenous RNA, Promotes ROCK1-Mediated Proliferation and Metastasis *via* Decoying of miR-335-5p and miR-1972 in Osteosarcoma. *Mol Cancer* (2018) 17(1):89. doi: 10.1186/s12943-018-0837-6
38. Zhou FC, Zhang YH, Liu HT, Song J, Shao J. LncRNA LINC00588 Suppresses the Progression of Osteosarcoma by Acting as a ceRNA for miRNA-1972. *Front Pharmacol* (2020) 11:255. doi: 10.3389/fphar.2020.00255
39. Liu K, Ni JD, Li WZ, Pan BQ, Yang YT, Xia Q, et al. The Sp1/FOXC1/HOTTIP/LATS2/ YAP/β-Catenin Cascade Promotes Malignant and Metastatic Progression of Osteosarcoma. *Mol Oncol* (2020) 14(10):2678–95. doi: 10.1002/1878-0261.12760
40. Liu J, Li M, Liu X, Liu F, Zhu J. miR-27a-3p Promotes the Malignant Phenotypes of Osteosarcoma by Targeting Ten-Eleven Translocation 1. *Int J Oncol* (2018) 52(4):1295–304. doi: 10.3892/ijo.2018.4275

Conflict of Interest: The authors declare that the research was conducted in the absence of any commercial or financial relationships that could be construed as a potential conflict of interest.

Publisher's Note: All claims expressed in this article are solely those of the authors and do not necessarily represent those of their affiliated organizations, or those of the publisher, the editors and the reviewers. Any product that may be evaluated in this article, or claim that may be made by its manufacturer, is not guaranteed or endorsed by the publisher.

frontiers in Immunology

ORIGINAL RESEARCH
published: 19 October 2021
doi: 10.3389/fimmu.2021.755639

Inclusion of the Inducible Caspase 9 Suicide Gene in CAR Construct Increases Safety of CAR.CD19 T Cell Therapy in B-Cell Malignancies

Marika Guercio[1†], Simona Manni[1†], Iolanda Boffa[1†], Simona Caruso[1], Stefano Di Cecca[1], Matilde Sinibaldi[1], Zeinab Abbaszadeh[1], Antonio Camera[1], Roselia Ciccone[1], Vinicia Assunta Polito[1], Francesca Ferrandino[1], Sofia Reddel[1], Maria Luigia Catanoso[1], Emilia Bocceri[1], Francesca Del Bufalo[1], Mattia Algeri[1], Biagio De Angelis[1‡], Concetta Quintarelli[1,2‡] and Franco Locatelli[1,3‡]*

[1] Department of Oncology-Haematology and Cell and Gene Therapy, Bambino Gesù Children Hospital, Istituto di Ricovero e Cura a Carattere Scientifico (IRCCS), Rome, Italy, [2] Department of Clinical Medicine and Surgery, University of Naples Federico II, Naples, Italy, [3] Department of Pediatrics, Sapienza University of Rome, Rome, Italy

T cells engineered with chimeric antigen receptor (CAR-T cells) are an effective treatment in patients with relapsed/refractory B-cell precursor acute lymphoblastic leukemia or B-cell non-Hodgkin lymphoma. Despite the reported exciting clinical results, the CAR-T cell approach needs efforts to improve the safety profile, limiting the occurrence of adverse events in patients given this treatment. Besides the most common side effects, such as cytokine release syndrome and CAR-T cell–related encephalopathy syndrome, another potential issue involves the inadvertent transduction of leukemia B cells with the CAR construct during the manufacturing process, thus leading to the possibility of a peculiar mechanism of antigen masking and treatment resistance. In this study, we investigated whether the inclusion of the inducible caspase 9 (iC9) suicide gene in the CAR construct design could be an effective safety switch to control malignant CAR+ B cells, ultimately counteracting this serious adverse event. iC9 is a suicide gene able to be activated through binding with an otherwise inert small biomolecule, known as AP1903. The exposure of iC9.CAR.CD19-DAUDI lymphoma and iC9.CAR.CD19-NALM-6 leukemia cells *in vitro* to 20 nM of AP1903 resulted into the prompt elimination of CAR^+ B-leukemia/lymphoma cell lines. The results obtained in the animal model corroborate *in vitro* data, since $iC9.CAR.CD19^+$ tumor cells were controlled *in vivo* by the activation of the suicide gene through administration of AP1903. Altogether, our data indicate that the inclusion of the iC9 suicide gene may result in a safe CAR-T cell product, even when manufacturing starts from biological materials characterized by heavy leukemia blast contamination.

Keywords: chimeric antigen receptor (CAR T), CD19, suicide gene, immunotherapy, B-cell Acute Lymphoblastic Leukemia

OPEN ACCESS

Edited by:
Nicholas Vitanza, Seattle Children's Hospital, United States

Reviewed by:
Luis De La Cruz-Merino, Virgen Macarena University Hospital, Spain
Sanjivan Gautam, National Cancer Institute (NIH), United States

***Correspondence:**
Concetta Quintarelli
concetta.quintarelli@opbg.net

†These authors share first authorship

‡These authors share last authorship

Specialty section:
This article was submitted to Cancer Immunity and Immunotherapy, a section of the journal Frontiers in Immunology

Received: *09 August 2021*
Accepted: *27 September 2021*
Published: *19 October 2021*

Citation:
Guercio M, Manni S, Boffa I, Caruso S, Di Cecca S, Sinibaldi M, Abbaszadeh Z, Camera A, Ciccone R, Polito VA, Ferrandino F, Reddel S, Catanoso ML, Bocceri E, Del Bufalo F, Algeri M, De Angelis B, Quintarelli C and Locatelli F (2021) Inclusion of the Inducible Caspase 9 Suicide Gene in CAR Construct Increases Safety of CAR.CD19 T Cell Therapy in B-Cell Malignancies. Front. Immunol. 12:755639. doi: 10.3389/fimmu.2021.755639

INTRODUCTION

Chimeric antigen receptor (CAR)-T cell therapy is one of the most innovative and revolutionary approaches in the fight against cancer, with growing evidence supporting its ability to induce complete remission of highly refractory malignancies in a significant proportion of patients (1).

It is based on autologous T cells engineered to express a CAR capable of specifically recognizing its cognate target antigen expressed on tumor cells through a single-chain variable fragment (scFv) binding domain, resulting in T-cell activation in a major histocompatibility complex (MHC)-independent manner.

To date, CAR-T cells targeting the CD19 antigen represent the first gene therapy approved for treatment of relapsed/refractory (r/r) B-cell acute lymphoblastic leukemia (B-ALL) and aggressive forms of r/r B-cell non-Hodgkin lymphoma, with up to 90% complete remission reported (1). In particular, the first two CAR-T cell products approved by the FDA (Food and Drug Administration) and EMA (European Medicinal Agency) regulatory authorities were Tisagenlecleucel (Kymriah®-Novartis) and Axicabtagene Ciloleucel (Yescarta®-Kite), but additional products are currently in an advanced stage of market authorization approval.

Despite the fact that CAR-T cell therapy represents a valid therapeutic strategy, it may induce severe toxicities, the most common being cytokine release syndrome (CRS) and CAR-T cell-related encephalopathy syndrome (CRES). Although rare, another adverse event was recently reported to potentially occur, raising the possibility of a peculiar mechanism of treatment resistance. In particular, the occurrence of an inadvertent leukemia cell transduction with CAR.CD19 vector during CAR-T cell manufacturing has been described (2,3). The CAR molecule expressed *in cis* on the surface of the leukemic cells masks the CD19 antigen, promoting the consequent expansion of a $CD19^{-}CAR^{+}$ leukemic clone (3). This phenomenon has been reported in a preclinical retroviral model (3), as well as in two patients treated with lentiviral-based CAR.CD19 T cells who relapsed with a CAR^{+} leukemia (2).

In this study, we investigated whether the inclusion of a suicide gene in the CAR construct could be an effective safety switch to control the event of inadvertent malignant B-cell transduction with the CAR construct, ultimately counteracting this serious adverse event.

Several safety switches have been developed, either by inclusion of transgenic enzymes selectively activated by a cytotoxic pro-drug (herpes simplex virus-thymidine kinase: HSV-TK; inducible caspase 9, iC9) or by expression of surface molecules (CD20, EGFR) that can be targeted using clinically approved monoclonal antibodies (4).

The iC9 suicide gene contains the intracellular portion of the human caspase 9 protein, fused to a drug-binding domain derived from the human FK506-binding protein. Intravenous administration of an otherwise inert small biomolecule AP1903 (Rimiducid) is able to induce dimerization of iC9, which activates the downstream apoptosome (5). In a pivotal study (6) conducted in patients given T-cell-depleted hematopoietic stem cell transplantation (HSCT) followed by post-transplant infusion of a titrated number of donor T cells transduced with iC9, it was shown that AP1903 administration can trigger chemically induced dimerization and eliminate genetically modified T cells from both peripheral blood and the central nervous system (CNS), leading to rapid resolution of graft-*versus*-host disease (GvHD) and CRS. iC9 has been used in CAR-T cell immunotherapy in several preclinical models (7), demonstrating the ability of eliminating CAR-T cells both *in vitro* and *in vivo*, although a large clinical application of this approach has been limited so far. An important aspect of iC9 is represented by its preferential killing of highly activated cells, which can be explained in view of their high expression of the transgene. As retroviral vectors preferentially integrate near transcription start sites and genes involved in proliferation (8–11), actively dividing cells typically have higher transgene expression and hence higher levels of iC9. Preclinical work suggests that transduced T cells that are not killed by AP1903 administration express an insufficient level of iC9 to allow functional activation by the dimerizing agent (5). However, it has been observed that after inducing the activation of T cells with low transgene expression that residue after the activation of iC9, it is possible to rapidly restore the AP1903 sensitivity of these cells (12).

MATERIALS AND METHODS

Cell Cultures

The human Burkitt lymphoma cell line DAUDI (WT and iC9.CAR.CD19 DAUDI) and B-ALL cell line NALM-6 (WT and iC9.CAR.CD19) were maintained in RPMI 1640 (EuroClone, Italy) supplemented with 10% heat-inactivated fetal bovine serum (EuroClone), 2 mM of l-glutamine (GIBCO, USA), 25 IU/ml of penicillin, and 25 mg/ml of streptomycin (EuroClone), in a humidified atmosphere containing 5% CO2 at 37°C. All cell lines were authenticated by PCR single-locus-technology (Promega, USA, PowerPlex 21 PCR) analysis in "BMR Genomics s.r.l." (Italy), and were periodically checked for mycoplasma (Venor®GeM Advance, MB Minerva Biolabs, UK) and surface markers expression.

Generation and Expansion of Effector Cells

Buffy coats (BC) from healthy donors (HDs), peripheral blood (PB), and bone marrow (BM) obtained from children with B-ALL were used to isolate unfractionated mononuclear cells using Lympholyte Cell Separation Media (Cedarlane, Canada). T cells were activated with OKT3 (1 μg/ml, ThermoFisher Scientific, USA) and anti-CD28 (1 μg/ml, BD Biosciences, USA) monoclonal antibodies (mAb) with a combination of recombinant human (rh) interleukin-7 (rh-IL7, 10 ng/ml; Bio-Techne; USA) and rh-IL15 (5 ng/ml; Bio-Techne; USA). NK cells were generated from BC of HDs following a previously described method (13). After 3/4 days, T and NK cells were transduced with a γ-retroviral supernatant, in 24-well plates precoated with rhRetroNectin (Takara-Bio; Japan). T and NK lymphocytes were expanded in the presence of cytokines, in TexMacs complete medium (Miltenyi, Germany) or NK MACS medium (Miltenyi, Germany) and replenished twice a week.

CAR Construct

T and NK cells from HD, as well as the B-cell leukemia/lymphoma cell lines DAUDI and NALM-6, were genetically modified using the retroviral construct iC9.CAR.CD19 ($1e^9$ retrovirus-copies/0.5×10^6 cells. Multiplicity of infection were quantified by Retro-X™ qRT-PCR Titration Kit from Takara, USA). The bicistronic CAR construct carries antihuman CD19-scFv from FMC63, CD8 stalk domain, CD8 transmembrane domain, 4.1bb, and CD3ζ cytoplasmic domains cloned in-frame with the iC9 suicide gene (3).

Phenotypic Analysis

Flow-cytometry (FACS) analysis was performed to determine cell surface antigen expression; monoclonal antibodies for CD19 and CD34 (all from Becton Dickinson, NJ, USA) combined with different fluorochromes were selected according to need. FACS analysis was performed using a BD LSRFortessa X-20 cytometer (BD Biosciences, USA) and analyzed by FACSDiva software (BD Biosciences, USA). FACS sorting of CAR-transduced tumor cell lines was performed on FACSAria (BD Biosciences, USA).

Activation of the Suicide Gene

To induce the activation of iC9 *in vitro*, cells were treated once with 20 nM of AP1903 (TOCRIS, Bio-Techne, USA), considering that this dose is in the low range of the observed Cmax for the drug (14). The percentage of residual CAR^+ cells after exposure to AP1903 was evaluated by FACS at the indicated time points. For the *in vivo* experiments, NOD-scid IL2Rgammanull mice (NSG, The Jackson Laboratory, USA) were infused with 0.25×10^6 iC9.CAR.CD19-DAUDI cells genetically modified with a retroviral construct to express FF-Luciferase. After tumor engraftment, documented through the IVIS imaging system, AP1903 was administered intraperitoneally from day 1 to day 28 (100 μg/day/mouse). The control cohort was infused with sterile PBS as vehicle solution. Tumors were monitored by weekly IVIS imaging analysis.

Quantitative Real-Time PCR

The average of vector copy number (VCN) per cell was determined by real-time PCR, using a TaqMan probe designed on the retroviral construct using the Primer Express® software (Applied Biosystems).

In Vivo CAR^+ Leukemia Mouse Model

Cg-Prkdcscid Il2rgtm1Wjl/SzJ (NSG) female mice were provided by Charles River and maintained in the Plaisant animal facility (Castel Romano, Rome, Italy). All procedures were performed in accordance with the Guidelines for Animal Care and Use of the National Institutes of Health (Ethical committee for animal experimentation Prot. N 088/2016-PR). At day −3, mice were infused intravenously with 0.25×10^6 iC9.CAR.CD19-DAUDI cells genetically modified to express firefly luciferase (FF-Luc). At day 0, mice were evaluated for leukemia engraftment by the IVIS imaging system and treated with AP1903, 100 μg/day/mouse, from day 0 to day +28. Tumor growth was monitored weekly by the IVIS Imaging System, after intraperitoneal D-Luciferin (PerkinElmer, D-Luciferin potassium salt, USA) administration.

Statistical Analysis

Unless otherwise noted, data are shown as mean ± standard deviation (SD). Student t-test (two-sided) was used to determine statistically significant differences between samples, with p-value <0.05 indicating a statistically significant difference.

Mice survival was analyzed using Kaplan-Meier survival curves, and the Log-rank (Mantel-Cox) test was used to measure statistically significant differences. No valuable samples were excluded from the analyses. Animals were excluded only in the event of death after tumor infusion, before treatment. Neither randomization nor blinding was applied. However, mice were matched in control and treatment groups based on the tumor signal. To compare the growth of tumors over time, bioluminescence signal intensity was collected in a blind fashion. Bioluminescence signal intensity was log-transformed and, then, compared using a two-sample t-test. We estimated the sample size considering no significant variation within each group of data and using a size as small as possible to obtain a significant result. The sample size was defined in order to detect a difference in averages of two standard deviations at the 0.05 level of significance, with an 80% power. Graphic representations and statistical analysis were performed using GraphPad Prism 6 (GraphPad Software, La Jolla, CA, USA).

RESULTS

Suicide Gene iC9 Activation Controls Expansion of CAR+ Leukemic Cells

We developed a γ-retroviral vector encoding for iC9.CAR.CD19. The bicistronic construct was cloned in-frame with the iC9 suicide gene. As proof of concept, we genetically modified $CD19^+$ B-leukemia/lymphoma cell lines with the bicistronic vector encoding for iC9.CAR.CD19, in order to reproduce a CAR^+ CD19-masked leukemic clonotype (**Figure 1A**). *In vitro*, we demonstrated the prompt elimination of CAR^+ B-leukemia/lymphoma cell lines after exposure of iC9.CAR.CD19-DAUDI and iC9.CAR.CD19-NALM-6 cells to 20 nM of AP1903. In particular, activation of the suicide gene iC9 led to a significant, early (6 h) reduction in the percentage of CAR^+ tumor cells (**Figures 1B, C** for DAUDI cells and **Figures 2A, B** for NALM-6 cells). Prolonged, 6-day culture of AP1903-treated iC9.CAR.CD19 DAUDI cells was not associated with re-expansion of iC9.CAR^+ lymphoma cells (**Figure 1C**). Similar results were also confirmed in the NALM-6 model: upon treatment with AP1903, no leukemia cell with high MFI of CAR expression could be detected by flow cytometry (**Figure 2B**). In particular, the CAR MFI on AP1903-treated cells (day 15) was 142 ± 22 (gray line, **Figure 3A**), a value not significantly different from un-transduced DAUDI cells (125.8 ± 20.6; dotted line), but significantly lower as compared to that of transduced cells not exposed to the dimerizing agent (7,933 ± 72, black line; p= 6E-09). Notably, AP1903 was able to eliminate not only CAR+ cells with a high CAR MFI, but also cells showing a low CAR expression (**Figure 3B** shows CAR expression before and after AP1903 treatment, respectively).

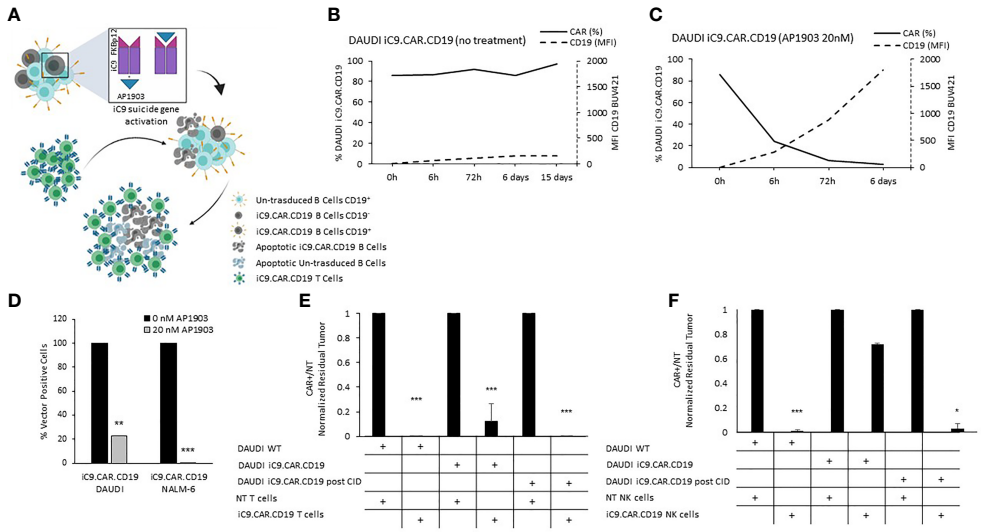

FIGURE 1 | iC9 activation in iC9.CAR.CD19 lymphoma cells leads to prompt elimination of the CAR+ fraction and redetection of CD19 antigen. **(A)** Schematic representation of iC9 dimerization in iC9.CAR.CD19 lymphoma cells leading to iC9.CAR.CD19 B cells apoptosis and to redetection of CD19 antigen by iC9.CAR.CD19 T cells (created with BioRender.com). **(B, C)** iC9.CAR.CD19 DAUDI cells were treated with 0 nM **(B)** and 20 nM **(C)** of AP1903; both CAR and CD19 expressions were monitored over time by flow cytometry. **(D)** Detection of iC9.CAR.CD19 vector in tumor cells by qRT-PCR after AP1903 exposure. Reactions were performed in triplicate. Black histograms represent the positive control of reference (0 nM of AP1903), and gray histograms represent results after drug exposure (20 nM of AP1903). **(E)** A 7-day co-culture assay was carried out using un-transduced T cells or iC9.CAR.CD19 T cells and WT DAUDI cells, iC9.CAR.CD19 DAUDI cells never exposed to AP1903, and iC9.CAR.CD19 DAUDI residual after AP1903 exposure and further re-expanded (at effector/target ratio of 1:1). **(F)** A 7-day co-culture assay was carried out using un-transduced NK cells or iC9.CAR.CD19 NK cells and WT DAUDI cells, iC9.CAR.CD19 DAUDI cells never exposed to AP1903, and iC9.CAR.CD19 DAUDI residual after AP1903 exposure and further re-expanded (at effector/target ratio of 1:1) *p-value ≤ 0.05, **p-value ≤ 0.01, ***p-value ≤ 0.001.

Moreover, we observed that residual leukemia cells after AP1903 exposure showed completely re-established levels of CD19 antigen expression (dotted line; **Figures 1C** and **2B**). Although qPCR analysis revealed the presence of the CAR transgene in residual blasts after AP1903 incubation, the proportion of positive cells was significantly lower as compared to that of untreated cells (**Figure 1D**, transgene positivity being observed in 22.8% of DAUDI cells, and 0.6% of NALM-6 cells).

AP1903-Treated CAR+ B Cells Are Recognized and Eliminated by CAR.CD19 Effector Cells

Since CD19 expression was completely re-established in iC9.CAR$^+$ B cells after AP1903 exposure, we evaluated whether they could be re-targeted by CAR.CD19 T cells. As shown in **Figure 1E** (DAUDI) and in **Figure 2C** (NALM-6), iC9.CAR.CD19 T cells were able to eliminate iC9.CAR$^+$ tumor B cells re-expanded after AP1903 exposure. Moreover, since generating the autologous CAR-T cell product from patients with CAR$^+$ B-cell relapse does not represent a feasible strategy in the clinical setting, we have also proved that *off-the-shelf*, third-party, HD-derived iC9.CAR.CD19 NK cells (13) are able to significantly control iC9.CAR.CD19$^+$ B cells rescued after AP1903 treatment (**Figure 1F** for the DAUDI model, and **Figure 2D** for the NALM-6 model).

In Vivo Suicide Gene Strategy to Control CAR+ Leukemia

We proved *in vivo* the ability of the suicide gene iC9 to eliminate CAR + leukemia expansion using AP1903. NSG mice were infused with iC9.CAR.CD19 DAUDI cells at day −3 (**Figure 4A**); after tumor engraftment, the dimerizing drug AP1903 was intraperitoneally administrated from day 0 to day 28 (**Figure 4A**). iC9 activation resulted in complete eradication of CAR+ leukemia in 9 out of 10 studied mice (**Figures 4B, C**). Moreover, AP1903 administration resulted in survival of all mice without leukemia but one, even after stopping drug administration, with 9 out of 10 mice showing absence of leukemia cell progression until day 63 (endpoint of the experiment; **Figure 4D**).

DISCUSSION

In this study, we provide evidence that the inclusion of the iC9 safety switch in a CAR vector represents a powerful and effective rescue strategy in case of inadvertent CAR.CD19$^+$ blast generation. In comparison to other suicide genes, the iC9 safety switch is non-immunogenic and is characterized by a rapid mechanism of action once activated by the binding with AP1903 (15). Our data confirm previously published *in vitro* (16) and *in vivo* studies (17) showing that AP1903 is highly efficient in eliminating the great majority of

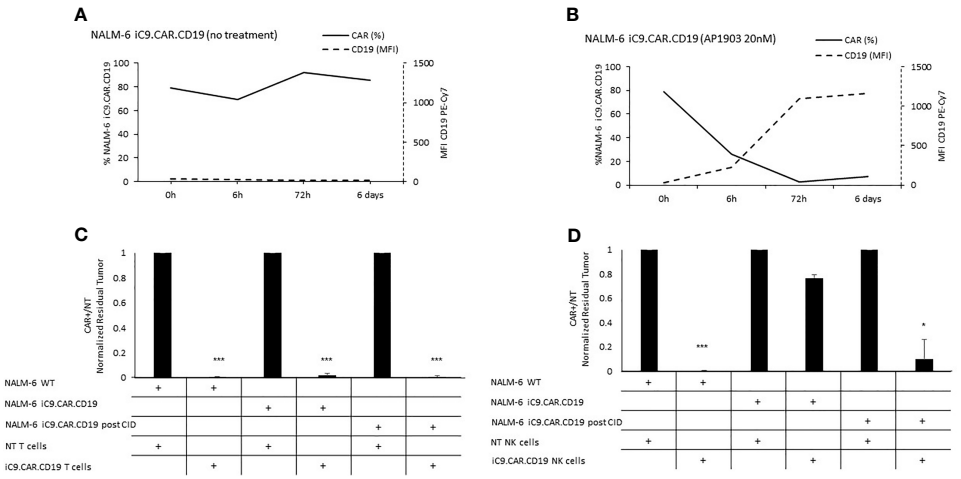

FIGURE 2 | Long-term *in vitro* assays to evaluate the activity of iC9 controlling CAR.CD19-positive leukemia cell lines. **(A, B)** iC9.CAR.CD19 NALM-6 cells were treated with 0 nM **(A)** and 20 nM **(B)** of AP1903; both CAR and CD19 expressions were monitored over time by flow cytometry. **(C)** A 7-day co-culture assay was carried out between un-transduced T cells or iC9.CAR.CD19 T cells and WT NALM-6 cells, iC9.CAR.CD19 NALM-6 cells never exposed to AP1903, and iC9.CAR.CD19 NALM-6 residual after AP1903 exposure and further re-expanded (at effector/target ratio of 1:1). **(D)** A 7-day co-culture assay was carried out using un-transduced NK cells or iC9.CAR.CD19 NK cells and WT NALM-6 cells, iC9.CAR.CD19 NALM-6 cells never exposed to AP1903, and iC9.CAR.CD19 NALM-6 residual after AP1903 exposure and further re-expanded (at effector/target ratio of 1:1) *p-value ≤ 0.05, ***p-value ≤ 0.001.

cells highly expressing iC9, while sparing cells with a lower level of iC9 expression. Indeed, in the context of genetically modified T cells, patients who received an infusion of haploidentical, donor-derived iC9-T cells after HSCT and were subsequently treated with Rimiducid to control GvHD, showed 1% of residual iC9-T cells a few hours after AP1903 administration. The residual iC9-T cells were characterized by a remarkably dim expression of the transgene, possibly related to a low level of T-cell activation. Elimination of iC9-T cells could be enhanced by T-cell activation during repeated AP1903 administrations (17). By contrast, when iC9 is expressed in tumor cells, AP1903 is able to induce massive and rapid apoptosis, leading to a significant elimination of tumor cells (16). With our CAR system, in case of an unlucky inadvertent transduction of leukemia blasts with iC9.CAR.CD19, we demonstrated that CAR+ B cells can be efficiently eliminated by exposure to AP1903 and that the expression level of the CAR in rescued leukemic cells after treatment is negligible. Leukemia cells that could not be eliminated by AP1903 and lacking a high expression of CAR on their surface express a standard level of CD19 antigen on their surface, this results in the possibility of efficiently targeting B-cell leukemia/lymphoma elements through CAR.CD19 T cells and CAR.CD19 allogenic NK cells.

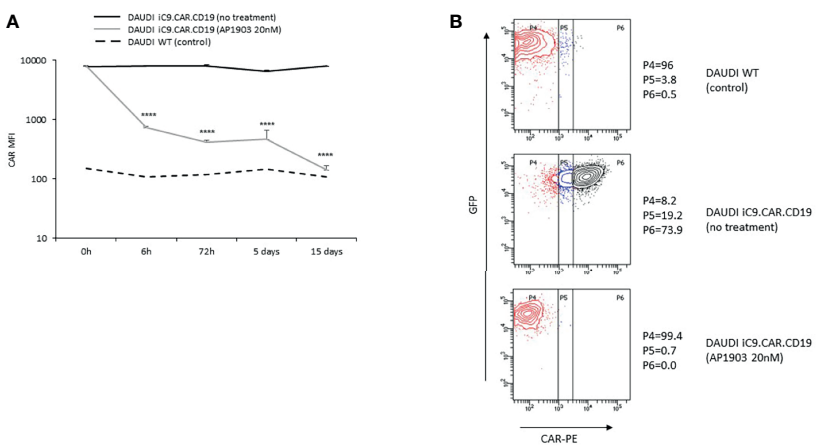

FIGURE 3 | iC9 activation controls CAR+ B-cells with dim expression of transgene. **(A)** iC9.CAR.CD19 DAUDI cell line were treated with 0 nM (black line) and 20 nM of AP1903 (gray line); CAR MFI was monitored over time by flow cytometry analysis from day 0 to day 15 after treatment and compared to the control WT DAUDI cell line. **(B)** CAR expression detected by flow cytometry in the DAUDI WT cell line (negative control; top panel), iC9.CAR.CD19 DAUDI cell line (no treatment, middle panel), or iC9.CAR.CD19 DAUDI cell line treated with 20 nM of AP1903 (day +15; bottom panel) ****p-value ≤ 0.00001.

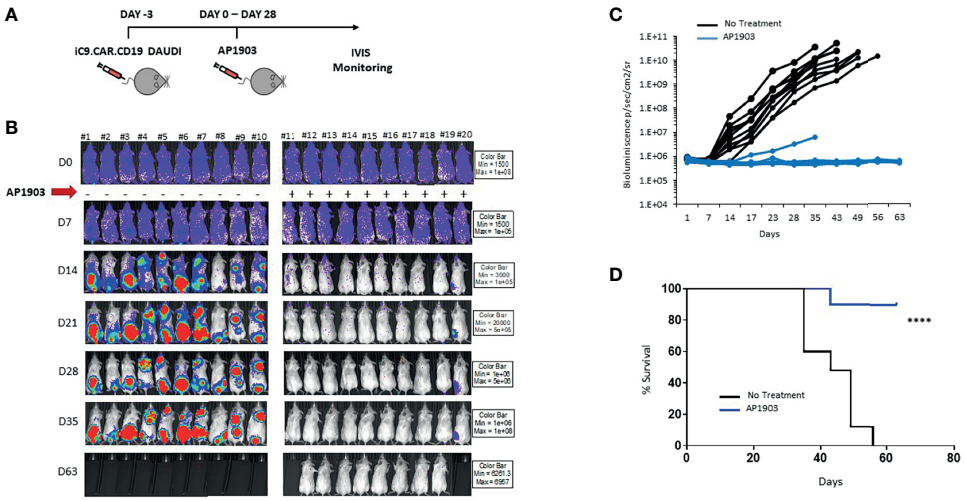

FIGURE 4 | iC9 activation is able to control *in vivo* expansion of CAR-positive lymphoma in a xenograft mouse model. **(A)** Schematic representation of the experimental design, with iC9.CAR.CD19-positive/FF-Luciferase-positive DAUDI cells infused at day –3. At day 0, mice were evaluated for leukemia engraftment and treated with 100 μg/mouse of AP1903 from day 0 to day 28. **(B)** Bioluminescence images of each control untreated mouse and each AP1903-treated mouse. Mice were monitored for more than 30 days after AP1903 withdrawal. **(C)** Bioluminescence values over time for each treated mouse in the two cohorts, untreated (black lines) or AP1903-treated (blue line) mice. **(D)** Kaplan-Meier survival curve analysis of leukemia-bearing mice untreated (black line) or AP1903-treated (blue line). ****p-value ≤ 0.00001. The only mouse (#20) showing a persisting positive signal at IVIS analysis after AP1903 administration was sacrificed at day+43 together with a negative control (#11), to characterize the leukemia cells.

The results we obtained in our animal model corroborated *in vitro* data, since iC9.CAR.CD19$^+$ DAUDI cells could be controlled *in vivo* by the activation of the suicide gene through administration of AP1903. In particular, NSG mice infused with iC9.CAR.CD19 DAUDI cells were treated with intraperitoneal administration of AP1903 from day 0 to day 28. iC9 activation resulted in complete eradication of CAR$^+$ B cells in the great majority of the mice (90%), without leukemia relapse after withdrawal of the drug for a prolonged period of time.

Altogether, our data support the hypothesis that for patient-derived CAR-T cell products, the inclusion of the iC9 suicide gene in the construct represents an important safety strategy, able to control and eliminate leukemia cells in case of inadvertent blast-cell transduction during CAR-T cell manufacturing, and meets the medical need of increasing the safety profile of CAR-T cell gene therapy. Moreover, the iC9 suicide gene could contribute to successfully treat other CAR-T cell therapy associated toxicities, such as CRS and CRES, if not adequately controlled by conventional pharmacological treatment. In this respect, we are now conducting a clinical trial in which we treat patients with B-ALL using CAR-T cells transduced with a retroviral construct including iC9 (NCT03373071).

DATA AVAILABILITY STATEMENT

The original contributions presented in the study are included in the article/supplementary material. Further inquiries can be directed to the corresponding author.

ETHICS STATEMENT

The animal study was reviewed and approved by the Ethical Committee of the Italian Ministry of Health, Prot. N 088/2016-PR.

AUTHOR CONTRIBUTIONS

FL, BDA, and CQ are the co-last author of the paper. SM, MG, and IB are the first authors of the paper. CQ, BDA, and FL designed experimental studies, supervised the project conduction, analyzed the data, and wrote the manuscript. IB, MG, SM, SDC, MS, SC, ZA, AC, RC, VP, FF, and SR developed the *in vitro* models and performed the *in vitro* experiments. IB, BDA, and CQ performed the *in vivo* experiments. CQ, IB, and BDA cloned the retroviral vector. IB, MG, SM, and MS performed FACS analysis. FDB, MA, MLC, EB, and FL provided healthy donor material, medical advice, and expertise in childhood B-ALL and B-NHL. All authors contributed to writing the paper and approved the final version of the manuscript.

FUNDING

The experimental work was supported by grants awarded by GR-2016-02364546 (BA), RF-2016-02364388 (FL), Accelerator Award–Cancer Research UK/AIRC–INCAR project (FL), Associazione Italiana Ricerca per la Ricerca sul Cancro (AIRC)-Special Project 5×1000 no. 9962 (FL), AIRC IG 2018 id. 21724 (FL), MFAG 21979 (CQ), Ricerca Corrente (CQ, BA),

Ministero dell'Università e della Ricerca (Grant PRIN 2017 to FL); Italian Healthy Ministry project on CAR T RCR-2019-23669115 (Coordinator FL), Independent Research grant AIFA (FL: 2016 call).

ACKNOWLEDGMENTS

We are very grateful to Bellicum Pharmaceuticals for the collaboration in supporting clinical trial programs on iC9.CAR T cells.

REFERENCES

1. Greenbaum U, Mahadeo KM, Kebriaei P, Shpall EJ, Saini NY. Chimeric Antigen Receptor T-Cells in B-Acute Lymphoblastic Leukemia: State of the Art and Future Directions. *Front Oncol* (2020) 10:1594. doi: 10.3389/fonc.2020.01594
2. Ruella M, Xu J, Barrett DM, Fraietta JA, Reich TJ, Ambrose DE, et al. Induction of Resistance to Chimeric Antigen Receptor T Cell Therapy by Transduction of a Single Leukemic B Cell. *Nat Med* (2018) 24:1499–503. doi: 10.1038/s41591-018-0201-9
3. Quintarelli C, Guercio M, Manni S, Boffa I, Sinibaldi M, Di Cecca S, et al. Strategy to Prevent Epitope Masking in CAR.CD19+ B-Cell Leukemia Blasts. *J Immunother Cancer* (2021) 9(6):e001514. doi: 10.1136/jitc-2020-001514
4. Jones BS, Lamb LS, Goldman F, Di Stasi A. Improving the Safety of Cell Therapy Products by Suicide Gene Transfer. *Front Pharmacol* (2014) 5:254. doi: 10.3389/fphar.2014.00254
5. Straathof KC, Pulè MA, Dotti PYG, Vanin EF, Malcolm K, Brenner MK, et al. An Inducible Caspase 9 Safety Switch for T-Cell Therapy. *Blood* (2005) 105:4247–54. doi: 10.1182/blood-2004-11-4564
6. Zhou X, Di Stasi A, Tey S, Krance RA, Martinez C, Leung KS, et al. Long-Term Outcome After Haploidentical Stem Cell Transplant and Infusion of T Cells Expressing the Inducible Caspase 9 Safety Transgene. *Blood* (2014) 123:3895–905. doi: 10.1182/blood-2014-01-551671
7. Guercio M, Orlando D, Di Cecca S, Sinibaldi M, Boffa I, Caruso S, et al. CD28.OX40 Co-Stimulatory Combination Is Associated With Long *In Vivo* Persistence and High Activity of CAR.CD30 T-Cells. *Haematologica* (2021) 106(4):987–99. doi: 10.3324/haematol.2019.231183
8. Wu X, Li Y, Crise B, Burgess SM. Transcription Start Regions in the Human Genome Are Favored Targets for MLV Integration. *Science* (2003) 300:1749–51. doi: 10.1126/science.1083413
9. Cattoglio C, Facchini G, Sartori D, Antonelli A, Miccio A, Cassani B, et al. Hot Spots of Retroviral Integration in Human CD34+ Hematopoietic Cells. *Blood* (2007) 110:1770–8. doi: 10.1182/blood-2007-01-068759
10. Recchia A, Bonini C, Magnani Z, Urbinati F, Sartori D, Muraro S, et al. Retroviral Vector Integration Deregulates Gene Expression But Has No Consequence on the Biology and Function of Transplanted T Cells. *Proc Natl Acad Sci U.S.A.* (2006) 103:1457–62. doi: 10.1073/pnas.0507496103
11. Schwarzwaelder K, Howe SJ, Schmidt M, Brugman MH, Deichmann A, Glimm H, et al. Gammaretrovirus-Mediated Correction of SCID-X1 is Associated With Skewed Vector Integration Site Distribution. *Vivo J Clin Invest* (2007) 117:2241–9. doi: 10.1172/JCI31661
12. Gargett T, Brown MP. The Inducible Caspase-9 Suicide Gene System as a "Safety Switch" to Limit on-Target, Off-Tumor Toxicities of Chimeric Antigen Receptor T Cells. *Front Pharmacol* (2014) 5:235. doi: 10.3389/fphar.2014.00235
13. Quintarelli C, Sivori S, Caruso S, Carlomagno S, Falco M, Boffa I, et al. Efficacy of Third-Party Chimeric Antigen Receptor Modified Peripheral Blood Natural Killer Cells for Adoptive Cell Therapy of B-Cell Precursor Acute Lymphoblastic Leukemia. *Leukemia* (2020) 34:1102–15. doi: 10.1038/s41375-019-0613-7
14. Iuliucci JD, Oliver SD, Morley S, Ward C, Ward J, Dalgarno D, et al. Intravenous Safety and Pharmacokinetics of a Novel Dimerizer Drug, AP1903, in Healthy Volunteers. *J Clin Pharmacol* (2001) 41:870–9. doi: 10.1177/00912700122010771
15. Marin V, Cribioli E, Philip B, Tettamanti S, Pizzitola I, Biondi A, et al. Comparison of Different Suicide-Gene Strategies for the Safety Improvement of Genetically Manipulated T Cells. *Hum Gene Ther Methods* (2012) 23:376–86. doi: 10.1089/hgtb.2012.050
16. Kemper K, Rodermond H, Colak S, Grandela C, Medema JP. Targeting Colorectal Cancer Stem Cells With Inducible Caspase-9. *Apoptosis* (2012) 17:528–37. doi: 10.1007/s10495-011-0692-z
17. Zhou X, Naik S, Dakhova O, Dotti G, Heslop HE, Brenner MK, et al. Serial Activation of the Inducible Caspase 9 Safety Switch After Human Stem Cell Transplantation. *Mol Ther* (2016) 24:823–31. doi: 10.1038/mt.2015.234

Conflict of Interest: The authors declare that the research was conducted in the absence of any commercial or financial relationships that could be construed as a potential conflict of interest.

Publisher's Note: All claims expressed in this article are solely those of the authors and do not necessarily represent those of their affiliated organizations, or those of the publisher, the editors and the reviewers. Any product that may be evaluated in this article, or claim that may be made by its manufacturer, is not guaranteed or endorsed by the publisher.

frontiers in Immunology

MINI REVIEW
published: 04 November 2021
doi: 10.3389/fimmu.2021.791206

Enhancing Natural Killer Cell Targeting of Pediatric Sarcoma

Natacha Omer[1,2,3]*, *Wayne Nicholls*[2,3], *Bronte Ruegg*[1], *Fernando Souza-Fonseca-Guimaraes*[1] *and Gustavo Rodrigues Rossi*[1]*

[1] The University of Queensland Diamantina Institute (UQDI), The University of Queensland, Brisbane, QLD, Australia, [2] Oncology Services Group, Queensland Children's Hospital, South Brisbane, QLD, Australia, [3] Faculty of Medicine, The University of Queensland, Brisbane, QLD, Australia

Osteosarcoma, Ewing sarcoma (EWS), and rhabdomyosarcoma (RMS) are the most common pediatric sarcomas. Conventional therapy for these sarcomas comprises neoadjuvant and adjuvant chemotherapy, surgical resection of the primary tumor and/or radiation therapy. Patients with metastatic, relapsed, or refractory tumors have a dismal prognosis due to resistance to these conventional therapies. Therefore, innovative therapeutic interventions, such as immunotherapy, are urgently needed. Recently, cancer research has focused attention on natural killer (NK) cells due their innate ability to recognize and kill tumor cells. Osteosarcoma, EWS and RMS, are known to be sensitive to NK cell cytotoxicity *in vitro*. In the clinical setting however, NK cell cytotoxicity against sarcoma cells has been mainly studied in the context of allogeneic stem cell transplantation, where a rapid immune reconstitution of NK cells plays a key role in the control of the disease, known as graft-versus-tumor effect. In this review, we discuss the evidence for the current and future strategies to enhance the NK cell-versus-pediatric sarcoma effect, with a clinical focus. The different approaches encompass enhancing antibody-dependent NK cell cytotoxicity, counteracting the NK cell mechanisms of self-tolerance, and developing adoptive NK cell therapy including chimeric antigen receptor-expressing NK cells.

Keywords: osteosarcoma, Ewing sarcoma, rhabdomyosarcoma, natural killer, immunotherapy

OPEN ACCESS

Edited by:
Orazio Vittorio, University of New South Wales, Australia

Reviewed by:
Alexander David Barrow, The University of Melbourne, Australia

***Correspondence:**
Natacha Omer
n.omer@uq.edu.au
Gustavo Rodrigues Rossi
g.rodriguesrossi@uq.edu.au

Specialty section:
This article was submitted to Cancer Immunity and Immunotherapy, a section of the journal Frontiers in Immunology

Received: *08 October 2021*
Accepted: *20 October 2021*
Published: *04 November 2021*

Citation:
Omer N, Nicholls W, Ruegg B, Souza-Fonseca-Guimaraes F and Rossi GR (2021) Enhancing Natural Killer Cell Targeting of Pediatric Sarcoma. Front. Immunol. 12:791206. doi: 10.3389/fimmu.2021.791206

INTRODUCTION

Osteosarcoma, Ewing sarcoma (EWS), and rhabdomyosarcoma (RMS) are the most common sarcomas in children. Patients with metastatic, relapsed, or refractory pediatric sarcoma have a dismal prognosis with less than 30% maintaining long-term survival (1). Further, no significant improvement in patient outcome has been made over the last 3 decades with currently available therapies (surgery, radiation, and chemotherapy) (2–4). Hence, there is an urgent need for innovative therapeutic interventions, such as immunotherapy.

Immunotherapy is not a new concept for sarcoma. The earliest described sarcoma immunotherapy was in 1891, when William B. Coley observed tumor regression after locally injecting *Streptococcus* bacteria into patient's sarcoma to generate an immune response (5). Now scientific and clinical evidence strongly supports the critical role for both early and late immune responses to control cancer growth. As an example, there is mounting evidence that hematopoietic stem cell transplantation (HSCT) has an allograft-versus-tumor effect in the treatment of leukemia

and in a subgroup of solid tumors including sarcomas (6). Rapid immune reconstitution post HSCT is critical for the anti-tumor effect, particularly due to the recovery of natural killer (NK) cells (7). Nevertheless, studies investigating the function of NK cells in sarcoma in the clinical field are limited and further work aiming to "unleash" the full potential of NK cells to improve their anti-sarcoma activity are needed. This review highlights the current knowledge in the field and future perspectives of applying NK cell-based immunotherapies to treat pediatric sarcomas. Possible strategies to increase NK cells efficiency discussed here are the use of monoclonal antibodies (mAb) targeting tumor antigens or of pharmacological agents to enhance antibody-dependent cell-mediated cytotoxicity (ADCC), the use of cytokines to enhance NK cell-mediated anti-tumor activity, strategies to counteract self-tolerance, and the development of adoptive therapy using NK cells, including chimeric antigen receptor (CAR)-expressing NK cells (**Figure 1**).

NK CELL ACTIVITY IN PEDIATRIC SARCOMA

NK cells are cytotoxic innate immune cells that can eliminate infected or transformed cells without prior sensitization. NK cells express inhibitory surface receptors, such as killer-cell immunoglobulin receptors (KIR), which recognizes specific human leucocyte antigen (HLA) class I molecules HLA-A, B and C, and CD94/NK group 2 member A (NKG2A), which recognizes HLA-E (8). NK cells are educated to lyse target cells lacking expression of major histocompatibility complex (MHC) class I molecules expressed by the host cells (9). Their activating surface receptors include natural cytotoxic receptors (NCRs) and NK group 2 member D (NKG2D), which recognize stress proteins on the surface of target cells such as MICA/B and ULBPs, and a Fcγ receptor CD16, that mediate ADCC through recognition of the Fc portion of antibodies on opsonized cells (10). Coreceptors of NCRs and NKG2D, such as DNAM-1, are capable of amplifying the NK cell activation (11). The balance between activating and inhibitory signals received by the NK cells determines their cytotoxic activity. This activity is mediated by the release of cytotoxic granules containing granzymes and perforin, expression of death receptor ligands on their surface, and the production of cytokines (e.g., tumor necrosis factor-α and interferon γ) promoting an anti-tumor immune response (12).

In pre-clinical studies, osteosarcoma, EWS, and RMS cells are sensitive to killing by NK cells. NK cells from healthy donors expanded for 7 days with K562-mb15-41BBL feeder cells showed a median cytotoxicity of 87.2%, 79.1% and 46.1% at a 1:1 effector: target ratio with EWS, RMS and osteosarcoma cells respectively. EWS cells were particularly sensitive with maintained cytotoxicity at considerably lower ratios (13). Cytotoxicity was not related to levels of expression of NK receptor ligands but was markedly

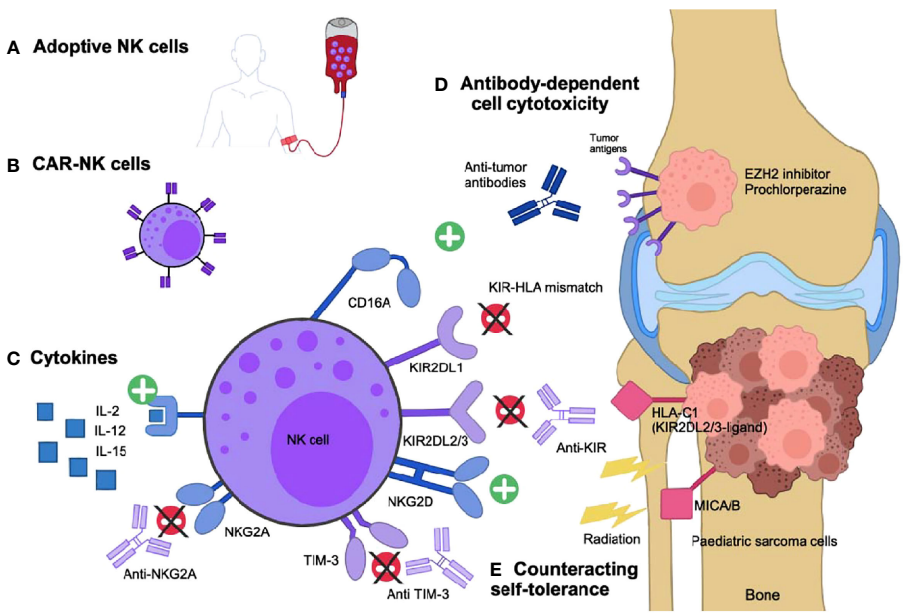

FIGURE 1 | Enhancing NK cells-versus-pediatric sarcoma effect. **(A)** Expanded and activated NK-cells *in vitro* or **(B)** engineered NK cells expressing combined antigen-receptors (CAR) specific to the sarcoma cells can be infused to the patients. **(C)** Infused cytokines can stimulate the NK cell cytotoxic activity. **(D)** Specific anti-tumor antibodies activate NK cells *via* their CD16 activating receptor and drive the antibody-dependent cell cytotoxicity (ADCC). Small molecules, such as EZH2 inhibitors and prochlorperazine, can increase antigen presentation to facilitate ADCC. **(E)** Self-tolerance can be counteracted if the NK cells are KIR-mismatched to the tumor, if the NK inhibitory receptors are targeted with specific inhibitory antibodies (anti-KIR, NKG2A or TIM-3) or if the NK activating receptors ligands, such as MIC-A/B, are overexpressed due to genotoxic stress such as radiation therapy.

inhibited by preincubation of NK cells with antibodies anti-NKG2D and anti-DNAM-1, when used in combination (13). Similarly, NKG2D receptor blockade, but not that of DNAM-1, significantly decreased NK cells cytotoxicity *in vitro* against osteosarcoma cells (14). KIRs were also shown to play an important role: KIR receptor-ligand mismatched NK cells showed higher cytotoxicity *in vitro* against osteosarcoma cells, and this was enhanced further when osteosarcoma cells HLA class I molecules were blocked (14). Furthermore, in a mouse xenograft model of EWS, weekly intravenous administration of expanded NK cells decreased significantly the number of lung metastases (15). In an orthotopic xenograft mouse model of osteosarcoma, intra-tumoral injection of *in vitro* activated and expanded NK cells and intraperitoneal IL-2 for 5 days limited bone damage and tumor growth, prevented lung metastases, and significantly prolonged mice survival (14). *Ex vivo* expanded NK cells with IL-15 and IL-21 injected after radiation therapy to mice with subcutaneous RMS slowed the tumor growth significantly (16). In another xenograft model of RMS, adoptive therapy of NK cells completely prevented the intraperitoneal implantation of RH30 tumor cells (17).

In the clinical setting, however, the specific NK-versus-sarcoma effect has only been studied in small case series. In one study, two patients with stage 4 EWS were in complete remission after haploidentical transplantation. Early post-transplant, their rapidly recovering NK cells demonstrated high cytotoxic activity against EWS cell lines *in vitro*, suggesting a potential role in systemic tumor control (18). In another study, one patient with relapsed metastatic RMS and one with EWS responded to a haploidentical transplantation after 3 lines of chemotherapy. The patient with RMS had a full donor NK genotype at 18 months post-transplantation and his NK cells exhibited high lysis of K562 cells, a classical target of NK cells due to their lack of HLA class I and II expression (19). These reports suggest that if the NK cells effector functions are maximized, clearance of high-risk sarcoma can be achieved.

THERAPEUTIC ENHANCEMENT OF NK CELL FUNCTIONS *VIA* ADCC

NK cells are the ideal candidate for adoptive therapy combined with mAbs targeting specific tumor antigens due to their unique mechanism of target cell lysis through ADCC mediated by their CD16 (FcγRIIIa) receptors (20). Multiple preclinical studies have shown the benefit of NK cells and mAbs in pediatric sarcomas (21–23). Several mAbs have been tested as single agent in phase I or II clinical trials, mainly in patients with osteosarcoma, including trastuzumab to target human epidermal growth factor receptor 2 (HER2) (24), cexutimab to target the epidermal growth factor receptor (EGFR) (25), glembatumumab-vedotin to target the glycoprotein non-metastatic B (GPNMB) (26), and dinutuxumab to target disialoganglioside GD2 (27). Cixutumumab, ganitumab, robatumumab, and figitumumab, targeting the insulin-like growth factor-1 receptor (IGF1R), have been tested in advanced RMS, EWS, and osteosarcoma (28, 29). Bevacizumab has been used to target vascular endothelial growth factor (VEGF) in RMS (30). Unfortunately, none of these clinical trials have shown a significant clinical benefit. Of note, most included patients with the tumor type of interest without restriction. Inclusion criteria based on the presence of predictive biomarkers identifying patients who would likely respond to these mAb are needed to determine the utility of these agents. The clinical response to mAb is also affected by a single nucleotide polymorphism in the FCGR3A (CD16) gene that affects binding affinity for IgG (increased affinity with valine at FCGR3A-158) (20).

Strategies to improve mAbs interactions with CD16 have been developed in other tumor types. Obinutuzumab, a humanized Fc-defucosylated anti-CD20 mAb, has an increased CD16 binding affinity, insensitive to CD16-V158F polymorphism (31). Bispecific or trispecific killer engagers have been generated and are composed of anti-CD16 Ab connected to the scFv of one or two of the tumor-antigen antibodies (31).

The ADCC can also be amplified by upregulating the expression of targeted surface antigens or by limiting their endocytosis. Kailayangari et al. demonstrated that the use of an enhancer of zeste homolog 2 (EZH2) inhibitor enhanced the expression of GD2 on the surface of EWS sarcoma cells, thus increasing their sensitivity to lysis by GD2 specific CAR-T cells (32). Prochlorperazine, used as anti-psychotic and anti-emetic agent in the clinic, reversibly inhibits dynamin-dependent endocytosis and, by enhancing target availability, improved the efficiency of NK cell-mediated ADCC by cetuximab, trastuzumab and avelumab in non-sarcoma solid tumor models (33).

Even though the mAbs bind to the activating receptor CD16 on NK cells, a potent activating signal, they have not shown positive results in pediatric sarcoma (20). Combination with adoptive NK cell therapy, small molecules or other strategies to amplify ADCC, as well as a better selection of patients to include in trials based on their tumor expression profile, could improve the mAbs efficacy.

MAXIMIZE EFFECTOR FUNCTIONS WITH CYTOKINES

Cytokines have raised interest as an adjuvant therapy in sarcomas since the 1980s. Mice treated with interferon (IFN)-α, IL-2, IL-12, IL-15, or IL-18 showed an increase in NK cell cytotoxicity against multiple sarcoma cell subtypes, but few have been translated successfully to the clinic (34). Pegylated IFN-2b in addition to conventional chemotherapy was tested in osteosarcoma in an international phase 3 clinical trial (35). Unfortunately, it showed no benefit as a maintenance therapy. This study had some limitations: approximately 45% of the patients did not start or complete the treatment with pegylated IFN-2b due to the intensity of treatment, patient's refusal, physician choice or toxicity (35). Similarly, IL-2 therapy is limited by its severe side-effects when used systematically (36). When administered

by aerosol in combination with NK cell infusion in a mouse model of metastatic pulmonary osteosarcoma, the NK cell number in the lungs was increased and IL-2 induced metastatic regression and improved overall survival of the animals (37). There is an ongoing clinical trial in metastatic osteosarcoma using aerosol IL-2 (NCT01590069). IL-15 was tested in a phase I clinical trial as a 10-day continuous infusion in 27 adults with advanced metastatic solid tumors, including 4 sarcomas (38). The maximum tolerated dose was reached, and 8 serious adverse events were reported including 2 deaths. A dramatic increase in NK cell number was induced: 38-fold in total circulating NK cells and 358-fold in the highly inflammatory $CD56^{bright}$ NK cell subset.

These reports demonstrate a clear activity of cytokines in boosting NK cell function in sarcoma, but the potential for toxicity make them difficult to apply in the clinic. The use of NK cells expanded and stimulated with cytokines before their therapeutic infusion, or the use of genetically modified NK cells may help overcome these limitations (12).

TIPPING THE BALANCE TOWARD ACTIVATION

There is a fine balance between activating and inhibitory signals regulating NK cell cytotoxicity and self-tolerance, and the tumor microenvironment (TME) of solid tumors is known to be immunosuppressive (39). A detailed characterization of the immune TME in sarcomas is lacking and it is currently unclear which approach should be applied to which type of sarcoma to target the TME appropriately (40). Proinflammatory cytokines, as discussed above, is a possible method. Immune checkpoint inhibitors reversing the exhausted phenotype of T cells are another strategy (12). However, the role of well-described T cell immune checkpoints such as PD-1, CTLA-4, TIM-3, and B7-H3 in the control of NK cell tolerance is unclear and they seem to promote different effects than those described and expected for T cells (41). Nevertheless, TIM-3 was found to be expressed on NK cells, and anti-TIM-3 antibody in combination with a superagonist of IL-15 (ALT-803) enhanced NK cell cytotoxicity against osteosarcoma cells *ex vivo* (42). Further, specific antibodies to block NK cell immune checkpoints have recently been developed and are currently undergoing trials in solid tumors, such as the anti-KIR mAb, lirilumab (NCT02813135), and the anti-NKG2A antibody, monalizumab (NCT02671435).

An alternative approach to break the self-tolerance and enhance NK cell anti-tumor activity is through their activating receptors. The ligands of the activating receptor NKG2D are upregulated following genotoxic stress such as viral infection or radiation therapy, alerting the immune system to potentially dangerous transformed or infected cells (12). The combination of NK cell and radiation therapy has shown promising results. Dogs with osteosarcoma die of metastatic progression to the lungs in 80% of the cases, but in a canine clinical trial, local radiation therapy before intralesional NK cell injection significantly increased NK cell homing to the tumor and, encouragingly, 50% of the dogs were metastasis-free 6 months after NK transfer (43).

Another method to avoid the inhibition of NK cells is the use of KIR-HLA mismatched cells. The interaction of KIR receptors on NK cells with their cognate HLA ligands provides a strong inhibitory signal preventing NK-mediated lysis of the self-target cells (8). Therefore, low MHC-I-expressing tumors are an ideal target for NK cells. MHC I downregulation or absence of expression has been reported in high-risk EWS and RMS (44). Osteosarcoma cells with surface expression of HLA molecules are less susceptible to killing by NK cells compared to cells lacking this expression (45). Similarly, KIR-HLA mismatching (i.e., donor cells expressing KIRs incompatible with recipient HLA ligands) can lessen the inhibitory signals from the sarcoma cells received by NK cells and result in enhanced anti-tumor function. Osteosarcoma cells target killing correlate with their degree of KIR-HLA incompatibility with the NK cells (45). Clinical data also demonstrate that KIR-mismatched NK cells exert enhanced antitumor activity in patients with solid tumors undergoing allogeneic HSCT and even in patients undergoing autologous HSCT (46, 47). A Japanese group has successfully developed KIR-mismatched cord-blood cells transplantation with reduced-intensity conditioning as a form of non-targeted immunotherapy (as the anti-GD2 antibodies are not approved by the regulatory authorities in Japan) to produce excellent outcomes in patients with high-risk neuroblastoma (48). KIR-mismatched stem cell transplantations have not been tested specifically in patients with pediatric sarcomas, but better overall responses were observed in patients who had undergone HLA-haploidentical stem cell transplantation with 1 to 2 KIR-HLA mismatches, when retrospectively studied (6, 46). Although not targeting sarcoma, anti-CD19 CAR-NK cells developed recently for relapsed or refractory anti-CD19-positive cancers have shown great clinical responses when produced from selected KIR-HLA mismatched cord-blood units (49).

These examples demonstrate the importance of breaking NK cell tolerance to enhance NK cell-versus-sarcoma activity, not only in the context of allogeneic stem cell transplant, but also of adoptive NK cell therapy.

ADOPTIVE THERAPY

NK cells for adoptive therapy can be derived from multiple autologous or allogeneic sources including peripheral blood, umbilical cord blood, $CD34^+$ hematopoietic progenitors, and human-induced pluripotent stem cells (12).

Multiple trials have tested adoptive NK cell (aNK) transfer post HSCT in high-risk sarcomas with the intent to amplify the graft-versus-tumor effect. In 2015, Shah et al. trialed donor-derived NK cell transfer in 9 children and young adults with high-risk solid tumors. The NK cells were activated *in vitro* with IL-15 and 4-1BBL and transferred following HLA-matched T cell depleted HSCT. Five patients with relapsed EWS and 1 with RMS were enrolled, and 3 of these 6 patients survived over 2 years, including 2 in complete remission. Interestingly, 5 of 9

transplant recipients experienced graft-versus-host disease following the NK cell infusion (50). Perez-Martinez et al. stimulated NK cells with IL-15 and infused them 30 days after haploidentical HSCT in 6 patients with high-risk solid tumors, including 3 EWS and 1 osteosarcoma, all with progressive disease (51). Four patients showed a clinical response (3 patients in partial remission of their tumor and 1 with stable disease). No toxicity secondary to the NK cell infusion was reported. Thakar et al. also tested adoptive transfer of donor NK cells post haploidentical HSCT in 14 patients with relapsed pediatric sarcomas (9 EWS, 4 RMS and 1 osteosarcoma) with stable disease, and demonstrated much better than expected survival in this high-risk population with an overall survival of 64% and 40% at 1 and 2 years respectively (75% and 45% for the EWS cohort) (52).

Outside of the post-HSCT context, aNK cells are only recently being tested in sarcoma with only 8 clinical trials ongoing, or recently completed (**Table 1**). Most of these trials are testing NK cell infusions in combination with a cytokine (IL-15 or IL-2) after chemotherapy conditioning with at least cyclophosphamide. The NK cells used are expanded from autologous or heterologous sources including universal donors, cord blood, or parental donors (haploidentical).

In a preliminary report, Chawla et al. tested activated autologous NK cells (SNK01) in a dose-escalation phase 1 study in patients with rapidly progressive metastatic solid tumors (53). Of the 7 patients enrolled so far, 5 had sarcomas and had received an average of 5 prior lines of therapy. The best overall response at 9 weeks was stable disease in 4 patients. No adverse events were reported and dose limiting toxicity had not been reached, but dose escalation is ongoing.

CAR-NK CELLS

CAR-NK cells are harder to engineer than CAR-T cells, but they are better tolerated and can be readily available as an allogeneic off-the-shelf product (54). CAR-NK cells maintain their ability to be activated by their innate receptors recognizing transformed cells, without prior antigen priming needed, while antigen recognition is redirected toward CAR-specific targets. Furthermore, CAR-NK cells can respond to levels of tumor-associated antigens that are too low to trigger ADCC (12).

In a phase I/II clinical trial of cord blood-derived CAR-NK cells treating patients with relapsed/refractory B-cell leukemia/lymphoma, the overall response rate was 73% including 64% with complete response (49). In contrast to large trials of CD19-directed CAR T-cell therapy with a comparable response rate of up to 80% (55), none of the patients showed evidence of neurotoxicity or cytokine-release syndrome. CAR-NK cells persisted up to 12 months after infusion.

In pediatric sarcoma, CAR-NK cells have shown anti-cancer activity *in vitro*. GD2-specific CAR-NK had an increased activity against EWS cells in an antigen-specific manner, but when

TABLE 1 | Clinical trials testing adoptive NK cell therapy in sarcoma.

Clinicaltrial.gov identifier	Tumor type included	NK cell type	Phase	Location	Methods	Status/ Publication
NCT02890758	Relapsed/refractory soft tissue sarcoma (EWS and RMS included)	Universal donor	I	USA	NK cell infusions (x2) +/- recombinant IL-15 - Dose escalation with 3 cell doses	Active, Not recruiting
NCT03420963	Relapsed/refractory solid tumor	Cord blood-derived expanded	I	USA	NK cell infusion (x1) on D8 - Conditioning with cyclophosphamide and etoposide (D1 to 5)	Recruiting
NCT03941262	Refractory cancer	*Ex-vivo* expanded autologous	I	USA	NK cell infusion weekly for 5 weeks +/- Avelumab or Pembrolizumab (anti-PD-L1 and anti-PD-1) - Dose escalation with 3 cell doses	Recruiting (53, ASCO abstract)
NCT04214730	Advanced solid tumor	*N/A*	?	China	NK cell infusion (x4) + chemotherapy vs chemotherapy only	Recruiting
NCT01875601	Relapsed/refractory solid tumor	Autologous activated	I	USA	NK cell infusion (x1) - Conditioning with cyclophosphamide +/- recombinant IL-15 - Dose escalation cell dose and IL-15	Completed (unpublished)
NCT02849366	Recurrent sarcoma	*N/A*	I/II	China	Cryosurgery +/- NK cells infusions (x3)	Completed (unpublished)
NCT03209869	Relapsed/refractory neuroblastoma and osteosarcoma	*Ex-vivo* expanded activated haploidentical	I	USA	NK cell infusion + humanized 14.18-IL2 (anti-GD2 immunocytokine) (D1 to 7)	Suspended (due to COVID-19)
NCT02409576	EWS, RMS	*Ex-vivo* expanded activated haploidentical	I/II	Singapore	NK cell infusion (x1) on D0 - Conditioning with cyclophosphamide, fludarabine and radiation 2Gy + IL-2	Unknown

This table outlines completed or ongoing clinical trials of NK cell adoptive therapy including patients with osteosarcoma, Ewing sarcoma or rhabdomyosarcoma. Underlined clinical trials include children. The aims of these clinical studies are to determine safety (phase I) and/or efficacy (phase II) of the interventional therapies. Most involve a conditioning with chemotherapy +/- radiation therapy before infusion of the cells (number of cell infusion planned in bracket), and cytokine injections to enhance the cell activity (IL-2 or IL-15). EWS, Ewing sarcoma; RMS, rhabdomyosarcoma; NK, natural killer; N/A, non available; Gy, Gray; D, Day.

transferred to mice with GD2-positive EWS xenografts they lacked efficiency due to inhibitory HLA-G hyper-expression on the tumor (56). Anti-receptor tyrosine kinase-like orphan receptor 1 (ROR1) CAR-NK cells also demonstrated significantly enhanced cytotoxicity *in vitro* against EWS and osteosarcoma cell lines compared to mock expanded NK cells (57). However, to date, there is no clinical trial of CAR-NK in sarcoma registered on clinicaltrial.gov.

Overall pre-clinical data in sarcoma and clinical trials of CAR-NK cells in other cancers show how promising CAR-NK cells could be as an immunotherapeutic approach in pediatric sarcomas.

CONCLUSION

NK cells have recently emerged as an exciting option to target sarcomas resistant to conventional anti-cancer therapy. Many immunotherapies use NK cells as one of the main effectors of their anti-cancer effect along with T cells, but this effect can be enhanced, and adoptive NK cell therapy and particularly CAR-NK cells are emerging from preclinical settings. Ongoing research appears promising to translate this into patient's benefit in the coming years.

AUTHOR CONTRIBUTIONS

Writing – original draft preparation, NO. Writing – review and editing, NO, WN, BR FS-F-G and GR. Figure creation - NO and BR. All authors contributed to the article and approved the submitted version.

FUNDING

NO is supported by the Queensland Children's Hospital and UQ PhD scholarship. FS-F-G is funded by a UQ Diamantina Institute laboratory start-up package, Australian and New Zealand Sarcoma Association Sarcoma Research Grant, a priority-driven collaborative cancer research scheme grant co-funded by Cancer Australia and Cure Cancer (#1158085), and a US Department of Defense – Breast Cancer Research Program – breakthrough award level 1 (#BC200025).

ACKNOWLEDGMENTS

The authors thank Timothy McCulloch for critical comments and editing support.

REFERENCES

1. Keegan TH, Ries LA, Barr RD, Geiger AM, Dahlke DV, Pollock BH, et al. Comparison of Cancer Survival Trends in the United States of Adolescents and Young Adults With Those in Children and Older Adults. *Cancer* (2016) 122(7):1009–16. doi: 10.1002/cncr.29869
2. Chen C, Dorado Garcia H, Scheer M, Henssen AG. Current and Future Treatment Strategies for Rhabdomyosarcoma. *Front Oncol* (2019) 9(1458). doi: 10.3389/fonc.2019.01458
3. Gill J, Gorlick R. Advancing Therapy for Osteosarcoma. *Nat Rev Clin Oncol* (2021) 18:609–24. doi: 10.1038/s41571-021-00519-8
4. Riggi N, Suvà ML, Stamenkovic I. Ewing's Sarcoma. *New Engl J Med* (2021) 384(2):154–64. doi: 10.1056/NEJMra2028910
5. Coley WBII. Contribution to the Knowledge of Sarcoma. *Ann Surg* (1891) 14 (3):199–220. doi: 10.1097/00000658-189112000-00015
6. Pérez-Martínez A, de Prada Vicente I, Fernández L, González-Vicent M, Valentín J, Martín R, et al. Natural Killer Cells can Exert a Graft-vs-Tumor Effect in Haploidentical Stem Cell Transplantation for Pediatric Solid Tumors. *Exp Hematol* (2012) 40(11):882–91.e1. doi: 10.1016/j.exphem.2012.07.004
7. Mehta RS, Rezvani K. Can We Make a Better Match or Mismatch With KIR Genotyping? *Hematology* (2016) 2016(1):106–18. doi: 10.1182/asheducation-2016.1.106
8. Pende D, Falco M, Vitale M, Cantoni C, Vitale C, Munari E, et al. Killer Ig-Like Receptors (KIRs): Their Role in NK Cell Modulation and Developments Leading to Their Clinical Exploitation. *Front Immunol* (2019) 10(1179). doi: 10.3389/fimmu.2019.01179
9. Boudreau JE, Hsu KC. Natural Killer Cell Education and the Response to Infection and Cancer Therapy: Stay Tuned. *Trends Immunol* (2018) 39 (3):222–39. doi: 10.1016/j.it.2017.12.001
10. Barrow AD, Martin CJ, Colonna M. The Natural Cytotoxicity Receptors in Health and Disease. *Front Immunol* (2019) 10:909–. doi: 10.3389/fimmu.2019.00909
11. Sivori S, Vacca P, Del Zotto G, Munari E, Mingari MC, Moretta L. Human NK Cells: Surface Receptors, Inhibitory Checkpoints, and Translational Applications. *Cell Mol Immunol* (2019) 16(5):430–41. doi: 10.1038/s41423-019-0206-4
12. Souza-Fonseca-Guimaraes F, Cursons J, Huntington ND. The Emergence of Natural Killer Cells as a Major Target in Cancer Immunotherapy. *Trends Immunol* (2019) 40(2):142–58. doi: 10.1016/j.it.2018.12.003
13. Cho D, Shook DR, Shimasaki N, Chang Y-H, Fujisaki H, Campana D. Cytotoxicity of Activated Natural Killer Cells Against Pediatric Solid Tumors. *Clin Cancer Res* (2010) 16(15):3901–9. doi: 10.1158/1078-0432.CCR-10-0735
14. Fernández L, Valentín J, Zalacain M, Leung W, Patiño-García A, Pérez-Martínez A. Activated and Expanded Natural Killer Cells Target Osteosarcoma Tumor Initiating Cells in an NKG2D-NKG2DL Dependent Manner. *Cancer Lett* (2015) 368(1):54–63. doi: 10.1016/j.canlet.2015.07.042
15. Tong AA, Hashem H, Eid S, Allen F, Kingsley D, Huang AY. Adoptive Natural Killer Cell Therapy is Effective in Reducing Pulmonary Metastasis of Ewing Sarcoma. *Oncoimmunology* (2017) 6(4):e1303586. doi: 10.1080/2162402X.2017.1303586
16. Wagner J, Pfannenstiel V, Waldmann A, Bergs JWJ, Brill B, Huenecke S, et al. A Two-Phase Expansion Protocol Combining Interleukin (IL)-15 and IL-21 Improves Natural Killer Cell Proliferation and Cytotoxicity Against Rhabdomyosarcoma. *Front Immunol* (2017) 8:676. doi: 10.3389/fimmu.2017.00676
17. Vela M, Bueno D, González-Navarro P, Brito A, Fernández L, Escudero A, et al. Anti-CXCR4 Antibody Combined With Activated and Expanded Natural Killer Cells for Sarcoma Immunotherapy. *Front Immunol* (2019) 10 (1814). doi: 10.3389/fimmu.2019.01814
18. Schlegel P, Feuchtinger T, Nitschke-Gérard C, Seidel UJ, Lang AM, Kyzirakos C, et al. Favorable NK Cell Activity After Haploidentical Hematopoietic Stem Cell Transplantation in Stage IV Relapsed Ewing's Sarcoma Patients. *Bone marrow Transplant* (2015) 50(Suppl 2):S72–6. doi: 10.1038/bmt.2015.100
19. Pérez-Martínez A, Leung W, Muñoz E, Iyengar R, Ramírez M, Vicario JL, et al. KIR–HLA Receptor-Ligand Mismatch Associated With a Graft-Versus-Tumor Effect in Haploidentical Stem Cell Transplantation for Pediatric Metastatic Solid Tumors. *Pediatr Blood Cancer* (2009) 53(1):120–4. doi: 10.1002/pbc.21955
20. Capuano C, Pighi C, Battella S, De Federicis D, Galandrini R, Palmieri G. Harnessing CD16-Mediated NK Cell Functions to Enhance Therapeutic Efficacy of Tumor-Targeting Mabs. *Cancers* (2021) 13(10):2500. doi: 10.3390/cancers13102500

21. Chu Y, Nayyar G, Jiang S, Rosenblum JM, Soon-Shiong P, Safrit JT, et al. Combinatorial Immunotherapy of N-803 (IL-15 Superagonist) and Dinutuximab With *Ex Vivo* Expanded Natural Killer Cells Significantly Enhances In Vitro Cytotoxicity Against GD2(+) Pediatric Solid Tumors and *In Vivo* Survival of Xenografted Immunodeficient NSG Mice. *J Immunother Cancer* (2021) 9(7):e002267. doi: 10.1136/jitc-2020-002267
22. Jamitzky S, Krueger AC, Janneschuetz S, Piepke S, Kailayangiri S, Spurny C, et al. Insulin-Like Growth Factor-1 Receptor (IGF-1R) Inhibition Promotes Expansion of Human NK Cells Which Maintain Their Potent Antitumor Activity Against Ewing Sarcoma Cells. *Pediatr Blood Cancer* (2015) 62 (11):1979–85. doi: 10.1002/pbc.25619
23. Pahl JH, Ruslan SE, Buddingh EP, Santos SJ, Szuhai K, Serra M, et al. Anti-EGFR Antibody Cetuximab Enhances the Cytolytic Activity of Natural Killer Cells Toward Osteosarcoma. *Clin Cancer Res* (2012) 18(2):432–41. doi: 10.1158/1078-0432.CCR-11-2277
24. Ebb D, Meyers P, Grier H, Bernstein M, Gorlick R, Lipshultz SE, et al. Phase II Trial of Trastuzumab in Combination With Cytotoxic Chemotherapy for Treatment of Metastatic Osteosarcoma With Human Epidermal Growth Factor Receptor 2 Overexpression: A Report From the Children's Oncology Group. *J Clin Oncol* (2012) 30(20):2545–51. doi: 10.1200/JCO.2011.37.4546
25. Ha HT, Griffith KA, Zalupski MM, Schuetze SM, Thomas DG, Lucas DR, et al. Phase II Trial of Cetuximab in Patients With Metastatic or Locally Advanced Soft Tissue or Bone Sarcoma. *Am J Clin Oncol* (2013) 36(1):77–82. doi: 10.1097/COC.0b013e31823a4970
26. Kopp LM, Malempati S, Krailo M, Gao Y, Buxton A, Weigel BJ, et al. Phase II Trial of the Glycoprotein non-Metastatic B-Targeted Antibody-Drug Conjugate, Glembatumumab Vedotin (CDX-011), in Recurrent Osteosarcoma AOST1521: A Report From the Children's Oncology Group. *Eur J Cancer* (2019) 121:177–83. doi: 10.1016/j.ejca.2019.08.015
27. Hingorani P, Krailo MD, Buxton A, Hutson PR, Davis J, Janeway KA, et al. Phase II Study of Antidisialoganglioside Antibody, Dinutuximab, in Combination With GM-CSF in Patients With Recurrent Osteosarcoma (AOST1421): A Report From the Children's Oncology Group. *J Clin Oncol* (2020) 38(15_suppl):10508–. doi: 10.1200/JCO.2020.38.15_suppl.10508
28. Anderson PM, Bielack SS, Gorlick RG, Skubitz K, Daw NC, Herzog CE, et al. A Phase II Study of Clinical Activity of SCH 717454 (Robatumumab) in Patients With Relapsed Osteosarcoma and Ewing Sarcoma. *Pediatr Blood Cancer* (2016) 63(10):1761–70. doi: 10.1002/pbc.26087
29. Weigel B, Malempati S, Reid JM, Voss SD, Cho SY, Chen HX, et al. Phase 2 Trial of Cixutumumab in Children, Adolescents, and Young Adults With Refractory Solid Tumors: A Report From the Children's Oncology Group. *Pediatr Blood Cancer* (2014) 61(3):452–6. doi: 10.1002/pbc.24605
30. Mascarenhas L, Chi YY, Hingorani P, Anderson JR, Lyden ER, Rodeberg DA, et al. Randomized Phase II Trial of Bevacizumab or Temsirolimus in Combination With Chemotherapy for First Relapse Rhabdomyosarcoma: A Report From the Children's Oncology Group. *J Clin Oncol* (2019) 37 (31):2866–74. doi: 10.1200/JCO.19.00576
31. Mössner E, Brünker P, Moser S, Püntener U, Schmidt C, Herter S, et al. Increasing the Efficacy of CD20 Antibody Therapy Through the Engineering of a New Type II Anti-CD20 Antibody With Enhanced Direct and Immune Effector Cell-Mediated B-Cell Cytotoxicity. *Blood* (2010) 115(22):4393–402. doi: 10.1182/blood-2009-06-225979
32. Kailayangiri S, Altvater B, Lesch S, Balbach S, Göttlich C, Kühnemundt J, et al. EZH2 Inhibition in Ewing Sarcoma Upregulates GD2 Expression for Targeting With Gene-Modified T Cells. *Mol Ther* (2019) 27(5):933–46. doi: 10.1016/j.ymthe.2019.02.014
33. Chew HY, De Lima PO, Gonzalez Cruz JL, Banushi B, Echejoh G, Hu L, et al. Endocytosis Inhibition in Humans to Improve Responses to ADCC-Mediating Antibodies. *Cell* (2020) 180(5):895–914.e27. doi: 10.1016/j.cell.2020.02.019
34. Lachota M, Vincenti M, Winiarska M, Boye K, Zagożdżon R, Malmberg K-J. Prospects for NK Cell Therapy of Sarcoma. *Cancers* (2020) 12(12):3719. doi: 10.3390/cancers12123719
35. Bielack SS, Smeland S, Whelan JS, Marina N, Jovic G, Hook JM, et al. Methotrexate, Doxorubicin, and Cisplatin (MAP) Plus Maintenance Pegylated Interferon Alfa-2b Versus MAP Alone in Patients With Resectable High-Grade Osteosarcoma and Good Histologic Response to Preoperative MAP: First Results of the EURAMOS-1 Good Response Randomized Controlled Trial. *J Clin Oncol* (2015) 33(20):2279–87. doi: 10.1200/JCO.2014.60.0734
36. Schwinger W, Klass V, Benesch M, Lackner H, Dornbusch HJ, Sovinz P, et al. Feasibility of High-Dose Interleukin-2 in Heavily Pretreated Pediatric Cancer Patients. *Ann Oncol* (2005) 16(7):1199–206. doi: 10.1093/annonc/mdi226
37. Guma SR, Lee DA, Ling Y, Gordon N, Kleinerman ES. Aerosol Interleukin-2 Induces Natural Killer Cell Proliferation in the Lung and Combination Therapy Improves the Survival of Mice With Osteosarcoma Lung Metastasis. *Pediatr Blood Cancer* (2014) 61(8):1362–8. doi: 10.1002/pbc.25019
38. Conlon KC, Potter EL, Pittaluga S, Lee C-CR, Miljkovic MD, Fleisher TA, et al. IL15 by Continuous Intravenous Infusion to Adult Patients With Solid Tumors in a Phase I Trial Induced Dramatic NK-Cell Subset Expansion. *Clin Cancer Res* (2019) 25(16):4945–54. doi: 10.1158/1078-0432.CCR-18-3468
39. Rossi GR, Trindade ES, Souza-Fonseca-Guimaraes F. Tumor Microenvironment-Associated Extracellular Matrix Components Regulate NK Cell Function. *Front Immunol* (2020) 11(73). doi: 10.3389/fimmu.2020.00073
40. Terry RL, Meyran D, Fleuren EDG, Mayoh C, Zhu J, Omer N, et al. Chimeric Antigen Receptor T Cell Therapy and the Immunosuppressive Tumor Microenvironment in Pediatric Sarcoma. *Cancers* (2021) 13(18):4704. doi: 10.3390/cancers13184704
41. McCulloch TR, Wells TJ, Souza-Fonseca-Guimaraes F. Towards Efficient Immunotherapy for Bacterial Infection. *Trends Microbiol* (2021). doi: 10.1016/j.tim.2021.05.005
42. Chu Y, Rosenblum J, Jeng EK, Alter S, Rhode PR, Lee JH, et al. Efficiently Targeting Metastatic Osteosarcoma, Neuroblastoma and Glioblastoma With Ex-Vivo Expanded Natural Killer Cells Combined With N-803 (ALT-803, IL-15 Superagonist) and TIM-3 Blockage. *Biol Blood Marrow Transplant* (2019) 25(3, Supplement):S336. doi: 10.1016/j.bbmt.2018.12.543
43. Canter RJ, Grossenbacher SK, Foltz JA, Sturgill IR, Park JS, Luna JI, et al. Radiotherapy Enhances Natural Killer Cell Cytotoxicity and Localization in Pre-Clinical Canine Sarcomas and First-in-Dog Clinical Trial. *J Immunother Cancer* (2017) 5(1):98. doi: 10.1186/s40425-017-0305-7
44. Haworth KB, Leddon JL, Chen C-Y, Horwitz EM, Mackall CL, Cripe TP. Going Back to Class I: MHC and Immunotherapies for Childhood Cancer. *Pediatr Blood Cancer* (2015) 62(4):571–6. doi: 10.1002/pbc.25359
45. Delgado D, Webster DE, DeSantes KB, Durkin ET, Shaaban AF. KIR Receptor-Ligand Incompatibility Predicts Killing of Osteosarcoma Cell Lines by Allogeneic NK Cells. *Pediatr Blood Cancer* (2010) 55(7):1300–5. doi: 10.1002/pbc.22665
46. Leung W, Handgretinger R, Iyengar R, Turner V, Holladay MS, Hale GA. Inhibitory KIR-HLA Receptor-Ligand Mismatch in Autologous Haematopoietic Stem Cell Transplantation for Solid Tumour and Lymphoma. *Br J Cancer* (2007) 97(4):539–42. doi: 10.1038/sj.bjc.6603913
47. Venstrom JM, Zheng J, Noor N, Danis KE, Yeh AW, Cheung IY, et al. KIR and HLA Genotypes are Associated With Disease Progression and Survival Following Autologous Hematopoietic Stem Cell Transplantation for High-Risk Neuroblastoma. *Clin Cancer Res* (2009) 15(23):7330–4. doi: 10.1158/1078-0432.CCR-09-1720
48. Matsuno R, Toyama D, Akiyama K, Isoyama K, Shiozawa E, Yamamoto S. Killer-Cell Immunoglobulin-Like Receptor Ligand Mismatch Cord Blood Transplantation in High-Risk Neuroblastoma. *Pediatr Int* (2019) 61(6):566–71. doi: 10.1111/ped.13861
49. Liu E, Marin D, Banerjee P, Macapinlac HA, Thompson P, Basar R, et al. Use of CAR-Transduced Natural Killer Cells in CD19-Positive Lymphoid Tumors. *New Engl J Med* (2020) 382(6):545–53. doi: 10.1056/NEJMoa1910607
50. Shah NN, Baird K, Delbrook CP, Fleisher TA, Kohler ME, Rampertaap S, et al. Acute GVHD in Patients Receiving IL-15/4-1BBL Activated NK Cells Following T-Cell-Depleted Stem Cell Transplantation. *Blood* (2015) 125 (5):784–92. doi: 10.1182/blood-2014-07-592881
51. Pérez-Martínez A, Fernández L, Valentín J, Martínez-Romera I, Corral MD, Ramírez M, et al. A Phase I/II Trial of Interleukin-15–Stimulated Natural Killer Cell Infusion After Haplo-Identical Stem Cell Transplantation for Pediatric Refractory Solid Tumors. *Cytotherapy* (2015) 17(11):1594–603. doi: 10.1016/j.jcyt.2015.07.011
52. Thakar MS, Browning M, Hari P, Charlson JA, Margolis DA, Logan B, et al. Phase II Trial Using Haploidentical Hematopoietic Cell Transplantation

(HCT) Followed by Donor Natural Killer (NK) Cell Infusion and Sirolimus Maintenance for Patients With High-Risk Solid Tumors. *J Clin Oncol* (2020) 38(15_suppl):e23551. doi: 10.1200/JCO.2020.38.15_suppl.e23551

53. Chawla SP, Kim KM, Chua VS, Jafari O, Song PY. Phase I Study of SNK01 (Autologous Non-Genetically Modified Natural Killer Cells With Enhanced Cytotoxicity) in Refractory Metastatic Solid Tumors. *J Clin Oncol* (2020) 38(15_suppl):e15024. doi: 10.1200/JCO.2020.38.15_suppl.e15024
54. Xie G, Dong H, Liang Y, Ham JD, Rizwan R, Chen J. CAR-NK Cells: A Promising Cellular Immunotherapy for Cancer. *EBioMedicine* (2020) 59:102975. doi: 10.1016/j.ebiom.2020.102975
55. Anagnostou T, Riaz IB, Hashmi SK, Murad MH, Kenderian SS. CD19 Directed Chimeric Antigen Receptor T Cell Therapy in Acute Lymphoblastic Leukemia: A Systematic Review and Meta-Analysis. *Biol Blood Marrow Transplant* (2019) 25(3, Supplement):S169–70. doi: 10.1016/j.bbmt.2018.12.308
56. Kailayangiri S, Altvater B, Spurny C, Jamitzky S, Schelhaas S, Jacobs AH, et al. Targeting Ewing Sarcoma With Activated and GD2-Specific Chimeric Antigen Receptor-Engineered Human NK Cells Induces Upregulation of Immune-Inhibitory HLA-G. *Oncoimmunology* (2016) 6(1):e1250050. doi: 10.1080/2162402X.2016.1250050
57. Park H, Awasthi A, Ayello J, Chu Y, Riddell S, Rosenblum J, et al. 108 - ROR1-Specific Chimeric Antigen Receptor (CAR) NK Cell Immunotherapy for High Risk Neuroblastomas and Sarcomas. *Biol Blood Marrow Transplant* (2017) 23 (3, Supplement):S136–S7. doi: 10.1016/j.bbmt.2017.01.056

Conflict of Interest: FS-F-G is a consultant and has a funded research agreement with Biotheus Inc.

The remaining authors declare that the research was conducted in the absence of any commercial or financial relationships that could be construed as a potential conflict of interest.

Publisher's Note: All claims expressed in this article are solely those of the authors and do not necessarily represent those of their affiliated organizations, or those of the publisher, the editors and the reviewers. Any product that may be evaluated in this article, or claim that may be made by its manufacturer, is not guaranteed or endorsed by the publisher.

frontiers in Oncology

REVIEW
published: 19 November 2021
doi: 10.3389/fonc.2021.772862

Immunotherapy and Radioimmunotherapy for Desmoplastic Small Round Cell Tumor

*Madelyn Espinosa-Cotton and Nai-Kong V. Cheung**

Department of Pediatrics, Memorial Sloan Kettering Cancer Center, New York, NY, United States

Desmoplastic small round cell tumor (DRSCT) is a highly aggressive primitive sarcoma that primarily affects adolescent and young adult males. The 5-year survival rate is 15-30% and few curative treatment options exist. Although there is no standard treatment for DSRCT, patients are most often treated with a combination of aggressive chemotherapy, radiation, and surgery. Targeted therapy inhibitors of PDGFA and IGF-1R, which are almost uniformly overexpressed in DSRCT, have largely failed in clinical trials. As in cancer in general, interest in immunotherapy to treat DSRCT has increased in recent years. To that end, several types of immunotherapy are now being tested clinically, including monoclonal antibodies, radionuclide-conjugated antibodies, chimeric antigen receptor T cells, checkpoint inhibitors, and bispecific antibodies (BsAbs). These types of therapies may be particularly useful in DSRCT, which is frequently characterized by widespread intraperitoneal implants, which are difficult to completely remove surgically and are the frequent cause of relapse. Successful treatment with immunotherapy or radioimmunotherapy following debulking surgery could eradiate these micrometasteses and prevent relapse. Although there has been limited success to date for immunotherapy in pediatric solid tumors, the significant improvements in survival seen in the treatment of other pediatric solid tumors, such as metastatic neuroblastoma and its CNS spread, suggest a potential of immunotherapy and specifically compartmental immunotherapy in DSRCT.

Keywords: DSRCT = desmoplastic small round cell tumor, antibodies, immunotherapy, targeted therapy, radioimmunotherapy, CAR T cell

OPEN ACCESS

Edited by:
Pouya Faridi,
Monash University, Australia

Reviewed by:
Pingping Chen,
University of Miami, United States
Tomas Sjöberg Bexelius,
Karolinska Institutet (KI), Sweden

***Correspondence:**
Nai-Kong V. Cheung
cheungn@mskcc.org

Specialty section:
This article was submitted to Cancer Immunity and Immunotherapy, a section of the journal Frontiers in Oncology

Received: *08 September 2021*
Accepted: *02 November 2021*
Published: *19 November 2021*

Citation:
Espinosa-Cotton M and Cheung N-KV (2021) Immunotherapy and Radioimmunotherapy for Desmoplastic Small Round Cell Tumor. Front. Oncol. 11:772862. doi: 10.3389/fonc.2021.772862

INTRODUCTION

Background

Desmoplastic small round cell tumor (DRSCT) was first described in 1989 by Gerald and Rosai as a highly aggressive primitive sarcoma characterized by nests of blue-staining tumor cells surrounded by dense stroma. Of note was the fact that these tumor cells were positive for markers of mesenchymal, neural, and epithelial lineages, suggesting that they may arise from

undifferentiated progenitor cells (1, 2). A (11:22), (p13:q12) chromosomal translocation is present in all cases, resulting in an EWS-WT1 gene fusion product (3–5). This feature is considered pathognomonic and is required for its definitive diagnosis (6). DSRCT is rare, with an age-adjusted incidence rate of 0.3/million in the United States (7), and primarily arises in adolescent and young adult males, with around 80% of patients being male and an average age of 18-22 years at diagnosis (2, 8). It may disproportionately affect African Americans (7, 9). Overall 5-year survival is a dismal 15-30% (7, 10).

Clinical Presentation and Staging

Most patients initially present with abdominal pain and distension, evidence of ascites caused by extensive tumor seeding of the peritoneum (6). The vast majority (>90%) of primary tumors are found on the serosal surfaces of the abdomen, but others have been found in the thoracic cavity, the skull, or even the hand (8). Rarely, early-stage DSRCT is discovered incidentally during surgery or imaging for other indications. More commonly, however, the disease has spread extensively and is considered Stage IV at the time of diagnosis. Because of this, a new staging system for DSRCT has been proposed by Hayes-Jordan and colleagues: Stage I would include patients with one or two abdominal tumors, Stage II would include patients with extensive peritoneal spread, Stage III would include patients with peritoneal disease plus liver metastases, and Stage IV would include patients with disease that has spread outside the abdomen (6).

Treatment

There is no standard therapy for DSRCT. Treatment typically consists of multimodal neoadjuvant chemotherapy followed by surgery and radiation. Treatment with the P6 protocol – cyclophosphamide, doxorubicin and vincristine alternating with ifosfamide and etoposide – is used in the United States, whereas a slightly different protocol used to treat Ewing Sarcoma patients (vincristine, doxorubicin, and cyclophosphamide alternating with ifosfamide and etoposide) is the most common regimen in other parts of the world (11, 12). Because of the extent of disease spread within the peritoneal cavity, surgery is most effective after neoadjuvant chemotherapy, since these tumors are typically responsive to chemotherapy and either shrink or become less vascularized (6). Complete surgical resection of all visible tumors was found to be essential for survival beyond 3 years, with 58% of patients who underwent complete resection surviving to 3 years compared to 0% of patients whose tumors were not resected and instead received only chemotherapy and radiation (10). While surgical excision of all visible tumors is critical, it may be impossible to remove every tumor cell from the peritoneal cavity. Hyperthermic intraperitoneal chemotherapy (HIPEC) has been proposed as a treatment for microscopic residual disease after complete surgical resection. A recent phase II clinical trial showed that HIPEC using cisplatin is effective at improving survival, with a 3-year overall survival rate of 79% (13). However, this treatment modality does not appear effective for patients whose tumors were not able to be completely removed during surgery (14). Whole abdominopelvic irradiation has also been used to treat residual disease following surgery and appears to reduce the incidence of peritoneal relapse, however, severe gastrointestinal and hematopoietic toxicity is common (15, 16). Intensity modulated radiation therapy reduces grade 2-4 toxicities without compromising efficacy (17). Autologous stem cell transplant has been investigated and does not appear to improve outcomes for DSRCT patients (18); allogenic stem cell transplant could be an alternative (19). Several clinical trials are currently underway to test new combinations of chemotherapy and targeted therapy (**Table 1**). Progress has been made in extending survival, however, cures are rare.

TABLE 1 | Current clinical trials using chemotherapy and targeted therapy for DSRCT.

Trial	Phase	Therapy	Status	Study term	Actual Enrollment
NCT01189643	Early 1	Irinotecan, temozolomide and bevacizumab in combination with existing high dose alkylator based chemotherapy	Active, not recruiting	08/2010 – 08/2022	15
NCT03478462	1	CLR 131 (phosopholipid drug conjugate)	Recruiting	04/2019 – 12/2024	30*
NCT03600649	1	Seclidemstat (LSD1 inhibitor)	Recruiting	06/2018 – 12/2021	50*
NCT04145349	1/2	Ramucirumab, cyclophosphamide, vinorelbine	Recruiting	01/2020 – 01/2024	34*
NCT04095221	1/2	Prexasertib, irinotecan, temozolomide	Recruiting	09/2019 – 09/2022	30*
NCT04901806	1/2	PBI-200 (TRK inhibitor)	Recruiting	07/2021 – 06/2024	74*
NCT01946529	2	Vincristine, doxorubicin, cyclophosphamide, ifosfamide, etoposide, temozolomide, temsirolimus, bevacizumab, sorafenib, surgery, and radiation	Active, not recruiting	12/2013 – 07/2026	24
NCT03275818	2	Nab-paclitaxel	Active, not recruiting	05/2017 – 05/2021	60*

**For ongoing studies the estimated enrollment is provided in lieu of actual enrollment.*

MUTATIONS, TARGETS, AND DYSREGULATED PATHWAYS

Many common mutations have been found in DSRCT (**Table 2**), some of which have been explored as targets for therapy. Several of these are targets of the EWS-WT1 fusion protein, which is present in every case of DSRCT and is required for positive diagnosis (6). This protein results from a chromosomal translocation involving breakage of chromosomes 11 and 22 at sites of genes known to be involved in Wilms' tumor (*WT1*) and Ewing's sarcoma (*EWSR1*), respectively (20). *WT1* is a tumor suppressor gene encoding a transcription factor (WT1) that generally represses gene expression and was first noted for its deletion in Wilms' tumor (21, 22). Fusion of the transcription-activating N-terminal domain of *EWS* to a set of zinc fingers in *WT1* produces a unique transcription factor capable of upregulating a number of genes that promote tumor progression, many of which are repressed by wild-type WT1 (20).

Platelet-Derived Growth Factor A

One of the most well-characterized gene targets of EWS-WT1 is *PDGFA*, whose role in DSRCT was first described by Haber and colleagues in 1997, just a few years after the identification of DSRCT as a distinct malignancy (23). This group found that *PDGFA* was upregulated in an osteosarcoma cell line following induced expression of EWS-WT1 (23). Additionally, *PDGFA* expression was found in 13/14 DSRCT tumor specimens and correlated with expression of EWS-WT1 (23). These results and subsequent publications (24, 25) confirming the role of *PDGFA* in DSRCT laid the groundwork for clinical trials using imatinib mesylate, a tyrosine kinase inhibitor that targets *abl*, c-Kit, and PDGF receptor (PDGFR) and is known for its use in the treatment of chronic myelogenous leukemia (26). Unfortunately none of these trials have shown any efficacy in DSRCT (27–29).

Insulin-Like Growth Factor 1 Receptor (IGF-1R)

Another target of EWS-WT1 is IGF-1R, a tyrosine kinase receptor that is frequently upregulated in cancer cells, leading to dysregulation of the IGF pathway (30). There are several reports of DSRCT patients presenting with severe hypoglycemia as a result of an elevated IGF-II : IGF-I ratio, a consequence of IGF pathway dysregulation (31, 32). Several IGF inhibitors have been tested in DSRCT patients in early phase clinical trials. In a phase II trial of 16 DSRCT patients treated with ganitumab [monoclonal antibody (mAb) IGF-1R inhibitor], 25% (4/16) achieved clinical benefit (PR + SD ≥ 24 weeks) (33). In another study combining cixutumumab (mAb IGF-1R inhibitor) and temsirolimus (mTOR inhibitor) in 20 patients with Ewing's sarcoma family tumors, two DSRCT patients achieved partial tumor regression and one progressed (34).

Androgen Receptor (AR)

Because DSRCT predominantly affects male patients, it has been hypothesized that androgen receptor (AR) could play a role in this disease. In one study of 27 patients with end-stage DSRCT, 10 (37%) had tumors that were positive for AR by IHC (35). Among the 10 AR-positive patients, 6 had been treated with combined androgen blockade (CAB). Three responded, with either stable disease or a reduction in tumor burden, though

TABLE 2 | Mutations and dysregulated pathways in DSRCT.

Mutation/pathway	Source material	Publication year	PMID
Acetylcholine receptor (AChR)	2 tumor specimens	2008	18568996
Androgen receptor (AR)	27 tumor specimens	2007	16896931
	7 tumor specimens	2017	28415643
BAIAP3 promoter	2 tumor specimens	2002	12498718
B7-H3	37 tumor specimens	2001	11358824
Connective tissue growth factor (CCN2)	3 tumor specimens	2004	15047749
c-Kit	27 tumor specimens	2007	16896931
DNA damage-response pathway	7 tumor specimens	2018	30486883
	2 PDX models	2019	30563935
Epidermal growth factor receptor (EGFR)	12 tumor specimens	2015	25906748
EMT/MET	7 tumor specimens	2018	30486883
	7 tumor specimens	2017	28415643
Equilibrative nucleotide transporter 4 (ENT4)	4 tumor specimens	2008	18523561
EWS-WT1	5 tumor specimens	1994	8187063
GD2	20 tumor specimens	2016	27304202
HER2	1 patient	2015	25800760
	23 patient specimens	2003	12640103
IL-2/15Rbeta	16 tumor specimens	2002	11960373
Insulin growth factor receptor I (IGF-1R)	2 EWS/WT1-transduced osteosarcoma cell lines	1996	8702614
LRRC15	8 tumor specimens	2003	12923058
PI3K/Akt/mTOR	1 tumor specimen	2013	23922674
	10 tumor specimens	2014	25119929
PDGFA	5 tumor specimens	1997	9354795
MET	10 tumor specimens	2014	25119929
NTRK3	2 cell lines, 2 tumor specimens, 3 PDX models	2020	33229458
TGFbeta	10 tumor specimens	1999	10074970

these responses were not durable, lasting only 3-4 months. The patients who responded to CAB had normal testosterone levels, whereas the patients who did not respond had castrate levels of testosterone, which could explain the lack of efficacy of CAB (35). A subsequent study found that AR-positive tumors were enriched for markers of stemness, which could also partially explain why the response to CAB in AR-positive patients with normal testosterone levels was short-lived (36).

In addition to the targets above, numerous other potential targets have been identified and are in various stages of pre-clinical investigation (**Table 2**). These include pathways common to many types of cancer (DNA damage-response pathway, epithelial-mesenchymal transition) as well as receptors that have been identified as overexpressed or activated specifically in DSRCT as targets of the EWS-WT1 transcription factor (LRRC15, NTRK3).

Targets for Immunotherapy

A suitable target for immunotherapy must be expressed consistently on tumor cells but be restricted in its normal tissue expression to prevent on-target, off-tumor toxicity. Several appropriate targets have been identified in DSRCT. B7-H3 (targeted by the monoclonal antibody 8H9) is expressed in almost all DSRCT (35/37 tumors in one study (37), 44/46 in another) (38). It is tightly regulated by microRNA-29; despite universal transcription in most normal tissues, protein expression is highly restricted (39). Its hepatic expression explained the liver sequestration after intravenous injection, forcing its clinical development into compartmental administrations (NCT00582608). A clinical trial using intraperitoneal compartmental RIT using ^{131}I-8H9 in DSRCT is ongoing (NCT01099644). Two studies have found GD2 expression in DSRCT, albeit to varying degrees (32/36 in one study (38), 2/20 in another.) (40) A T-cell engaging bispecific antibody (BsAb) trial is currently open for GD2(+) DSRCT (NCT03860207). EGFR, which is frequently mutated or overexpressed in cancer, was found to be amplified in 2/10 (20%) DSRCT tumors (41), and an EGFR CAR T cell trial for children and young adults with refractory/recurrent solid tumors (including DSRCT) is currently underway (NCT03618381). Another phase I CAR T cell trial was carried out for patients with HER2-positive sarcomas and the one DSRCT patient included achieved stable disease for 14 months (42). In a study assessing expression of various markers in DSRCT, HER2 was found to be expressed in 7/18 tumors, albeit at a low level for the majority of the positive-staining tumors (43). The use of these targets for immunotherapy in DSRCT is discussed in more detail below.

IMMUNOTHERAPY AND RADIOIMMUNOTHERAPY FOR DSRCT

Although there has been a relatively recent resurgence in interest in cancer immunotherapy, the practice of using immunomodulatory agents to activate an anti-tumor immune response is over a hundred years old (44). Immunotherapy holds the potential for durable responses and even cures of metastatic disease. Immune cells activated against the tumor can seek out and destroy micrometastases and prevent recurrence. This type of treatment is particularly useful in DSRCT because of the extensive intraperitoneal seeding that typically has occurred at the time of diagnosis. While it is practically impossible to surgically remove every tumor cell when there are often dozens or hundreds of tumor implants on the peritoneum, removing all visible tumors surgically and following up with consolidation treatment to "clean up" leftover tumor cells is a viable strategy already in use for DSRCT in the form of HIPEC and abdominal radiation (14, 15, 17).

Another way in which immunotherapy is particularly well-suited for DSRCT and other cancers that affect mainly children and young adults is the lack of long-term adverse effects, or at least side effects that do not overlap with classic genotoxic chemoradiotherapy. Because these patients are treated early in life, any lasting adverse effects of treatment have the potential to impact them for decades. Furthermore, some treatments, including cranial radiation and intrathecal chemotherapy used to treat CNS metastases, have the potential to cause cognitive deficits and endocrinopathies (45). Although the wide-spread use of immunotherapy in children and young adults is relatively new, it also appears to be generally safe, though long-term follow-up will be required to identify any late adverse effects.

Because of these enormous potential benefits, various types of immunotherapy are being investigated for DSRCT. A summary of current clinical trials involving immunotherapy for DSRCT, and their molecular targets can be found in **Table 3**. Cellular targets that have been used for immunotherapy in other types of cancer have been identified on DSRCT tumors. For example, GD2 is reportedly expressed on the surface of DSRCT and is the target of a clinical trial (NCT00445965) employing the radionuclide-conjugated anti-GD2 antibody ^{131}I-3F8 for patients with DSRCT and other tumors that either spread to or originate in the CNS. Neuroblastoma cells uniformly express GD2 and the use of monoclonal antibody therapy in high-risk neuroblastoma has been particularly encouraging (46).

Antibody-Based Therapies

Several types of antibody-based therapies are used in the treatment of cancer, all of which rely on the specificity of an antibody-antigen interaction and require an appropriate tumor antigen to be identified that is expressed highly in tumor tissue and not in normal tissue. The most basic antibodies are monoclonal antibodies directed against a tumor antigen and designed to engage effectors cells through their Fc receptors, to mediate antibody-dependent, cell-mediated cytotoxicity (ADCC) either by natural killer cells (NK-ADCC) or by myeloid cells such as neutrophils and macrophages (myeloid-ADCC). In some tumors (e.g. neuroblastoma), complement-mediated cytotoxicity (CDC) can also play a role in the anti-tumor response. Enoblituzumab specific for B7-H3, is being tested in a phase I clinical trial in children and young adults with B7-H3-expressing relapsed/refractory solid tumors including DSRCT (NCT02982941). Enoblituzumab is also being tested in combination with checkpoint inhibitors

TABLE 3 | Previous and current clinical trials using immunotherapy to treat DSRCT.

Trial	Phase	Therapy	Type	Target	Status	Study term	Actual enrollment
NCT00043979	2	Allogenic hematopoietic stem cell transplant	STC	n/a	Completed	09/2002 – 12/2011	60
NCT00089245	1	^{131}I-8H9	RIT	B7-H3	Active, not recruiting	07/2004 – 07/2021	120*
NCT00445965	2	^{131}I-3F8	RIT	GD2	Active, not recruiting	01/2006 – 01/2022	78
NCT00562380	1	AMG-479	mAb	IGF-1R	Completed	04/2010 – 06/2010	64*
NCT00720174	1	Cixutumumab	mAb	IGF-1R	Completed	06/2008 – 01/2013	30
NCT01099644	1	^{131}I-8H9	RIT	B7-H3	Active, not recruiting	04/2010 – 09/2021	54
NCT02982486	2	Nivolumab + ipilimumab	ICI	PD-1/CTLA-4	Unknown	12/2017 – 12/2020	60*
NCT02982941	1	Enoblituzumab	mAb	B7-H3	Completed	12/2016 – 05/2019	25
NCT03618381	1	EGFR806 CAR T Cells	CAR T	EGFR	Recruiting	06/2019 – 06/2038	36*
NCT03860207	1/2	Hu3F8-BsAb	BsAb	GD2	Recruiting	02/2019 – 02/2022	30*
NCT04022213	2	^{131}I-8H9	RIT	B7-H3	Recruiting	07/2019 – 07/2024	55*
NCT04483778	1	B7-H3 CAR T cells	CAR T	B7-H3	Recruiting	07/2020 – 12/2040	68*
NCT04530487	2	Allogenic hematopoietic stem cell transplant	SCT	n/a	Recruiting	08/2020 – 05/2025	40*
NCT04897321	1	B7-H3 CAR T cells	CAR T	B7-H3	Not yet recruiting	04/2022 – 03/2027	32*

**For ongoing studies the estimated enrollment is provided in lieu of actual enrollment. STC, stem cell transplant; RIT, radioimmunotherapy; mAb, monoclonal antibody; ICI, immune checkpoint inhibitor; CAR T, chimeric antigen receptor T cell; BsAb, bispecific antibody.*

pembrolizumab (NCT02475213) and ipilimumab (NCT02381314) among patients with B7-H3-expressing tumors.

There is also an ongoing trial to test the efficacy of a T cell-engaging BsAb in patients with advanced GD2+ tumors including DSRCT (NCT03860207). These BsAb are wide-ranging in structure, with one or more domains designed to engage T cells (usually targeting CD3) and one or more domains specific for a tumor antigen and serve as a sort of link between T cells and tumor cells, turning polyclonal T cells into specific killers. The advantage of BsAb over traditional antibody therapy is that they can initiate a robust T cell response against tumors at comparatively very low antibody concentrations and low target density. So far just one BsAb, blinatumomab, which targets CD3 and CD19, has been approved for use in cancer, in this case for ALL (47). Many others are in phase I-II trials, but only in adults (48).

Additionally, tumor antigen-specific antibodies can be used as vehicles to deliver radionuclide conjugates selectively to tumors in a process called radioimmunotherapy (RIT). This type of therapy has been successful clinically and two drugs have so far been approved for non-Hodgkin lymphoma (49). Currently, two radionuclide-conjugated antibodies are in trials for DSRCT: ^{131}I-3F8, directed against GD2, which has previously been tested in medulloblastoma (50) and as a diagnostic tool in neuroblastoma (51), and ^{131}I-8H9, directed against B7-H3, which has been previously tested in neuroblastoma (52). A recent Phase I trial (NCT01099644) of intraperitoneal ^{131}I-8H9 in 48 DSRCT patients and four patients with other B7-H3-positive sarcomas found the treatment to be safe and well-tolerated with no dose-limiting toxicities (53). A Phase II trial for DSRCT is now accruing patients (NCT04022213).

CAR T Cells

In addition to using bi-specific antibodies to direct T cells to tumors, it is also possible to redirect T cells by genetically engineering them to express receptors specific for more classic antibody targets, i.e. not T cell receptor (TCR) peptide-MCH targets. These engineered cells are termed chimeric antigen receptor (CAR) T cells. In the past two years, two CAR T cell therapies have been approved by the FDA for treating CD19-expressing cancers based on clinical trials that showed they can induce complete responses in a significant proportion of patients (54, 55). Although current success with CAR T cell therapy has been largely limited to liquid tumors, clinical trials for solid tumors, including DSRCT and other sarcomas, are ongoing (56). HER2-CAR T cells were used in a phase I/II trial of sarcoma patients (including one with DSRCT) because evidence shows that HER2 is expressed at low levels by many types of sarcoma, including DSRCT (43, 57). While this low level of expression precludes immunotherapy with IgG monoclonal antibodies, CAR T cell therapy could be effective (57). This trial showed that HER2-CAR T cells delivered at low doses were safe, tolerable, and effective in maintaining stable disease in a subset of patients, with one DSRCT patient stable for >14 months (42). Phase I trials testing CAR T cells targeting EGFR (NCT03618381) and B7-H3 (NCT04483778, NCT04897321) are currently underway for patients with solid tumors including DSRCT.

Cancer Vaccines

It has been proposed that chromosomal translocation products can serve as tumor-specific antigens in sarcomas including DSRCT (58). This occurs when mutant proteins are processed by proteasomes and displayed as peptides on MHC molecules on the surface of tumor cells, as was demonstrated with mutant p53 (59, 60). A 9-amino acid epitope from the EWS-WT1 fusion protein has been described that binds to HLA-A3, providing the potential target for cytotoxic T cells (61). In one study among sarcoma patients, 2 patients with DSRCT were treated with autologous lymphocytes, tumor-pulsed dendritic cells and IL-7; unfortunately, neither had any measurable response (62). In another WT1 peptide vaccine trial among a group of 20 children with glioma, rhabdomyosarcoma, neuroblastoma, osteosarcoma, and clear cell sarcoma of the kidney (63), WT1-specific immune response was demonstrated in 4/18 (22%) evaluable patients (63). Although no DSRCT patients were included in this study, these results may provide a rationale for using peptide vaccines in DSRCT and other tumors with chromosomal translocation products that contain WT1.

Hematopoietic Stem Cell Transplantation

Allogenic stem cell transplants (SCT) have been transformative in the treatment of hematological cancers. Although intense pre-transplant chemotherapy drastically reduces tumor burden, it rarely eliminates all tumor cells from the marrow compartment (64). Rather, a graft-*versus*-tumor effect is probably responsible for long term tumor control (65, 66). In this way, SCT is a form of cancer immunotherapy. Allogenic SCT has been shown to increase survival in advanced DSRCT (11.4 months *vs.* 1.9 months) (19). Autologous SCT has also been used but does not appear to be effective in increasing survival or reducing recurrence (18, 67). Yet, one DSRCT patient treated with CD34+ selected peripheral blood stem cells (PBSC) following surgical resection and high-dose chemotherapy, has maintained remission for over 10 years (68).

Checkpoint Inhibitors

The field of immunotherapy was revolutionized by the advent of immune checkpoint inhibitors, drugs meant to release the "brakes" on T cells to reboot or to recruit T cells in their anti-tumor immune responses. Drugs targeting CTLA4 (ipilimumab) and PD-1 (programmed cell death protein 1) (nivolumab and pembrolizumab) have proven effective in treating melanoma, and, most excitingly, many of the patients who respond are alive years after treatment, suggesting that their remission is durable (69). Unfortunately, DSRCT, like sarcomas in general, do not respond well to checkpoint inhibition (36, 70). Typical among pediatric cancers driven by gene fusion, DSRCT has low tumor mutation burden, and hence few neoepitopes and insufficient anti-tumor T cell clonal frequencies (71). Tumor mutation burden, which often also correlates with a low degree of lymphocyte infiltration, is a predictor of response to checkpoint inhibitors (72). In contrast to melanoma and other tumors that are responsive to checkpoint inhibition, DSRCT appears to be an immunologically "cold" tumor, that is to say it is not heavily populated by tumor infiltrating lymphocytes (TILs) (73). DSCRT has low or no expression of PD-1/PD-L1 (programmed death ligand 1), suggesting that signaling along this axis is uncommon (41, 74). Put simply, removing the "brakes" from T cells is only effective if the host already has T cells capable of recognizing tumor epitopes just waiting to be rebooted, or if the naive T cells can be recruited to go after neoepitopes. Despite their failure as monotherapies in DSRCT, they could still hold promise when combined with other forms of immunotherapy, such as CAR T cells, cancer vaccines, and BsAb (75–77).

Challenges in Immunotherapy for DSRCT

Low mutation load is now a well-recognized Achilles heel for most solid tumors in children and adolescents/young adults (71). This partly explained the paucity of TILs, which is made worse by the upfront use of aggressive chemotherapy, adopted as the standard of care from the time of diagnosis (6, 78). While this chemotherapy often succeeds at reducing tumor burden, it also depletes the patient's immune cells, which may lead to depletion of effector cells, and especially T cells, thereby reducing the efficacy of immunotherapies (78).

Another challenge lies in achieving sufficient concentrations of antibody or large proteins in the tumor. When delivered intravenously, it may be difficult to achieve therapeutic doses of antibodies without on-target, off-tumor toxicity and other adverse effects. One solution for this is to deliver the immunotherapeutic agent regionally or to a specific biological compartment (56). Currently, a clinical trial (NCT00445965) is underway to test the efficacy of intrathecal delivery of the radiolabeled antibody ^{131}I-3F8 to DSRCT and other tumors that have spread to or originated in the brain. Another clinical trial (NCT04022213) is in progress to determine the efficacy of ^{131}I-8H9 delivered intraperitoneally for DSRCT and other solid tumors which metastasize within the peritoneum. Regional delivery has also been tested in radioimmunotherapy of neuroblastoma that has spread to the CNS, and even CAR T cells in ovarian cancer (52, 56, 79). These delivery methods aim to allow the treatment to reach sufficient levels in and around the tumor while protecting other normal tissues from the deleterious effects of high concentrations of these immunotherapeutic agents. Given the peripatetic presence across all tissues, T cells have the capability to penetrate deep into tissues unlike antibodies. Hence BsAbs that arm T cells either *in vivo* or *ex vivo* may be able to overcome penetration hurdles.

Although speculative, regional or compartmental delivery of BsAb may reduce on-target, off-tumor effects, which can be life-threatening. The most common adverse effect experienced by patients in these T cell-based therapy is cytokine release syndrome, which occurs when large numbers of T cells become activated and release cytokines such as IFN-y, GM-CSF, IL-10, and IL-6 (80). This occurs because of immediate contact between active T cells with targets in the hematogenous compartment (e.g. CD19), or direct activation of T cells even before arriving at the tumor site. The effects of this "cytokine storm" range from mild to severe, and can cause fever, fatigue, pain, nausea, hypotension, and organ failure (80). One patient treated with 1×10^{10} HER2 CAR T cells experienced respiratory distress within minutes of the infusion and died 5 days later (81). It is thought that the CAR T cells localized to her lungs and became active upon recognition of low levels of HER2 expressed in lung tissue (81). However, patients have safely been treated with HER2 CAR T cells at much lower doses, including one DSRCT patient treated with $1 \times 10^7/m^2$ cells (42). Such life-threatening complications can potentially be avoided if the BsAbs are first administered into a "cold" compartment to bind to tumors before TILs arrive.

Finally, it is well known that tumors evolve resistance to treatments by downregulating expression of target molecules, and by upregulating expression of immune checkpoint molecules. In the context of immunotherapy, this is called immune escape (82). It has been demonstrated that tumors upregulate PD-1 and CD47 in response to treatment with BsAbs (77, 83). It has also been shown that tumors are capable of downregulating the targets of CARs, evidenced by the fact that 11% of B-cell malignancy patients who initially responded to treatment with CD19 CAR T cells eventually relapsed with CD19- tumors (84). One potential strategy to combat this

phenomenon is to develop treatments that target multiple tumor antigens, including bispecific CAR T cells and T cell engaging antibodies with more than one tumor-targeting domain (82).

DISCUSSION

Overall cancer death rates have steadily declined over the past several decades in the United States, owing to prevention, early detection, and advances in treatment (85). Deaths from childhood cancers have also declined, though this is primarily due to the availability of better treatments, since childhood cancers (which are rarely caused by infection or exposure to carcinogens) can only rarely be prevented (86, 87). Furthermore, while the adult cancer death rate has been improved by efforts to regularly screen at-risk populations (through cervical cancer screening, mammograms, and colonoscopies, for example), for childhood cancers including DSRCT it is not feasible to implement any screening programs because no at-risk populations have been identified and no suitable screening tests exist to implement on a population-wide scale (88–90). For these reasons, efforts to reduce deaths from DSRCT and other childhood cancers can only be focused on improving treatments. While some novel approaches, such as the use of HIPEC, could delay progression, few have yielded few long-term DSRCT survivors who can be considered cured (6, 14). Immunotherapy and radioimmunotherapy are attractive options for DSRCT because they have the potential to produce durable responses without long-term side effects.

So far most of the reports on immunotherapy success in DSRCT are anecdotal. However, it is useful to learn from the successful implementation of immunotherapy in other pediatric solid tumors, like high-risk metastatic neuroblastoma which was incurable three decades ago. As mentioned previously, GD2-targeted immunotherapy has revolutionized treatment of high-risk neuroblastoma even when recurrent (46). Beginning with murine monoclonal antibodies, anti-GD2 treatment has evolved into chimeric and humanized monoclonal antibodies, and trials are underway testing CAR T cells (NCT03294954), an antibody vaccine(NCT00911560), and BsAb therapy (NCT03860207) (46). Though decades behind neuroblastoma, DSRCT could benefit from similar types of immunotherapies.

While DSRCT and other immunologically "cold" tumors don't have *de novo* anti-tumor immune responses, passive immunotherapy, such as monoclonal antibodies, may still be effective. The success of monoclonal antibody therapy in neuroblastoma and leukemia, even in patients who are immunocompromised by prior chemoradiotherapy, suggests that these passive immunotherapeutic approaches could be successfully implemented even after receiving dose-intensive therapies among DSRCT patients. In fact, a monoclonal antibody against B7-H3 (NCT02982941) and two radionuclide-labeled monoclonal antibodies against B7-H3 (NCT04022213) and GD2 (NCT00445965) are currently being tested in clinical trials open to patients with DSRCT.

Immunotherapy may also be made more efficacious for DSRCT by compartmental delivery to the peritoneum. While DSRCT is often advanced at diagnosis, in a substantial proportion of patients their disease is contained within the peritoneum. By delivering the immunotherapeutic agent intraperitoneally, the concentration of the agent in and around the tumor could be substantially higher compared to systemic delivery. The likelihood of adverse on-target, off-tumor effects would also likely be reduced for tissues expressing the target but located outside the peritoneal cavity. In this way, the impact of the agent on the tumors would be maximized while the impact of the agent on normal tissue would be minimized. Intraperitoneal delivery of CAR T cells has proven superior to systemic delivery in an animal model of metastatic peritoneal colorectal cancer (91) and this strategy is being implemented in clinical trials for ovarian cancer (NCT02498912), peritoneal mesothelioma (NCT03608618) and advanced gastric cancer (NCT03563326) with peritoneal spread. When DSRCT does spread beyond the peritoneum, it often metastasizes to the CNS, which is walled off by the blood brain barrier from most treatments that are delivered parenterally. To reach these tumors treatment must be delivered intrathecally or intraparenchymally using catheters connected to an Ommaya reservoir. A clinical trial testing intrathecal ^{131}I-3F8 (NCT00445965) is ongoing for patients with CNS tumors, including metastatic DSRCT.

Another challenge to consider which may inform the future direction of immunotherapy in DSRCT is antigen heterogeneity and antigen loss, a process in which tumors lose expression of antigens targeted by immunotherapy and thereby "escape" immune surveillance. This is now a well-known mechanism of resistance in CD19 CAR T cells, where recurrent leukemia cells no longer express CD19 following treatment. A proposed solution for this problem is to target two antigens instead of one, since the probability of two distinct mutations arising in the tumor that would downregulate both targets and allow for antigen escape during treatment is statistically unlikely (92). Since DSRCT expresses several tumor-associated targets, they should be suitable for this dual targeting approach. Targeting multiple antigens would also increase efficacy of immunotherapy in tumors where the expression of targets is heterogenous, where no single target is expressed uniformly on every tumor cell. Radionuclide-conjugated antibodies offer a similar benefit, as they can kill not only the tumor cells that express their antibody targets but other tumor cells in the vicinity. This killing is achieved by way of cross-firing during radioactive decay by high energy particles such as electrons and positrons that travel millimeter distances, and alpha particles that travel micron distances. By combining antibody formats that target multiple targets with novel radioimmunotherapy platforms, the potential exists for designing a radioimmunotherapy strategy for DSRCT, which is well-known to be radiation-responsive.

In addition to the scientific challenges confronting immunotherapy approaches, it is important to take into consideration the logistical hurdles, including the cost of these therapies and the accessibility for the general public world-wide. These issues have surfaced quickly in the field of CAR T cells,

which must be tailor-made for each patient using *ex vivo* T cell expansion and viral transduction. In the case of Kymriah and Yescarta, the two FDA-approved CAR T cell therapies, the drug cost is currently $475,000 and $373,000 per patient, respectively (93). These prices make them inaccessible for many patients, even those in developed countries. In addition to the cost, the treatment can take several weeks to prepare for each individual patient. Although these therapies have undoubtedly saved lives, the fact remains that they are time-consuming and expensive to produce. While antibody therapy is less personalized and therefore does not have to be tailored made for each patient, it is still expensive in the current market. In the United States, a course of treatment with dinutuximab, an anti-GD2 monoclonal antibody, for example, can cost upwards of $150,000 for the drug only, and the only BsAb approved for cancer, blinatumomab, costs over $170,000 per year. The cost of these revolutionary treatments needs to be considered when evaluating the success of immunotherapy, considering that patients cannot benefit from drugs they cannot access.

Until recently, the improvements in survival for DSRCT have been incremental, owing mostly to the use of multi-agent chemotherapy. These combinations of drugs are highly toxic, have debilitating side effects, and only serve to prolong survival by a few months or years, at best. Today, there are numerous ongoing trials of various types of immunotherapy for DSRCT patients, including a BsAb, radionuclide-conjugated antibodies, a monoclonal antibody, CAR T cells, and checkpoint inhibitors (**Table 3**). New clinical studies aiming to collate information on clinical attributes (NCT04690374) and immune characteristics (NCT03967834) of patients with DSRCT will improve our knowledge this rare disease. Immunotherapy offers the promise of eradicating chemotherapy-resistant, microscopic tumors that cause relapse and eventually death in a majority of DSRCT patients, without the same adverse long-term effects encountered by genotoxic therapies. It is instructive to look at the successes of immunotherapy in other diseases, such as neuroblastoma and leukemia, which have seen children with relapsed tumors cured for the first time by antibody therapy and CAR T cells. At the same time, it is important to learn from the challenges experienced in the development and evolution of these treatments so that they may be implemented most efficiently and effectively in DSRCT.

AUTHOR CONTRIBUTIONS

N-KC and ME-C both wrote and edited this manuscript. All authors contributed to the article and approved the submitted version.

FUNDING

The authors acknowledge support of the NCI Cancer Center Support Grant P30 CA008748, NCI Predoctoral to Postdoctoral Fellow Transition Award K00 CA223062, and support from the following donors and organizations: Runway Heroes, Renaissance Charitable Foundation, Tay-Bandz, Inc., The Steven Vanover Foundation, and Brenda D. Vanover.

REFERENCES

1. Gerald WL, Rosai J. Case 2. Desmoplastic Small Cell Tumor With Divergent Differentiation. *Pediatr Pathol* (1989) 9:177–83. doi: 10.3109/15513818909022347
2. Gerald WL, Miller HK, Battifora H, Miettinen M, Silva EG, Rosai J. Intra-Abdominal Desmoplastic Small Round-Cell Tumor. Report of 19 Cases of a Distinctive Type of High-Grade Polyphenotypic Malignancy Affecting Young Individuals. *Am J Surg Pathol* (1991) 15:499–513. doi: 10.1097/00000478-199106000-00001
3. Sawyer JR, Tryka AF, Lewis JM. A Novel Reciprocal Chromosome Translocation T(11;22)(P13;Q12) in an Intraabdominal Desmoplastic Small Round-Cell Tumor. *Am J Surg Pathol* (1992) 16:411–6. doi: 10.1097/00000478-199204000-00010
4. Rodriguez E, Sreekantaiah C, Gerald W, Reuter VE, Motzer RJ, Chaganti RS. A Recurring Translocation, T(11;22)(P13;Q11.2), Characterizes Intra-Abdominal Desmoplastic Small Round-Cell Tumors. *Cancer Genet Cytogenet* (1993) 69:17–21. doi: 10.1016/0165-4608(93)90105-U
5. Ladanyi M, Gerald W. Fusion of the EWS and WT1 Genes in the Desmoplastic Small Round Cell Tumor. *Cancer Res* (1994) 54:2837–40.
6. Hayes-Jordan A, LaQuaglia MP, Modak S. Management of Desmoplastic Small Round Cell Tumor. *Semin Pediatr Surg* (2016) 25:299–304. doi: 10.1053/j.sempedsurg.2016.09.005
7. Lettieri CK, Garcia-Filion P, Hingorani P. Incidence and Outcomes of Desmoplastic Small Round Cell Tumor: Results From the Surveillance, Epidemiology, and End Results Database. *J Cancer Epidemiol* (2014) 2014:680126. doi: 10.1155/2014/680126
8. Gerald WL, Ladanyi M, de Alava E, Cuatrecasas M, Kushner BH, LaQuaglia MP, et al. Clinical, Pathologic, and Molecular Spectrum of Tumors Associated With T(11;22)(P13;Q12): Desmoplastic Small Round-Cell Tumor and its Variants. *J Clin Oncol* (1998) 16:3028–36. doi: 10.1200/jco.1998.16.9.3028
9. Worch J, Cyrus J, Goldsby R, Matthay KK, Neuhaus J, DuBois SG. Racial Differences in the Incidence of Mesenchymal Tumors Associated With EWSR1 Translocation. *Cancer Epidemiol Biomarkers Prev* (2011) 20:449–53. doi: 10.1158/1055-9965.Epi-10-1170
10. Lal DR, Su WT, Wolden SL, Loh KC, Modak S, La Quaglia MP. Results of Multimodal Treatment for Desmoplastic Small Round Cell Tumors. *J Pediatr Surg* (2005) 40:251–5. doi: 10.1016/j.jpedsurg.2004.09.046
11. Kushner BH, LaQuaglia MP, Wollner N, Meyers PA, Lindsley KL, Ghavimi F, et al. Desmoplastic Small Round-Cell Tumor: Prolonged Progression-Free Survival With Aggressive Multimodality Therapy. *J Clin Oncol* (1996) 14:1526–31. doi: 10.1200/JCO.1996.14.5.1526
12. Whelan J, Khan A, Sharma A, Rothermundt C, Dileo P, Michelagnoli M, et al. Interval Compressed Vincristine, Doxorubicin, Cyclophosphamide Alternating With Ifosfamide, Etoposide in Patients With Advanced Ewing's and Other Small Round Cell Sarcomas. *Clin Sarcoma Res* (2012) 2:12. doi: 10.1186/2045-3329-2-12
13. Hayes-Jordan AA, Coakley BA, Green HL, Xiao L, Fournier KF, Herzog CE, et al. Desmoplastic Small Round Cell Tumor Treated With Cytoreductive Surgery and Hyperthermic Intraperitoneal Chemotherapy: Results of a Phase 2 Trial. *Ann Surg Oncol* (2018) 25:872–7. doi: 10.1245/s10434-018-6333-9
14. Hayes-Jordan A, Green HL, Lin H, Owusu-Agyemang P, Fitzgerald N, Arunkumar R, et al. Complete Cytoreduction and HIPEC Improves Survival in Desmoplastic Small Round Cell Tumor. *Ann Surg Oncol* (2014) 21:220–4. doi: 10.1245/s10434-013-3269-y
15. Goodman KA, Wolden SL, La Quaglia MP, Kushner BH. Whole Abdominopelvic Radiotherapy for Desmoplastic Small Round-Cell Tumor.

Int J Radiat Oncol Biol Phys (2002) 54:170–6. doi: 10.1016/S0360-3016(02)02871-7

16. Honore C, Atallah V, Mir O, Orbach D, Ferron G, LePechoux C, et al. Abdominal Desmoplastic Small Round Cell Tumor Without Extraperitoneal Metastases: Is There a Benefit for HIPEC After Macroscopically Complete Cytoreductive Surgery? *PloS One* (2017) 12:e0171639. doi: 10.1371/journal.pone.0171639
17. Desai NB, Stein NF, LaQuaglia MP, Alektiar KM, Kushner BH, Modak S, et al. Reduced Toxicity With Intensity Modulated Radiation Therapy (Imrt) for Desmoplastic Small Round Cell Tumor (Dsrct): An Update on the Whole Abdominopelvic Radiation Therapy (Wap-Rt) Experience. *Int J Radiat Oncol Biol Phys* (2013) 85:e67–72. doi: 10.1016/j.ijrobp.2012.09.005
18. Forlenza CJ, Kushner BH, Kernan N, Boulad F, Magnan H, Wexler L, et al. Myeloablative Chemotherapy With Autologous Stem Cell Transplant for Desmoplastic Small Round Cell Tumor. *Sarcoma* (2015) 2015:269197. doi: 10.1155/2015/269197
19. Baird K, Fry TJ, Steinberg SM, Bishop MR, Fowler DH, Delbrook CP, et al. Reducedintensity Allogeneic Stem Cell Transplantation in Children and Young Adults With Ultrahigh-Risk Pediatric Sarcomas. *Biol Blood Marrow Transplant* (2012) 18:698–707. doi: 10.1016/j.bbmt.2011.08.020
20. Gerald WL, Haber DA. The EWS-WT1 Gene Fusion in Desmoplastic Small Round Cell Tumor. *Semin Cancer Biol* (2005) 15:197–205. doi: 10.1016/j.semcancer.2005.01.005
21. Gessler M, Poustka A, Cavenee W, Neve RL, Orkin SH, Bruns GA. Homozygous Deletion in Wilms Tumours of a Zinc-Finger Gene Identified by Chromosome Jumping. *Nature* (1990) 343:774–8. doi: 10.1038/343774a0
22. Rauscher FJ3rd. The Wt1 Wilms Tumor Gene Product: A Developmentally Regulated Transcription Factor in the Kidney That Functions as a Tumor Suppressor. *FASEB J* (1993) 7:896–903. doi: 10.1096/fasebj.7.10.8393820
23. Lee SB, Kolquist KA, Nichols K, Englert C, Maheswaran S, Ladanyi M, et al. The EWSWT1 Translocation Product Induces PDGFA in Desmoplastic Small Round-Cell Tumour. *Nat Genet* (1997) 17:309–13. doi: 10.1038/ng1197-309
24. Froberg K, Brown RE, Gaylord H, Manivel C. Intra-Abdominal Desmoplastic Small Round Cell Tumor: Immunohistochemical Evidence for Up-Regulation of Autocrine and Paracrine Growth Factors. *Ann Clin Lab Sci* (1999) 29:78–85.
25. Zhang PJ, Goldblum JR, Pawel BR, Pasha TL, Fisher C, Barr FG. PDGF-a, Pdgfrbeta, Tgfbeta3 and Bone Morphogenic Protein-4 in Desmoplastic Small Round Cell Tumors With EWS-WT1 Gene Fusion Product and Their Role in Stromal Desmoplasia: An Immunohistochemical Study. *Mod Pathol* (2005) 18:382–7. doi: 10.1038/modpathol.3800264
26. Druker BJ, Talpaz M, Resta DJ, Peng B, Buchdunger E, Ford JM, et al. Efficacy and Safety of a Specific Inhibitor of the BCR-ABL Tyrosine Kinase in Chronic Myeloid Leukemia. *N Engl J Med* (2001) 344:1031–7. doi: 10.1056/nejm200104053441401
27. Bond M, Bernstein ML, Pappo A, Schultz KR, Krailo M, Blaney SM, et al. A Phase II Study of Imatinib Mesylate in Children With Refractory or Relapsed Solid Tumors: A Children's Oncology Group Study. *Pediatr Blood Cancer* (2008) 50:254–8. doi: 10.1002/pbc.21132
28. Chao J, Budd GT, Chu P, Frankel P, Garcia D, Junqueira M, et al. Phase II Clinical Trial of Imatinib Mesylate in Therapy of KIT and/or Pdgfralpha-Expressing Ewing Sarcoma Family of Tumors and Desmoplastic Small Round Cell Tumors. *Anticancer Res* (2010) 30:547–52.
29. De Sanctis R, Bertuzzi A, Bisogno G, Carli M, Ferrari A, Comandone A, et al. Imatinib Mesylate in Desmoplastic Small Round Cell Tumors. *Future Oncol* (2017) 13:1233–7. doi: 10.2217/fon-2016-0305
30. Werner H, LeRoith D. The Role of the Insulin-Like Growth Factor System in Human Cancer. *Adv Cancer Res* (1996) 68:183–223. doi: 10.1016/S0065-230X(08)60354-1
31. Barra WF, Castro G, Hoff AO, Siqueira SA, Hoff PM. Symptomatic Hypoglycemia Related to Inappropriately High Igf-Ii Serum Levels in a Patient With Desmoplastic Small Round Cell Tumor. *Case Rep Med* (2010) 2010:684045. doi: 10.1155/2010/684045
32. Almaghraby A, Brickman WJ, Goldstein JA, Habiby RL. Refractory Hypoglycemia in a Pediatric Patient With Desmoplastic Small Round Cell Tumor. *J Pediatr Endocrinol Metab JPEM* (2018) 31:947–50. doi: 10.1515/jpem-2018-0107
33. Tap WD, Demetri G, Barnette P, Desai J, Kavan P, Tozer R, et al. Phase II Study of Ganitumab, a Fully Human Anti-Type-1 Insulin-Like Growth Factor Receptor Antibody, in Patients With Metastatic Ewing Family Tumors or Desmoplastic Small Round Cell Tumors. *J Clin Oncol* (2012) 30:1849–56. doi: 10.1200/JCO.2011.37.2359
34. Naing A, LoRusso P, Fu S, Hong DS, Anderson P, Benjamin RS, et al. Insulin Growth Factor-Receptor (IGF-1R) Antibody Cixutumumab Combined With the Mtor Inhibitor Temsirolimus in Patients With Refractory Ewing's Sarcoma Family Tumors. *Clin Cancer Res* (2012) 18:2625–31. doi: 10.1158/1078-0432.CCR-12-0061
35. Fine RL, Shah SS, Moulton TA, Yu IR, Fogelman DR, Richardson M, et al. Androgen and C-Kit Receptors in Desmoplastic Small Round Cell Tumors Resistant to Chemotherapy: Novel Targets for Therapy. *Cancer Chemother Pharmacol* (2007) 59:429–37. doi: 10.1007/s00280-006-0280-z
36. Negri T, Brich S, Bozzi F, Volpi CV, Gualeni AV, Stacchiotti S, et al. New Transcriptionalbased Insights Into the Pathogenesis of Desmoplastic Small Round Cell Tumors (Dsrcts). *Oncotarget* (2017) 8:32492–504. doi: 10.18632/oncotarget.16477
37. Modak S, Kramer K, Gultekin SH, Guo HF, Cheung NK. Monoclonal Antibody 8H9 Targets a Novel Cell Surface Antigen Expressed by a Wide Spectrum of Human Solid Tumors. *Cancer Res* (2001) 61:4048–54.
38. Modak S, Gerald W, Cheung NK. Disialoganglioside GD2 and a Novel Tumor Antigen: Potential Targets for Immunotherapy of Desmoplastic Small Round Cell Tumor. *Med Pediatr Oncol* (2002) 39:547–51. doi: 10.1002/mpo.10151
39. Xu H, Cheung IY, Guo HF, Cheung NK. Microrna Mir-29 Modulates Expression of Immunoinhibitory Molecule B7-H3: Potential Implications for Immune Based Therapy of Human Solid Tumors. *Cancer Res* (2009) 69:6275–81. doi: 10.1158/0008-5472.CAN-08-4517
40. Dobrenkov K, Ostrovnaya I, Gu J, Cheung IY, Cheung NK. Oncotargets GD2 and GD3 are Highly Expressed in Sarcomas of Children, Adolescents, and Young Adults. *Pediatr Blood Cancer* (2016) 63:1780–5. doi: 10.1002/pbc.26097
41. Movva S, Wen W, Chen W, Millis SZ, Gatalica Z, Reddy S, et al. Multi-Platform Profiling of Over 2000 Sarcomas: Identification of Biomarkers and Novel Therapeutic Targets. *Oncotarget* (2015) 6:12234–47. doi: 10.18632/oncotarget.3498
42. Ahmed N, Brawley VS, Hegde M, Robertson C, Ghazi A, Gerken C, et al. Human Epidermal Growth Factor Receptor 2 (HER2) -Specific Chimeric Antigen Receptor-Modified T Cells for the Immunotherapy of HER2-Positive Sarcoma. *J Clin Oncol* (2015) 33:1688–96. doi: 10.1200/jco.2014.58.0225
43. Zhang PJ, Goldblum JR, Pawel BR, Fisher C, Pasha TL, Barr FG. Immunophenotype of Desmoplastic Small Round Cell Tumors as Detected in Cases With EWS-WT1 Gene Fusion Product. *Mod Pathol* (2003) 16:229–35. doi: 10.1097/01.Mp.0000056630.76035.F3
44. Decker WK, da Silva RF, Sanabria MH, Angelo LS, Guimaraes F, Burt BM, et al. Cancer Immunotherapy: Historical Perspective of a Clinical Revolution and Emerging Preclinical Animal Models. *Front Immunol* (2017) 8:829. doi: 10.3389/fimmu.2017.00829
45. Duffner PK. Long-Term Effects of Radiation Therapy on Cognitive and Endocrine Function in Children With Leukemia and Brain Tumors. *Neurol* (2004) 10:293–310. doi: 10.1097/01.nrl.0000144287.35993.96
46. Keyel ME, Reynolds CP. Spotlight on Dinutuximab in the Treatment of High-Risk Neuroblastoma: Development and Place in Therapy. *Biologics* (2019) 13:1–12. doi: 10.2147/btt.S114530
47. Curran E, Stock W. Taking a "Bite Out of ALL" - Blinatumomab Approval for MRD Positive ALL. *Blood* (2019) 133:1715–9. doi: 10.1182/blood-2018-12-852376
48. Sedykh SE, Prinz VV, Buneva VN, Nevinsky GA. Bispecific Antibodies: Design, Therapy, Perspectives. *Drug Design Dev Ther* (2018) 12:195–208. doi: 10.2147/dddt.S151282
49. Kawashima H. Radioimmunotherapy: A Specific Treatment Protocol for Cancer by Cytotoxic Radioisotopes Conjugated to Antibodies. *Sci World J* (2014) 2014:492061. doi: 10.1155/2014/492061
50. Kramer K, Pandit-Taskar N, Humm JL, Zanzonico PB, Haque S, Dunkel IJ, et al. A Phase II Study of Radioimmunotherapy With Intraventricular (131) I-3F8 for Medulloblastoma. *Pediatr Blood Cancer* (2018) 65. doi: 10.1002/pbc.26754
51. Yeh SD, Larson SM, Burch L, Kushner BH, Laquaglia M, Finn R, et al. Radioimmunodetection of Neuroblastoma With Iodine-131-3F8: Correlation

With Biopsy, Iodine- 131-Metaiodobenzylguanidine and Standard Diagnostic Modalities. *J Nucl Med* (1991) 32:769–76.
52. Kramer K, Kushner BH, Modak S, Pandit-Taskar N, Smith-Jones P, Zanzonico P, et al. Compartmental Intrathecal Radioimmunotherapy: Results for Treatment for Metastatic Cns Neuroblastoma. *J Neurooncol* (2010) 97:409–18. doi: 10.1007/s11060-009-0038-7
53. Modak S, Zanzonico P, Grkovski M, Slotkin EK, Carrasquillo JA, Lyashchenko SK, et al. B7H3-Directed Intraperitoneal Radioimmunotherapy With Radioiodinated Omburtamab for Desmoplastic Small Round Cell Tumor and Other Peritoneal Tumors: Results of a Phase I Study. *J Clin Oncol* (2020) 38:4283–91. doi: 10.1200/jco.20.01974
54. Schuster SJ, Bishop MR, Tam CS, Waller EK, Borchmann P, McGuirk JP, et al. Primary Analysis of Juliet: A Global, Pivotal, Phase 2 Trial of CTL019 in Adult Patients With Relapsed or Refractory Diffuse Large B-Cell Lymphoma. *Blood* (2017) 130:577–7.
55. Maude SL, Laetsch TW, Buechner J, Rives S, Boyer M, Bittencourt H, et al. Tisagenlecleucel in Children and Young Adults With B-Cell Lymphoblastic Leukemia. *N Engl J Med* (2018) 378:439–48. doi: 10.1056/NEJMoa1709866
56. Schmidts A, Maus MV. Making CAR T Cells a Solid Option for Solid Tumors. *Front Immunol* (2018) 9:2593. doi: 10.3389/fimmu.2018.02593
57. Ahmed N, Salsman VS, Yvon E, Louis CU, Perlaky L, Wels WS, et al. Immunotherapy for Osteosarcoma: Genetic Modification of T Cells Overcomes Low Levels of Tumor Antigen Expression. *Mol Ther* (2009) 17:1779–87. doi: 10.1038/mt.2009.133
58. Goletz TJ, Mackall CL, Berzofsky JA, Helman LJ. Molecular Alterations in Pediatric Sarcomas: Potential Targets for Immunotherapy. *Sarcoma* (1998) 2:77–87. doi: 10.1080/13577149878037
59. Houbiers JG, Nijman HW, van der Burg SH, Drijfhout JW, Kenemans P, van de Velde CJ, et al. *In Vitro* Induction of Human Cytotoxic T Lymphocyte Responses Against Peptides of Mutant and Wild-Type P53. *Eur J Immunol* (1993) 23:2072–7. doi: 10.1002/eji.1830230905
60. Yanuck M, Carbone DP, Pendleton CD, Tsukui T, Winter SF, Minna JD, et al. A Mutant P53 Tumor Suppressor Protein is a Target for Peptide-Induced CD8+ Cytotoxic T-Cells. *Cancer Res* (1993) 53:3257–61.
61. Worley BS, van den Broeke LT, Goletz TJ, Pendleton CD, Daschbach EM, Thomas EK, et al. Antigenicity of Fusion Proteins From Sarcoma-Associated Chromosomal Translocations. *Cancer Res* (2001) 61:6868–75.
62. Merchant MS, Bernstein D, Amoako M, Baird K, Fleisher TA, Morre M, et al. Adjuvant Immunotherapy to Improve Outcome in High-Risk Pediatric Sarcomas. *Clin Cancer Res* (2016) 22:3182–91. doi: 10.1158/1078-0432.CCR-15-2550
63. Hirabayashi K, Yanagisawa R, Saito S, Higuchi Y, Koya T, Sano K, et al. Feasibility and Immune Response of WT1 Peptide Vaccination in Combination With OK-432 for Paediatric Solid Tumors. *Anticancer Res* (2018) 38:2227–34. doi: 10.21873/anticanres.12465
64. Srinivasan R, Barrett J, Childs R. Allogeneic Stem Cell Transplantation as Immunotherapy for Nonhematological Cancers. *Semin Oncol* (2004) 31:47–55. doi: 10.1053/j.seminoncol.2003.11.002
65. Horowitz MM, Gale RP, Sondel PM, Goldman JM, Kersey J, Kolb HJ, et al. Graftversus- Leukemia Reactions After Bone Marrow Transplantation. *Blood* (1990) 75:555–62. doi: 10.1182/blood.V75.3.555.555
66. Weiden PL, Flournoy N, Thomas ED, Prentice R, Fefer A, Buckner CD, et al. Antileukemic Effect of Graft-Versus-Host Disease in Human Recipients of Allogeneic-Marrow Grafts. *N Engl J Med* (1979) 300:1068–73. doi: 10.1056/nejm197905103001902
67. Bertuzzi A, Castagna L, Quagliuolo V, Ginanni V, Compasso S, Magagnoli M, et al. Prospective Study of High-Dose Chemotherapy and Autologous Peripheral Stem Cell Transplantation in Adult Patients With Advanced Desmoplastic Small Round-Cell Tumour. *Br J Cancer* (2003) 89:1159–61. doi: 10.1038/sj.bjc.6601304
68. Houet L, Moller I, Engelhardt M, Kohler G, Schmidt H, Herchenbach D, et al. Long-Term Remission After CD34+-Selected PBSCT in a Patient With Advanced Intra-Abdominal Desmoplastic Small Round-Cell Tumor. *Bone Marrow Transplant* (2010) 45:793–5. doi: 10.1038/bmt.2009.226
69. Lugowska I, Teterycz P, Rutkowski P. Immunotherapy of Melanoma. *Contemp Oncol (Poznan Poland)* (2018) 22:61–7. doi: 10.5114/wo.2018.73889
70. Tawbi HA, Burgess M, Bolejack V, Van Tine BA, Schuetze SM, Hu J, et al. Pembrolizumab in Advanced Soft-Tissue Sarcoma and Bone Sarcoma (SARC028): A Multicentre, Two-Cohort, Single-Arm, Open-Label, Phase 2 Trial. *Lancet Oncol* (2017) 18:1493–501. doi: 10.1016/s1470-2045(17)30624-1
71. Watson IR, Takahashi K, Futreal PA, Chin L. Emerging Patterns of Somatic Mutations in Cancer. *Nat Rev Genet* (2013) 14:703–18. doi: 10.1038/nrg3539
72. Chan TA, Yarchoan M, Jaffee E, Swanton C, Quezada SA, Stenzinger A, et al. Development of Tumor Mutation Burden as an Immunotherapy Biomarker: Utility for the Oncology Clinic. *Ann Oncol* (2019) 30:44–56. doi: 10.1093/annonc/mdy495
73. Maleki Vareki S. High and Low Mutational Burden Tumors Versus Immunologically Hot and Cold Tumors and Response to Immune Checkpoint Inhibitors. *J Immunother Cancer* (2018) 6:157. doi: 10.1186/s40425-018-0479-7
74. Inaguma S, Wang Z, Lasota J, Sarlomo-Rikala M, McCue PA, Ikeda H, et al. Comprehensive Immunohistochemical Study of Programmed Cell Death Ligand 1 (Pd-L1): Analysis in 5536 Cases Revealed Consistent Expression in Trophoblastic Tumors. *Am J Surg Pathol* (2016) 40:1133–42. doi: 10.1097/pas.0000000000000653
75. Rosewell Shaw A, Porter CE, Watanabe N, Tanoue K, Sikora A, Gottschalk S, et al. Adenovirotherapy Delivering Cytokine and Checkpoint Inhibitor Augments CAR T Cells Against Metastatic Head and Neck Cancer. *Mol Ther* 25:2440–51. doi: 10.1016/j.ymthe.2017.09.010 (2017
76. Kim H, Khanna V, Kucaba TA, Zhang W, Ferguson DM, Griffith TS, et al. Combination of Sunitinib and PD-L1 Blockade Enhances Anticancer Efficacy of TLR7/8 Agonist-Based Nanovaccine. *Mol Pharm* (2019) 16:1200–10. doi: 10.1021/acs.molpharmaceut.8b01165
77. Krupka C, Kufer P, Kischel R, Zugmaier G, Lichtenegger FS, Kohnke T, et al. Blockade of the PD-1/PD-L1 Axis Augments Lysis of AML Cells by the CD33/CD3 Bite Antibody Construct AMG 330: Reversing a T-Cell-Induced Immune Escape Mechanism. *Leukemia* (2016) 30:484–91. doi: 10.1038/leu.2015.214
78. Das RK, Vernau L, Grupp SA, Barrett DM. Naive T-Cell Deficits at Diagnosis and After Chemotherapy Impair Cell Therapy Potential in Pediatric Cancers. *Cancer Discovery* (2019) 9:492–9. doi: 10.1158/2159-8290.Cd-18-1314
79. Heiss MM, Strohlein MA, Jager M, Kimmig R, Burges A, Schoberth A, et al. Immunotherapy of Malignant Ascites With Trifunctional Antibodies. *Int J Cancer* (2005) 117:435–43. doi: 10.1002/ijc.21165
80. Bonifant CL, Jackson HJ, Brentjens RJ, Curran KJ. Toxicity and Management in CAR Tcell Therapy. *Mol Ther Oncolytics* (2016) 3:16011. doi: 10.1038/mto.2016.11
81. Morgan RA, Yang JC, Kitano M, Dudley ME, Laurencot CM, Rosenberg SA. Case Report of a Serious Adverse Event Following the Administration of T Cells Transduced With a Chimeric Antigen Receptor Recognizing ERBB2. *Mol Ther* (2010) 18:843–51. doi: 10.1038/mt.2010.24
82. Zhang X, Yang Y, Fan D, Xiong D. The Development of Bispecific Antibodies and Their Applications in Tumor Immune Escape. *Exp Hematol Oncol* (2017) 6:12. doi: 10.1186/s40164-017-0072-7
83. Piccione EC, Juarez S, Liu J, Tseng S, Ryan CE, Narayanan C, et al. A Bispecific Antibody Targeting CD47 and CD20 Selectively Binds and Eliminates Dual Antigen Expressing Lymphoma Cells. *MAbs* (2015) 7:946–56. doi: 10.1080/19420862.2015.1062192
84. Maude SL, Frey N, Shaw PA, Aplenc R, Barrett DM, Bunin NJ, et al. Chimeric Antigen Receptor T Cells for Sustained Remissions in Leukemia. *N Engl J Med* (2014) 371:1507–17. doi: 10.1056/NEJMoa1407222
85. Siegel RL, Miller KD, Jemal A. *Cancer Statistics, 2018*, Vol. 68. *CA Cancer J Clin* (2018). pp. 7–30. doi: 10.3322/caac.21442.
86. Smith MA, Seibel NL, Altekruse SF, Ries LA, Melbert DL, O'Leary M, et al. Outcomes for Children and Adolescents With Cancer: Challenges for the Twenty-First Century. *J Clin Oncol* (2010) 28:2625–34. doi: 10.1200/jco.2009.27.0421
87. Islami F, Goding Sauer A, Miller KD, Siegel RL, Fedewa SA, Jacobs EJ, et al. Proportion and Number of Cancer Cases and Deaths Attributable to Potentially Modifiable Risk Factors in the United States. *CA Cancer J Clin* (2018) 68:31–54. doi: 10.3322/caac.21440
88. Wiegering A, Ackermann S, Riegel J, Dietz UA, Gotze O, Germer CT, et al. Improved Survival of Patients With Colon Cancer Detected by Screening Colonoscopy. *Int J Colorectal Dis* (2016) 31:1039–45. doi: 10.1007/s00384-015-2501-6
89. Kaplan HG, Malmgren JA, Atwood MK, Calip GS. Effect of Treatment and Mammography Detection on Breast Cancer Survival Over Time: 1990-2007. *Cancer* (2015) 121:2553–61. doi: 10.1002/cncr.29371
90. Holmquist ND. Revisiting the Effect of the Pap Test on Cervical Cancer. *Am J Public Health* (2000) 90:620–3. doi: 10.2105/AJPH.90.4.620

91. Katz SC, Point GR, Cunetta M, Thorn M, Guha P, Espat NJ, et al. Regional CAR-T Cell Infusions for Peritoneal Carcinomatosis are Superior to Systemic Delivery. *Cancer Gene Ther* (2016) 23:142–8. doi: 10.1038/cgt.2016.14
92. Jackson HJ, Brentjens RJ. Overcoming Antigen Escape With CAR T-Cell Therapy. *Cancer Discovery* (2015) 5:1238–40. doi: 10.1158/2159-8290.Cd-15-1275
93. de Lima Lopes G, Nahas GR. Chimeric Antigen Receptor T Cells, a Savior With a High Price. *Chin Clin Oncol* (2018) 7:21. doi: 10.21037/cco.2018.04.02

Conflict of Interest: N-KC reports receiving commercial research grants from Y-mAbs Therapeutics and Abpro-Labs Inc.; holding ownership interest/equity/options in Y-mAbs Therapeutics Inc., and in Abpro-Labs, and owning stock options in Eureka Therapeutics. N-KC is the inventor of pending and issued patents filed by MSK, including hu3F8 and 8H9 licensed to Y-mAbs Therapeutics, beta-glucan to Biotec Pharmacon, and HER2 bispecific antibody to Abpro-labs. N-KC is an advisory board member for Abpro-Labs and Eureka Therapeutics.

The remaining author declares that the research was conducted in the absence of any commercial or financial relationships that could be construed as a potential conflict of interest.

Publisher's Note: All claims expressed in this article are solely those of the authors and do not necessarily represent those of their affiliated organizations, or those of the publisher, the editors and the reviewers. Any product that may be evaluated in this article, or claim that may be made by its manufacturer, is not guaranteed or endorsed by the publisher.

frontiers in Immunology

ORIGINAL RESEARCH
published: 03 March 2022
doi: 10.3389/fimmu.2022.837013

Conventional Therapies Deplete Brain-Infiltrating Adaptive Immune Cells in a Mouse Model of Group 3 Medulloblastoma Implicating Myeloid Cells as Favorable Immunotherapy Targets

Zahra Abbas[1,2], *Courtney George*[2,3], *Mathew Ancliffe*[2,4], *Meegan Howlett*[1,2], *Anya C. Jones*[1,5], *Mani Kuchibhotla*[2], *Robert J. Wechsler-Reya*[6], *Nicholas G. Gottardo*[1,2,7] *and Raelene Endersby*[1,2]*

[1] Centre for Child Health Research, University of Western Australia, Perth, WA, Australia, [2] Brain Tumour Research Program, Telethon Kids Cancer Centre, Telethon Kids Institute, Perth, WA, Australia, [3] School of Medical and Health Sciences, Edith Cowan University, Perth, WA, Australia, [4] School of Veterinary and Life Sciences, Murdoch University, Perth, WA, Australia, [5] Cancer Centre Core Research, Telethon Kids Cancer Centre, Telethon Kids Institute, Perth, WA, Australia, [6] NCI-Designated Cancer Center, Sanford Burnham Prebys Medical Discovery Institute, La Jolla, CA, United States, [7] Department of Paediatric and Adolescent Oncology and Haematology, Perth Children's Hospital, Perth, WA, Australia

OPEN ACCESS

Edited by:
Orazio Vittorio,
University of New South Wales,
Australia

Reviewed by:
Maria Vinci,
Bambino Gesù Children's Hospital
(IRCCS), Italy
Toni Jue,
Children's Cancer Institute Australia,
Australia

***Correspondence:**
Raelene Endersby
raelene.endersby@telethonkids.org.au

Specialty section:
This article was submitted to
Cancer Immunity
and Immunotherapy,
a section of the journal
Frontiers in Immunology

Received: 16 December 2021
Accepted: 08 February 2022
Published: 03 March 2022

Citation:
Abbas Z, George C, Ancliffe M,
Howlett M, Jones AC, Kuchibhotla M,
Wechsler-Reya RJ, Gottardo NG and
Endersby R (2022) Conventional
Therapies Deplete Brain-Infiltrating
Adaptive Immune Cells in a Mouse
Model of Group 3 Medulloblastoma
Implicating Myeloid Cells as Favorable
Immunotherapy Targets.
Front. Immunol. 13:837013.
doi: 10.3389/fimmu.2022.837013

Medulloblastoma is the most common childhood brain cancer. Mainstay treatments of radiation and chemotherapy have not changed in decades and new treatment approaches are crucial for the improvement of clinical outcomes. To date, immunotherapies for medulloblastoma have been unsuccessful, and studies investigating the immune microenvironment of the disease and the impact of current therapies are limited. Preclinical models that recapitulate both the disease and immune environment are essential for understanding immune-tumor interactions and to aid the identification of new and effective immunotherapies. Using an immune-competent mouse model of aggressive *Myc*-driven medulloblastoma, we characterized the brain immune microenvironment and changes induced in response to craniospinal irradiation, or the medulloblastoma chemotherapies cyclophosphamide or gemcitabine. The role of adaptive immunity in disease progression and treatment response was delineated by comparing survival outcomes in wildtype C57Bl/6J and in mice deficient in *Rag1* that lack mature T and B cells. We found medulloblastomas in wildtype and *Rag1*-deficient mice grew equally fast, and that craniospinal irradiation and chemotherapies extended survival equally in wildtype and *Rag1*-deficient mice, suggesting that tumor growth and treatment response is independent of T and B cells. Medulloblastomas were myeloid dominant, and in wildtype mice, craniospinal irradiation and cyclophosphamide depleted T and B cells in

the brain. Gemcitabine treatment was found to minimally alter the immune populations in the brain, resulting only in a depletion of neutrophils. Intratumorally, we observed an abundance of Iba1^{+} macrophages, and we show that CD45^{high} cells comprise the majority of immune cells within these medulloblastomas but found that existing markers are insufficient to clearly delineate resident microglia from infiltrating macrophages. Ultimately, brain resident and peripheral macrophages dominate the brain and tumor microenvironment and are not depleted by standard-of-care medulloblastoma therapies. These populations therefore present a favorable target for immunotherapy in combination with front-line treatments.

Keywords: medulloblastoma, immune microenvironment, microglia, immunocharacterization, chemotherapy, craniospinal irradiation, group 3

INTRODUCTION

Medulloblastoma is the most common malignant brain cancer in children, accounting for over 60% of childhood embryonal brain tumors [reviewed in (1)]. Extensive molecular analyses by multiple groups have revealed that medulloblastomas can be classified according to molecular and histopathological features into four major subgroups (WNT, SHH, Group 3, and Group 4) which vary in their clinical outcomes (2, 3). Standard-of-care treatment consists of radiotherapy and chemotherapy following surgical resection which has not changed for decades, survival outcomes have plateaued (4), and severe treatment-induced toxicity remains a major problem for survivors (1). Approximately 30% of children with medulloblastoma will fail conventional therapy (5). While certain molecular features can identify tumors at high risk of treatment failure, including amplification and/or overexpression of *MYC* in Group 3 medulloblastoma (6), limited therapeutic options exist for patients following relapse and there are minimal genetic changes in Group 3 tumors that can be therapeutically targeted at this disease stage (7). Consequently, there is an urgent and unmet need to identify new therapies for the treatment of medulloblastoma and to improve quality-of-life following disease control.

Immunotherapy has arisen as a possible adjunct to conventional therapy to improve the efficacy and mitigate the profound neurotoxicity of current medulloblastoma treatments; however, there have been few studies defining the mechanisms by which medulloblastomas evade anti-tumoral immune activity. Despite the successes immunotherapies have had in other cancers, no clinically approved immunotherapy has had proven success in clinical trials for medulloblastoma to date. Although there are several different immunotherapeutic approaches currently in clinical trials for children with medulloblastoma, including immune checkpoint inhibitors, oncolytic viruses, and dendritic cell vaccines, all of these are early phase studies, and none have progressed beyond phase 2. Moreover, as with many early phase clinical trials for pediatric cancer, these agents are being evaluated in children with recurrent or relapsed disease; whereas past clinical trial experience indicates that new therapies for medulloblastoma have the greatest chance of success when applied early in the course of the disease. This is because relapsed medulloblastoma is typically highly treatment resistant and a patient's likelihood of responding to salvage therapy is low at this disease stage (<5% long-term survival) (5, 8, 9). It is therefore important that new immuno-therapies being considered for medulloblastoma are rationally designed based on the immune cells present within tumors and tested for efficacy in combination with standard first-line therapies like radiotherapy and chemotherapy. However, studies investigating the impact of radiotherapy and chemotherapy on the immune microenvironment of medulloblastoma are limited. As a result, it is poorly understood how compatible standard therapies are with existing or emerging immunotherapeutics.

Here, we have utilized both immune-competent and immunodeficient murine models of aggressive *Myc*-driven medulloblastoma (10) and characterized adaptive and innate immune cell infiltration in the brain. We describe the impact of the adaptive immune system on tumor growth and treatment response using *Rag1* knockout mice. These mice are deficient in V(D)J recombination, resulting in the arrest of T and B cell differentiation at an early stage and subsequent severe combined immunodeficiency (11). In addition, we have defined how the immune microenvironment changes in response to clinically-relevant fractionated craniospinal irradiation (CSI) protocols, or to the clinically used medulloblastoma chemotherapies cyclophosphamide (CPA) or gemcitabine (GEM). We show that these first-line therapies deplete lymphocyte populations in the brain/medulloblastoma microenvironment, and recommend these impacts be considered when designing future up-front treatment protocols that incorporate immunotherapies for medulloblastoma.

MATERIALS AND METHODS

Preclinical Models

6-12 week old female C57Bl/6J (WT) mice were obtained from the Animal Resource Centre (Perth, Australia). 6-12 week old female C57Bl/6J *Rag1*$^{-/-}$ (Rag1KO) mice, that lack mature T and B cells (11), were obtained from an on-site breeding colony at the Telethon Kids Institute Bioresources Facility. Mice were group-housed in a pathogen-free facility at the Telethon Kids Institute

(12:12 hour light:dark cycle) with access to standard chow and water *ad libitum*. Mice received sunflower seeds during treatment for enrichment and to maintain healthy weight. All animal procedures were approved by the Animal Ethics Committee of the Telethon Kids Institute and performed in accordance with Australia's Code for the Care and use of Animals for Scientific Purposes.

The murine allograft model of aggressive *Myc*-amplified Group 3 medulloblastoma (Myc/p53^{DD}) was generated through retroviral-driven expression of *Myc*^{T58A}, a dominant negative carboxy-terminal fragment of *Tp53*, GFP and firefly luciferase in CD133-positive cerebellar stem cells as previously described (10). For intracranial implantation, Myc/p53^{DD} cells were harvested from female C57Bl/6J donor mice, suspended in Matrigel (BD Biosciences), and 5,000 cells were implanted per mouse as previously described (12).

Tumor size was monitored using bioluminescence imaging with an IVIS Spectrum (Caliper, USA). Prior to imaging, fur was removed with electric clippers and depilatory cream. Mice received intraperitoneal injections of D-Luciferin [15 mg/kg in Dulbecco's phosphate-buffered saline (DPBS)] and were anesthetized with isoflurane. During image acquisition, isoflurane was maintained at 1.5-1.8% in oxygen (flow rate 0.5 L/min) and images were acquired every minute for 10 minutes until peak photon flux was recorded. Bioluminescence was used as a surrogate measure of tumor burden and mice were randomized into groups such that the average flux ± standard deviation (SD) was equal across all groups at the start of treatment.

Craniospinal Irradiation (CSI)

Irradiation was performed using a X-RAD SmART small animal image-guided radiation therapy system (Precision X-Ray, USA) employing cone-beam CT guidance with fully assessed spatial and dosimetric accuracy (13). Treatment planning and dose calculations were performed using Monte Carlo simulations in SmART-Plan software (14). Mice were anesthetized with isoflurane, maintained at 1-2% in air delivered *via* nose cone during treatment. Mice were secured to the irradiation stage with non-adhesive athletic tape to flatten the spine and avoid irradiating abdominal organs. CSI was achieved using two sets of two lateral coplanar beams with 40 mm square collimation delivered to two separate isocenters, with the first set of beams targeting the brain and cervical spine, the second targeting the thoracic and lumbar spine. Mice received a total of 20 Gy CSI fractionated as 10 doses of 2 Gy, delivered on a 5-days-on, 2-days-off schedule for two weeks (15) (**Figure 1A**). For the sham control group, mice were anesthetized with isoflurane on a 5-days-on, 2-days-off schedule for two weeks for an equal length of time per day as the CSI treatment protocol. Animals were humanely euthanized upon the onset of tumor-related morbidity.

Chemotherapy

Cyclophosphamide (CPA, Baxter) and gemcitabine (GEM, MedChemExpress) were diluted in phosphate-buffered saline (PBS) and delivered twice weekly (day 7, 10, 14, 17, etc.). CPA was delivered intraperitoneally (i.p.) at 120 mg/kg and GEM was delivered intravenously (i.v.) at 60 mg/kg. Control mice received saline injections *via* the equivalent route on the same schedule (**Figure 1A**). Treatment was continued until mice required euthanasia due to tumor-related morbidity.

Flow Cytometry

Single cell suspensions were prepared from whole brains for flow cytometric analysis. Whole brains were minced on a sterile petri dish with a scalpel blade, prior to addition of 5 mL digestion buffer (100 U/mL Collagenase IV (Life Technologies), 10 U/mL DNAse (Sigma-Aldrich) in Hank's balanced salt solution (HBSS, Gibco)), followed by trituration to obtain a uniform suspension. The tissue suspension was transferred to a gentleMACS C tube (Miltenyi) and further digested on a gentleMACS Octo Dissociator (Miltenyi) for 30 minutes, with constant stirring at 50 RPM at 37°C. Digestion was halted with the addition of 10 mL cold FACS buffer (2% fetal calf serum, 5 mM EDTA in HBSS) and the suspension was strained through a 100 µm filter (Miltenyi). Red blood cells were lysed with red blood cell lysis solution (Miltenyi), cells were resuspended in 10 mL FACS buffer and strained through a 30 µm filter (Miltenyi). To remove myelin, cells were resuspended in 10 mL of 30% Percoll (Sigma-Aldrich) diluted in FACS buffer and centrifuged at 800 g for 30 min at room temperature. The myelin layer was removed, and cells resuspended in DPBS before staining.

Given that chemotherapy is known to have systemic effects, spleen tissue was routinely collected and analyzed alongside brain tissue as a control to characterize the effects of chemotherapy on immune cells outside the central nervous system. In addition, the spleens of mice treated with CSI would have received some off-target irradiation when radiotherapy was delivered to the thoracic and lumbar spine. Spleen dissociation protocols and results can be found in the **Supplementary Data** (**Supplementary Figure 1**).

Single cell suspensions were labelled with a viability stain (BD Bioscience Cat #564997) then stained with the following fluorochrome conjugated cell surface marker antibodies: CD45-BV421 (BD Bioscience Cat #563890), IAIE-BV510 (Biolegend Cat #107635), CD11b-BV605 (Biolegend Cat #101257), CD4-BV650 (BD Bioscience Cat #563747), CD8a-BV711 (BD Bioscience Cat #563046), NK1.1-BV786 (Biolegend Cat #108749), B220-PerCP-Cy5.5 (BD Bioscience Cat #552771), F4/80-PE (BD Bioscience Cat #565410), CD3e-PE-CF594 (BD Bioscience Cat #562286), CD19-PECy7 (BD Bioscience Cat #552854), CD11c-APC (BD Bioscience Cat #550261), Ly6G-APC-Cy7 (BD Bioscience Cat #560600). Antibody dilutions and the staining protocol can be found in the **Supplementary Material** (**Supplementary Methods** and **Supplementary Table 1**). Data were acquired on a LSRFortessa X-20 (BD Bioscience, USA) and immune populations were gated using FlowJo (**Figure 2**). The combination of markers used to define different immune populations is described in **Supplementary Table 2**. Positively stained cells are presented as a proportion of all CD45-positive cells. Alternatively, calibration beads (BD Bioscience Cat #556296) were added to cell suspensions to quantify the total numbers of immune cells within each tissue sample by comparing the ratio of bead events to cell events. Population statistics were compared and graphed in GraphPad

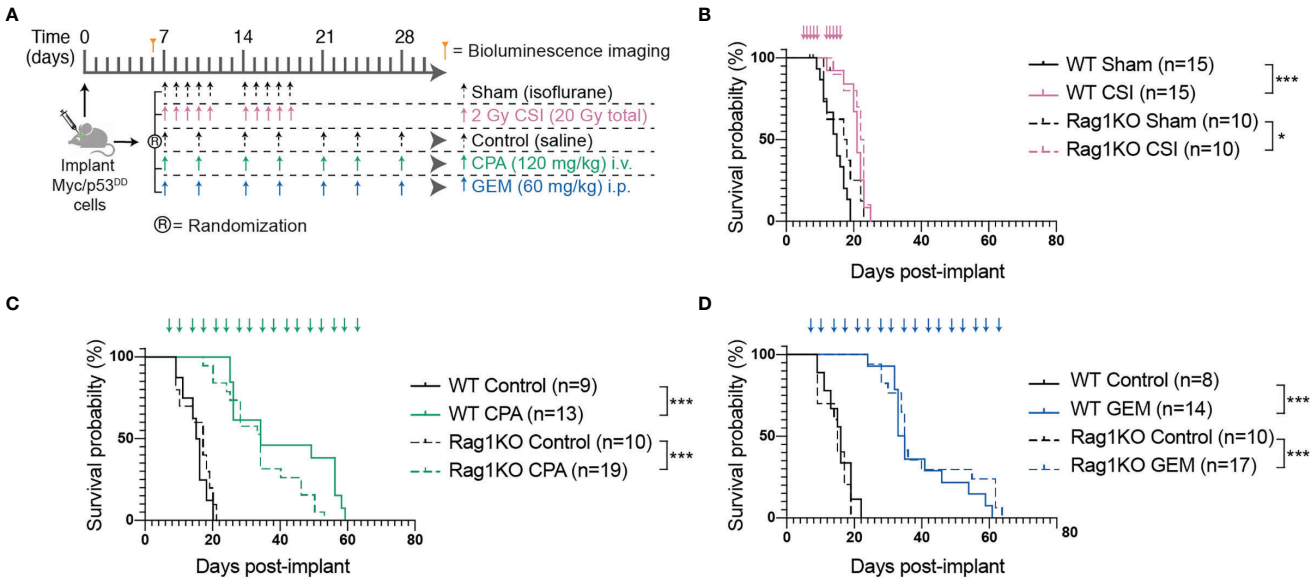

FIGURE 1 | The adaptive immune system does not play a role in Myc/p53^{DD} tumor progression nor treatment efficacy. **(A)** Schematic diagram illustrating the treatment protocols for craniospinal irradiation (CSI), cyclophosphamide (CPA) and gemcitabine (GEM). **(B–D)** Survival curves of multiple independent experiments (minimum of two independent experiments per treatment) of WT (*solid lines*) or Rag1KO (*dashed lines*) mice treated with **(B)** CSI (*pink*), **(C)** CPA (*green*), or **(D)** GEM (*blue*). Arrows on graphs indicate when treatment was administered. The number of mice per group (n) is shown and significant differences between survival curves determined using log-rank tests is indicated (*P < 0.05; ***P < 0.001).

PRISM v8. Gating strategy for populations from Rag1KO mice are shown in **Supplementary Figure 2**.

For CSI treated mice, immune cell populations were assessed at two experimental time points. Firstly, tissue was harvested 24 hours following the final (10th) dose of CSI (referred to as "acute") to capture transient changes in immune populations following CSI. A second time point was captured approximately 1-2 weeks after the cessation of CSI (referred to as "late stage"), when tumor burden was high and mice were moribund, to determine lasting effects of CSI. For all chemotherapy experiments, brains were analyzed when tumor burden was high and caused morbidity requiring euthanasia. Due to the continual dosing schedule (**Figure 1**), tumor related morbidity and tissue analyses occurred within 2-3 days of chemotherapy dosing. Healthy, non-tumor bearing mice were time-matched to Myc/p53^{DD} bearing mice. To determine proportions of CD45^{high} and CD45^{intermediate} (CD45^{int}) tumor-infiltrating immune cells, untreated Myc/p53^{DD} medulloblastomas from C57Bl/6J WT mice were dissected out from the brain, dissociated as above, and labelled with viability stain (BD Bioscience Cat #564997) and CD45-BV421 (BD Bioscience Cat #563890).

Immunohistochemistry (IHC)

Mice were transcardially perfused with PBS, followed by 4% paraformaldehyde (PFA) in PBS. Brains were further fixed overnight in 4% PFA at 4°C before embedding into paraffin. IHC was performed on 5 µm sections. Briefly, sections were deparaffinized and rehydrated using an ST5010 AutoStainer XL (Leica, Germany). Antigen retrieval was performed using a sodium citrate buffer (1.8 mM citric acid, 8.2 mM sodium citrate), sections were incubated in 3% H_2O_2 to block endogenous peroxidases, blocked with 10% normal goat serum in Tris buffered saline containing 0.01% Tween 20 (TBS-T) for one hour at room temperature, and incubated with primary antibodies overnight at 4°C in 2% goat serum in TBS-T. Slides were incubated with biotinylated secondary antibodies, then incubated with an streptavidin-conjugated peroxidase reagent (Elite ABC, Vector Labs). Slides were incubated with NovaRED peroxidase substrate (Vector Labs), counterstained with Gill's Hematoxylin (Vector Labs), dehydrated, and coverslipped with Permount (Fisher Scientific). Slides were stained with the following antibodies: Iba1 (1:800, Wako Chemicals, Cat #019-19741), Tmem119 (1:300, Abcam, Cat #ab209064). Positively-stained cells with evident nuclei were counted from four 1mm^2 areas per mouse corresponding to three different areas: normal cortex, areas where the image consisted of 50% tumor and 50% normal brain, or tumor. Data are presented as cells per mm^2.

RNA Isolation and Bulk RNA Sequencing

Tumor tissue was dissected from the brain, snap frozen using dry ice and stored at -80°C. Total RNA was isolated from 5-20 mg tumor tissue using the RNeasy Plus Mini Kit (Qiagen) as per the supplied protocol. RNA concentration and purity was assessed on a spectrophotometer (NanoDrop) and total RNA was submitted to GenomicsWA (Perth, Australia) (CSI and Sham samples) or the Australian Genome Research Facility (AGRF) (CPA, GEM, control samples). Samples had an average ± SD RNA integrity number (RIN) of 9.8 ± 0.36 prior to library

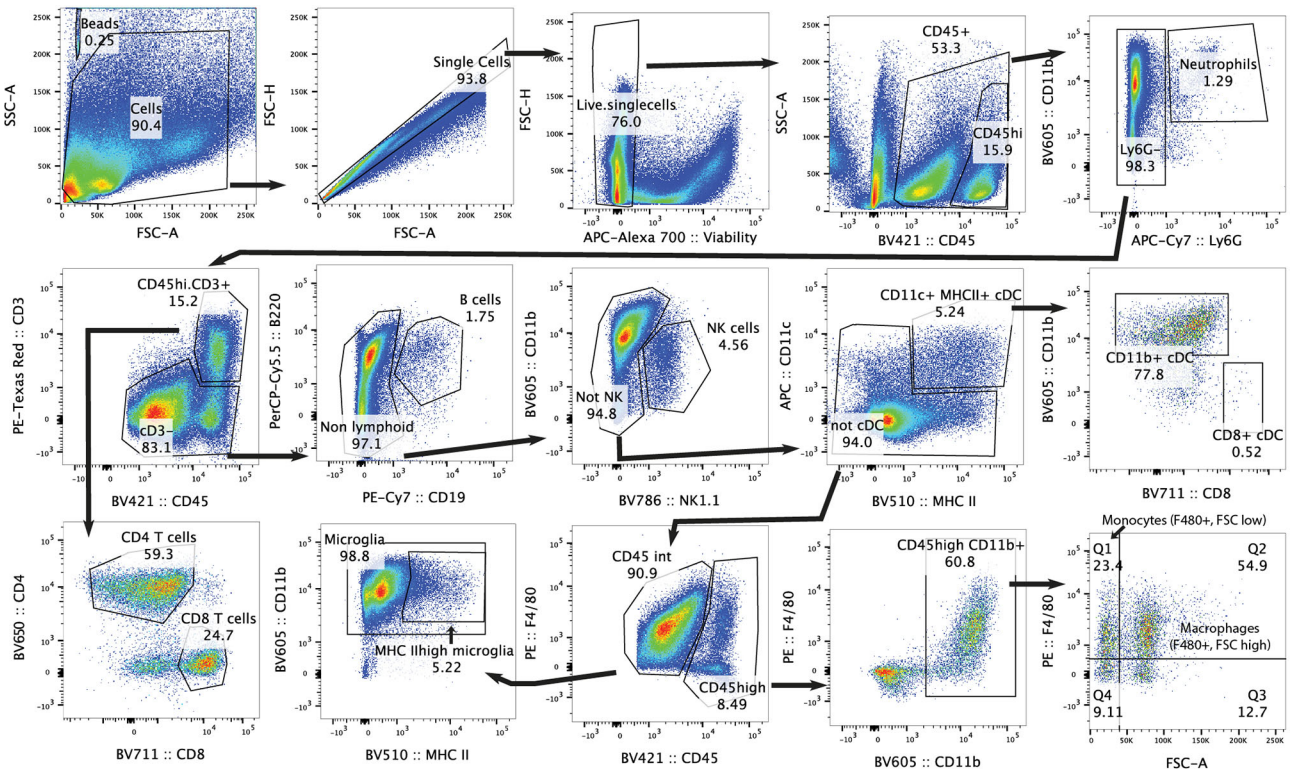

FIGURE 2 | Gating strategy for flow cytometry analysis of mouse brain. Representative plots of gating strategy for immune populations in C57Bl/6J WT brain.

preparation. Total RNA library preparation (SureSelect, Agilent), rRNA depletion (Ribo-Zero Plus, Illumina) and sequencing were carried out by GenomicsWA or AGRF. Libraries were sequenced on NovaSeq 6000 S1 flow cells as paired-end 150bp reads (Illumina). Raw sequencing data for two independent datasets are available from the European Genome Archives (EGAS0000 1005847 and EGAS00001005846).

Pre-Processing, Quality Control (QC) and Exploratory Data Analysis

Adapter and quality trimming were applied using CutAdapt (16). Pre-alignment and post-alignment QC were carried out with FastQC (17) and SAMStat (18) respectively. Reads were aligned to the mouse reference genome (GRCm38) using HISAT2 (19) and quantified at the gene-level with *summarizedOverlaps()* (20). The proportion of mapped reads was 84% (79.7-87%) in CPA/GEM/Control samples and 90% (89.3-91.5%) in CSI/Sham samples.

Data analysis was carried out in the statistical computing environment R (version 4.1.1). Genes with an official MGI Gene Nomenclature Committee symbol and a count per million corresponding to 10 in ≥3 were retained for downstream analysis. Exploratory data analysis was carried out using EDASeq (21) and standard QC plots were used to identify potential outlying samples pre- and post-global-scale median normalization of gene counts. Unwanted variation was removed employing RUVSeq (21).

Estimation of the Cellular Composition With CIBERSORTx

CIBERSORTx (22) was used to estimate the immune cell proportions in medulloblastoma tissue. A published C57Bl/6J WT whole brain single cell dataset (23) (GEO accession GSE128855) was used as the reference dataset containing 8 annotated brain immune cell types (microglia, B cells, NK/NKT cells, T cells, cDC, monocytes, border associated macrophages, neutrophils). The following parameters were used: disabled batch correction, relative run mode, 100 permutations. Cell fractions calculated by CIBERSORTx in treatment groups were compared to their control (CSI vs Sham, CPA and GEM vs Control) by unpaired two-tailed *t tests*.

Differential Expression Analysis

Differentially expressed genes were identified using edgeR (24). A linear binomial model was fit to the data and a false discovery rate (FDR) for multiple testing was applied. An adjusted $P < 0.05$ and an absolute log2 fold change > 0.5 (fold change = 1.5) was deemed significant.

Pathway Analysis

Up- and downregulated genes were assessed separately for pathways enrichment using InnateDB (25) version 5.4. Enrichment testing is based on a hypergeometric distribution

and P values are corrected using the Benjamini-Hochberg method for multiple testing.

Upstream Driver Analysis

Putative molecular drivers of the observed gene expression patterns were identified using upstream regulator analysis from Ingenuity Systems KnowledgeBase (26). Significance testing is based on a Fisher's exact test, testing for enrichment against known upstream drivers. The Benjamini-Hochberg method was used to correct for multiple testing. An adjusted P-value < 0.01 and absolute z-score > 2.0 (predicting activation/inhibition of the driver) were deemed significant.

Statistical Analyses

Kaplan-Meier survival curves were compared using the log-rank test. In each survival experiment, treatment groups were compared to their equivalent controls. Unpaired two-tailed *t* tests were used to compare immune populations for flow cytometry data. Treatments were compared to their control (CSI vs Sham, CPA and GEM vs Control). For CSI experiments, each time-point group was only compared to its time-matched sham (late-stage/acute). Being an exploratory study, P values are stated without multiplicity adjustments (27) and significant differences were defined as $P < 0.05$ in flow cytometry, IHC, and CIBERSORTx comparisons.

RESULTS

Myc/p53^{DD} Tumor Growth Is Unaffected by a Functional Adaptive Immune System

The majority of preclinical medulloblastoma mouse models utilize immune-deficient strains and the role of the immune system in medulloblastoma growth is poorly defined. To address this, we took advantage of a murine model of Group 3 medulloblastoma that engrafts in C57Bl/6J mice following intracranial implantation and compared tumor growth in wildtype C57Bl/6J mice and C57Bl/6J mice deficient in *Rag1*. Tumor-free survival of control mice (sham/isoflurane or control/saline) was not different between WT and Rag1KO animals, indicating that growth of this model of Group 3 medulloblastoma is not impacted by the presence or absence of mature T and B cells (**Figure 1**). To determine the role of the adaptive immune system in response to conventional first-line therapies, medulloblastoma-bearing mice of either strain were treated with CSI or two DNA-damaging chemotherapies used as part of clinical care: CPA or GEM (28) (NCT01878617) (**Figure 1A**). Compared to control groups, CSI prolonged median survival similarly in WT mice (21 compared to 15 days; P<0.0001) and Rag1KO mice (22.5 compared to 17.5 days; P=0.03). Likewise, response of Myc/p53^{DD} tumors to chemotherapy was similar in WT and Rag1KO mice. CPA prolonged median survival to 34 days in both WT mice (P<0.001) and Rag1KO mice (P<0.0001); while GEM prolonged median survival from 16 days to 34 days in WT mice (P<0.0001) and from 15 to 35 days in Rag1KO mice (P<0.0001). These results indicate that treatment-mediated tumor control is independent of T and B cells in this model of medulloblastoma (**Figures 1B–D**).

Group 3 Medulloblastoma Growth Stimulates Immune Cell Influx Into the Brain

The finding that the adaptive immune system did not appear to modulate response to therapy was surprising given previous reports of increased CD8$^+$ T cells in murine Group 3 medulloblastoma (29). Furthermore, it is unknown what impact conventional medulloblastoma treatments have on immune cells within the brain. To understand whether these treatments were altering the immune populations in the whole brain, mice harboring Myc/p53^{DD} tumors were administered treatment (or control) as described above, and the immune cells present in brain tissue were assessed by flow cytometry when mice required euthanasia due to tumor-related morbidity, using the gating strategy defined in **Figure 2**.

In the absence of treatment, we observed that medulloblastoma growth induced an overall influx of immune cells into the brain (**Figure 3**). Brain-resident microglia in adult mice express lower levels of CD45 compared to bone-marrow derived immune cells, thus can be distinguished using flow cytometry (30, 31). The addition of calibration beads enabled us to analyze absolute cell numbers in the cell suspensions of the entire brain and we observed a significant increase in immune cell numbers (CD45$^+$), both CD45^{high} and microglia (CD45^{int} CD11b$^+$) in the brains of tumor-bearing WT mice compared to healthy age-matched brains. Moreover, we observed increased counts of activated microglia (CD45^{int} CD11b$^+$ MHC II^{high}) (32), classical dendritic cells (cDCs) (CD45^{high} CD11c$^+$ MHC II$^+$, CD11b$^+$), NK cells (CD45^{high} NK1.1$^+$), CD4$^+$ T cells (CD45^{high} CD3$^+$ CD4$^+$), and CD8$^+$ T cells (CD45^{high} CD3$^+$ CD8$^+$), (**Figure 3**). CD8$^+$ cDCs accounted for a very small proportion of the immune cells, and their counts are not shown. No significant changes were detected in neutrophil (CD45^{high} Ly6G$^+$), B cell (CD45^{high} CD19$^+$ B220$^+$), monocyte (CD45^{high} CD11b$^+$ F4/80$^+$ FSC^{low}) or macrophage (CD45^{high} CD11b$^+$ F4/80$^+$ FSC^{high}) numbers between normal brains or brains harboring Myc/p53^{DD} medulloblastomas.

To further demonstrate the changes in immune cell populations caused by medulloblastoma growth in WT mouse brain we compared the changes in immune cell populations relative to each other by quantifying differences as a percentage of all CD45$^+$ cells. As a proportion of all CD45$^+$ immune cells in the brain, significant increases in cDCs, CD4$^+$ T cells, CD8$^+$ T cells, and activated microglia were observed in tumor-bearing brains compared to healthy brains. As a consequence of this influx, the proportion of microglia relative to all immune cells was decreased in tumor-bearing brains compared to healthy brain (**Supplementary Figure 3**), although as described above, microglial numbers were increased overall.

In Rag1KO mice, growth of Myc/p53^{DD} medulloblastoma also induced an increase in the absolute numbers of microglia in the brain as well as an influx of bone marrow-derived immune cells in the absence of treatment. In addition, we observed a significant increase in CD11b$^+$ cDCs, NK cells, neutrophils, and monocytes (**Supplementary Figure 4**), reiterating the finding

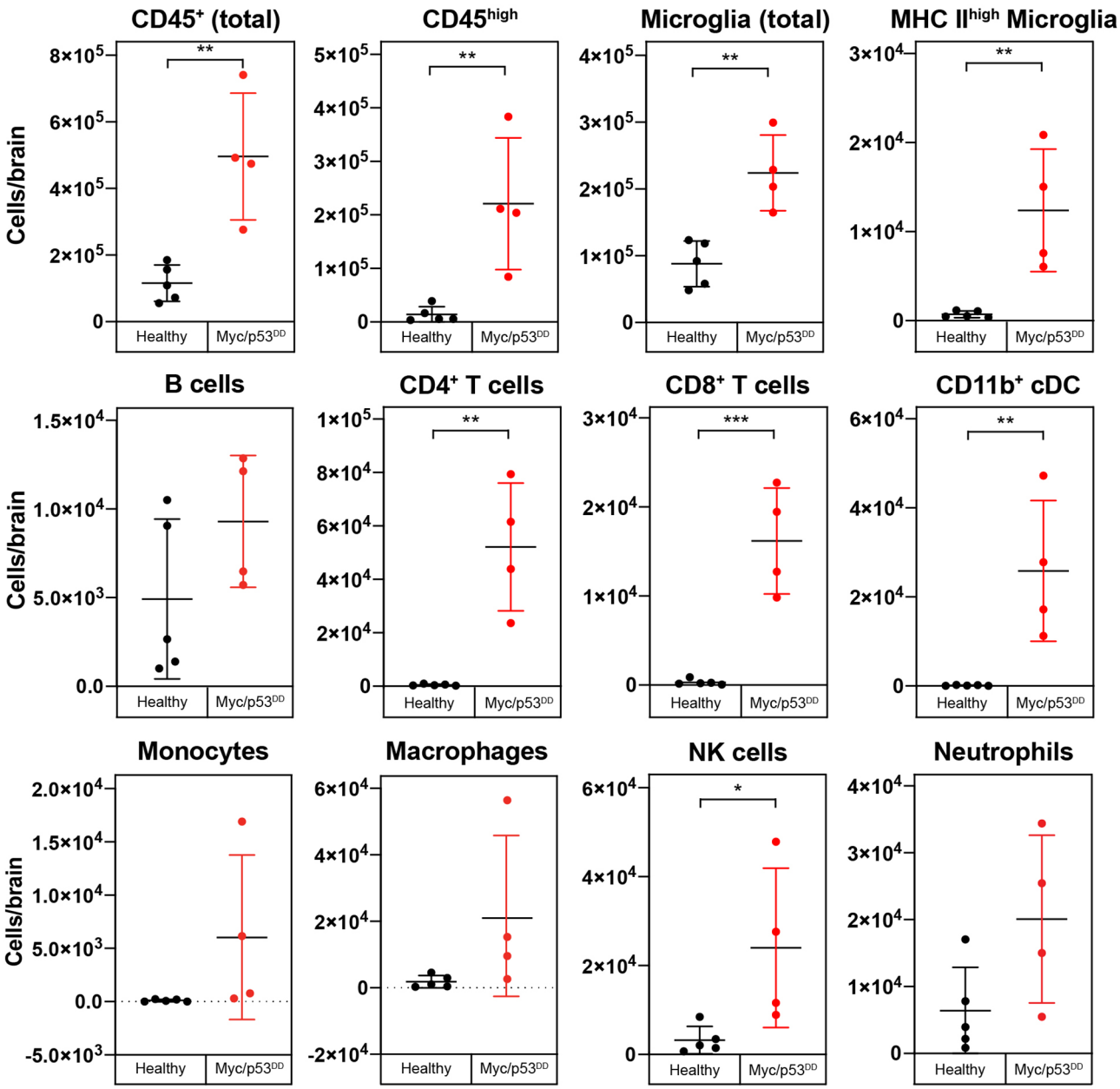

FIGURE 3 | Growth of Myc/p53^{DD} medulloblastoma increases the numbers of infiltrating and resident immune cells in the brain. The immune cell populations from healthy brains of C57Bl/6J WT mice (*black circles*, n=5) were determined using flow cytometry and compared with the brains of WT mice bearing Myc/p53^{DD} tumors (*red circles*, n=4). Beads were used and the entire sample was analyzed to determine the total number of the indicated cells in each sample. Tumor-containing brains had significantly higher overall counts of immune cells (CD45^{+}), both infiltrating (CD45^{high}) and resident (microglia) compared to healthy brain. Moreover, an increase in activated microglia (MHC II^{high}), CD4^{+} T cells, CD8^{+} T cells, NK cells, and CD11b^{+} cDCs was observed in Myc/p53^{DD} tumor bearing brains. No significant change in neutrophils, B cells, monocytes or macrophages was observed. Horizontal lines indicate the mean and error bars indicate SD. Comparisons shown to be statistically significant by *t* test are shown (*P < 0.05; **P < 0.01; ***P < 0.001).

that even in mice lacking an adaptive immune system, medulloblastoma growth induces influx of bone marrow-derived immune cells to the brain. As observed in WT mice, Myc/p53^{DD} tumor growth significantly elevated the number of activated microglia in Rag1KO brains.

CSI Transiently Depletes Bone Marrow-Derived Immune Populations in the Brain

Given this understanding of how the immune microenvironment of brain is altered with medulloblastoma growth, we next characterized the effects of clinical treatments on the

immunology of medulloblastoma, starting with CSI. We analyzed brains at two time points following CSI – 24 hours after the final dose of radiation (acute), and at high tumor burden when mice required euthanasia (late-stage) – to determine transient and long-term impacts. In WT mice, CSI resulted in a significant, but transient, reduction in infiltrating bone marrow derived immune cells ($CD45^{high}$). The proportion of $CD4^+$ T cells, $CD8^+$ T cells, B cells, and $CD11b^+$ cDCs in the brain were all observed to be significantly reduced 24 hours following delivery of the last CSI fraction (**Figure 4**, *squares*). In consequence, the proportion of microglia as a percentage of the total immune milieu was significantly higher in CSI treated mice compared to sham treated mice at this time point (**Figure 4**, *squares*). Proportions of monocytes and macrophages were unchanged with treatment (**Supplementary Figure 5**). In contrast, when we examined acute CSI-induced changes in the

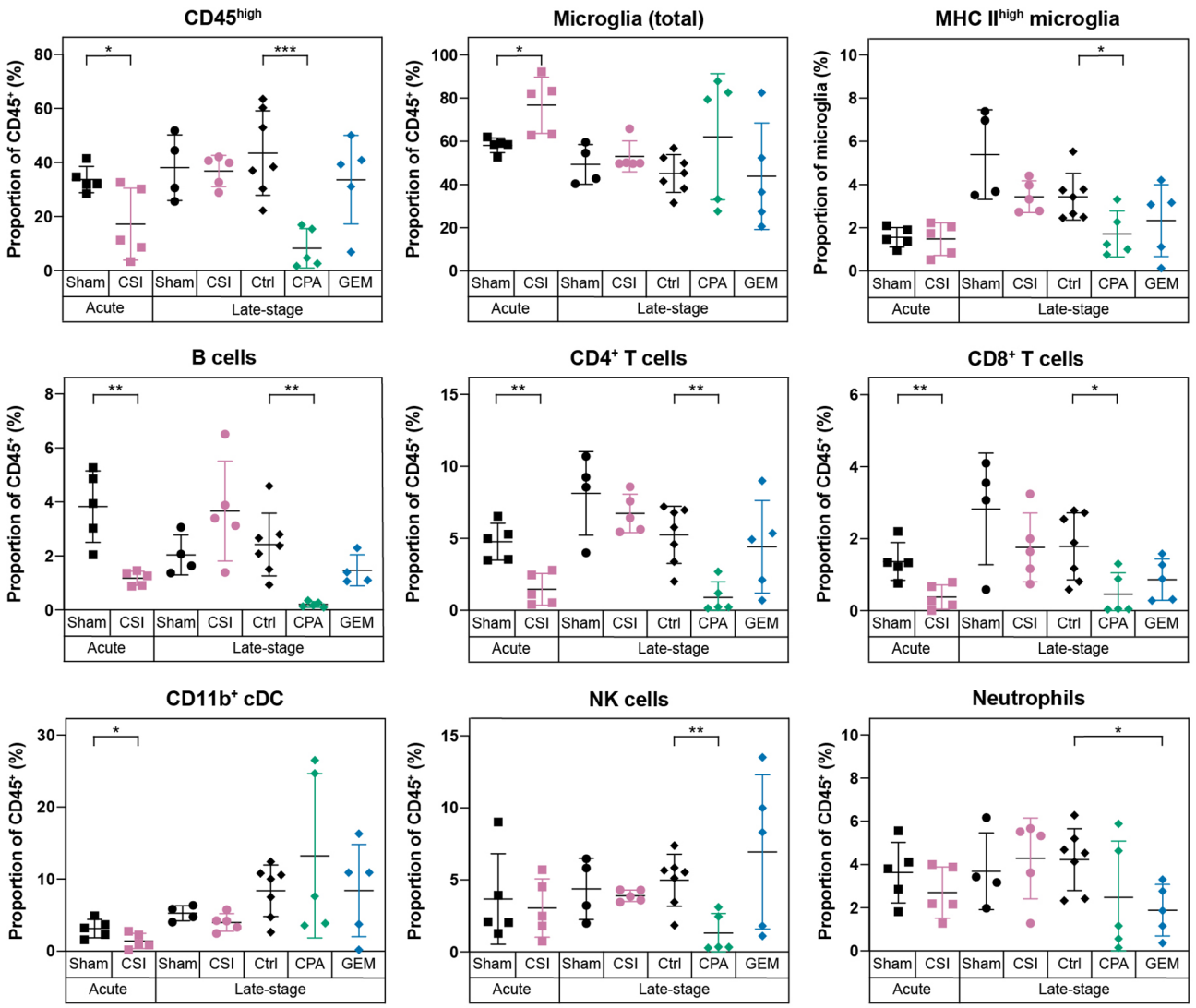

FIGURE 4 | Radiotherapy and chemotherapy alter the immune microenvironment in the brains of C57Bl/6J WT mice with Myc/$p53^{DD}$ medulloblastoma. Immune cell populations (shown as a percentage of all $CD45^+$ cells) in WT brains harboring medulloblastoma following a range of different treatments are shown. From left to right, mice with Myc/$p53^{DD}$ medulloblastoma were treated with either sham (*black squares*, n=5) or CSI (*pink squares*, n=5) and harvested 24 hours after the tenth dose (labeled "Acute"), sham (*black circles*, n=4) or CSI (*pink circles*, n=5) and harvested upon the development of tumor-related morbidity (labeled "Late stage"), or after treatment with saline ("Ctrl", *black diamonds*, n=7), CPA (*green diamonds*, n=5), or GEM (*blue diamonds*, n=5) and harvested upon the development of tumor-related morbidity (also labeled "Late stage"). Fractionated CSI resulted in a temporary depletion of infiltrating $CD45^{high}$ immune cells. Specifically, B cells, $CD4^+$ T cells, $CD8^+$ T cells, and $CD11b^+$ cDCs were decreased (*pink squares*) and in consequence a proportional increase of microglia was observed, whereas this was not observed at a later time point (*pink circles*). CPA reduced the abundance of B cells, $CD4^+$ T cells, $CD8^+$ T cells, and NK cells, while GEM only significantly depleted neutrophils. Horizontal lines indicate the mean and error bars indicate SD. Each treatment group was compared to the appropriate treatment and time-point matched control by *t* test, with statistically significant differences indicated (*P < 0.05; **P < 0.01; ***P < 0.001).

brains of Rag1KO mice with Myc/p53^{DD} medulloblastoma, only a significant reduction of NK cells was observed 24 hours following CSI (**Supplementary Figure 6**, *squares*). WT mouse brains were also assessed upon the development of tumor-related morbidity, which occurred 1-2 weeks following the cessation of CSI. No differences in immune cell populations were detected in CSI treated mice compared to time-matched controls at this late stage (**Figure 4**, *circles*), indicating that immune population changes induced by CSI in the brain were temporary. These findings contrast recent reports of irradiation-mediated enhanced immune cell infiltration in a model of SHH medulloblastoma (33).

CPA Depletes Infiltrating CD45^{high} Immune Cells While GEM has Minimal Impacts on the Immune Microenvironment

Chemotherapeutics, including first-line medulloblastoma drugs CPA and GEM, can achieve an anti-tumor response directly *via* DNA damaging activity, or indirectly *via* induction of an immune response through immunogenic cell death, stimulating immune effectors, or inhibiting immune suppressors [reviewed in (34)]. Thus, we sought to characterize the effects of these clinically used chemotherapies on the immune cells within medulloblastoma bearing brains. Brains were analyzed when tumor burden was high ("Late-stage"), which was within 3-4 days of the last chemotherapy dose due to the continual dosing protocol. WT mice treated with CPA had significantly lower proportions of infiltrating immune cells in the brain compared to controls. Proportions of CD4$^+$ T cells, CD8$^+$ T cells, B cells, NK cells and activated microglia were all significantly reduced in CPA treated mice (**Figure 4**, *green diamonds*). It is known that CPA can cause leukopenia [reviewed in (35)]. Consistent with this, significant decreases in multiple immune cell populations were also observed in the spleens of mice treated with CPA (**Supplementary Figure 1**). In contrast, GEM treatment had minimal effects on the immunology of WT mouse brain, resulting only in a proportional reduction of neutrophils (**Figure 4**, *blue diamonds*).

Surprisingly, chemotherapy-induced immunodepletion was not observed in the brains of Rag1KO mice. Instead, we observed a significant increase in CD45^{high} immune cells in Rag1KO mice treated with either CPA or GEM (**Supplementary Figure 6**). The increase of CD45^{high} cells was higher in CPA treated mice, and we observed a concomitant decrease in the proportion of microglia in CPA treated Rag1KO brains.

Medulloblastoma-Infiltrating Myeloid Cells Express Iba1 but Not the Microglial Marker Tmem119

Not surprisingly, our results show that microglia dominate the brain/medulloblastoma immune microenvironment; however, our flow cytometry data did not indicate the spatial distribution of these cells or define if they were interacting with medulloblastoma cells, or instead if they were retained in normal brain. To determine intratumoral distribution of resident (CD45^{int}) and infiltrating (CD45^{high}) immune cells, we dissected out Myc/p53^{DD} tumors from WT mice and assessed proportions of intratumor immune cells with flow cytometry. We found that immune cells account for only 1-2% of the cells within these tumors, and that a majority (76.9 ± 3.88%) of the immune cells within the tumor were CD45^{high} (**Figure 5A**). However, it has been shown that microglia may up-regulate CD45 under pathological conditions; therefore, our approach of delineating microglia from tumor-infiltrating macrophages on the basis of intermediate versus high CD45 expression may be insufficient (36, 37). To characterize and further delineate the location of resident microglia and infiltrating peripheral myeloid cells in the brain and within Myc/p53^{DD} medulloblastomas, we performed IHC for two myeloid cell markers, Iba1 and Tmem119. Cells staining positively for Iba1, which is a marker of both bone marrow derived macrophages and microglia (38), were observed throughout the brain parenchyma and tumors. The morphology of cells stained with Iba1 varied from ramified in the normal brain, which typifies the resting state of microglia, to a more ameboid state, which typifies the active state, for cells located at the tumor periphery and within medulloblastomas (**Figures 5B, C**). Cells staining positively for the marker Tmem119, reported to be a specific marker of microglia (39), were observed throughout the normal brain displaying ramified morphology. Tmem119 also stained cells around the tumor edge and these cells displayed more ameboid morphology. However, IHC staining for Tmem119 was completely absent within the tumors suggesting these cells were not microglia (**Figures 5B, C**), although this is inconsistent with our flow cytometry findings which indicated that at least 23% of intratumoral immune cells should be microglia based on their lower expression of CD45 (CD45^{int}, **Figure 5A**). Together, our findings suggest that either bone-marrow derived immune cells comprise the majority of the intratumoral immune cells and that microglia do not penetrate the tumor, or, given reports of microglia upregulating CD45 in pathological conditions (36, 37), that microglia downregulate Tmem119 and upregulate CD45 in response to medulloblastoma.

Immunological Signatures in Medulloblastoma Are Poorly Interpretable Using Bulk RNA Sequencing

To understand what was driving the immunological changes we observed following the administration of first line medulloblastoma treatments, and due to the inability to clearly delineate microglia from macrophages or monocytes through flow cytometry or IHC, we employed bulk RNA sequencing on medulloblastomas following control, sham, CSI, CPA, or GEM treatment. RNA sequencing was carried out on late-stage tumors, as tumors were too small to be isolated at earlier stages. As such, CSI treated samples were harvested 1-2 weeks after treatment cessation, while chemotherapy-treated tumors were harvested within 48-72 hours of drug administration. For scientific rigor, CSI treated mice were compared to sham controls, while chemotherapy-treated mice were compared to saline controls. Principal component analysis plots were used to visualize and identify whether samples clustered by treatment across both mouse strains (**Figure 6A**). Samples treated with CSI or sham did

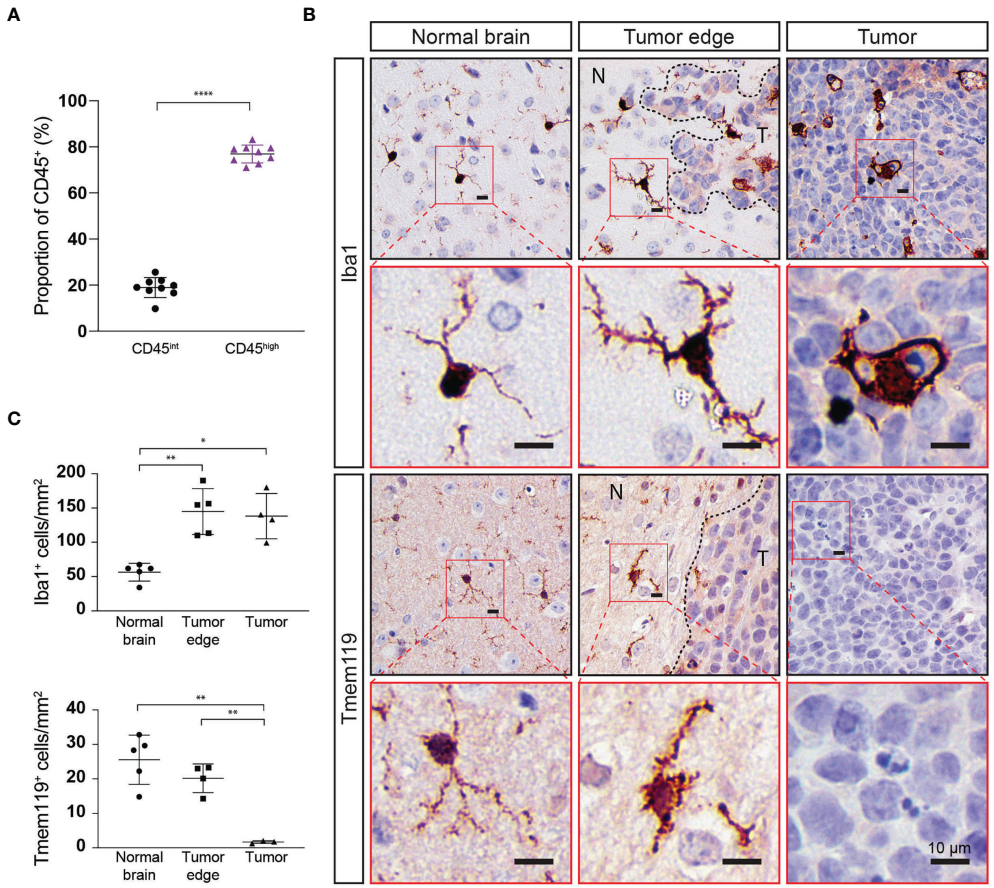

FIGURE 5 | Immune cell populations within Myc/p53^{DD} tumors in WT mouse brain highly express CD45 and do not express Tmem119. **(A)** Myc/p53^{DD} medulloblastomas (n=8) were dissected away from normal C57Bl6/J WT brain and cells were analyzed by flow cytometry for CD45^{int} (*black circles*) or CD45^{high} immune cells (*purple triangles*). Horizontal lines indicate the mean and error bars indicate SD. Comparison by paired *t test* is shown (****P < 0.0001) demonstrating that CD45^{high} immune cells account for the majority of intratumoral immune cells within Myc/p53^{DD} tumors. **(B)** WT mouse brain implanted with Myc/p53^{DD} medulloblastoma were examined using IHC for Iba1 and Tmem119. Representative low (*black border*) and high (*red border*) magnification images of Iba1 (*top*) or Tmem119 (*bottom*) expressing cells demonstrate a resting or ramified appearance in the normal brain (*left*), but have an activated or ameboid appearance around the edge of medulloblastomas (*middle, N* indicates normal brain and *T* indicates tumor), characterized by an increase and thickening of membrane projections. Within tumors (*right*), Iba1^{+} cells appear phagocytic, while Tmem119 staining is absent. Nuclei have been counterstained with hematoxylin and the scale bar on each image indicates 10 µm. **(C)** Quantitation of Iba1 or Tmem119 expressing cells from the brain regions indicated. Each symbol represents an individual mouse, horizontal lines indicate the mean and error bars indicate SD. Each area was compared using t test, with statistically significant differences indicated (*P < 0.05; **P < 0.01).

not cluster according to treatment or genetic background. For chemotherapy treated mice, Rag1KO samples clustered by treatment (Ctrl, CPA, GEM), whilst in WT mice, GEM clustered separately to CPA and Ctrl samples, which overlapped.

Through differential gene expression analysis, we identified 210 differentially expressed genes (DEGs) in WT CSI treated mice compared to sham (132 upregulated genes, 78 downregulated genes), while no significant changes in gene expression were observed in CSI treated Rag1KO samples compared to sham (**Figure 6B**, *left*). In WT mice, there were no DEGs in response to CPA treatment, whilst in Rag1KO CPA treated mice there were 3440 DEGs compared to Ctrl (2334 up, 1106 down). GEM treatment in WT mice induced 403 DEGs (245 up, 158 down) and 1857 DEGs in Rag1KO (934 up, 923 down) compared to Ctrl (**Figure 6B**).

We applied CIBERSORTx to determine the abundance of immune cell types within the bulk sequenced data and to clarify if these were altered following treatment. Immune signatures were very low, and only microglia, border associated macrophages (BAMs), and monocyte signatures were detected (**Figures 6C, D**), although these estimates were non-significant (P>0.05). CSI did not appear to significantly alter immune cell composition (**Figure 6C**). Despite the low signature values, when the computed cell fractions were compared from Rag1KO mice treated with CPA or GEM, microglia were decreased compared to control mice ($P=2x10^{-4}$ and $P=2x10^{-5}$, respectively), consistent with our flow cytometry findings (**Supplementary Figure 6**), and BAMs were significantly elevated (P=0.04 and $P=1.8x10^{-5}$, respectively) (**Figure 6D**); no significant differences were observed in WT mice. Ultimately, immune cell composition

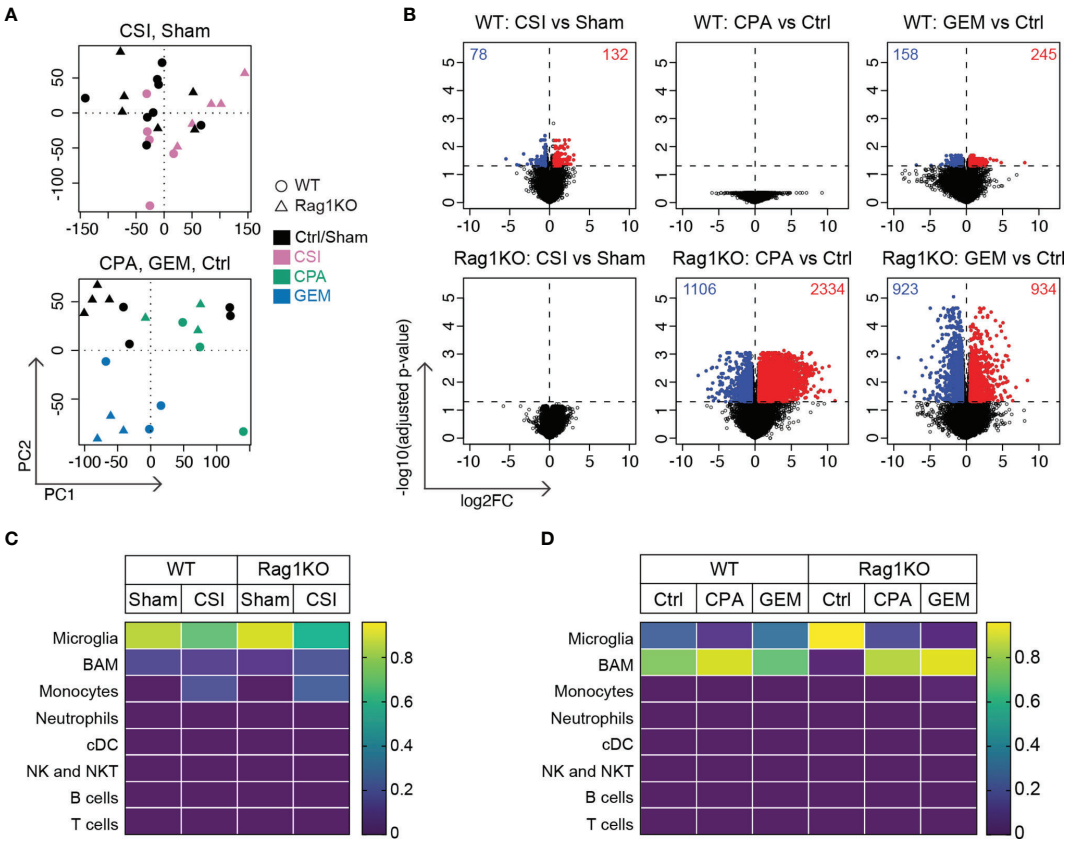

FIGURE 6 | Radiotherapy and chemotherapy induce distinctly different gene expression changes in Group 3 medulloblastoma in immune-competent versus immune-deficient mice. RNA sequencing was performed on Myc/p53^{DD} medulloblastomas from either C57Bl/6J WT mice (*circles*) or C57Bl/6J Rag1KO mice (*triangles*) that were harvested upon the development of tumor-related morbidity following treatment with sham, CSI, saline, CPA, or GEM. **(A)** Principal component analysis plots showing sham treated tumors (*black*) compared with CSI treated tumors (*pink*, upper panel), or saline treated tumors (Ctrl, *black*) compared with CPA (*green*) or GEM (*blue*) treated tumors (lower panel). **(B)** Volcano plots showing DEGs identified using EdgeR in response to CSI, CPA, and GEM treatment in tumors from WT or Rag1KO mice compared to their respective controls (*red* = upregulated, *blue* = downregulated) for the six comparisons indicated. The number of significantly differentially expressed genes is shown in each plot. **(C)** Immune cell fractions in WT and **(D)** Rag1KO tumor tissue were estimated using CIBERSORTx. Color scale indicates the predicted fraction of the indicated immune cells deconvoluted from bulk tumor transcriptome data. CSI did not significantly alter predicted immune fractions in either strain, nor did chemotherapy in WT tumors. Despite non-significant deconvolution, a reduction in microglial signatures was observed in Rag1KO mice following treatment with either CPA (P=2.0x10^{-4}) or GEM (P=2.0x10^{-5}) compared to control, with an increase in transcripts associated with border associated macrophages (BAMs) (P=0.04 and P=1.8x10^{-5} respectively). Number of mice in each group were: WT/Sham = 8, WT/CSI = 5, Rag1KO/Sham = 6, Rag1KO/CSI = 5, WT/Ctrl = 4, WT/CPA = 3, WT/GEM = 3, Rag1KO/Ctrl = 4, Rag1KO/CPA = 3, Rag1KO/GEM = 3.

could not be accurately quantified by deconvoluting our bulk RNA sequencing data likely due to the low abundance of immune cells relative to tumor cells in Myc/p53^{DD} tumors.

Pathway analysis also showed very few differentially expressed genes were associated with the immune system, owing to most genes being from tumor cells rather than from immune cells. Activated pathways in medulloblastomas in WT mice treated with CSI were associated with muscle contraction (P=3.70x10^{-5}) and myogenesis (P=0.0143), whilst inhibited pathways were related to the neuronal system/ion channels (P=2.32x10^{-4}). While there were no DEGs identified in CPA-treated medulloblastomas from WT mice, activated pathways in CPA-treated medulloblastomas from Rag1KO mice related to the neuronal system/ion channels (e.g. voltage ion channels, GABA receptors; P=1.94x10^{-46}), signaling by GPCRs (P=7.26x10^{-7}), MAPK signaling pathway (P=1.62x10^{-5}), axon guidance (P=4.01x10^{-5}), and hemostasis (P=3.6x10^{-4}). Downregulated pathways were associated with ribosomal translation/gene expression (P=5.12x10^{-13}), collagen biosynthesis/degradation & extracellular matrix (P<2.20x10^{-8}) and cell cycle/proliferation (P=1.73x10^{-7}). In response to GEM treatment, common activated pathways in both WT and Rag1KO mice were associated with metabolism (P<7.76x10^{-5}), whilst ribosomal translation was unique to WT mice, and Hedgehog (P=0.0242), PPAR (P=0.0277) and interleukin signaling pathways (P=0.0281) were only activated in Rag1KO. Common downregulated pathways were associated with hemostasis (P<0.0229) and axon guidance (P<2.82x10^{-4}); unique pathways in WT were linoleic acid metabolic (P=3.02x10^{-4}) and p53 signaling (p=0.0449); inhibited

pathways in Rag1KO mice only were developmental biology ($P=1.70x10^{-5}$), MAPK signaling (P=0.00499), neuronal system (P=0.0277), cell cycle/proliferation (P=0.0262) and WNT signaling (P=0.0439).

Upstream regulator analysis was performed to identify putative drivers of the differentially expressed genes (**Supplementary Figure 7**). Overall, as expected given the above findings, the data showed limited immune system drivers and an array of activated chemical signatures, particularly in chemotherapy treated Rag1KO mice. In WT mice, the CSI response was driven by growth factor signaling (e.g. EGF, NRG1, ERBB3) and pro-inflammatory regulators (STAT3, PTGS2). In WT mice, GEM responses are driven by metabolic regulators (primarily lipid metabolism), while in Rag1KO mice, CPA and GEM responses are driven by chemical drivers, and cancer associated drivers were inhibited (MYC, SOX4, MYB).

DISCUSSION

Medulloblastoma is one of the most prevalent pediatric cancers. While 5-year survival rates are approximately 70%, particular genetic features are associated with worse prognosis and current clinical approaches require innovative rethinking to identify ways to improve outcomes for those patients. Immunotherapy has recently become a major focus of novel therapy development and there are multiple clinical trials that aim to increase immune cell recognition of medulloblastoma, including oncolytic viral therapy, cancer vaccines and immune checkpoint blockade [reviewed in (40)]. To develop future immunotherapy clinical trials for medulloblastoma that have a strong chance of improved efficacy with reduced adverse effects, a deeper understanding of the interactions between medulloblastoma and either brain resident immune cells or infiltrating immune cells is crucial.

While patient derived xenograft models provide insight into the genetic and molecular basis of medulloblastoma and are valuable in the investigation of molecularly targeted therapies, they do not allow for the study of the whole immune system due to their use of immunocompromised hosts. Ideally, preclinical models for testing novel immunotherapies must recapitulate orthotopic medulloblastoma as well as the immune microenvironment. Immune competent preclinical models are therefore required to complement patient-derived xenograft models in a robust and comprehensive preclinical drug testing pipeline. Here we used an immune-competent murine model of *Myc*-amplified Group 3 medulloblastoma to investigate changes in intracerebral immune cell populations induced by tumor growth, and for the first time describe the impact of several first line medulloblastoma therapies on the immune microenvironment. Moreover, we repeated this work in *Rag1* knockout mice lacking T and B cells to elucidate the role of adaptive immune cells in treatment response.

Our data show that adaptive immune cells account for a small proportion of immune cells in the brains of mice harboring Myc/$p53^{DD}$ tumors. T cells account for between 10-15% of the immune population in Myc/$p53^{DD}$ bearing brain, and B cells account for between 2-6% of the immune populations. Using *Rag1* deficient mice, we found that the adaptive immune system does not play a significant role in Myc/$p53^{DD}$ tumor engraftment or growth, nor in treatment-mediated tumor control. Furthermore, both CSI and CPA were found to significantly deplete T cells in the brain. This, combined with the fact that lymphocytes are rare in human Group 3 medulloblastoma (41) and medulloblastoma patients have demonstrated low to undetectable levels of PD-L1 and PD-1 (42–44), suggests that T cell targeted antibody therapies, such as anti-PD-1, are unlikely to succeed in combination with radiotherapy or chemotherapy in medulloblastoma.

On the other hand, microglia dominate the immune milieu of the tumor bearing brain, accounting for between 50-65% of all immune cells. Further, we show that following either radiotherapy or chemotherapy, microglia remain the most abundant immune cell in the brain and thus present as a favorable target for immunotherapy in Group 3 medulloblastoma in combination with frontline therapies. Indeed, recent preclinical data has excitingly shown that treatments targeting myeloid cell immune checkpoints, such as the CD47-SIRPα axis, are highly effective in mouse models of medulloblastoma and other childhood brain cancers (45). Furthermore, it has been suggested that radiotherapy may synergize with monoclonal antibody therapies, on the basis that radiation enhances the visibility of medulloblastoma to the immune system [reviewed in (40)]. Recently, it has been shown that a single 10 Gy dose of radiation can induce an increase in tumor associated macrophages in SHH medulloblastoma (33), however, in our study using a clinically-relevant fractionated CSI protocol did not result in an increase in absolute counts of microglia nor macrophage at either acute or late-stage time points, and no increase in $Iba1^{+}$ staining was observed in late-stage tumors after CSI (**Supplementary Figure 8**). For laboratory-based experiments to accurately inform new clinical trials in medulloblastoma, future work should aim to characterize the immune response to fractionated versus unfractionated radiotherapy doses across different medulloblastoma subtypes to better understand the optimal preclinical radiotherapy methods to apply.

In contrast to the effects of fractionated CSI, we found that CPA treatment reduced the proportions of MHC II^{+} microglia in mouse brain, suggesting this chemotherapy suppresses microglial function. We also examined the effects of GEM on immune cell populations in medulloblastoma, as this drug is currently being investigated as a first-line chemotherapy in Group 3 and Group 4 medulloblastoma (NCT01878617). The only cell population in the brain observed to be affected by GEM were neutrophils which were decreased following treatment. This was unexpected, as in previous cancer studies, GEM selectively depleted myeloid cells and B cells, in both a tumor microenvironment and in lymphoid organs (46, 47), and we observed depletion of T and B cells in the spleen of GEM treated WT mice (**Supplementary Figure 1**). Importantly, exposure to GEM can also increase tumor antigenicity through upregulation

of MHC-I (48), inhibition of tumor-associated macrophages, and improving antigen cross-presentation (49, 50) to aid in immune stimulation and tumor elimination. Our data did not indicate that GEM treatment had these same effects in medulloblastoma, although given these previous studies, additional experiments to better delineate the effects of GEM on medulloblastoma-associated macrophages would be valuable.

Limitations of this study include the techniques and cellular markers used to identify immune populations from brains of mice with medulloblastoma. Flow cytometry is unable to determine the spatial interactions of microglia and infiltrating macrophages within murine medulloblastoma, and importantly our data suggest that the marker Tmem119, often used to distinguish microglia from macrophages, may be an unreliable cellular marker in this context. Using IHC, we observed an abundance of $Iba1^+$ cells throughout medulloblastomas and an absence of $Tmem119^+$ cells, suggesting intratumoral $Iba1^+$ cells were not microglia. However, the absence of intratumoral Tmem119 staining is not consistent with our findings that 23.1% of intratumoral immune cells were $CD45^{int}$, and presumed microglia. Given previous reports have shown microglia can upregulate CD45 expression in pathological conditions (36, 37), we hypothesize that bone marrow-derived macrophages do not account for the entirety of tumor-infiltrative $Iba1^+$ $Tmem119^-$ cells observed, and that microglia may downregulate Tmem119 as they enter medulloblastomas, suggesting a transition of these cells into a more macrophage-like state. While there are a number of methods that can clarify if these cells are activated microglia, such as MHC Class II, Sca-1 (51) or CD68 (52), these markers are also expressed on other myeloid cells, and would need to be assessed in combination with a microglia specific marker such as Sall1 (53).

Microglia and infiltrating macrophages are complex and dynamic in the context of cancer, and they cannot be easily delineated by simple markers. Indeed, recent single cell transcriptomics analysis of human samples revealed that an unexpectedly diverse spectrum of myeloid populations infiltrate medulloblastoma (41). Here, we set out to use transcriptomics to further characterize immune responses to treatment. However, we found that bulk RNA sequencing lacked sensitivity to probe the immunology of these tumors, largely due to the low abundance of intratumoral immune cells within this model of medulloblastoma. As a result, cell fractions were not significantly deconvoluted by CIBERSORTx and downstream comparisons of cell abundances should be carried out with caution. Our RNAseq data suggests that chemotherapy may alter the ratio of myeloid subsets (specifically microglia and BAMs) within the brain, but this requires additional experimental validation, particularly given the flow cytometry markers used here were not able to discriminate between these two cell types. Further examination using makers such as CD206, Siglec-H and CD38 that are expressed on BAMs and not microglia (51), as well as using histological techniques to define the locations of the chemotherapy-affected cells will be important to more accurately define the impacts of chemotherapy on the brain immune microenvironment especially given that the vasculature in the border regions would have different barrier properties compared to the blood-brain barrier of the parenchyma. Future work aimed at better understanding the immune cell dynamics within medulloblastomas may also consider first enriching for $CD45^+$ cells prior to bulk RNA sequencing or employing single cell sequencing or single cell proteomics technologies to detect immune signatures in medulloblastoma tissue, though these methods are accompanied with the caveat of tissue processing induced artefacts [reviewed in (54)]. Our sequencing data was limited by small sample sizes in this exploratory study and, in the case of CSI-treated tumors, by the choice to sample later time points when tumors were larger, but possibly too late after treatment cessation to detect gene expression differences. Further, this study is limited by the intracranial implantation procedure disrupting the skull and meninges, which may mediate peripheral immune influx by promoting an inflammatory response and disrupting the blood brain barrier. Though we have found that the intracranial implantation procedure does not detectably change immune populations in the brain of non-tumor bearing animals (data not shown), genetically engineered spontaneous models of Group 3 medulloblastoma with an intact blood-brain barrier would improve the study of the tumor-immune microenvironment.

The study of the immune infiltrate within medulloblastoma is critical not only for the implementation of optimal radiotherapy and chemotherapy protocols, but very relevant to immunotherapy, a therapeutic modality with increasing use in oncology. Immunotherapies are not standard in the treatment of medulloblastoma, and clinical trials investigating the use of T-cell targeting immunotherapies have proven unsuccessful to date (40). This lack of success is likely a consequence of the immune microenvironment in pediatric brain tumors being very different from that of adult solid tumors in which immune-based therapies have proven successful. Overall, the most consistently abundant immune cell within this model of Group 3 medulloblastoma following radiotherapy or chemotherapy are myeloid cells, which we speculate are a mixture of both brain-resident and bone marrow-derived cells. Should myeloid cell-targeting therapies continue to be developed for medulloblastoma, future work should assess the impacts of radiotherapy and chemotherapy on microglial and macrophage activation and function, to dissect out mechanisms of treatment-induced changes and how this might impact the efficacy of immunotherapies. Building upon our study will be important to address this issue and will facilitate the rational selection of optimal immunotherapeutics for future medulloblastoma clinical trials.

DATA AVAILABILITY STATEMENT

The data presented in the study are deposited in the European Genome-Phenome Archive, accession numbers EGAS00001005846 and EGAS00001005847.

ETHICS STATEMENT

All animal studies in this work were reviewed and approved by the Animal Ethics Committee of the Telethon Kids Institute.

AUTHOR CONTRIBUTIONS

ZA, CG, MH, RE, and NG designed the experiments. ZA, CG, MA, AJ, MK, and RE performed experiments or analyzed data. ZA, CG, MA, AJ, MH, RW-R, NG, and RE were involved in data discussion, drafting, and editing the manuscript. All authors contributed to the article and approved the submitted version.

FUNDING

This research was funded by The Pirate Ship Foundation. RNA sequencing experiments were partially funded through the Australian Lions Children's Cancer Research Fund and the Stan Perron Charitable Foundation. RE has support from a Cancer Council of Western Australia Research Fellowship and a Brainchild Fellowship from the Pirate Ship Foundation. NG is supported by the Stan Perron Chair of Paediatric Haematology and Oncology. ZA is supported by a Richard Walter Gibbon Medical Research Scholarship and an Australian Government Research Training Program Scholarship at the University of Western Australia. MA and CG were supported by an Australian Postgraduate Award from the Australian Government. AJ is supported by the Stan Perron Foundation, Australian Lions Children's Cancer Research Foundation and Channel 7 Telethon Trust. RW-R is supported by funds from the National Cancer Institute (2R01 CA159859, P30 CA30199), the National Institute of Neurological Disorders and Stroke (R35 NS122339, R01 NS096368) and the V Foundation for Cancer Research (D2018-021).

ACKNOWLEDGMENTS

We thank Drs. Bree Foley and Jason Waithman for their invaluable advice and discussions in designing the flow cytometry panels, and for sharing *Rag1*$^{-/-}$ C57Bl/6J mice. We also thank Dr. Tanja Eisemann for her input and assistance in the editing of this manuscript. Library preparation and sequencing was conducted in the Genomics WA Laboratory in Perth, Australia. This facility is supported by BioPlatforms Australia, State Government Western Australia, Australian Cancer Research Foundation, Cancer Research Trust, Harry Perkins Institute of Medical Research, Telethon Kids Institute and the University of Western Australia. We gratefully acknowledge the Australian Cancer Research Foundation and the Centre for Advanced Cancer Genomics for making available Illumina Sequencers for the use of Genomics WA. We also acknowledge support from Bright Blue, the Police Commissioner's Fund for Sick Kids for other equipment. We thank the Australian Federal Government Department of Health for funding to establish infrastructure used here that support the Zero Childhood Cancer personalized medicine program. Thank you to the Bioresources teams of Telethon Kids Institute for the care of our animals, and the Laboratory Management team, particularly Pradeep Kumar, for maintenance of the flow cytometry and histology facilities. We thank all members of the Telethon Kids Institute Brain Tumour Research team and Cancer Immunotherapy Unit for their advice, suggestions, and discussions during the course of this project.

SUPPLEMENTARY MATERIAL

The Supplementary Material for this article can be found online at: https://www.frontiersin.org/articles/10.3389/fimmu.2022.837013/full#supplementary-material

REFERENCES

1. Northcott PA, Robinson GW, Kratz CP, Mabbott DJ, Pomeroy SL, Clifford SC, et al. Medulloblastoma. *Nat Rev Dis Primers* (2019) 5(1):11. doi: 10.1038/s41572-019-0063-6
2. Cavalli FMG, Remke M, Rampasek L, Peacock J, Shih DJH, Luu B, et al. Intertumoral Heterogeneity Within Medulloblastoma Subgroups. *Cancer Cell* (2017) 31(6):737–54.e6. doi: 10.1016/j.ccell.2017.05.005
3. Schwalbe EC, Lindsey JC, Nakjang S, Crosier S, Smith AJ, Hicks D, et al. Novel Molecular Subgroups for Clinical Classification and Outcome Prediction in Childhood Medulloblastoma: A Cohort Study. *Lancet Oncol* (2017) 18(7):958–71. doi: 10.1016/S1470-2045(17)30243-7
4. Leary SES, Olson JM. The Molecular Classification of Medulloblastoma. *Curr Opin Pediatr* (2012) 24(1):33–9. doi: 10.1097/MOP.0b013e32834ec106
5. Hill RM, Richardson S, Schwalbe EC, Hicks D, Lindsey JC, Crosier S, et al. Time, Pattern, and Outcome of Medulloblastoma Relapse and Their Association With Tumour Biology at Diagnosis and Therapy: A Multicentre Cohort Study. *Lancet Child Adolesc Health* (2020) 4(12):865–74. doi: 10.1016/S2352-4642(20)30246-7
6. Kool M, Korshunov A, Remke M, Jones DT, Schlanstein M, Northcott PA, et al. Molecular Subgroups of Medulloblastoma: An International Meta-Analysis of Transcriptome, Genetic Aberrations, and Clinical Data of WNT, SHH, Group 3, and Group 4 Medulloblastomas. *Acta Neuropathol* (2012) 123(4):473–84. doi: 10.1007/s00401-012-0958-8
7. Richardson S, Hill RM, Kui C, Lindsey JC, Grabovksa Y, Keeling C, et al. Emergence and Maintenance of Actionable Genetic Drivers at Medulloblastoma Relapse. *Neuro Oncol* (2022) 24(1):153–65. doi: 10.1093/neuonc/noab178
8. Koschmann C, Bloom K, Upadhyaya S, Geyer JR, Leary SES. Survival After Relapse of Medulloblastoma. *J Pediatr Hematol/Oncol* (2016) 38(4):269–73. doi: 10.1097/MPH.0000000000000547
9. Sabel M, Fleischhack G, Tippelt S, Gustafsson G, Doz F, Kortmann R, et al. Relapse Patterns and Outcome After Relapse in Standard Risk Medulloblastoma: A Report From the HIT-SIOP-PNET4 Study. *J Neuro-Oncol* (2016) 129(3):515–24. doi: 10.1007/s11060-016-2202-1
10. Pei Y, Moore CE, Wang J, Tewari AK, Eroshkin A, Cho YJ, et al. An Animal Model of MYC-Driven Medulloblastoma. *Cancer Cell* (2012) 21(2):155–67. doi: 10.1016/j.ccr.2011.12.021
11. Mombaerts P, Iacomini J, Johnson RS, Herrup K, Tonegawa S, Papaioannou VE. RAG-1-Deficient Mice Have No Mature B and T Lymphocytes. *Cell* (1992) 68(5):869–77. doi: 10.1016/0092-8674(92)90030-G
12. Endersby R, Zhu X, Hay N, Ellison DW, Baker SJ. Nonredundant Functions for Akt Isoforms in Astrocyte Growth and Gliomagenesis in an Orthotopic Transplantation Model. *Cancer Res* (2011) 71(12):4106–16. doi: 10.1158/0008-5472.CAN-10-3597
13. Feddersen TV, Rowshanfarzad P, Abel TN, Ebert MA. Commissioning and Performance Characteristics of a Pre-Clinical Image-Guided Radiotherapy

System. *Australas Phys Eng Sci Med* (2019) 42(2):541–51. doi: 10.1007/s13246-019-00755-4
14. van Hoof SJ, Granton PV, Verhaegen F. Development and Validation of a Treatment Planning System for Small Animal Radiotherapy: Smart-Plan. *Radiother Oncol* (2013) 109(3):361–6. doi: 10.1016/j.radonc.2013.10.003
15. Smith SMC, Bianski BM, Orr BA, Harknett G, Onar-Thomas A, Gilbertson RJ, et al. Preclinical Modeling of Image-Guided Craniospinal Irradiation for Very-High-Risk Medulloblastoma. *Int J Radiat Oncol Biol Phys* (2019) 103 (3):728–37. doi: 10.1016/j.ijrobp.2018.10.015
16. Martin M. Cutadapt Removes Adapter Sequences From High-Throughput Sequencing Reads. *EMBnetjournal* (2011) 17(1):10. doi: 10.14806/ej.17.1.200
17. Andrews SFASTQC. *A Quality Control Tool for High Throughput Sequence Data* (2010). Available at: https://www.bioinformatics.babraham.ac.uk/projects/fastqc/.
18. Lassmann T, Hayashizaki Y, Daub CO. Samstat: Monitoring Biases in Next Generation Sequencing Data. *Bioinformatics* (2011) 27(1):130–1. doi: 10.1093/bioinformatics/btq614
19. Kim D, Langmead B, Salzberg SL. HISAT: A Fast Spliced Aligner With Low Memory Requirements. *Nat Methods* (2015) 12(4):357–60. doi: 10.1038/nmeth.3317
20. Lawrence M, Huber W, Pagès H, Aboyoun P, Carlson M, Gentleman R, et al. Software for Computing and Annotating Genomic Ranges. *PloS Comput Biol* (2013) 9(8):e1003118. doi: 10.1371/journal.pcbi.1003118
21. Risso D, Ngai J, Speed TP, Dudoit S. Normalization of RNA-Seq Data Using Factor Analysis of Control Genes or Samples. *Nat Biotechnol* (2014) 32 (9):896–902. doi: 10.1038/nbt.2931
22. Newman AM, Steen CB, Liu CL, Gentles AJ, Chaudhuri AA, Scherer F, et al. Determining Cell Type Abundance and Expression From Bulk Tissues With Digital Cytometry. *Nat Biotechnol* (2019) 37(7):773–82. doi: 10.1038/s41587-019-0114-2
23. Van Hove H, Martens L, Scheyltjens I, De Vlaminck K, Pombo Antunes AR, De Prijck S, et al. A Single-Cell Atlas of Mouse Brain Macrophages Reveals Unique Transcriptional Identities Shaped by Ontogeny and Tissue Environment. *Nat Neurosci* (2019) 22(6):1021–35. doi: 10.1038/s41593-019-0393-4
24. Robinson MD, McCarthy DJ, Smyth GK. Edger: A Bioconductor Package for Differential Expression Analysis of Digital Gene Expression Data. *Bioinformatics* (2010) 26(1):139–40. doi: 10.1093/bioinformatics/btp616
25. Breuer K, Foroushani AK, Laird MR, Chen C, Sribnaia A, Lo R, et al. Innatedb: Systems Biology of Innate Immunity and Beyond–Recent Updates and Continuing Curation. *Nucleic Acids Res* (2013) 41(Database issue):D1228–D33. doi: 10.1093/nar/gks1147
26. Krämer A, Green J, Pollard JJr., Tugendreich S. Causal Analysis Approaches in Ingenuity Pathway Analysis. *Bioinformatics* (2014) 30(4):523–30. doi: 10.1093/bioinformatics/btt703
27. Bender R, Lange S. Adjusting for Multiple Testing—When and How? *J Clin Epidemiol* (2001) 54(4):343–9. doi: 10.1016/S0895-4356(00)00314-0
28. Martin AM, Raabe E, Eberhart C, Cohen KJ. Management of Pediatric and Adult Patients With Medulloblastoma. *Curr Treat Options Oncol* (2014) 15 (4):581–94. doi: 10.1007/s11864-014-0306-4
29. Pham CD, Flores C, Yang C, Pinheiro EM, Yearley JH, Sayour EJ, et al. Differential Immune Microenvironments and Response to Immune Checkpoint Blockade Among Molecular Subtypes of Murine Medulloblastoma. *Clin Cancer Res* (2016) 22(3):582–95. doi: 10.1158/1078-0432.CCR-15-0713
30. Sedgwick JD, Schwender S, Imrich H, Dorries R, Butcher GW, Ter Meulen V. Isolation and Direct Characterization of Resident Microglial Cells From the Normal and Inflamed Central Nervous System. *Proc Natl Acad Sci* (1991) 88 (16):7438–42. doi: 10.1073/pnas.88.16.7438
31. O'Koren EG, Mathew R, Saban DR. Fate Mapping Reveals That Microglia and Recruited Monocyte-Derived Macrophages Are Definitively Distinguishable by Phenotype in the Retina. *Sci Rep* (2016) 6(1):20636. doi: 10.1038/srep20636
32. Wyss-Coray T, Mucke L. Inflammation in Neurodegenerative Disease–A Double-Edged Sword. *Neuron* (2002) 35(3):419–32. doi: 10.1016/S0896-6273(02)00794-8
33. Dang MT, Gonzalez MV, Gaonkar KS, Rathi KS, Young P, Arif S, et al. Macrophages in SHH Subgroup Medulloblastoma Display Dynamic Heterogeneity That Varies With Treatment Modality. *Cell Rep* (2021) 34 (13):108917. doi: 10.1016/j.celrep.2021.108917
34. Galluzzi L, Buque A, Kepp O, Zitvogel L, Kroemer G. Immunological Effects of Conventional Chemotherapy and Targeted Anticancer Agents. *Cancer Cell* (2015) 28(6):690–714. doi: 10.1016/j.ccell.2015.10.012
35. Ahlmann M, Hempel G. The Effect of Cyclophosphamide on the Immune System: Implications for Clinical Cancer Therapy. *Cancer Chemother Pharmacol* (2016) 78(4):661–71. doi: 10.1007/s00280-016-3152-1
36. Honarpisheh P, Lee J, Banerjee A, Blasco-Conesa MP, Honarpisheh P, D'Aigle J, et al. Potential Caveats of Putative Microglia-Specific Markers for Assessment of Age-Related Cerebrovascular Neuroinflammation. *J Neuroinflamm* (2020) 17(1):366. doi: 10.1186/s12974-020-02019-5
37. Muller A, Brandenburg S, Turkowski K, Muller S, Vajkoczy P. Resident Microglia, and Not Peripheral Macrophages, Are the Main Source of Brain Tumor Mononuclear Cells. *Int J Cancer* (2015) 137(2):278–88. doi: 10.1002/ijc.29379
38. Sasaki Y, Ohsawa K, Kanazawa H, Kohsaka S, Imai Y. Iba1 Is an Actin-Cross-Linking Protein in Macrophages/Microglia. *Biochem Biophys Res Commun* (2001) 286(2):292–7. doi: 10.1006/bbrc.2001.5388
39. Bennett ML, Bennett FC, Liddelow SA, Ajami B, Zamanian JL, Fernhoff NB, et al. New Tools for Studying Microglia in the Mouse and Human CNS. *Proc Natl Acad Sci USA* (2016) 113(12):E1738–46. doi: 10.1073/pnas.1525528113
40. Kabir TF, Kunos CA, Villano JL, Chauhan A. Immunotherapy for Medulloblastoma: Current Perspectives. *Immunotarg Ther* (2020) 9:57–77. doi: 10.2147/ITT.S198162
41. Riemondy KA, Venkataraman S, Willard N, Nellan A, Sanford B, Griesinger AM, et al. Neoplastic and Immune Single Cell Transcriptomics Define Subgroup-Specific Intra-Tumoral Heterogeneity of Childhood Medulloblastoma. *Neuro Oncol* (2021) 24(2):273–86. doi: 10.1093/neuonc/noab135
42. Vermeulen JF, Van Hecke W, Adriaansen EJM, Jansen MK, Bouma RG, Villacorta Hidalgo J, et al. Prognostic Relevance of Tumor-Infiltrating Lymphocytes and Immune Checkpoints in Pediatric Medulloblastoma. *Oncoimmunology* (2018) 7(3):e1398877. doi: 10.1080/2162402X.2017.1398877
43. Hwang K, Koh EJ, Choi EJ, Kang TH, Han JH, Choe G, et al. PD-1/PD-L1 and Immune-Related Gene Expression Pattern in Pediatric Malignant Brain Tumors: Clinical Correlation With Survival Data in Korean Population. *J Neurooncol* (2018) 139(2):281–91. doi: 10.1007/s11060-018-2886-5
44. Martin AM, Nirschl CJ, Polanczyk MJ, Bell WR, Nirschl TR, Harris-Bookman S, et al. PD-L1 Expression in Medulloblastoma: An Evaluation by Subgroup. *Oncotarget* (2018) 9(27):19177–91. doi: 10.18632/oncotarget.24951
45. Gholamin S, Mitra SS, Feroze AH, Liu J, Kahn SA, Zhang M, et al. Disrupting the CD47-Sirpα Anti-Phagocytic Axis by a Humanized Anti-CD47 Antibody Is an Efficacious Treatment for Malignant Pediatric Brain Tumors. *Sci Trans Med* (2017) 9(381):eaaf2968. doi: 10.1126/scitranslmed.aaf2968
46. Nowak AK, Robinson BWS, Lake RA. Gemcitabine Exerts a Selective Effect on the Humoral Immune Response. *Cancer Res* (2002) 62(8):2353.
47. Suzuki E, Kapoor V, Jassar AS, Kaiser LR, Albelda SM. Gemcitabine Selectively Eliminates Splenic Gr-1+/CD11b+ Myeloid Suppressor Cells in Tumor-Bearing Animals and Enhances Antitumor Immune Activity. *Clin Cancer Res* (2005) 11(18):6713–21. doi: 10.1158/1078-0432.CCR-05-0883
48. McDonnell AM, Lesterhuis WJ, Khong A, Nowak AK, Lake RA, Currie AJ, et al. Tumor-Infiltrating Dendritic Cells Exhibit Defective Cross-Presentation of Tumor Antigens, But Is Reversed by Chemotherapy. *Eur J Immunol* (2015) 45(1):49–59. doi: 10.1002/eji.201444722
49. Homma Y, Taniguchi K, Murakami T, Nakagawa K, Nakazawa M, Matsuyama R, et al. Immunological Impact of Neoadjuvant Chemoradiotherapy in Patients With Borderline Resectable Pancreatic Ductal Adenocarcinoma. *Ann Surg Oncol* (2014) 21(2):670–6. doi: 10.1245/s10434-013-3390-y
50. Eriksson E, Wenthe J, Irenaeus S, Loskog A, Ullenhag G. Gemcitabine Reduces Mdscs, Tregs and Tgfβ-1 While Restoring the Teff/Treg Ratio in Patients With Pancreatic Cancer. *J Trans Med* (2016) 14(1):282. doi: 10.1186/s12967-016-1037-z
51. Mrdjen D, Pavlovic A, Hartmann FJ, Schreiner B, Utz SG, Leung BP, et al. High-Dimensional Single-Cell Mapping of Central Nervous System Immune Cells Reveals Distinct Myeloid Subsets in Health, Aging, and Disease. *Immunity* (2018) 48(2):380–95 e6. doi: 10.1016/j.immuni.2018.01.011
52. Stankov A, Belakaposka-Srpanova V, Bitoljanu N, Cakar L, Cakar Z, Rosoklija G. Visualisation of Microglia With the Use of Immunohistochemical Double

Staining Method for CD-68 and Iba-1 of Cerebral Tissue Samples in Cases of Brain Contusions. *Pril (Makedon Akad Nauk Umet Odd Med Nauki)* (2015) 36 (2):141–5. doi: 10.1515/prilozi-2015-0062
53. Buttgereit A, Lelios I, Yu X, Vrohlings M, Krakoski NR, Gautier EL, et al. Sall1 is a Transcriptional Regulator Defining Microglia Identity and Function. *Nat Immunol* (2016) 17(12):1397–406. doi: 10.1038/ni.3585
54. Machado L, Relaix F, Mourikis P. Stress Relief: Emerging Methods to Mitigate Dissociation-Induced Artefacts. *Trends Cell Biol* (2021) 31(11):888–97. doi: 10.1016/j.tcb.2021.05.004

Conflict of Interest: The authors declare that the research was conducted in the absence of any commercial or financial relationships that could be construed as a potential conflict of interest.

Publisher's Note: All claims expressed in this article are solely those of the authors and do not necessarily represent those of their affiliated organizations, or those of the publisher, the editors and the reviewers. Any product that may be evaluated in this article, or claim that may be made by its manufacturer, is not guaranteed or endorsed by the publisher.

frontiers | Frontiers in Immunology

REVIEW
published: 07 April 2022
doi: 10.3389/fimmu.2022.864423

A Toolkit for Profiling the Immune Landscape of Pediatric Central Nervous System Malignancies

Jacob S. Rozowsky[1†], Joyce I. Meesters-Ensing[1†], Julie A. S. Lammers[1], Muriël L. Belle[1], Stefan Nierkens[1,2], Mariëtte E. G. Kranendonk[1], Lennart A. Kester[1], Friso G. Calkoen[1] and Jasper van der Lugt[1]*

[1] Princess Máxima Center for Pediatric Oncology, Utrecht, Netherlands, [2] Center for Translational Immunology, University Medical Center Utrecht, Utrecht, Netherlands

OPEN ACCESS

Edited by:
Orazio Vittorio, University of New South Wales, Australia

Reviewed by:
Jiyang Yu, St. Jude Children's Research Hospital, United States
Raelene Endersby, University of Western Australia, Australia

***Correspondence:**
Jasper van der Lugt
j.vanderlugt@prinsesmaximacentrum.nl

[†]These authors have contributed equally to this work

Specialty section:
This article was submitted to Cancer Immunity and Immunotherapy, a section of the journal Frontiers in Immunology

Received: *28 January 2022*
Accepted: *11 March 2022*
Published: *07 April 2022*

Citation:
Rozowsky JS, Meesters-Ensing JI, Lammers JAS, Belle ML, Nierkens S, Kranendonk MEG, Kester LA, Calkoen FG and van der Lugt J (2022) A Toolkit for Profiling the Immune Landscape of Pediatric Central Nervous System Malignancies. Front. Immunol. 13:864423. doi: 10.3389/fimmu.2022.864423

The prognosis of pediatric central nervous system (CNS) malignancies remains dismal due to limited treatment options, resulting in high mortality rates and long-term morbidities. Immunotherapies, including checkpoint inhibition, cancer vaccines, engineered T cell therapies, and oncolytic viruses, have promising results in some hematological and solid malignancies, and are being investigated in clinical trials for various high-grade CNS malignancies. However, the role of the tumor immune microenvironment (TIME) in CNS malignancies is mostly unknown for pediatric cases. In order to successfully implement immunotherapies and to eventually predict which patients would benefit from such treatments, in-depth characterization of the TIME at diagnosis and throughout treatment is essential. In this review, we provide an overview of techniques for immune profiling of CNS malignancies, and detail how they can be utilized for different tissue types and studies. These techniques include immunohistochemistry and flow cytometry for quantifying and phenotyping the infiltrating immune cells, bulk and single-cell transcriptomics for describing the implicated immunological pathways, as well as functional assays. Finally, we aim to describe the potential benefits of evaluating other compartments of the immune system implicated by cancer therapies, such as cerebrospinal fluid and blood, and how such liquid biopsies are informative when designing immune monitoring studies. Understanding and uniformly evaluating the TIME and immune landscape of pediatric CNS malignancies will be essential to eventually integrate immunotherapy into clinical practice.

Keywords: tumor immune microenvironment, immunotherapy, immune monitoring, central nervous system malignancy, immunohistochemistry, flow cytometry, transcriptomics

INTRODUCTION

Central nervous system (CNS) malignancies are the leading cause of cancer-related death in children. Extensive molecular profiling has resulted in a better understanding and further subclassification of many pediatric CNS tumors (1). So far, these significant advances are not reflected in clinical benefit for the patients, and the prognosis remains dismal for most of the

subtypes. Five-year survival rates for children range from 2% for diffuse midline glioma, 20% for glioblastoma, to 75% for medulloblastoma and ependymoma (2, 3).

Current treatment of children with CNS malignancies is facing a lot of challenges. The diffuse infiltration of some high-grade malignancies into critical neural circuits only permits partial resection or biopsy (4, 5). Depending on diagnosis and age of the patient, either craniospinal or local radiotherapy is added to optimize survival and reduce the risk of (local) recurrence (6). However, radiation can predispose patients to hearing, endocrine, and neuro-cognitive dysfunction (7). Despite the fact that the blood–brain barrier restricts the bioavailability of most of the currently available anti-neoplastic medication, chemotherapy can improve survival. This holds true for the embryonal tumors in particular, though tumors from glial origin tend to be more intrinsically resistant (8). Alternative therapeutic approaches such as molecular-targeted therapies, in particular MEK, BRAF, and tyrosine kinase inhibitors, have manifested improved outcomes in pediatric low-grade and infantile hemispheric gliomas (9). In summary, these highly aggressive and heterogeneous malignancies require an arsenal of agents to achieve meaningful clinical improvement albeit at the cost of significant long-term morbidity. It is clear that conventional treatments fall short, stressing the urge to explore alternative therapeutic modalities.

The field of immunotherapy is a promising area to investigate in the field of pediatric CNS malignancies given its previous success in other solid tumors and superior safety-profile (10–14). Immunomodulating approaches that are currently under investigation comprise vaccination therapy, oncolytic viruses, immune checkpoint inhibition, and CAR T cell therapy. However, there are many hurdles to overcome when applying immunotherapy.

Pediatric CNS malignancies generally exhibit an immunologically "cold" phenotype, lacking infiltrating T and natural killer (NK) cells (15–17). The pathophysiology behind the absence of T cell infiltration has not been fully elucidated. However, the low tumor mutational burden, deficiencies in antigen presentation on cells, and T cell homing to the tumor bed potentially play an important role (18). Additionally, tumor-associated microglia and macrophages (TAMs), cells of the innate immune system, are the most abundant immune cell type in the tumor immune microenvironment (TIME). In healthy control brain tissue biopsies, microglia are the dominant myeloid-derived cell type in the brain. During disease, microglia are activated, and bone marrow-derived macrophages are recruited to the tumor site, where they polarize towards different activation states ranging from classically activated (M1) to alternatively activated (M2) phenotypes (19–21). They can secrete inhibitory cytokines (such as TGF-B and IL-10) promoting immunosuppression and malignant proliferation (22, 23). Macrophages can also secrete endothelial growth factors that stimulate angiogenesis, thus advancing tumor growth and metastatic invasion into surrounding tissues (24).

Cells of the TIME interact with the tumor through paracrine signaling, which can stimulate tumor progression and enable immune escape. Moreover, in other solid tumor types, different components of the TIME may function as a predictive marker of response to immunotherapy (25); therefore, characterizing the TIME, as well as other immune compartments [e.g., blood, cerebral spinal fluid (CSF), and bone marrow], is necessary for evaluating current immunotherapies and clinical implementation. Comprehensive immune monitoring programs are needed for a better understanding of the TIME, but also to find surrogate markers in blood that can be helpful in designing future immunotherapies. Currently, literature about this association is lacking.

In this review, we provide an overview of different cellular and molecular profiling techniques for a multidimensional characterization of the immunophenotypes in pediatric CNS malignancies. We focus on immunohistochemistry (IHC), flow hen implemented simultaneously, these techniques characterize and quantify the immune cells in the microenvironment and provide detailed information into immune-status and function (**Figure 1**). We aim to discuss the advantages and pitfalls of these technologies to study the immune landscape at time of diagnosis and throughout therapy. Understanding the subtype-specific inflammatory milieu of pediatric CNS malignancies will advance our knowledge when evaluating current immunotherapies, designing new treatments, and predicting the clinical responses of patients, ultimately laying groundwork for a more personalized and safe treatment design.

IMMUNOHISTOCHEMISTRY

Introduction to Immunohistochemistry

IHC is an essential method for detecting, quantifying, and localizing a specified protein in tissue with antibody–antigen interactions. Since its introduction in the 1970s, the clinical diagnostics field rapidly advanced wherein pathologists can better classify tumors based on their expression of lineage-specific markers (glial tumors selectively expressing GFAP), oncogenic somatic mutations (oligodendrogliomas express IDH1 R132H mutation), and epigenetic modifications (diffuse midline gliomas show H3K27me3 loss) (26, 27).

IHC is performed on formalin-fixed paraffin-embedded (FFPE) tumor slides, which allows for a retrospective analysis of preserved tissue. Antibodies are used in conjunction with a coloring dye to visualize and detect the antigen of interest on the tissue section. In the clinical diagnostics setting, automated IHC machines have standardized this process, which improved reproducibility and reduced experimental biases. Both intensity and location of the stained marker can be interpreted, which is usually done by manual scoring; however, sophisticated programs and algorithms for automatic quantification are available nowadays, which reduce interpretation biases. We refer to Kim et al. who provided a detailed overview of IHC for pathologists (28).

Characterizing the TIME of Pediatric CNS Malignancies Using IHC

In addition to the valuable applications for cancer diagnostics, IHC can provide details into the composition of the TIME.

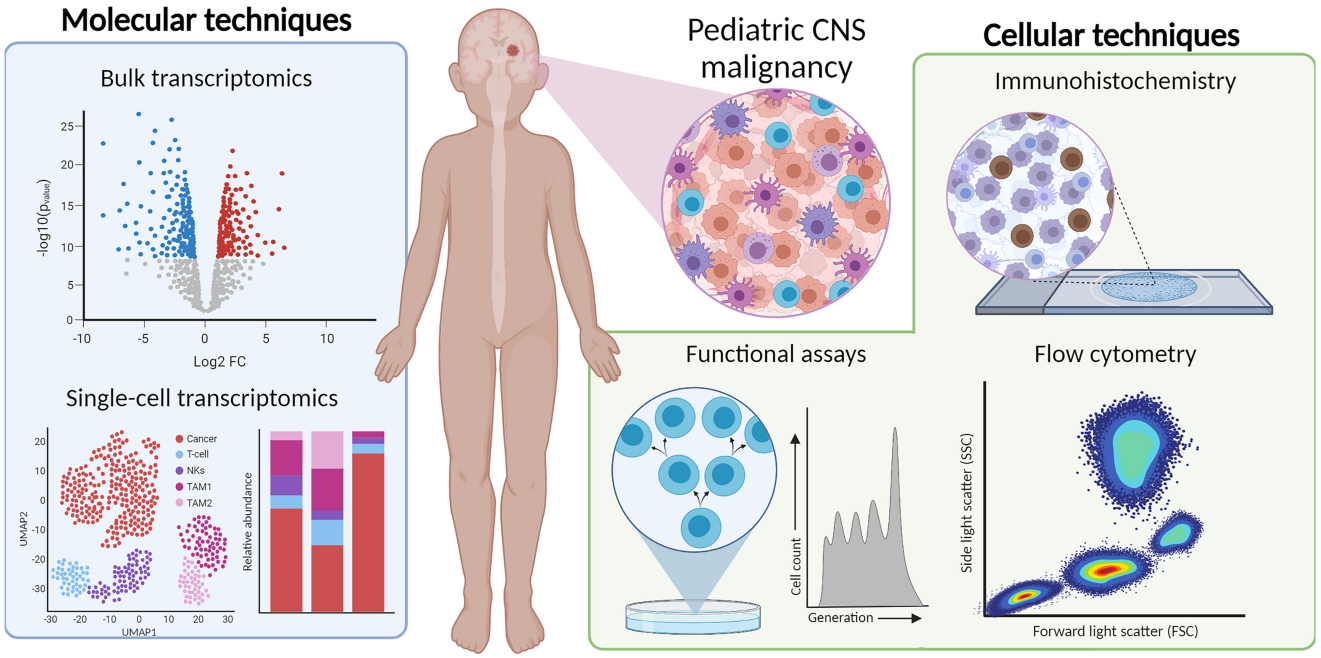

FIGURE 1 | Multi-dimensional immunophenotyping of TIME from tumor tissue using IHC, flow cytometry, bulk- and scRNA-seq, and functional assays.

Antibodies that target antigens found on infiltrating lymphocytes, macrophages, and stromal cells are especially useful for immunophenotyping pediatric CNS malignancies (28). As IHC is an *in situ* technique, it can also describe the spatial distribution of infiltrating immune cells in the TIME. An overview of commonly used cell markers to dissect the TIME can be found in **Figure 2**.

Multiple studies used IHC to characterize the TIME of pediatric CNS malignancies, which shed unprecedented light on the composition of the TIME and revealed tumor type-specific immunophenotypes (17, 29, 30). The results demonstrated that myeloid cells are major components of the TIME of pediatric gliomas, encompassing infiltrating macrophages, myeloid-derived suppressor cells (MDSCs), and microglia, whereas there are few infiltrating lymphocytes (17, 29, 31). Analysis of the immune cell infiltration in pediatric gliomas shows an enrichment of $CD8^+$ T cells and $CD45^+$ leukocytes in low-grade compared to high-grade gliomas (17). In a similar way, Lieberman et al. use IHC to study immune cell infiltration in pediatric low-grade gliomas, high-grade gliomas, and diffuse midline glioma tumor samples. While the percentage of tumor-associated $CD68^+$ macrophages is comparable across indications, diffuse midline gliomas have the lowest number of infiltrating $CD8^+$ T cells and $CD163^+$ macrophages, which contributes to its immunosuppressive phenotype (29). Moreover, multiple studies have described the subgroup-specific TIME composition of medulloblastomas. The SHH subgroup are the most enriched in $CD163^+$ macrophages, suggesting different roles of tumor-associated macrophages in medulloblastoma subgroups (32). Comparing immune cell infiltration in the peritumoral area and tumor core of glioblastomas showed that $CD163^+$ cells were more abundant in the tumor core. Similarly, the expression of the immunosuppressive markers PD-L1, IDO, and TIGIT was higher in the tumor core (31).

Immune profiling using IHC can be predictive of prognoses and help inform treatment strategy by detecting targets of immune checkpoint therapies, such as PD-L1. Pediatric ependymomas with higher infiltration of $CD3^+$ and $CD8^+$ T cells in the microenvironment at diagnosis have a longer progression-free survival (PFS), while elevated FOXP3 regulatory T cells and $CD68^+$ macrophages correlate with a shorter PFS. Patients in this cohort were treated according to standard of care consisting of surgery only (59.5%), adjuvant radiotherapy (32.8%), and chemotherapy (14.6%) (33). For medulloblastoma, an increased infiltration of $CD8^+$ T cells and decreased PD-L1 expression are correlated to PFS (34); however, the prognostic relevance between lymphocyte infiltration and medulloblastoma survival has been disputed (35). Other studies have quantified the presence of other checkpoint proteins, such as B7-H3 and CD155, and found that they vary largely based on cancer type (36–38). In summary, IHC is integral for characterizing the TIME in a spatial context and patient-specific manner.

Advances in Immunohistochemistry and Spatial Proteomics

One of the major drawbacks of using IHC to characterize the TIME is the limited number of antibodies that can be used on a single tumor slide, which hampers evaluation of numerous immune cell subsets on a single slide. This is even more relevant

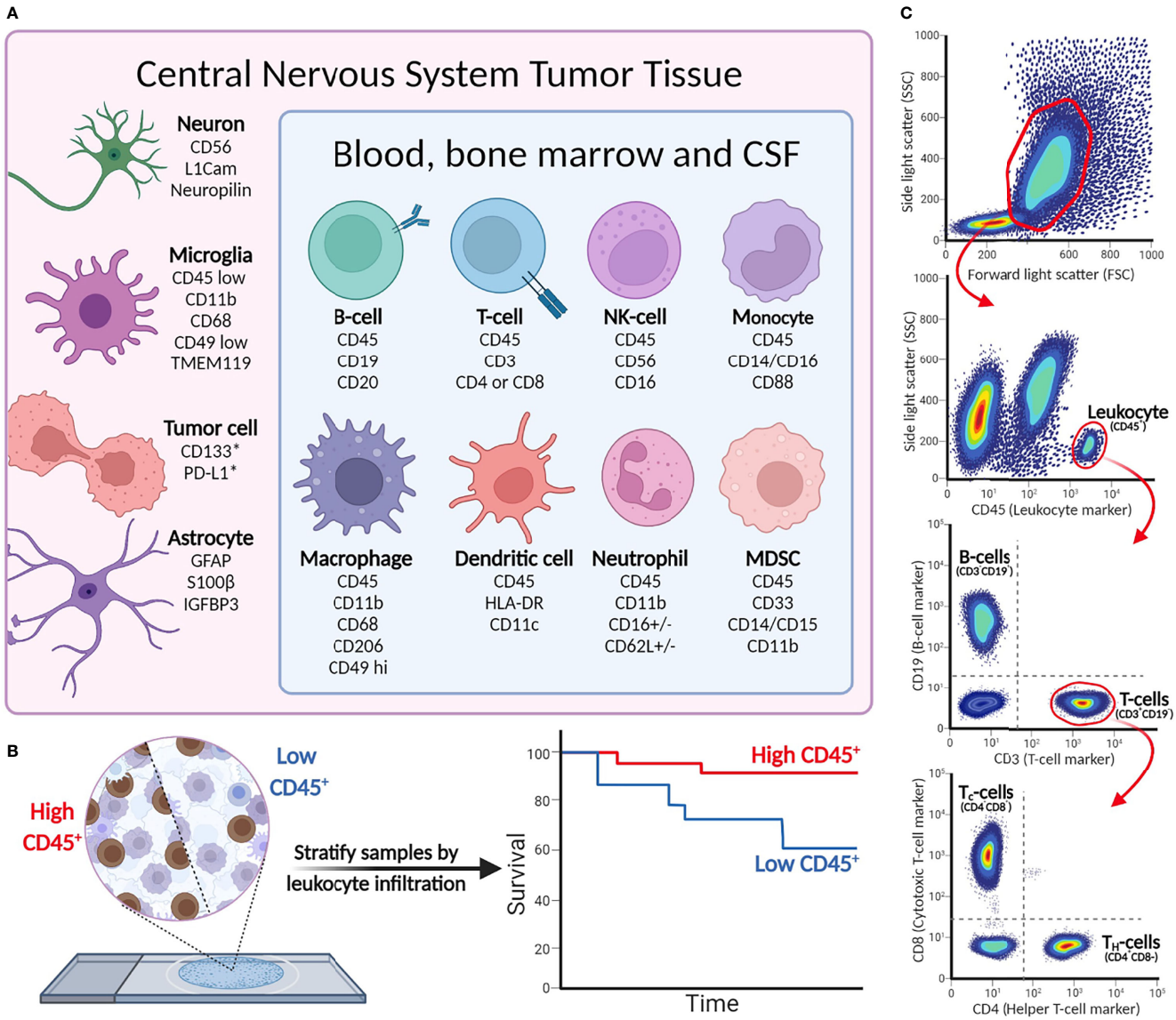

FIGURE 2 | **(A)** Cell-type markers for identification of immunological, tumor, and stromal cells in CNS malignancies. **(B)** Immunohistochemistry detects leukocytes in tumor tissue, and can be used to stratify patient tumor tissue (as demonstrated in Murata et al.). *Cell surface expression may vary between tumor cells and indications. **(C)** Example of flow cytometry gating strategy. More elaborate flow panels can be used for in-depth phenotyping of immune cells, providing information on specific cell subsets and status (activation/anergic/suppressive).

when describing functionally active subsets of immune cells, or co-localization of antigens on tumor or immune cells. Over the last few years, more advanced techniques—such as multiplex IHC, multiplex immunofluorescence, and spatial proteomics—have been developed to study the complex spatial architecture of tissues. These methods allow for simultaneous visualization of multiple proteins, allowing to study the spatial distribution and co-localization of immune cells in the TIME in much greater detail (39, 40). Conceptually, multiplexed immunofluorescence is similar to IHC, though each antibody is labeled with a fluorophore with a unique excitation wavelength, which allows for multiple targets to be visualized on one tumor slide. Interestingly, one study designed a panel of 18 antibodies to study the effect of oncolytic virus therapy on the distribution and functional states of immune cells in a pediatric patient with glioblastoma (41). They noticed a significant increase of $CD8^+$ T cells, macrophages and microglia in post-treatment tissue compared to pre-treatment tissue. Moreover, T cells expressed higher levels of CTLA-4 and PD-1 after treatment, suggesting a potential role of checkpoint inhibition. However, multiplex immunofluorescence uses frozen tissue slides that often have poorer morphology, making spatial interpretation more difficult.

Therefore, current spatial profiling approaches are based on antibodies linked to photocleavable oligonucleotide tags (such as

GeoMx® Protein Assays of NanoString), or use an agonistic approach by detection of isotope-labeled antibodies with mass spectrometry (42, 43). Other methods use a combination of DNA-conjugated antibodies and multicyclic addition of complementary fluorescently labeled DNA probes (44). A significant advantage of spatial proteomics over other protein-detection methods is the ability to spatially profile and quantify the high-dimensional composition of the TIME with high resolution; for example, CODEX can visualize up to 60 antigens on a single slide (44, 45). Using multiplex IHC and spatial proteomics to study the TIME of pediatric CNS malignancies could greatly enhance our understanding of the spatial composition and interactions between cells in a high-throughput manner using only a single tissue slide. To summarize, IHC is considered a highly reliable and robust method to detect protein expression and is often used to study the TIME composition.

FLOW CYTOMETRY

Introduction to Flow Cytometry

Since its invention in the 1960s, flow cytometry has been widely applied to characterize and quantify immune cells (46). Whereas IHC provides information on *in situ* protein expression, flow cytometry measures the expression of surface and intra-cellular proteins at the single-cell resolution. Using panels of fluorophore-conjugated antibodies directed against specific proteins, distinct (sub)populations of cells can be characterized and quantified based on their unique protein expression profiles.

Flow cytometry is used to profile various types of patient materials, such as blood, bone marrow, cerebral spinal fluid, and tissue samples once processed in a single-cell suspension. A viable single-cell suspension can be obtained from solid tissue by enzymatic digestion and/or mechanical dissociation (47–49). It is important to select a tissue-dissociation method that retains cell viability, as dead cells interfere with analysis due to their increased autofluorescence and non-specific binding of antibodies (50). Dead cells can be excluded from analysis by incorporating a specific live/dead marker in the antibody panel (50–52).

Cell handling with either freeze–thawing cycles or a Ficoll gradient to select mononuclear cells results in a loss of specific cells, and therefore, it is essential to standardize methods when initiating an immune monitoring program. Granulocytic cells are generally lost upon a freeze–thaw cycle, whereas mononuclear cells are more stable. Red blood cells are often lysed as they may interfere with the fluorescence readout (53, 54). With recent technical advances in flow cytometry, spectral flow cytometers can now analyze over 40 different extra- and intracellularly markers simultaneously.

Characterization of Immune Cells Using Flow Cytometry

Based on the size and granularity, immune cells can be distinguished from the generally larger non-immune cells and tumor cells that are present in tumor material. Subsequently, cells can be further profiled based on the light emitted by the different cell-bound fluorophores, showing a unique phenotype for each single cell detected. An overview of the most relevant cell-specific lineage markers to discriminate subsets of leukocytes and tumor cells is given in **Figure 2**. CD45 is a general marker to identify hematopoietic cells (except erythrocytes and plasma cells). Cell-type-specific surface markers can be used for further subtyping; for example, CD3 is a lineage marker for T cells that can be further divided into $CD4^+$ and $CD8^+$ T cells, while CD19 is a part of the B-cell receptor complex and thus identifies B cells. The extensive multi-color options of flow cytometry allow analyses of surface-expressed markers for differentiation [naïve (effector), memory, etc.], activation [i.e., CD69 and CD137 (4-1BB)] and terminal differentiation/exhaustion (e.g., CTLA-4 and PD-1), and intracellular markers for proliferation (Ki67), production of effector molecules (cytokines/granzymes), or transcription factors (e.g., FoxP3 to define regulatory T cells). Intracellular staining requires fixation to retain cell structure and prevent intracellular proteins from diffusing out of the cells, followed by permeabilization to allow antibodies to enter the cells (55). To analyze intracellular cytokine production, cells require *ex vivo* stimulation with, for instance, phorbol myristate acetate (PMA; a NF-κB activator) and ionomycin for several hours, coinciding with Golgistop to prevent cytokine secretion, prior to performing antibody staining procedure. Detecting pro- or anti-inflammatory cytokines in the cells then provides insight into the activity of individual cells in the TIME. In conclusion, different combinations of both extra- and intracellular stains are useful for in-depth characterization of different subpopulations of cells present in TIME and periphery.

Applications of Flow Cytometry to Pediatric CNS Malignancy Research

Though flow cytometry is not generally used for diagnosing CNS malignancies, studies have used this technique to characterize the abundance of immune cell infiltration across multiple pediatric CNS malignancies. Griesinger et al. showed differences in immune infiltration and the degree of immune suppression on biopsy material, in patients diagnosed with pilocytic astrocytoma, ependymoma, glioblastoma, and medulloblastoma (56). Compared with glioblastoma and medulloblastoma, pilocytic astrocytomas and ependymomas had significant myeloid (characterized as $CD45^+CD11b^+$) and lymphocyte infiltration. Infiltrating immune cells were shown to express low levels of PD-1, which was suggested to represent a more permissive TIME for immunotherapy. However, the authors did not investigate any additional activation markers such as CD69 or CD137. Remarkably, PD-1 expression was significantly decreased on $CD4^+$ and $CD8^+$ T cells in the TIME of all indications, except glioblastoma. These data were later confirmed by Plant et al. Additional flow cytometric analysis of low- and high-grade glioma, atypical teratoid rhabdoid tumor, and medulloblastoma demonstrated a trend towards increased (activated) B-cell infiltration in high- versus low-grade gliomas. Interestingly, flow analysis of peripheral blood showed low absolute lymphocyte counts in both low- and high-grade

tumors, regardless of steroid treatment, which could indicate an immunosuppressive effect induced by the tumor (17).

Importantly, we are beginning to appreciate how the immunophenotype of pediatric CNS malignancies differs significantly from that of adults. Flow cytometric analysis of adult gliomas and brain metastases revealed that *IDH* mutation status and tumor origin are important in shaping the TIME. Compared to brain metastases, gliomas exhibited lower lymphocyte counts, and higher composition of microglia- and monocyte-derived infiltrating macrophages. Moreover, glioblastomas with *IDH*-wt status exhibited more lymphocyte and less macrophage infiltration compared to lower-grade *IDH*-mut gliomas (57). This correlation between tumor grading and lymphocyte infiltration has not been found in pediatric subtypes. Moreover, flow cytometric analysis demonstrated that tumor immune infiltrate in pediatric CNS malignancies does not correlate with tumor grade, as seen in adults. Low-grade gliomas have more lymphocyte and myeloid infiltration than higher-grade brain tumors (17, 56). These findings highlight that simply deducing results obtained from adult brain tumor research may not necessarily lead to the design of effective immunotherapies for children.

In addition to characterizing the TIME upon diagnosis, flow cytometry is readily used in clinical care for monitoring health and disease in various hematological indications. In hemato-oncology, immune monitoring with flow cytometry is performed on blood, CSF, or bone marrow to detect disease progression, recurrence, and to survey systemic effects of therapeutics (58, 59). However, in the context of CNS malignancies, repetitive tumor biopsies are uncommon. Studying more accessible immune compartments of solid tumors (such as blood, CSF or bone marrow) could provide valuable information on changes in the immune landscape and functional dynamics in a patient, which would otherwise be overlooked and may correlate to the TIME. To this note, a study using a glioblastoma mouse model showed evidence of glioblastoma-induced homing and accumulation of T cells (both $CD4^+$ and $CD8^+$) in the bone marrow. This T cell sequestration resulted in mice suffering from peripheral blood lymphopenia, a symptom that is also observed in patients diagnosed with glioblastoma (60). They also showed that T cell sequestration is a result of location rather than tumor origin, by introducing tumors of different histology in either brain or flank of the mice. Interestingly, all intracranial tumors induced T cell accumulation in the bone marrow regardless of tumor type, which was not found for subcutaneous xenografts (60). A flow cytometric and CyTOF study of adult glioblastoma patients found that MDSCs, but not regulatory T cells, are increased in the blood of glioblastoma patients compared to other CNS tumor indications. Additionally, they showed that the immune composition of blood changes during course of treatment, with reduced B cells and increased $CD8^+$ T cells, dendritic cells, and MDSCs in the blood at 2 months after surgery. Finally, they showed that MDSC levels correlate with overall survival, indicating MDSCs as a possible target for immunotherapy (61). These studies provide strong evidence why investigation of other less invasive immune compartments is essential. Longitudinal flow cytometric analysis of these compartments will not only provide information on disease progression but could also be used as a tool in predicting immune treatment responsiveness.

BULK TRANSCRIPTOMICS

Introduction to Bulk Transcriptomics

Gene expression profiling has become an indispensable tool in translational cancer research. In oncology, expression of genes provides valuable insights into the biological processes and pathways that are regulated in a tumor. For CNS malignancies, the transcriptome enables tumor subgrouping and is gaining interest as a standard tool for detection of driver mutations (62–64).

Procedures for quantifying specific RNA transcripts were first introduced with quantitative reverse transcription polymerase chain reaction (qRT-PCR), which is a robust and highly reproducible method to measure RNA expression (65). The subsequent development of microarrays allowed for the quantification of thousands of gene transcripts at the same time (66). Microarrays are based on hybridization of fluorescently labeled cDNA transcripts (obtained by reverse transcription of RNA from tissue) to complementary DNA probes (67). Nowadays, multiplex, fluorescence-based hybridization methods, such as the NanoString nCounter® platform, are also frequently used to study gene expression. These techniques are based on direct detection of mRNA or miRNA from tissue and permit the use of lower-quality RNA (68, 69). A particularly interesting panel for studying the TIME is the nCounter® Pancancer Immune Profiling Panel, which contains 770 genes associated with immune functions and tumor-specific antigens, spanning 24 immune cell types (70). However, these platforms only permit the quantification of a pre-defined panel of genes, and therefore the discovery of novel biomarkers is limited.

High-throughput whole transcriptome RNA-seq (from here on, referred to as "RNA-seq") has largely replaced microarrays for gene expression profiling in onco-immunology (71). The vast amount of data that can be generated with RNA-seq from a single tumor sample has revolutionized the oncology and clinical research field (66, 72). This technique uses next-generation sequencing technologies and allows for unbiased characterization of the complete transcriptome. Briefly, RNA is isolated from fresh, frozen, or FFPE tumor tissue using preparation kits, followed by ribosomal RNA depletion. Total RNA (including mRNA, lncRNA, and miRNA) undergoes reverse transcription to convert it to cDNA libraries, which are subsequently fragmented, amplified by PCR, and sequenced (73). The sequence reads are then aligned to a reference genome and expression counts can be determined or other analyses can be performed. In contrast to hybridization-based approaches, RNA-seq can detect isoform and splice variants, and identify clinically relevant gene fusions, which are common oncogenic drivers in pediatric CNS malignancies, such as *KIAA1549::BRAF* in pilocytic astrocytomas and *C11orf95::RELA*, primarily in supratentorial ependymomas (64, 74, 75). Additionally, as prospective selection

of genes is not required, the resulting expression profile is unbiased, and discovery of novel biomarkers and transcripts is possible.

Applications of Bulk Transcriptomics to CNS Malignancy and Immune-Oncology Research

The most straightforward analysis of transcriptomic data is comparing the expression of individual genes between samples or diagnoses. For example, Lieberman et al. measured RNA expression of chemokines, pro-inflammatory cytokines, and immunosuppressive factors across pediatric gliomas and normal brain tissue. Low-grade gliomas highly express *CCL2-4*, high-grade gliomas express *CCL5*, while diffuse midline gliomas have basal expression of all chemokines (29). These results are consistent with previous studies that used IHC and flow cytometry, which described the increased lymphocyte and myeloid chemoattraction in pediatric low-grade gliomas (17, 56). Similarly, a signature, or panel of genes, can be created to study the presence and activation state of specific immune cells. These gene expression panels can incorporate functional exhaustion markers or immune checkpoints (e.g., *PD-L1*, *CTLA-4*, and *LAG-3*), to explore the possibility of targeting those with immunotherapy in pediatric brain cancers. Several tools have been developed [e.g., MCP-counter (76)] to compare the abundance of immune cell populations, based on the expression of immune-cell specific genes, between samples.

More sophisticated computational methods can be used to robustly analyze RNA-seq datasets and derive biologically meaningful results, such as targetable genes or pathways implicated in cancers. Unsupervised clustering and dimensionality reduction are useful for observing the inter-sample variability in the transcriptome. Hierarchical and k-means clustering are popular methods for identifying groups of samples with similar global gene expression patterns (77). Dimensionality reduction, such as principal component analysis or uniform manifold approximation, reduces the number of features by transforming gene expression variables into a lower-dimensional space. This retains meaningful properties of the original high-dimensional dataset and can detect heterogeneity or confounding variables among samples (78). Groups of samples identified through these approaches can be clinically relevant, as transcriptomes have been shown to correspond to anatomical location [for pilocytic astrocytomas (79, 80)], diagnosis subgroups [for medulloblastoma (81)], oncogenic drivers [H3K27 mutation status for pediatric high-grade gliomas (82)], and survival [adult and pediatric high-grade gliomas (83)].

Methods such as differential gene expression and gene-set enrichment analysis provide a deeper perspective on the implicated genes and biological pathways, respectively (**Figure 3**). Differential gene expression analysis identifies quantitative differences in gene expression between two or more predefined groups; frequently used algorithms are DESeq2 (84) and edgeR (85). Differentially expressed genes can serve as diagnostic or prognostic biomarkers (83, 86). The next step is usually to translate the findings from differential gene expression analysis into pathways or gene sets to further denominate the biological processes involved. Functional enrichment analysis is useful for quantifying the expression of gene sets within groups of samples (87). There are multiple databases of gene sets, including Kyoto Encyclopedia of Genes and Genomes (88) and Molecular Signatures Database (89). In the context of immune-oncology, enrichment analysis has the potential to quantify the expression of inflammatory, cytotoxicity, or angiogenesis-related pathways. High-grade gliomas driven by alterations in MAPK pathway showed enrichment of immune-response pathways, including elevated M2-macrophage and $CD8^+$ T cell signatures, compared to non-MAPK altered gliomas (90). Furthermore, gene-set analysis resolved medulloblastoma subgroup-specific TIME differences. Bockmayr et al. found that tumors of the SHH subgroup highly expressed genes related in fibroblasts, macrophages, and T cells compared with other subgroups (91).

While RNA-seq on whole tumor samples can give a broad overview of immune cell status, it is impossible to quantify changes in the individual components and cell populations of the TIME. Studies have integrated the isolation and sorting of immune cells by FACS with RNA-seq, to study transcriptional programs in cell populations. In this way, Lin et al. compared expression profiles of tumor-associated macrophages, by selecting $CD11b^+/CD45^+$ cells, of adult glioblastomas and pediatric diffuse midline gliomas. They observed a notably different gene expression profile, in which diffuse midline glioma-associated macrophages expressed lower levels of inflammatory genes (e.g., *IL6* and *CCL4*) compared to glioblastoma-associated macrophages (92). In another study, macrophages and microglia from adult *IDH*-wt and *IDH*-mut glioma showed a disease-specific enrichment of inflammatory pathways: *IDH*-wt macrophages were enriched in gene sets associated with antigen presentation, and MHC I and II presentation (57). Mononuclear immune cells can also be isolated from the blood or CSF for transcriptomic profiling to define genes and gene sets implicated in various immune cells (93).

Furthermore, miRNA and lncRNA levels can also be measured with RNA-seq. The importance of non-coding RNA types in development and progression of cancer is gaining attention, both as biomarkers and as potential therapeutic targets (94). By integrating RNA-seq and miRNA expression profiling on glioblastoma tissue, Yeh et al. found that miR-138 is downregulated in glioblastomas. Subsequent *in vitro* experiments demonstrated that miR-138 downregulates CD44 expression (95). Other studies have also shown the differential expression of miRNAs or lncRNAs in brain cancers (96). While measuring miRNA and lncRNA levels with RNA-seq is still in its infancy, further studies should delineate the critical roles these RNAs play in oncogenesis and how they could be optimally targeted.

Finally, RNA-seq can further be integrated with whole-exome DNA sequencing to discover tumor-specific neoantigens. These neoantigens can be targets for tumor vaccines (97, 98). Although pediatric CNS malignancies are believed to have a low mutational burden, and therefore, a lack of targetable neoantigen expression, deep exome and transcriptome sequencing can still predict the presence of neoantigens (99, 100). For example, Rivero-Hinojosa et al. employed a multi-omics approach to detect immunogenic

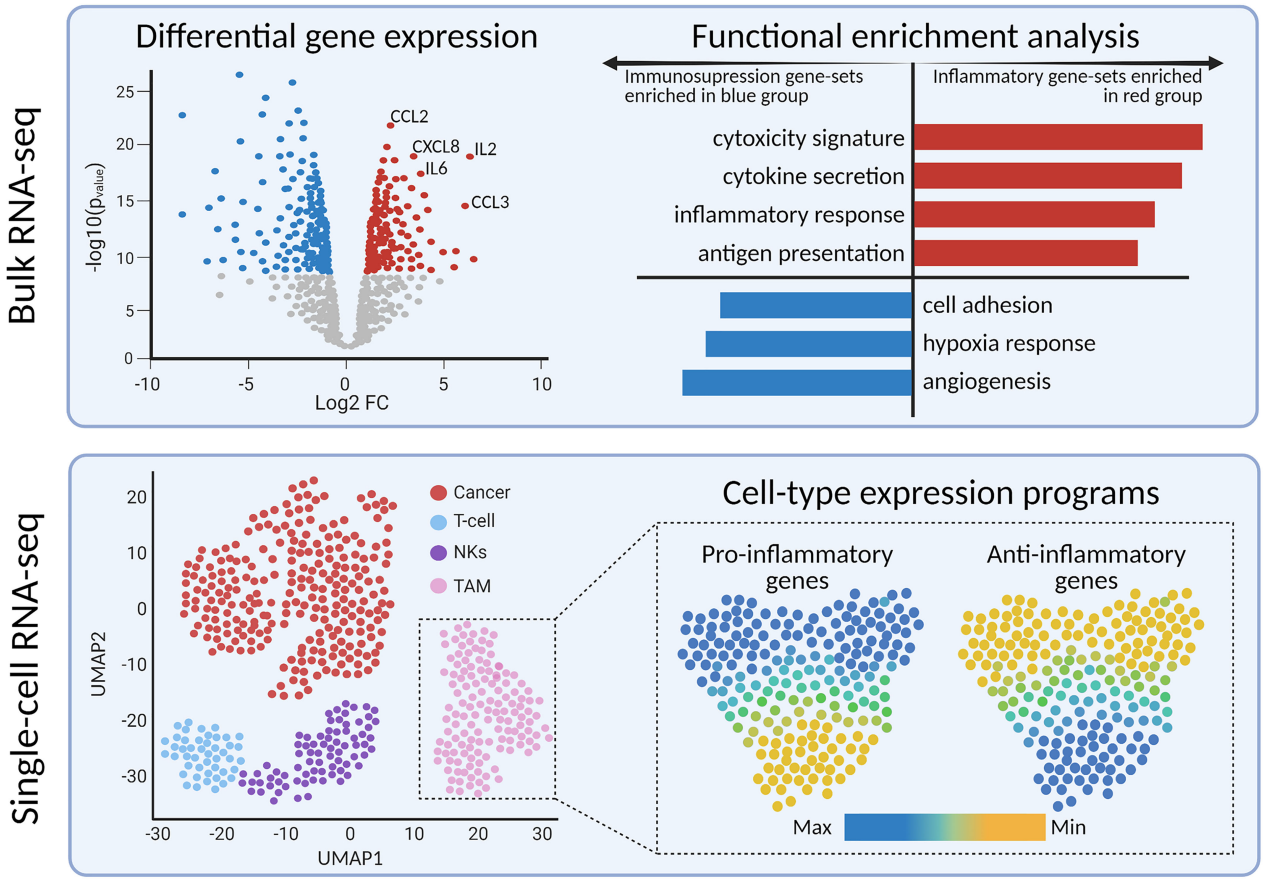

FIGURE 3 | Bulk and single-cell transcriptomics reveals differentially expressed genes and pathways between tumor sub-types or cell sub-populations, respectively.

tumor-specific neoantigens in pediatric medulloblastomas (101). Another study detected neo-antigens in paired primary and recurrent adult glioma samples. While there was no significant difference in the amount of neoantigens between primary and recurrent samples, the expression of neoantigens was reduced at recurrence, which indicates that gliomas downregulate expression of neoantigens to evade immune recognition (102). Two phase I trials of adult glioblastoma patients have already demonstrated that personalized neo-antigen vaccines can elicit neoantigen-specific $CD4^+$ and $CD8^+$ T cell responses (103, 104). These findings highlight the potential of neo-antigen discovery and monitoring, which paves the way towards personalized immune cell therapy.

SINGLE-CELL TRANSCRIPTOMICS

Introduction to Single-Cell RNA Sequencing

Whereas bulk RNA-seq averages the expression of all cells in a sample, the unique advantage of scRNA-seq is the ability to profile the transcriptome of thousands of individual cells. This technique has proven advantageous to characterize the expression programs and cell states of neoplastic and microenvironmental cells in primary and recurrent CNS malignancies (105, 106). Moreover, scRNA-seq profiling has been performed on CSF and blood to monitor the dynamic changes of leukocytes and myeloid cells during treatment (107, 108).

It is important to consider the technical and methodological challenges when designing scRNA-seq studies. First, during sample preparation, single cells must be isolated and lysed separately before sequencing, similar to flow cytometry. Tissue dissociation by enzymatic digestion can result in the loss of rare and vulnerable cell types, which would introduce experimental bias. Moreover, rare populations may not be detected as 10,000 cells are profiled in one scRNA-seq experiment. Single-nucleus RNA-seq (snRNA-seq) was developed to sequence tissues that cannot be easily dissociated into viable single-cells, including frozen tissue. snRNA-seq seems especially useful for research institutions with an extensive biobank, thus enabling a retrospective snRNA-seq on samples that were cryopreserved. Slyper et al. published a toolkit for sequencing fresh and frozen tumor samples using sc- and snRNA-seq, respectively, with recommendations for pediatric high-grade gliomas: CHAPS detergent with salts and Tris for nuclei dissociation; sequencing

with the Chromium platform (109). For the purposes of simplicity in this review, we will refer to both single cell and single nucleus as "scRNA-seq".

Additionally, researchers must decide upon sequencing technology. Full-length transcripts [produced by plate-based platforms such as Smart-Seq2 (110), RamDA-seq (111), and MATQ-seq (112)] are useful for detecting lowly expressed mRNA, splice variants, and isoforms. Droplet-based platforms [such as Chromium, DROP-seq (113), and inDrop (114)] mark the 3' end of mRNA with a 10 base-pair unique molecular identifier (UMI); this allows for higher throughput of cells at the cost of lower resolution, which is more suitable for complex tissues with rare cell types. Batch effect from tissue type, sample preparation protocols, or research facility can be a source of confounding variation. Computational workflows may be able to correct for these uncontrolled variations (**Table 1**).

Applications of scRNA-seq to CNS Malignancy and Immuno-Oncology Research

With advances in sequencing technologies and computational biology, dimensionality reduction and clustering can characterize the diversity of cell populations (115, 116). Prior knowledge of marker genes and cell types is needed to annotate clusters within these datasets, though published packages have been developed to annotate cell types automatically. ScRNA-seq has been utilized for describing the malignant programs and developmental origins of pediatric CNS malignancies (105, 117–120).

Detailed scRNA-seq studies have also been useful for appreciating the heterogeneity and functional differences in brain residing macrophages, as some subtypes play an immunosuppressive role in high-grade gliomas (121). Compared to control brains, diseased brains with epilepsy or tumors have a greater diversity in TAM phenotypes. This suggests that TAMs functionally specialize or differentiate in brain pathologies, which was confirmed in mouse models of adult CNS malignancies (122–124). Pro-tumor and anti-inflammatory macrophages are more abundant in *IDH*-wt gliomas than *IDH*-mut, which is consistent with the poorer survival associated with *IDH*-wt glioblastoma (121). Chen et al. identified that the *MARCO* gene (macrophage receptor with collagenous structure) is selectively expressed in TAMs of *IDH*-wt glioblastomas; interestingly, *MARCO* was not expressed in TAMs of low-grade gliomas or *IDH*-mut glioma (125).

Additionally, the infiltration of TAMs and T cells has been described across various brain regions. Reitman et al. profiled the TAMs in childhood pilocytic astrocytomas using scRNA-seq (126). They found that compared to infra-tentorial pilocytic astrocytomas, supra-tentorial tumors are enriched in microglia. This provided strong evidence for differences in the glioma TIME based on anatomical location. Altogether, future studies should comprehensively characterize the contribution of macrophages and microglia to the TIME, to understand how the tumor location and genomic aberrations affect the immunophenotype.

Further characterization of the expression profiles and surface receptors of T cells have shed light into how these infiltrating lymphocytes are activated in brain cancers. As the T cell receptors (TCRs) mediate T cells' response to cancer, computational methods have been developed to sequence the TCRs to understand how these cells proliferate and specialize (127). ScRNA-seq reads can be used to computationally reconstruct the TCR chains. These powerful methods allow for simultaneous measurements of the transcriptional profile and TCR of T cells from scRNA-seq data (128–130). A recent study by Mathewson et al. extensively profiled the transcriptomes and TCRs of infiltrating T cells in *IDH*-wt glioblastomas and *IDH*-mut high-grade gliomas (131). CD8+ and CD4+ T cells in IDH-wt glioblastoma had higher expression of cytotoxicity, interferon, and cellular stress pathways than *IDH*-mut gliomas. Additionally, they used TraCeR, a computational method to reconstruct the TCRs, to describe the clonal expansion of T cells upon infiltration. On average, each tumor contains 13 distinct T cell clonotypes, which provides evidence for T cell activation and expansion in high-grade gliomas. Of note, more clonal $CD8^+$ T cells have higher expression of reactivity and cytotoxicity signatures, which was confirmed by Rubio-Perez et al. (108). Overall, these analyses highlight the utility of scRNA-seq to investigate transcriptional programs and expansion of T cells in adult brain cancers. However, it may be challenging to profile TCRs in pediatric CNS malignancies as they typically exhibit low levels of T cell infiltration. Therefore, it would be necessary to first sort for $CD3^+$ T cells, thereby excluding the neoplastic, TAMs, and other infiltrating immune cells present in tumor tissue (131).

Overall, scRNA-seq has the potential to identify transcriptional changes in the neoplastic and microenvironmental cells throughout treatment, which is reliant on longitudinal sampling. Ruiz-Moreno et al. monitored the expression profiles of microglia, macrophages, and T cells in a patient with a diffuse midline glioma at diagnosis and metastasis (132). Upon biopsy, the immune component made

TABLE 1 | Comparison of single-cell RNA-seq technologies.

Sequencing type	*Procedure*	*Tissue compatibility*	*Platforms*	*Advantages*
Full-length transcripts	Plate based: single cells are flow sorted into individual wells before library preparation	Single-cell (fresh) and single-nuclei (fresh and frozen)	Smart-Seq2 (most popular); also MATQ-seq, RamDA-seq	Captures more genes per cell; can detect splice variants and isoforms
Unique molecular identifier (UMI)	Droplet based: cells are encapsulated into a gel bead and 3' or 5' end of mRNA is marked with UMI	Single-cell (fresh) and single-nuclei (fresh and frozen)	Chromium (most popular); also DROP-seq, inDrop	Captures more cells per sample; can detect rarer cell types

up half of the primary tumor, mostly consisting of microglia and a few macrophages. These tumor-associated macrophages expressed an anti-inflammatory/pro-tumor phenotype, which supported their finding of few infiltrative T cells. Three serial samples of the abdominal tumor metastasis were obtained; interestingly, they found that, over time, macrophages obtained a more pro-tumor phenotype with few infiltrating pro-inflammatory macrophages or T cells. Finally, the researchers also used scRNA-seq to describe changes in the TIME after the patient started treatment with hydroxychloroquine, an immunomodulator that increases the anti-tumor activity of macrophages (132). Their analysis revealed a dramatic increase in naïve and pro-inflammatory macrophages, and antigen-presenting dendritic cells. Their results highlight the utility of longitudinal sampling and scRNA-seq to understand the evolution of the TIME throughout disease course and immunotherapies.

Due to difficulties with re-sampling primary tumor tissues, researchers have used scRNA-seq to characterize other compartments of the immune system, including CSF and peripheral blood (108, 133). However, the question remains if the immune cells in the CSF or blood are informative for the brain TIME and should be further elucidated in future studies. In a study of adults with brain metastasis, Rubio-Perez et al. obtained simultaneous scRNA-seq datasets of brain metastasized tumor and CSF (108). The TIME and CSF had consistent proportions of $CD8^+$ T, $CD4^+$ T, and NK cells, highlighting how scRNA-seq data of lymphocytes in liquid biopsies recapitulate the TIME of primary tumors (108). As the TIME is correlated to patient's response to immunotherapies, future studies need to explore if liquid biopsies do reflect the TIME in pediatric brain malignancies, with the ultimate goal to have a surrogate for response to (immune) therapy (25). However, not all compartments of the immune system behave similarly. Prakadan et al. also obtained scRNA-seq datasets of peripheral blood and CSF of patients enrolled in clinical trials for immune checkpoint inhibitors for leptomeningeal disease (133). Lymphocytes and myeloid cells expressed gene signatures for antigen presentation and IFN-gamma response higher in the CSF compared to the blood. They also found that myeloid cells in the CSF showed an increase in the pro-inflammatory phenotype, while the opposite was seen in myeloid cells in the blood.

Longitudinal samples of liquid biopsies are useful when relating immune system dynamics with clinical outcomes. Soon after treatment with checkpoint inhibitors, Prakadan et al. identified an increased inflammatory gene signature in the CSF, which was not identified at later time points (133). Additionally, compared with pre-treatment samples, $CD8^+$ T cells significantly expressed genes associated with antigen presentation and IFN-gamma signaling. These results could explain the clinical benefits of the immune checkpoint inhibitors in leptomeningeal disease. Furthermore, Rubio-Perez et al. mapped the abundance of immune cells in the CSF for two patients that underwent re-surgery; their serial samples of CSF showed an increase in naïve T cells and decrease in macrophages (108). Together, these papers provide evidence that scRNA-seq should be further investigated for children with a CNS malignancy; preferably including longitudinal sampling to understand, and hopefully improve, (immuno)therapies in pediatric high-grade brain tumors (**Figure 4**).

Advances in Transcriptomic Profiling

With advancements in transcriptomics technologies and computational methods, we have seen a surge in creative applications using scRNA-seq to investigate the tumor ecosystem. Computational methods referred to as "deconvolution" integrate bulk and scRNA-seq, and have been developed to predict the cell-type composition from homogenized bulk RNA-seq data. Algorithms for cell-type deconvolution include CIBERSORTx, MuSiC, and DWLS (134–136). Though they differ in their mathematical methods, the results are highly robust and correlated (137). Results from deconvolution should be benchmarked with representative IHC staining or flow cytometry, to ensure that differences in RNA expression correspond to cell-type quantification from the protein and microscopy level. Additionally, cell–cell interactions have been predicted from scRNA-seq datasets of heterogeneous tissues, which is especially useful for characterizing the TIME. Simply, these algorithms utilize literature-derived datasets of ligand–receptor interactions, and predict which cells communicate based on the cell-type expression of these proteins (138). Physical location information from spatial transcriptomics or proteomics would increase the power of these data-driven predictions, as interacting cells are located near one another. Both deconvolution and cell–cell interaction algorithms will advance research studies aiming to quantify the immune cell composition and interactions within the TIME.

scRNA-seq has been adapted to profile transcriptomics in parallel with additional biomolecules. CITE-seq was developed to allow for simultaneous profiling of multiplexed protein markers and transcriptomes of single cells from fresh tissue (139). In this procedure, single cells are incubated with DNA-barcoded antibodies. Upon sequencing, a quantitative read out is obtained for the expression and immunophenotyping of single cells. CITE-seq has been used to profile the immune cells in the glioblastoma microenvironment (123). TAMs and dendritic cell clusters were identified in CITE-seq and scRNA-seq analyses, proving the robustness of the protocols. One unique benefit of CITE-seq is identifying novel cell surface protein markers; for example, markers were identified that captured monocyte-to-macrophage differentiation and characterized blood-derived macrophages from microglia (139).

Finally, as bulk- and scRNA-seq sample preparation requires tissue dissociation, spatial transcriptomics methods have been developed to retain spatial information of mRNA transcripts that is lost with other sequencing platforms (140–142). Fresh-frozen or FFPE tissues are transferred onto a slide with millions of oligonucleotide probes containing a "spatial barcode". The RNA binds with the oligonucleotides on the slide; upon sequencing, the tissue's RNA can be spatially resolved and mapped to histology images of the tissue. Commonly used scRNA-seq analysis tools [such as Seurat (115)] are compatible with spatial transcriptomics and allow for similar clustering analysis of distinct tumor regions. It is important to note that the

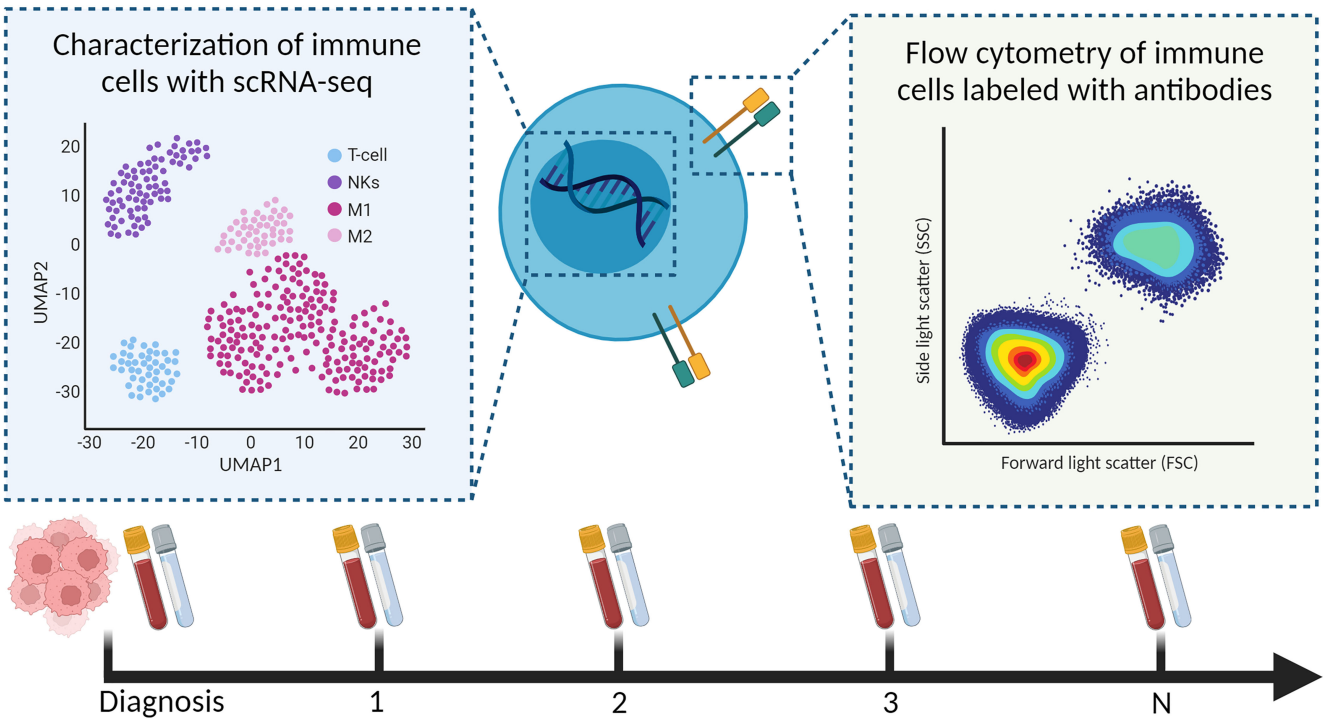

FIGURE 4 | Characterization of immune cells from longitudinal liquid biopsies (as shown, blood and CSF) using scRNA-seq and flow cytometry.

resolution of spatial transcriptomics is less than that of scRNA-seq; each spatial barcode can contain between 3 and 30 cells on the Visium platform, and profiles the expression of far fewer genes. It may be more challenging to detect intra-patient heterogeneity for embryonal tumors that have malignant cells that are densely packed together.

Spatial transcriptomics seems especially useful for resolving the biology at the tumor–microenvironment interface in solid tumors. A recent study from Ravi et al. identified a subset of myeloid cells that are co-localized with mesenchymal-like glioblastoma cells that drive T cell exhaustion, thus contributing to the anti-inflammatory TIME (143). Another study characterized a unique cell state localized at the tumor–microenvironment boundary, which had upregulation of cilia gene sets (144). For heterogeneous and infiltrative pediatric CNS malignancies such as high-grade gliomas, spatial transcriptomics can radically advance our understanding of how cancer cells interact with neurons, astrocytes, and immune cells, and eventually, how the microenvironment architecture changes due to therapeutic interventions.

FUNCTIONAL ASSAYS

IHC, flow cytometry, and transcriptomics are important for describing the composition of immune cells in the TIME. The presence of proliferation markers or enrichment of inflammatory gene sets is suggestive of a cell's potential to mediate humoral or cellular immunity. However, the true capacity of these immune cells to proliferate or kill target cells (referred to as "cytotoxicity") can only be confirmed using functional cellular assays. To this end, tumor-infiltrating lymphocytes (TILs) can be isolated from tumor material or liquid biopsies using cell sorting selective for CD45 markers and evaluated *ex vivo*. As an alternative to single-cell preparation and sorting, TILs can also be expanded directly from tumor materials by culturing the material for several weeks in the presence of stimulatory agents (IL-2, with or without anti-CD3 stimulus) (104, 145). This method for TIL expansion has been used successfully in adoptive cell therapy in multiple cancer indications (146–148); however, it has the disadvantage that cellular diversity is lost, as these culture conditions only promote clonal expansion of a select subset of TILs (mainly T cells).

The proliferative capacity of lymphocytes, indicative for an active immune response, can be investigated by fluorescently labeling the cells with a cell tracer dye [such as cell tracer violet or carboxyfluorescein diacetate succinimidyl ester (CFSE)] and culturing in the presence of an activating agent (149). Polyclonal activation of TILs can be induced with either a lectin mitogen (i.e., phytohemagglutinin) or with anti-CD3 or CD3/CD28 beads in the presence or absence of stimulatory cytokines [i.e., IL-2 (149)]. Upon proliferation, the cell tracer dye will get divided among daughter cells and, therefore, multiple peaks will be visible with a decreased fluorescence.

Clonal activation and expansion of TILs is performed by coculturing the cells for several weeks with irradiated and

peptide loaded feeder cells, in the presence of IL-2 (150). Feeder cells can be either autologous or allogeneic antigen-presenting cells (APCs) or tumor cells expressing the peptide(s) of interest (e.g., pp65 or H3K27M) on their MHC (151). The use of these feeder cells dates back to the 1980s and has shown to promote T cell culture (152). A clinical study using a similar procedure to clonally expand TILs from melanoma patients showed the presence of neo-antigen-specific T cells. Adoptive cell transfer of these TILs, supplemented with IL-2 dosing, resulted in a clinical response in 5 out of 10 patients of which 2 were complete responders (153). Additionally, brain metastases from melanoma have been shown to be susceptible to TIL therapy. In a retrospective study, 7 of 17 (41%) melanoma patients with brain metastases receiving adoptive TIL therapy achieved complete response (154). These results are promising and provide hope that TIL therapies could also be of benefit for the treatment of primary CNS malignancies, although more hurdles will need to be overcome, such as an immune-suppressive environment and the blood–brain barrier. Liu et al. demonstrated that TILs from glioma can be efficiently expanded using a combination of IL-2, IL-15, and IL-21, enhancing CD8 T cell reactivity to autologous tumor cells (155). More recently, a clinical phase I trial has started, investigating the safety and efficacy of TIL therapy in malignant glioma patients (NCT04943913).

Finally, cytokine secretion and cytotoxicity assays are essential for determining the capability of immune cells to induce direct cytotoxicity. The cytokine secretome can be measured directly from patient samples (including tumor tissue, CSF, or plasma), or from conditioned mediums of tumor cell cultures. Measuring both pro-inflammatory (e.g., IFNγ, TNFα, and IL-2) and anti-inflammatory cytokines (e.g., IL-4, IL-6, and IL-10) provides an indication of immune activity in the tumor. Several multiplex techniques such as Olink and Luminex were developed to measure over 25 different cytokines in a limited amount of material. Findings from these assays highlight the anti-inflammatory nature of pediatric CNS malignancies. The secretome of diffuse midline gliomas and pediatric glioblastomas are remarkably different to that of adult glioblastomas. Pediatric high-grade gliomas do not secrete substantial levels of inflammatory cytokines that recruit lymphocytes to the TIME, which contributes to their immunosuppressive phenotype (92). Moreover, assays wherein pediatric glioma cells were co-cultured with T and NK cells suggest therapeutic strategies for immunotherapies. T cells could not effectively lyse diffuse midline glioma cell lines, while NK cells exhibited cytotoxic effects (29). Altogether, cytotoxicity assays are essential in immune monitoring programs to validate hypotheses regarding the anti-inflammatory TIME of pediatric CNS malignancies.

DISCUSSION

Towards an Immunological Atlas of Pediatric CNS Malignancies

Current neuro-oncological practice is increasingly dependent on molecular and cellular profiling of CNS tumor tissue. These histo-molecular findings contribute to a more accurate diagnosis and have the potential to direct personalized and targeted treatment, especially in the context of immunotherapies. A comprehensive evaluation of the pediatric CNS tumor microenvironment and immune system at diagnosis, across treatment and at relapse will be necessary to not only understand how the immune system responds to radio- and systemic therapies, but also to evaluate how novel immunotherapies modulate the immune system. Without aiming to discuss all available methods, we selected various techniques that provide a comprehensive atlas of multiple compartments of the immune system at diagnosis and throughout treatment. We analyzed the clinical utility and feasibility of IHC, flow cytometry, bulk and single-cell transcriptomics, and functional assays for monitoring the immune system and TIME of pediatric CNS malignancies (**Table 2**).

Studies of IHC are useful to determine the quantity and location of a specific cell type in the TIME. In summary, IHC is

TABLE 2 | Utility and feasibility of selected techniques for immune profiling of tumor tissue.

Technique	Tissue type	Utility	Advantages	Disadvantages
Immuno-histochemistry	FFPE	Quantification and phenotyping	• Routine use in diagnostics • Validation for other techniques • Retains spatial information	• Low throughput
Flow Cytometry	Fresh	Quantification and phenotyping	• Millions of cells profiled • Fast data acquisition and analysis	• Panel of antigens or cell types (biased) • Loss of spatial information
Bulk Transcriptomics	Fresh, frozen, FFPE	Biomarkers, functional pathways	• Routine use in diagnostics • Identify pathways for targeted treatment	• Loss of spatial and cell-type information • Computationally intensive
Single-cell Transcriptomics	Fresh, frozen	Quantification, functional pathways	• Thousands of cells profiled • Retains cell-type information • Identify rare or novel cell types	• Expensive ($2,000/sample) • Time-consuming analysis • Computationally intensive • Loss of spatial information
Functional assays	Fresh	Immune-cell function	• Cytotoxicity or proliferation potential of TILs • *Ex vivo* and *in vitro* activity	• Low throughput • Reproducibility of assays

performed on formalin-fixed paraffin embedded tissue, thus retains spatial information, and enables retrospective analyses. With developments in multiplex IHC and flow cytometry, multiple cell types can be quantified to provide a more detailed atlas. Flow cytometry is beneficial as it profiles up to millions of cells in a short period of time (approximately 3 h). However, flow cytometry requires a viable suspension of millions of live single cells; therefore, the sample must be substantially larger than required for IHC or sequencing (where scRNA-seq requires a few thousand cells) and should be either viably cryopreserved or processed directly after surgery (where the latter is preferred to better characterize the myeloid components of the TIME). Additionally, antibody-based technologies require the development and assessment of a panel, which pre-selects the proteins (and therefore, cells) that can be interrogated. Another limitation is that certain cell types may have similar surface proteins compared to other cells, complicating the identification of the cells of interest (i.e., distinguishing MDSCs from myeloid cells). However, as both IHC and flow cytometry are cost-effective and readily available at almost all academic research hospitals, their utility should not be overlooked. Overall, they are useful for quantifying and phenotyping the immune cells present in the TIME; however, the analysis is hypothesis driven, and this introduces a selection bias when using a panel of antibodies. As we described, there is already much prognostic value in quantification metrics alone: for example, T cell infiltration is related to tumor grade in pediatric gliomas and progression-free survival in ependymomas (29, 33).

High-throughput genomic techniques, such as bulk and single-cell transcriptomics, quantify thousands of genes by sequencing. As these methods are unbiased (i.e., not relying on a panel of pre-selected RNA transcripts), they can be useful for identifying gene expression patterns with prognostic value. With bulk RNA-seq, evaluating the expression of immune-related genes and enrichment of immune-related pathways can reveal the inflammatory state of the TIME (29, 90). A possible, and promising, solution is to perform RNA-seq on immune cells found in blood or CSF, which could be correlated to the TIME (93, 156). Although, to our knowledge, no such experiments have been performed to monitor pediatric CNS malignancies yet, studies on other cancers have shown the potential of using these more readily accessible biomaterials to monitor the anti-tumor immune response during therapy. For example, circulating miRNA levels were found to be correlated to the absolute neutrophil count in pancreatic cancer (93). Moreover, comparing immune signatures of patients who respond to those who do not respond to a particular type of therapy can eventually guide therapy decision (157). However, the low number of tumor-infiltrating immune cells compared to the high density of tumor cells can limit the sensitivity of this technique. Furthermore, scRNA-seq can uniquely distinguish rare cell types and cell states; for example, scRNA-seq datasets of T cells in adult gliomas revealed differences in the expression of cytotoxicity and stress pathways between *IDH*-mut and *IDH*-wt tumors that could not be identified *via* IHC or flow cytometry alone (131). Though they are incredibly useful for investigating biological pathways implicated in diseases, transcriptomic methods are costly and computationally intensive. Spatial transcriptomics has been developed to retain the spatial information lost due to tissue dissociation protocols.

These cellular and molecular techniques are essential for immunophenotyping CNS malignancies. Additional functional experiments that assess the TIME cells' cytokine secretion profile or cytotoxicity capacity of immune cells are necessary to evaluate hypotheses generated from the prior methods. Such assays helped us realize that diffuse midline gliomas have a non-inflammatory TIME by secreting much fewer cytokines than adult high-grade gliomas (92). Additionally, they revealed that NK cells can lyse diffuse midline glioma cells, while T cells and macrophages cannot (29). Results from functional assays suggest that immunotherapies that recruit and activate NK cells could be plausible strategies for new treatment designs. In summary, integrating IHC, flow cytometry, transcriptomic methods, and functional assays allow for a detailed atlas of the quantity, location, and functionality of immune cells in both TIME and periphery, which cannot be achieved by one methodology alone.

Clinical Perspective

We recognize that there are significant challenges with designing studies that monitor the immune system during cancer treatment. Pediatric normal brain tissue is a necessary control for characterizing the infiltration and activation of immune cells in CNS malignancies but is scarce and difficult to obtain. Fresh CNS material can be obtained from epilepsy surgeries and tumor-free autopsy material (56); however, there are still confounding factors to consider, such as cause of mortality and time since death. Additionally, "brain banks" dedicated to storing and distributing postmortem brain tissues for the research community have been established worldwide, though these typically consist of adult specimens (158). The National Institute of Child Health and Human Development and the Harvard Brain Tissue Resource Center are two brain banks specific for collecting and distributing brain tissue from children and fetuses (159).

Furthermore, obtaining high-quality CNS tumor samples remains the biggest hurdle, especially for cases when the tumor is in a vulnerable location (i.e., the brain stem for diffuse midline gliomas). CUSA material (tissue obtained using a Cavitron Ultrasonic Surgical aspirator during brain surgery), which contains buffered solution, brain tumor and non-tumor fragments, and blood, can also be used for cellular and molecular analyses. CUSA material has been used for diagnostic purposes, and in studies of cellular heterogeneity of malignant cells and immune microenvironment (160–163). To what extent the CUSA material reflects the microenvironment of the tumor in children is subject to further research.

Longitudinal sampling to evaluate treatment effects is also particularly challenging. In a recent pre-print, Spitzer et al. obtained scRNA-seq datasets of two matched pre- and post-treatment glioma samples that responded well to a targeted treatment and identified changes in the malignant cell states that explained the observed clinical response. To increase the power and confidence of their analysis, they included pre-treatment scRNA-seq data of non-responders, and noticed a

distinct differentiation pattern that could explain their lack of clinical response (164). Additionally, we suggest utilizing liquid biopsies to characterize the immunological system response to treatment. Liquid biopsies are currently a hot topic for assessing progression of pediatric CNS malignancies, with a recent paper demonstrating that serial analysis of circulating DNA in the CSF can predict tumor burden and disease progression in medulloblastomas (165). As we described, flow cytometry and scRNA-seq datasets of immune cells in blood, bone marrow, and CSF can also be informative for advancing our understanding of the immune system's response to current treatment regimens and designing future immunotherapies (108, 133). Ideally, we can use liquid biopsies as surrogate markers for the TIME, avoiding invasive surgical procedures.

Looking forward, we predict that a detailed description of the microenvironment and immune system of pediatric CNS malignancies throughout the disease course will be paramount to implementing and evaluating the efficacy of immunotherapies (**Figure 5**). In our field, we are beginning to recognize substantial biological differences between pediatric and adult CNS malignancies, which could also be attributed to the role of the immune system in childhood neurodevelopment. Studies of pre- and post-natal mice have been essential in describing the unique role that microglia take as modulators in the formation of neural circuits: they clear excess neurons, assist with vascularization, and regulate neural-stem cell commitment to astrocyte and neuron lineages (166). During adulthood, microglia become ramified and survey the brain parenchyma for tissue injury or disease (166). Interestingly, in the setting of brain cancers, microglia do not phagocytize the glioma cells, and can be reprogrammed to promote tumor growth (167). Detailed scRNA-seq studies of adult and mouse gliomas could resolve the heterogeneity of microglia states (121–125); however, similar studies in children are lacking but will be necessary to unravel the complex activity of microglia in malignancy and development.

In the field of pediatric neuro-oncology, trials of vaccine approaches, oncolytic viruses, checkpoint blockade, and adoptive cellular therapy are currently under investigation in preclinical and clinical settings. Small trials thus far show noteworthy clinical outcomes but raise a broad spectrum of unique challenges that need to be evaluated (168). Specific challenges while developing immunotherapies for children with CNS malignancies include a cold immunophenotype with minimal T cell infiltration, a relatively low mutational burden, intra-tumoral heterogeneity, and blood–brain barrier penetration. The potency of immunotherapy needs to be evaluated for optimal application of immunotherapy targeting this highly specific neoplasm and challenging environment. Clinical outcomes targeting a single tumor-associated antigen failed to show adequate, durable anti-tumor responses, suggesting that selective targeting of one antigen may be insufficient (168, 169). Combination therapy might help overcome tumor heterogeneity and penetrate the highly immunosuppressive TIME, and clinical trials are underway (i.e., NCT03130959, NCT00634231, and NCT03396575). Furthermore, clinical research studies should focus on elucidating the long-term side effects of immune modulators in children, especially when addressing effects to their developing immune system, and neurodevelopment and cognition.

To move forward, we need a multifaceted and comprehensive description of the microenvironment of pediatric CNS malignancies. Understanding the subtype-specific immunological phenotype and how the treatment protocol, anatomical location, and grade of each tumor influences the TIME is essential to efficiently redirect the immune system towards cancer eradication. Within the Princess Maxima Center, Utrecht, Netherlands, a prospective observational longitudinal study is initiated including 60 newly diagnosed and relapsed children with various CNS malignancies (Trial NL8967). At diagnosis, biopsy tumor tissue will be profiled by IHC, bulk, and single-cell transcriptomics. CSF, bone marrow, and peripheral blood will be collected during surgery and subsequent follow-up visits; these liquid biopsies are profiled by flow cytometry and scRNA-seq (depending on sample size and tissue availability).

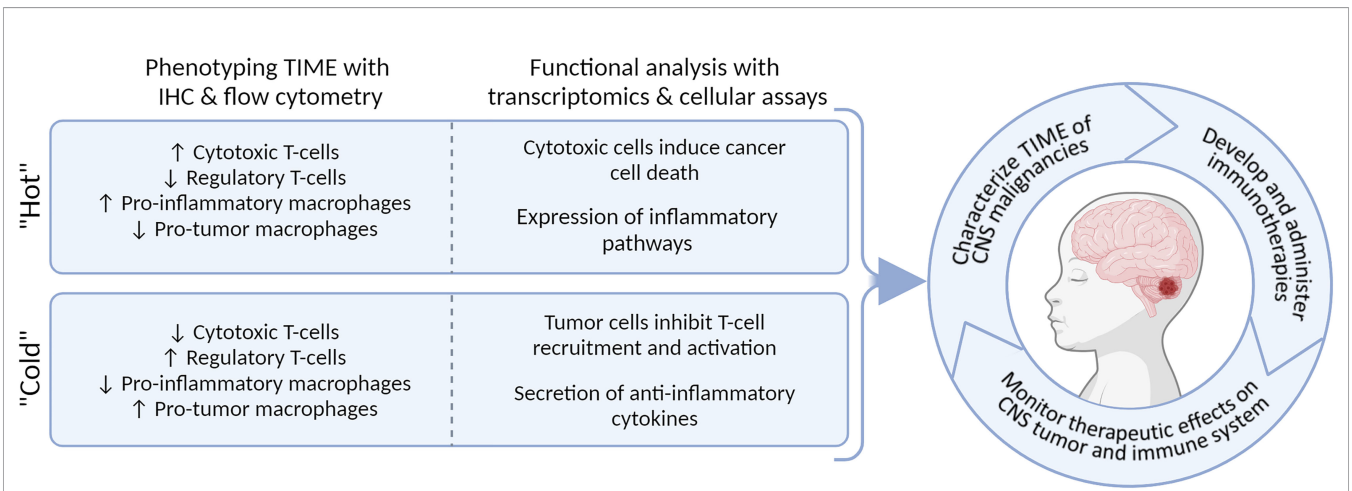

FIGURE 5 | Integrating methodologies allows for multi-dimensional characterization of TIME and will enable personalized immunotherapeutic strategies.

Accurate immune profiling could help pave the way for future immunotherapeutic interventions in pediatric neuro-oncology.

AUTHOR CONTRIBUTIONS

JSR, JIM-E, JASL, MLB, FGC, and JvdL wrote the review. JSR coordinated the writing and review process. SN, MEGK, and LAK critically revised the drafts. JSR, JIM-E, JASL, and MLB made the figures and tables. All authors contributed to the conception of this review and have made a substantial, direct, and intellectual contribution to the work and approved it for publication.

FUNDING

This study received funding from the Team Westland Foundation. JSR was supported by the Fulbright U.S. Student Grant and Netherland-American Foundation Pediatric Cancer Award. The funders were not involved in the study design, collection, analysis, interpretation of data, the writing of this article, or the decision to submit it for publication.

ACKNOWLEDGMENTS

All figures were created using BioRender.com.

REFERENCES

1. Louis DN, Perry A, Wesseling P, Brat DJ, Cree IA, Figarella-Branger D, et al. The 2021 WHO Classification of Tumors of the Central Nervous System: A Summary. *Neuro Oncol* (2021) 23(8):1231–51. doi: 10.1093/neuonc/noab106
2. Miller KD, Ostrom QT, Kruchko C, Patil N, Tihan T, Cioffi G, et al. Brain and Other Central Nervous System Tumor Statistics, 2021. *CA Cancer J Clin* (2021) 71(5):381–406. doi: 10.3322/caac.21693
3. Packer RJ, Zhou T, Holmes E, Vezina G, Gajjar A. Survival and Secondary Tumors in Children With Medulloblastoma Receiving Radiotherapy and Adjuvant Chemotherapy: Results of Children's Oncology Group Trial A9961. *Neuro Oncol* (2013) 15(1):97–103. doi: 10.1093/neuonc/nos267
4. Fangusaro J. Pediatric High Grade Glioma: A Review and Update on Tumor Clinical Characteristics and Biology. *Front Oncol* (2012) 2:105. doi: 10.3389/fonc.2012.00105
5. El-Ayadi M, Ansari M, Sturm D, Gielen GH, Warmuth-Metz M, Kramm CM, et al. High-Grade Glioma in Very Young Children: A Rare and Particular Patient Population. *Oncotarget* (2017) 8(38):64564–78. doi: 10.18632/oncotarget.18478
6. Grundy R. The Development of Cell Line Models of Childhood Brain Tumours. *ATLA* (2010) 38(Supplement 1):11–3. doi: 10.1177/026119291003801S09
7. Denunzio NJ, Yock TI. Modern Radiotherapy for Pediatric Brain Tumors. *Cancers (Basel)* (2020) 12(1533):1–16. doi: 10.3390/cancers12061533
8. Pollack IF, Agnihotri S, Broniscer A. Childhood Brain Tumors: Current Management, Biological Insights, and Future Directions. *J Neurosurg Pediatr* (2019) 23(3):261–73. doi: 10.3171/2018.10.PEDS18377
9. Miklja Z, Pasternak A, Stallard S, Nicolaides T, Kline-nunnally C, Cole B, et al. Neuro-Oncology Gliomas: Review and Consensus Recommendations. *Neuro Oncol* (2019) 21(February):968–80. doi: 10.1093/neuonc/noz022
10. Wolchok JD, Chiarion-Sileni V, Gonzalez R, Rutkowski P, Grob JJ, Cowey CL, et al. Overall Survival With Combined Nivolumab and Ipilimumab in Advanced Melanoma. *N Engl J Med* (2017) 377(14):1345–56. doi: 10.1056/NEJMoa1709684
11. Larkin J, Chiarion-Sileni V, Gonzalez R, Grob JJ, Cowey CL, Lao CD, et al. Combined Nivolumab and Ipilimumab or Monotherapy in Previously Untreated Melanoma. *N Engl J Med* (2015) 373(1):23–34. doi: 10.1056/NEJMoa1504030
12. Motzer RJ, Escudier B, McDermott DF, George S, Hammers HJ, Srinivas S, et al. Nivolumab Versus Everolimus in Advanced Renal Cell Carcinoma. *N Engl J Med* (2015) 373(19):1803–13. doi: 10.1056/NEJMoa1510665
13. Borghaei H, Paz-Ares L, Horn L, Spigel DR, Steins M, Ready NE, et al. Nivolumab Versus Docetaxel in Advanced Non-Squamous Non- Small Cell Lung Cancer. *N Engl J Med* (2017) 373(17):1627–39. doi: 10.1056/NEJMoa1507643
14. Vitanza NA, Johnson AJ, Wilson AL, Brown C, Yokoyama JK, Künkele A, et al. Locoregional Infusion of HER2-Specific CAR T Cells in Children and Young Adults With Recurrent or Refractory CNS Tumors: An Interim Analysis. *Nat Med* (2021) 27(9):1544–52. doi: 10.1038/s41591-021-01404-8
15. Jones C, Karajannis MA, Jones DTW, Kieran MW, Monje M, Baker SJ, et al. Neuro-Oncology in Need of New Thinking. *Neuro Oncol* (2017) 19(June 2016):153–61. doi: 10.1093/neuonc/now101
16. Yalon M, Toren A, Jabarin D, Fadida E, Constantini S. Elevated NLR May Be a Feature of Pediatric Brain Cancer Patients. *Front Oncol* (2019) 9(April):1–5. doi: 10.3389/fonc.2019.00327
17. Plant AS, Koyama S, Sinai C, Solomon IH, Griffin GK, Ligon KL, et al. Immunophenotyping of Pediatric Brain Tumors: Correlating Immune Infiltrate With Histology, Mutational Load, and Survival and Assessing Clonal T Cell Response. *J Neurooncol* (2018) 137(2):269–78. doi: 10.1007/s11060-017-2737-9
18. Bonaventura P, Shekarian T, Alcazer V, Valladeau-Guilemond J, Valsesia-Wittmann S, Amigorena S, et al. Cold Tumors: A Therapeutic Challenge for Immunotherapy. *Front Immunol* (2019) 10:168. doi: 10.3389/fimmu.2019.00168
19. Ajami B, Bennett JL, Krieger C, McNagny KM, Rossi FMV. Infiltrating Monocytes Trigger EAE Progression, But do Not Contribute to the Resident Microglia Pool. *Nat Neurosci* (2011) 14(9):1142–9. doi: 10.1038/nn.2887
20. Sampson JH, Gunn MD, Fecci PE, Ashley DM. Brain Immunology and Immunotherapy in Brain Tumours. *Nat Rev Cancer* (2020) 20(1):12–25. doi: 10.1038/s41568-019-0224-7
21. Murray PJ, Allen JE, Biswas SK, Fisher EA, Gilroy DW, Goerdt S, et al. Macrophage Activation and Polarization: Nomenclature and Experimental Guidelines. *Immunity* (2014) 41(1):14–20. doi: 10.1016/j.immuni.2014.06.008
22. Gate D, Danielpour M, Rodriguez J, Kim G, Levy R, Bannykh S. T-Cell TGF-β Signaling Abrogation Restricts Medulloblastoma Progression. *PNAS* (2014) 111(33):E3458–E3466. doi: 10.1073/pnas.1412489111
23. Huettner C, Czub S, Kerkau S, Roggendorf W, Tonn JC. Interleukin 10 is Expressed in Human Gliomas In Vivo and Increases Glioma Cell Proliferation and Motility *In Vitro*. *Anticancer Res* (1997) 17(5A):3217–24.
24. Ostuni R, Kratochvill F, Murray PJ, Natoli G. Macrophages and Cancer: From Mechanisms to Therapeutic Implications. *Trends Immunol* (2015) 36(4):229–39. doi: 10.1016/j.it.2015.02.004
25. Taube JM, Klein A, Brahmer JR, Xu H, Pan X, Kim JH, et al. Association of PD-1, PD-1 Ligands, and Other Features of the Tumor Immune Microenvironment With Response to Anti–PD-1 Therapy. *Clin Cancer Res* (2014) 20(19):5064–74. doi: 10.1158/1078-0432.CCR-13-3271
26. Gajjar A, Pfister SM, Taylor MD, Gilbertson RJ. Molecular Insights Into Pediatric Brain Tumors Have the Potential to Transform Therapy. *Clin Cancer Res* (2014) 20(22):5630–40. doi: 10.1158/1078-0432.CCR-14-0833
27. Huang T, Garcia R, Qi J, Lulla R, Horbinski C. Detection of Histone H3 K27M Mutation and Post-Translational Modifications in Pediatric Diffuse Midline Glioma *via* Tissue Immunohistochemistry Informs Diagnosis and Clinical Outcomes. *Oncotarget* (2018) 9(98):37112–24. doi: 10.18632/oncotarget.26430
28. Kim SW, Roh J, Park CS. Immunohistochemistry for Pathologists: Protocols , Pitfalls , and Tips. *J Pathol Transl Med* (2016) 50:411–8. doi: 10.4132/jptm.2016.08.08
29. Lieberman NAP, Degolier K, Kovar HM, Davis A, Hoglund V, Stevens J, et al. Characterization of the Immune Microenvironment of Diffuse Intrinsic Pontine Glioma: Implications for Development of Immunotherapy. *Neuro Oncol* (2019) 21(1):83–94. doi: 10.1093/neuonc/noy145
30. Ott M, Prins RM, Heimberger AB. The Immune Landscape of Common CNS Malignancies: Implications for Immunotherapy. *Nat Rev Clin Oncol* (2021) 18(November):729–44. doi: 10.1038/s41571-021-00518-9

31. Rahimi Koshkaki H, Minasi S, Ugolini A, Trevisi G, Napoletano C, Zizzari IG, et al. Immunohistochemical Characterization of Immune Infiltrate in Tumor Microenvironment of Glioblastoma. *J Pers Med* (2020) 10(3):1–16. doi: 10.3390/jpm10030112
32. Teo W-Y, Elghetany MT, Shen J, Man T-K, Li X, Chintagumpala M, et al. Therapeutic Implications of CD1d Expression and Tumor-Infiltrating Macrophages in Pediatric Medulloblastomas. *J Neurooncol* (2014) 120 (2):293–301. doi: 10.1007/s11060-014-1572-5
33. Nam SJ, Kim Y-H, Park JE, Ra Y, Khang SK, Cho YH, et al. Tumor-Infiltrating Immune Cell Subpopulations and Programmed Death Ligand 1 (PD-L1) Expression Associated With Clinicopathological and Prognostic Parameters in Ependymoma. *Cancer Immunol Immunother* (2019) 68 (2):305–18. doi: 10.1007/s00262-018-2278-x
34. Murata D, Mineharu Y, Arakawa Y, Liu B, Tanji M, Yamaguchi M, et al. High Programmed Cell Death 1 Ligand–1 Expression: Association With CD8+ T-Cell Infiltration and Poor Prognosis in Human Medulloblastoma. *J Neurosurg* (2018) 128(March):710–6. doi: 10.3171/2016.11.JNS16991
35. Vermeulen JF, Van Hecke W, Adriaansen EJM, Jansen MK, Bouma RG, Villacorta Hidalgo J, et al. Prognostic Relevance of Tumor-Infiltrating Lymphocytes and Immune Checkpoints in Pediatric Medulloblastoma. *Oncoimmunology* (2018) 7(3):e1398877. doi: 10.1080/2162402X.2017.1398877
36. Theruvath J, Sotillo E, Mount CW, Graef CM, Delaidelli A, Heitzeneder S, et al. Locoregionally Administered B7-H3-Targeted CAR T Cells for Treatment of Atypical Teratoid / Rhabdoid Tumors. *Nat Med* (2020) 26 :712–9. doi: 10.1038/s41591-020-0821-8
37. Maachani UB, Tosi U, David J, Mukherjee S, Christopher S. B7 E H3 as a Prognostic Biomarker and Therapeutic Target in Pediatric Central Nervous System Tumors. *Transl Oncol* (2020) 13(2):365–71. doi: 10.1016/j.tranon.2019.11.006
38. Thompson EM, Brown M, Dobrikova E, Ramaswamy V, Taylor MD, Mclendon R, et al. Poliovirus Receptor (CD155) Expression in Pediatric Brain Tumors Mediates Oncolysis of Medulloblastoma and Pleomorphic Xanthoastrocytoma. *J Neuropathol Exp Neurol* (2018) 77(8):696–702. doi: 10.1093/jnen/nly045
39. Widodo SS, Hutchinson RA, Fang Y, Mangiola S, Neeson PJ, Darcy PK, et al. Toward Precision Immunotherapy Using Multiplex Immunohistochemistry and in Silico Methods to Define the Tumor Immune Microenvironment. *Cancer Immunol Immunother* (2021) 70(7):1811–20. doi: 10.1007/s00262-020-02801-7
40. Marcelis L, Antoranz A, Delsupehe A-M, Biesemans P, Ferreiro JF, Debackere K, et al. In-Depth Characterization of the Tumor Microenvironment in Central Nervous System Lymphoma Reveals Implications for Immune-Checkpoint Therapy. *Cancer Immunol Immunother* (2020) 69(9):1751–66. doi: 10.1007/s00262-020-02575-y
41. Bernstock JD, Vicario N, Rong L, Valdes PA, Choi BD, Chen JA, et al. A Novel *in Situ* Multiplex Immunofluorescence Panel for the Assessment of Tumor Immunopathology and Response to Virotherapy in Pediatric Glioblastoma Reveals a Role for Checkpoint Protein Inhibition. *Oncoimmunology* (2019) 8(12):1–12. doi: 10.1080/2162402X.2019.1678921
42. Lundberg E, Borner GHH. Spatial Proteomics: A Powerful Discovery Tool for Cell Biology. *Nat Rev Mol Cell Biol* (2019) 20:285–302. doi: 10.1038/s41580-018-0094-y
43. Taylor MJ, Lukowski JK, Anderton CR. Spatially Resolved Mass Spectrometry at the Single Cell: Recent Innovations in Proteomics and Metabolomics. *J Am Soc Mass Spectrom* (2021) 32:872–984. doi: 10.1021/jasms.0c00439
44. Black S, Phillips D, Hickey JW, Kennedy-darling J, Venkataraaman VG, Samusik N, et al. CODEX Multiplexed Tissue Imaging With DNA-Conjugated Antibodies. *Nat Protoc* (2021) 16:3802–35. doi: 10.1038/s41596-021-00556-8
45. Phillips D, Schürch CM, Khodadoust MS, Kim YH, Nolan GP, Jiang S. Highly Multiplexed Phenotyping of Immunoregulatory Proteins in the Tumor Microenvironment by CODEX Tissue Imaging. *Front Immunol* (2021) 12(May):1–12. doi: 10.3389/fimmu.2021.687673
46. Jaye DL, Bray RA, Gebel HM, Harris WAC, Waller EK. Translational Applications of Flow Cytometry in Clinical Practice. *J Immunol* (2012) 188:4715–9. doi: 10.4049/jimmunol.1290017
47. Volovitz I, Shapira N, Ezer H, Gafni A, Lustgarten M, Alter T, et al. A non-Aggressive, Highly Efficient, Enzymatic Method for Dissociation of Human Brain-Tumors and Brain-Tissues to Viable Single-Cells. *BMC Neurosci* (2016) 17(1):1–10. doi: 10.1186/s12868-016-0262-y
48. Leelatian N, Doxie DB, Greenplate AR, Sinnaeve J, Ihrie RA, Irish JM. Preparing Viable Single Cells From Human Tissue and Tumors for Cytomic Analysis. *Curr Protoc Mol Biol* (2017) 118:1–31. doi: 10.1002/cpmb.37
49. Woroniecka K, Chongsathidkiet P, Elsamadicy A, Farber H, Cui X, Fecci PE. Flow Cytometric Identification of Tumor-Infiltrating Lymphocytes From Glioblastoma. *Methods Mol Biol* (2018) 1741:221–6. doi: 10.1007/978-1-4939-7659-1_18
50. Cossarizza A, Chang H, Radbruch A, Andr I, Martin B, Foster J, et al. Guidelines for the Use of Flow Cytometry and Cell Sorting in Immunological Studies *. *Eur J Immunol* (2017) 47(October 2017):1584–797. doi: 10.1002/eji.201646632
51. Johnson S, Nguyen V, Coder D. Assessment of Cell Viability. *Curr Protoc Cytom* (2013) SUPPL.64):1–26. doi: 10.1002/0471142956.cy0902s64
52. Bradford J, Buller G. *Dead Cell Stains in Flow Cytometry: A Comprehensive Analysis* . Available at: http://www.invitrogen.com/etc/medialib/en/filelibrary/cell_tissue_analysis/pdfs.Par.45053.File.tmp/ISAC-2008-DEAD-CELL-STAINS-IN-FLOW-CYTOMETRY-A-COMPREHENSIVE-ANALYSISl.pdf.
53. Hokland P, Heron I. Lymphocyte Isolation Estimate of Total Leucocyte and Differential Counts Preparation of Ery Throcy Tes. *J Imminulogical Methods* (1980) 32:31–9. doi: 10.1016/0022-1759(80)90114-3
54. Dagur PK, McCoy JP. Collection, Storage, and Preparation of Human Blood Cells. *Curr Protoc Cytom* (2015) 2015:5.1.1–5.1.16. doi: 10.1002/0471142956.cy0501s73
55. Cossarizza A, Cossarizza A, Chang H, Radbruch A, Acs A, Adam D, et al. Guidelines for the Use of Flow Cytometry and Cell Sorting in Immunological Studies (Second Edition). *Eur J Immunol* (2019) 49:1457–973. doi: 10.1002/eji.201970107
56. Griesinger AM, Birks DK, Donson AM, Amani V, Hoffman LM, Waziri A, et al. Characterization of Distinct Immunophenotypes Across Pediatric Brain Tumor Types. *J Immunol* (2013) 191(9):1–19. doi: 10.4049/jimmunol.1301966
57. Klemm F, Maas RR, Bowman RL, Kornete M, Soukup K, Nassiri S, et al. Interrogation of the Microenvironmental Landscape in Brain Tumors Reveals Disease-Specific Alterations of Immune Cells. *Cell* (2020) 181 (7):1643–1660.e17. doi: 10.1016/j.cell.2020.05.007
58. Riva G, Nasillo V, Ottomano AM, Bergonzini G, Paolini A, Forghieri F, et al. Multiparametric Flow Cytometry for MRD Monitoring in Hematologic Malignancies: Clinical Applications and New Challenges. *Cancers (Basel)* (2021) 13(18):4582. doi: 10.3390/cancers13184582
59. van der Velden VHJ, Hochhaus A, Cazzaniga G, Szczepanski T, Gabert J, van Dongen JJM. Detection of Minimal Residual Disease in Hematologic Malignancies by Real-Time Quantitative PCR: Principles, Approaches, and Laboratory Aspects. *Leukemia* (2003) 17(6):1013–34. doi: 10.1038/sj.leu.2402922
60. Chongsathidkiet P, Jackson C, Koyama S, Loebel F, Cui X, Farber SH, et al. Sequestration of T-Cells in Bone Marrow in the Setting of Glioblastoma and Other Intracranial Tumors. *Nat Methods* (2018) 24(9):1459–68. doi: 10.1038/s41591-018-0135-2
61. Alban TJ, Alvarado AG, Sorensen MD, Bayik D, Volovetz J, Serbinowski E, et al. Global Immune Fingerprinting in Glioblastoma Patient Peripheral Blood Reveals Immune-Suppression Signatures Associated With Prognosis. *JCI Insight* (2018) 3(21):1–15. doi: 10.1172/jci.insight.122264
62. Verhaak RGW, Hoadley KA, Purdom E, Wang V, Qi Y, Wilkerson MD, et al. An Integrated Genomic Analysis Identifies Clinically Relevant Subtypes of Glioblastoma Characterized by Abnormalities in PDGFRA, IDH1, EGFR and NF1. *Cancer Cell* (2010) 17(1):98. doi: 10.1016/j.ccr.2009.12.020
63. Byron S, Van Keuren-Jensen K, Engelthaler D, Carpten JD, Craig DW. Translating RNA Sequencing Into Clinical Diagnostics: Opportunities and Challenges. *Nat Rev Immunol* (2016) 17:257–71. doi: 10.1038/nrg.2016.10
64. van Belzen IAEM, Cai C, van Tuil M, Badloe S, Strengman E, Janse A, et al. Systematic Discovery of Gene Fusions in Pediatric Cancer by Integrating RNA-Seq and WGS. *Genomics* (2021) 2012:2021.08.31.458342. doi: 10.1101/2021.08.31.458342
65. Vanguilder HD, Vrana KE, Freeman WM, Facility GC. Twenty-Five Years of Quantitative PCR for Gene Expression. *Biotechniques* (2008) 44(5):619–26. doi: 10.2144/000112776

66. Rogawski DS, Vitanza NA, Gauthier AC, Ramaswamy V, Koschmann C. Integrating RNA Sequencing Into Neuro-Oncology Practice. *Trans Res J Lab Clin Med* (2017) 189:93–104. doi: 10.1016/j.trsl.2017.06.013
67. Mantione KJ, Kream RM, Kuzelova H, Ptacek R, Raboch J, Samuel JM, et al. Comparing Bioinformatic Gene Expression Profiling Methods: Microarray and RNA-Seq. *Mol Biol* (2014) 20:138–41. doi: 10.12659/MSMBR.892101
68. M'Boutchou MN, van Kempen LC. Analysis of the Tumor Microenvironment Transcriptome *via* NanoString mRNA and miRNA Expression Profiling. *Methods Mol Biol* (2016) 1458:291–310. doi: 10.1007/978-1-4939-3801-8_21
69. Veldman-jones MH, Brant R, Rooney C, Geh C, Emery H, Harbron CG, et al. Evaluating Robustness and Sensitivity of the NanoString Technologies Ncounter Platform to Enable Multiplexed Gene Expression Analysis of Clinical Samples. *Cancer Res* (2015) 75:2587–93. doi: 10.1158/0008-5472.CAN-15-0262
70. Cesano A. Ncounter ® PanCancer Immune Profiling Panel (NanoString Technologies , Inc. *J Immunother Cancer* (2015) 3:42. doi: 10.1186/s40425-015-0088-7
71. Hong M, Tao S, Zhang L, Diao L-T, Huang X, Huang S, et al. RNA Sequencing: New Technologies and Applications in Cancer Research. *J Hematol Oncol* (2020) 13(1):166. doi: 10.1186/s13045-020-01005-x
72. Kuksin M, Gautheret D. ScienceDirect Applications of Single-Cell and Bulk RNA Sequencing in. *ScienceDirect* (2021) 149:193–210. doi: 10.1016/j.ejca.2021.03.005
73. Smith CC, Bixby LM, Miller KL, Selitsky SR, Bortone DS, Hoadley KA, et al. Using RNA Sequencing to Characterize the Tumor Microenvironment. *Methods Mol Biol* (2019) 2055:245–72. doi: 10.1007/978-1-4939-9773-2_12
74. Jones DTW, Kocialkowski S, Liu L, Pearson DM, Ba LM, Ichimura K, et al. Tandem Duplication Producing a Novel Oncogenic BRAF Fusion Gene Defines the Majority of Pilocytic Astrocytomas. *Cancer Immunol Immunother* (2008) 68(21):8673–8. doi: 10.1158/0008-5472.CAN-08-2097
75. Parker M, Mohankumar KM, Punchihewa C, Weinlich R, Dalton JD, Li Y, et al. NF- K B Signalling in Ependymoma. *Nature* (2014) 506:451–5. doi: 10.1038/nature13109
76. Becht E, Giraldo NA, Lacroix L, Buttard B, Elarouci N, Petitprez F, et al. Estimating the Population Abundance of Tissue-Infiltrating Immune and Stromal Cell Populations Using Gene Expression. *Genome Biol* (2016) 17:218. doi: 10.1186/s13059-016-1070-5
77. Koch CM, Chiu SF, Akbarpour M, Bharat A, Ridge KM, Bartom ET, et al. A Beginner's Guide to Analysis of RNA Sequencing Data. *Am J Respir Cell Mol Biol* (2018) 59(2):145–57. doi: 10.1165/rcmb.2017-0430TR
78. Yang Y, Sun H, Zhang Y, Zhang T, Gong J, Wei Y, et al. Dimensionality Reduction by UMAP Reinforces Sample Heterogeneity Analysis in Bulk Transcriptomic Data. *Cell Rep* (2021) 36(4):109442. doi: 10.1016/j.celrep.2021.109442
79. Bergthold G, Bandopadhayay P, Hoshida Y, Ramkissoon S, Ramkissoon L, Rich B, et al. Expression Profiles of 151 Pediatric Low-Grade Gliomas Reveal Molecular Differences Associated With Location and Histological Subtype. *Neuro Oncol* (2015) 17(11):1486–96. doi: 10.1093/neuonc/nov045
80. Zakrzewski K, Jarząb M, Pfeifer A, Oczko-Wojciechowska M, Jarząb B, Liberski PP, et al. Transcriptional Profiles of Pilocytic Astrocytoma are Related to Their Three Different Locations, But Not to Radiological Tumor Features. *BMC Cancer* (2015) 15(1):778. doi: 10.1186/s12885-015-1810-z
81. Northcott PA, Buchhalter I, Morrissy AS, Hovestadt V, Weischenfeldt J, Ehrenberger T, et al. The Whole-Genome Landscape of Medulloblastoma Subtypes. *Nature* (2017) 547(7663):311–7. doi: 10.1038/nature22973
82. Wang L-B, Karpova A, Gritsenko MA, Kyle JE, Cao S, Li Y, et al. Proteogenomic and Metabolomic Characterization of Human Glioblastoma. *Cancer Cell* (2021) 39(4):509–528.e20. doi: 10.1016/j.ccell.2021.01.006
83. Donson AM, Birks DK, Schittone SA, Kleinschmidt-DeMasters BK, Sun DY, Hemenway MF, et al. Increased Immune Gene Expression and Immune Cell Infiltration in High Grade Astrocytoma Distinguish Long From Short-Term Survivors. *J Immunol* (2012) 189(4):1920–7. doi: 10.4049/jimmunol.1103373
84. Love MI, Huber W, Anders S. Moderated Estimation of Fold Change and Dispersion for RNA-Seq Data With Deseq2. *Genome Biol* (2014) 15(550):1–21. doi: 10.1186/s13059-014-0550-8
85. Robinson MD, Mccarthy DJ, Smyth GK. Edger: A Bioconductor Package for Differential Expression Analysis of Digital Gene Expression Data. *Bioinformatics* (2010) 26(1):139–40. doi: 10.1093/bioinformatics/btp616
86. Yin W, Tang G, Zhou Q, Cao Y, Li H, Fu X, et al. Expression Profile Analysis Identifies a Novel Five-Gene Signature to Improve Prognosis Prediction of Glioblastoma. *Front Genet* (2019) 10:419. doi: 10.3389/fgene.2019.00419
87. Subramanian A, Tamayo P, Mootha VK, Mukherjee S, Ebert BL. Gene Set Enrichment Analysis: A Knowledge-Based Approach for Interpreting Genome-Wide. *PNAS* (2005) 102(43):15545–50. doi: 10.1073/pnas.0506580102
88. Kanehisa M, Goto S. KEGG: Kyoto Encyclopedia of Genes and Genomes. *Nucleic Acids Res* (2000) 28(1):27–30. doi: 10.1093/nar/28.1.27
89. Liberzon A, Subramanian A, Pinchback R, Thorvaldsdóttir H, Tamayo P, Mesirov JP. Molecular Signatures Database (MSigDB) 3.0. *Bioinformatics* (2011) 27(12):1739–40. doi: 10.1093/bioinformatics/btr260
90. Mackay A, Burford A, Molinari V, Jaspan T, Varlet P, Jones C. Molecular, Pathological, Radiological, and Immune Profiling of Non-Brainstem Pediatric High-Grade Glioma From the HERBY Phase II Randomized Trial. *Cancer Cell* (2018) 33:829–42. doi: 10.1016/j.ccell.2018.04.004
91. Bockmayr M, Mohme M, Klauschen F, Winkler B, Budczies J, Rutkowski S, et al. Subgroup-Specific Immune and Stromal Microenvironment in Medulloblastoma. *Oncoimmunology* (2018) 7(9):e1462430. doi: 10.1080/2162402X.2018.1462430
92. Lin GL, Nagaraja S, Filbin MG, Suvà ML, Vogel H, Monje M. Non-Inflammatory Tumor Microenvironment of Diffuse Intrinsic Pontine Glioma. *Acta Neuropathol Commun* (2018) 6(51):1–12. doi: 10.1186/s40478-018-0553-x
93. van der Sijde F, Li Y, Schraauwen R, de Koning W, van Eijck C, Mustafa D. RNA From Stabilized Whole Blood Enables More Comprehensive Immune Gene Expression Profiling Compared to RNA From Peripheral Blood Mononuclear Cells. *PloS One* (2020) 15(6):1–12. doi: 10.1371/journal.pone.0235413
94. Turner JD, Williamson R, Almefty KK, Nakaji P, Porter R, Tse V, et al. The Many Roles of microRNAs in Brain Tumor Biology. *Neurosurg Focus* (2010) 28(1):E3. doi: 10.3171/2009.10.FOCUS09207
95. Yeh M, Wang YY, Yoo JY, Oh C, Otani Y, Kang JM, et al. MicroRNA – 138 Suppresses Glioblastoma Proliferation Through Downregulation of CD44. *Sci Rep* (2021) 11:9219. doi: 10.1038/s41598-021-88615-8
96. Aloizou A, Pateraki G, Siokas V, Mentis AA, Liampas I, Lazopoulos G, et al. The Role of MiRNA-21 in Gliomas: Hope for a Novel Therapeutic Intervention? *Toxicol Rep* (2020) 7(November):1514–30. doi: 10.1016/j.toxrep.2020.11.001
97. Blass E, Ott PA. Advances in the Development of Personalized Neoantigen-Based Therapeutic Cancer Vaccines. *Nat Rev Clin Oncol* (2021) 18:215–29. doi: 10.1038/s41571-020-00460-2
98. Zhang Z, Lu M, Qin Y, Gao W, Tao L, Su W, et al. Neoantigen: A New Breakthrough in Tumor Immunotherapy. *Front Immunol* (2021) 12 (April):1–9. doi: 10.3389/fimmu.2021.672356
99. Vogelstein B, Papadopoulos N, Velculescu VE, Zhou S, Diaz LA, Kinzler KW. CancerGenomeLandscape. *Sci (80-).* (2013) 339(6127):1546–58. doi: 10.1126/science.1235122
100. Blaeschke F, Paul MC, Schuhmann MU, Rabsteyn A, Schroeder C, Casadei N, et al. Low Mutational Load in Pediatric Medulloblastoma Still Translates Into Neoantigens as Targets for Specific T-Cell Immunotherapy. *Cytotherapy* (2019) 21(9):973–86. doi: 10.1016/j.jcyt.2019.06.009
101. Rivero-hinojosa S, Grant M, Panigrahi A, Zhang H, Caisova V, Bollard CM, et al. Proteogenomic Discovery of Neoantigens Facilitates Personalized Multi-Antigen Targeted T Cell Immunotherapy for Brain Tumors. *Nat Commun* (2021) 12(6689):1–15. doi: 10.1038/s41467-021-26936-y
102. Nejo T, Matsushita H, Karasaki T, Nomura M, Saito K, Tanaka S, et al. Reduced Neoantigen Expression Revealed by Longitudinal Multiomics as a Possible Immune Evasion Mechanism in Glioma. *Cancer Immunol Res* (2019) 7(7):1148–62. doi: 10.1158/2326-6066.CIR-18-0599
103. Keskin DB, Anandappa AJ, Sun J, Tirosh I, Mathewson ND, Li S, et al. Neoantigen Vaccine Generates Intratumoral T Cell Responses in Phase Ib Glioblastoma Trial. *Nature* (2018) 565:234–9. doi: 10.1038/s41586-018-0792-9
104. Hilf N, Kuttruff-Coqui S, Frenzel K, Bukur V, Stevanović S, Gouttefangeas C, et al. Actively Personalized Vaccination Trial for Newly Diagnosed Glioblastoma. *Nature* (2019) 565(7738):240–5. doi: 10.1038/s41586-018-0810-y
105. Filbin MG, Tirosh I, Hovestadt V, Shaw ML, Escalante LE, Mathewson ND, et al. Developmental and Oncogenic Programs in H3K27M Gliomas

Dissected by Single-Cell RNA-Seq. *Sci (80-)* (2018) 360(6386):331–5. doi: 10.1126/science.aao4750

106. Neftel C, Laffy J, Filbin MG, Hara T, Shore ME, Rahme GJ, et al. An Integrative Model of Cellular States, Plasticity, and Genetics for Glioblastoma. *Cell* (2019) 178(4):835–849.e21. doi: 10.1016/j.cell.2019.06.024
107. Schafflick D, Xu CA, Hartlehnert M, Cole M, Schulte-Mecklenbeck A, Lautwein T, et al. Integrated Single Cell Analysis of Blood and Cerebrospinal Fluid Leukocytes in Multiple Sclerosis. *Nat Commun* (2020) 11(1):247. doi: 10.1038/s41467-019-14118-w
108. Rubio-Perez C, Planas-Rigol E, Trincado JL, Bonfill-Teixidor E, Arias A, Marchese D, et al. Immune Cell Profiling of the Cerebrospinal Fluid Enables the Characterization of the Brain Metastasis Microenvironment. *Nat Commun* (2021) 12:1503. doi: 10.1038/s41467-021-21789-x
109. Slyper M, Porter CBM, Ashenberg O, Waldman J, Drokhlyansky E, Wakiro I, et al. A Single-Cell and Single-Nucleus RNA-Seq Toolbox for Fresh and Frozen Human Tumors. *Nat Med* (2020) 26(5):792–802. doi: 10.1038/s41591-020-0844-1
110. Picelli S, Björklund ÅK, Faridani OR, Sagasser S, Winberg G, Sandberg R. Smart-Seq2 for Sensitive Full-Length Transcriptome Profiling in Single Cells. *Nat Methods* (2013) 10(11):1096–8. doi: 10.1038/nmeth.2639
111. Hayashi T, Ozaki H, Sasagawa Y, Umeda M, Danno H, Nikaido I. Single-Cell Full-Length Total RNA Sequencing Uncovers Dynamics of Recursive Splicing and Enhancer RNAs. *Nat Commun* (2018) 9(1):619. doi: 10.1038/s41467-018-02866-0
112. Sheng K, Cao W, Niu Y, Deng Q, Zong C. Effective Detection of Variation in Single-Cell Transcriptomes Using MATQ-Seq. *Nat Methods* (2017) 14 (3):267–70. doi: 10.1038/nmeth.4145
113. Macosko EZ, Basu A, Satija R, Nemesh J, Shekhar K, Goldman M, et al. Highly Parallel Genome-Wide Expression Profiling of Individual Cells Using Nanoliter Droplets. *Cell* (2015) 161(5):1202–14. doi: 10.1016/j.cell.2015.05.002
114. Klein AM, Mazutis L, Akartuna I, Tallapragada N, Veres A, Li V, et al. Droplet Barcoding for Single Cell Transcriptomics Applied to Embryonic Stem Cells. *Cell* (2015) 161(5):1187–201. doi: 10.1016/j.cell.2015.04.044
115. Satija R, Farrell JA, Gennert D, Schier AF, Regev A. Spatial Reconstruction of Single-Cell Gene Expression Data. *Nat Biotechnol* (2015) 33(5):495–502. doi: 10.1038/nbt.3192
116. Wolf FA, Angerer P, Theis FJ. SCANPY: Large-Scale Single-Cell Gene Expression Data Analysis. *Genome Biol* (2018) 19(1):15. doi: 10.1186/s13059-017-1382-0
117. Gojo J, Englinger B, Jiang L, Hübner JM, Shaw ML, Hack OA, et al. Single-Cell RNA-Seq Reveals Cellular Hierarchies and Impaired Developmental Trajectories in Pediatric Ependymoma. *Cancer Cell* (2020) 38(1):44–59.e9. doi: 10.1016/j.ccell.2020.06.004
118. Hovestadt V, Smith KS, Bihannic L, Filbin MG, Shaw ML, Baumgartner A, et al. Resolving Medulloblastoma Cellular Architecture by Single-Cell Genomics. *Nature* (2019) 572(7767):74–9. doi: 10.1038/s41586-019-1434-6
119. Jessa S, Blanchet-Cohen A, Krug B, Vladoiu M, Coutelier M, Faury D, et al. Stalled Developmental Programs at the Root of Pediatric Brain Tumors. *Nat Genet* (2019) 51(12):1702–13. doi: 10.1038/s41588-019-0531-7
120. Vladoiu MC, El-Hamamy I, Donovan LK, Farooq H, Holgado BL, Sundaravadanam Y, et al. Childhood Cerebellar Tumours Mirror Conserved Fetal Transcriptional Programs. *Nature* (2019) 572(7767):67–73. doi: 10.1038/s41586-019-1158-7
121. Alghamri MS, McClellan BL, Avvari RP, Thalla R, Carney S, Hartlage MS, et al. G-CSF Secreted by Mutant IDH1 Glioma Stem Cells Abolishes Myeloid Cell Immunosuppression and Enhances the Efficacy of Immunotherapy. *Sci Adv* (2021) 7(40):eabh3243. doi: 10.1126/sciadv.abh3243
122. Sankowski R, Böttcher C, Masuda T, Geirsdottir L, Sagar, Sindram E, et al. Mapping Microglia States in the Human Brain Through the Integration of High-Dimensional Techniques. *Nat Neurosci* (2019) 22(12):2098–110. doi: 10.1038/s41593-019-0532-y
123. Pombo Antunes AR, Scheyltjens I, Lodi F, Messiaen J, Antoranz A, Duerinck J, et al. Single-Cell Profiling of Myeloid Cells in Glioblastoma Across Species and Disease Stage Reveals Macrophage Competition and Specialization. *Nat Neurosci* (2021) 24(4):595–610. doi: 10.1038/s41593-020-00789-y
124. Ochocka N, Segit P, Walentynowicz KA, Wojnicki K, Cyranowski S, Swatler J, et al. Single-Cell RNA Sequencing Reveals Functional Heterogeneity of Glioma-Associated Brain Macrophages. *Nat Commun* (2021) 12(1):1151. doi: 10.1038/s41467-021-21407-w
125. Chen AX, Gartrell RD, Zhao J, Upadhyayula PS, Zhao W, Yuan J, et al. Single-Cell Characterization of Macrophages in Glioblastoma Reveals MARCO as a Mesenchymal Pro-Tumor Marker. *Genome Med* (2021) 13 (1):88. doi: 10.1186/s13073-021-00906-x
126. Reitman ZJ, Paolella BR, Bergthold G, Pelton K, Becker S, Jones R, et al. Mitogenic and Progenitor Gene Programmes in Single Pilocytic Astrocytoma Cells. *Nat Commun* (2019) 10:3731. doi: 10.1038/s41467-019-11493-2
127. Pai JA, Satpathy AT. High-Throughput and Single-Cell T Cell Receptor Sequencing Technologies. *Nat Methods* (2021) 18(8):881–92. doi: 10.1038/s41592-021-01201-8
128. Redmond D, Poran A, Elemento O. Single-Cell TCRseq: Paired Recovery of Entire T-Cell Alpha and Beta Chain Transcripts in T-Cell Receptors From Single-Cell RNAseq. *Genome Med* (2016) 8(1):80. doi: 10.1186/s13073-016-0335-7
129. Stubbington MJT, Lönnberg T, Proserpio V, Clare S, Speak AO, Dougan G, et al. T Cell Fate and Clonality Inference From Single-Cell Transcriptomes. *Nat Methods* (2016) 13(4):329–32. doi: 10.1038/nmeth.3800
130. Rizzetto S, Koppstein DNP, Samir J, Singh M, Reed JH, Cai CH, et al. B-Cell Receptor Reconstruction From Single-Cell RNA-Seq With VDJPuzzle. *Bioinformatics* (2018) 34(16):2846–7. doi: 10.1093/bioinformatics/bty203
131. Mathewson ND, Ashenberg O, Tirosh I, Gritsch S, Perez EM, Marx S, et al. Inhibitory CD161 Receptor Identified in Glioma-Infiltrating T Cells by Single-Cell Analysis. *Cell Anal* (2021) 184(5):1281–98. doi: 10.1016/j.cell.2021.01.022
132. Ruiz-Moreno C, Keramati F, Brazda P, Megchelenbrink W, te PB, Boshuisen K, et al. Reprogramming of Pro-Tumor Macrophages by Hydroxychloroquine in an Abdominally Metastasized Diffuse Midline Glioma. *Oncology* (2021) 2021:2021.07.19.21259735. doi: 10.1101/2021.07.19.21259735
133. Prakadan SM, Alvarez-Breckenridge CA, Markson SC, Kim AE, Klein RH, Nayyar N, et al. Genomic and Transcriptomic Correlates of Immunotherapy Response Within the Tumor Microenvironment of Leptomeningeal Metastases. *Nat Commun* (2021) 12(1):5955. doi: 10.1038/s41467-021-25860-5
134. Newman AM, Steen CB, Liu CL, Gentles AJ, Chaudhuri AA, Scherer F, et al. Determining Cell Type Abundance and Expression From Bulk Tissues With Digital Cytometry. *Nat Biotechnol* (2019) 37(7):773–82. doi: 10.1038/s41587-019-0114-2
135. Wang X, Park J, Susztak K, Zhang NR, Li M. Bulk Tissue Cell Type Deconvolution With Multi-Subject Single-Cell Expression Reference. *Nat Commun* (2019) 10(1):380. doi: 10.1038/s41467-018-08023-x
136. Tsoucas D, Dong R, Chen H, Zhu Q, Guo G, Yuan G-C. Accurate Estimation of Cell-Type Composition From Gene Expression Data. *Nat Commun* (2019) 10(1):2975. doi: 10.1038/s41467-019-10802-z
137. Qi Z, Liu Y, Mints M, Mullins R, Sample R, Law T, et al. Single-Cell Deconvolution of Head and Neck Squamous Cell Carcinoma. *Cancers (Basel)* (2021) 13(6):1230. doi: 10.3390/cancers13061230
138. Armingol E, Officer A, Harismendy O, Lewis NE. Deciphering Cell–Cell Interactions and Communication From Gene Expression. *Nat Rev Genet* (2021) 22(2):71–88. doi: 10.1038/s41576-020-00292-x
139. Stoeckius M, Hafemeister C, Stephenson W, Houck-Loomis B, Chattopadhyay PK, Swerdlow H, et al. Simultaneous Epitope and Transcriptome Measurement in Single Cells. *Nat Methods* (2017) 14 (9):865–8. doi: 10.1038/nmeth.4380
140. Ståhl PL, Salmén F, Vickovic S, Lundmark A, Navarro JF, Magnusson J, et al. Visualization and Analysis of Gene Expression in Tissue Sections by Spatial Transcriptomics. *Science* (2016) 353(6294):78–82. doi: 10.1126/science.aaf2403
141. Rodriques SG, Stickels RR, Goeva A, Martin CA, Murray E, Vanderburg CR, et al. Slide-Seq: A Scalable Technology for Measuring Genome-Wide Expression at High Spatial Resolution. *Sci (80-).* (2019) 363(6434):1463–7. doi: 10.1126/science.aaw1219
142. Stickels RR, Murray E, Kumar P, Li J, Marshall JL, Di Bella DJ, et al. Highly Sensitive Spatial Transcriptomics at Near-Cellular Resolution With Slide-Seqv2. *Nat Biotechnol* (2021) 39(3):313–9. doi: 10.1038/s41587-020-0739-1
143. Ravi VM, Neidert N, Will P, Joseph K, Maier JP, Kückelhaus J, et al. T-Cell Dysfunction in the Glioblastoma Microenvironment is Mediated by Myeloid Cells Releasing Interleukin-10. *Nat Commun* (2022) 13(1):925. doi: 10.1038/s41467-022-28523-1

144. Hunter MV, Moncada R, Weiss JM, Yanai I, White RM. Spatially Resolved Transcriptomics Reveals the Architecture of the Tumor-Microenvironment Interface. *Nat Commun* (2021) 12(1):6278. doi: 10.1038/s41467-021-26614-z
145. Poch M, Hall M, Joerger A, Kodumudi K, Beatty M, Innamarato PP, et al. Expansion of Tumor Infiltrating Lymphocytes (TIL) From Bladder Cancer. *Oncoimmunology* (2018) 7(9):1–7. doi: 10.1080/2162402X.2018.1476816
146. Besser MJ, Shapira-Frommer R, Treves AJ, Zippel D, Itzhaki O, Hershkovitz L, et al. Clinical Responses in a Phase II Study Using Adoptive Transfer of Short-Term Cultured Tumor Infiltration Lymphocytes in Metastatic Melanoma Patients. *Clin Cancer Res* (2010) 16(9):2646–55. doi: 10.1158/1078-0432.CCR-10-0041
147. Stevanović S, Draper LM, Langhan MM, Campbell TE, Kwong ML, Wunderlich JR, et al. Complete Regression of Metastatic Cervical Cancer After Treatment With Human Papillomavirus-Targeted Tumor-Infiltrating T Cells. *J Clin Oncol* (2015) 33(14):1543–50. doi: 10.1200/JCO.2014.58.9093
148. Fujita K, Ikarashi H, Akiteru K. Prolonged Disease-Free Period in Patients With Advanced Epithelial Ovarian Cancer After Adoptive Transfer of Tumor-Infiltrating Lymphocytes. *Clin Cancer Res* (1995) 1(May):501–7.
149. Brinke AT, Marek-Trzonkowska N, Mansilla MJ, Turksma AW, Piekarska K, Iwaszkiewicz-Grzes D, et al. Monitoring T-Cell Responses in Translational Studies: Optimization of Dye-Based Proliferation Assay for Evaluation of Antigen-Specific Responses. *Front Immunol* (2017) 8(DEC):1–15. doi: 10.3389/fimmu.2017.01870
150. Riddell SR, Greenberg PD. The Use of Anti-CD3 and Anti-CD28 Monoclonal Antibodies to Clone and Expand Human Antigen-Specific T Cells. *J Immunol Methods* (1990) 128(2):189–201. doi: 10.1016/0022-1759(90)90210-M
151. Hulen TM, Chamberlain CA, Svane IM, Met Ö. ACT Up TIL Now: The Evolution of Tumor-Infiltrating Lymphocytes in Adoptive Cell Therapy for the Treatment of Solid Tumors. *Immuno* (2021) 1(3):194–211. doi: 10.3390/immuno1030012
152. Alessandro Moretta B, Pantaleo G, Moreti L, Cerottini J, Maria Cristina Mingari A. Clonal Analysis of HLA-DR Expression and Cytolytic Activity*. *J Exp Med* (1983) 157(February):743–54. doi: 10.1084/jem.157.2.743
153. Van Den Berg JH, Heemskerk B, Van Rooij N, Gomez-Eerland R, Michels S, Van Zon M, et al. Tumor Infiltrating Lymphocytes (TIL) Therapy in Metastatic Melanoma: Boosting of Neoantigen-Specific T Cell Reactivity and Long-Term Follow-Up. *J Immunother Cancer* (2020) 8(2):1–11. doi: 10.1136/jitc-2020-000848
154. Hong JJ, Rosenberg SA, Dudley ME, Yang JC, Whit DE, Butman JA, et al. Successful Treatment of Melanoma Brain Metastases With Adoptive Cell Therapy. *Clin Cancer Res* (2010) 16(19):4892–8. doi: 10.1158/1078-0432.CCR-10-1507
155. Liu Z, Meng Q, Bartek J, Poiret T, Persson O, Rane L, et al. Tumor-Infiltrating Lymphocytes (TILs) From Patients With Glioma. *Oncoimmunology* (2017) 6(2):e1252894. doi: 10.1080/2162402X.2016.1252894
156. Li Y, Polyak D, Lamsam L, Connolly ID, Johnson E, Khoeur LK, et al. Comprehensive RNA Analysis of CSF Reveals a Role for CEACAM6 in Lung Cancer Leptomeningeal Metastases. *NPJ Precis Oncol* (2021) 90:1–8. doi: 10.1038/s41698-021-00228-6
157. Chen P, Roh W, Reuben A, Cooper ZA, Spencer CN, Prieto PA, et al. Analysis of Immune Signatures in Longitudinal Tumor Samples Yields Insight Into Biomarkers of Response and Mechanisms of Resistance to Immune Checkpoint Blockade. *Cancer Discovery* (2016) 6:827–3. doi: 10.1158/2159-8290.CD-15-1545
158. Kretzschmar H. Brain Banking: Opportunities, Challenges and Meaning for the Future. *Nat Rev Neurosci* (2009) 10(1):70–8. doi: 10.1038/nrn2535
159. Abbott A. Tissue-Bank Shortage: Brain Child. *Nature* (2011) 478(7370):442–3. doi: 10.1038/478442a
160. Day BW, Brett SW, Wilson J, Jeffree RL, Jamieson PR, Ensbey KS, et al. Glioma Surgical Aspirate: A Viable Source of Tumor Tissue for Experimental Research. *Cancers (Basel)* (2013) 5(2):357–71. doi: 10.3390/cancers5020357
161. Vaskova M, Tichy M, Zamecnik J, Liby P, Kuzilkova D, Vicha A, et al. Cytometric Analysis of Cell Suspension Generated by Cavitron Ultrasonic Surgical Aspirator in Pediatric Brain Tumors. *J Neurooncol* (2019) 143(1):15–25. doi: 10.1007/s11060-019-03135-w
162. Rao S, Vazhayil V, Nandeesh B, Beniwal M, Rao K, Yasha T, et al. Diagnostic Utility of CUSA Specimen in Histopathological Evaluation of Tumors of Central Nervous System. *Neurol India* (2020) 68(6):1385–8. doi: 10.4103/0028-3886.304072
163. Jacobs JFM, Idema AJ, Bol KF, Nierkens S, Grauer OM, Wesseling P, et al. Regulatory T Cells and the PD-L1/PD-1 Pathway Mediate Immune Suppression in Malignant Human Brain Tumors. *Neuro Oncol* (2009) 11(4):394–402. doi: 10.1215/15228517-2008-104
164. Spitzer A, Gritsch S, Weisman HR, Gonzalez Castro LN, Nomura M, Druck N, et al. Mutant IDH Inhibitors Induce Lineage Differentiation in IDH-Mutant Oligodendroglioma. *Oncology* (2021) 2021:2021.11.16.21266364. doi: 10.1101/2021.11.16.21266364
165. Liu APY, Smith KS, Kumar R, Paul L, Bihannic L, Lin T, et al. Serial Assessment of Measurable Residual Disease in Medulloblastoma Liquid Biopsies. *Cancer Cell* (2021) 39(11):1519–1530.e4. doi: 10.1016/j.ccell.2021.09.012
166. Harry GJ. Microglia During Development and Aging. *Pharmacol Ther* (2013) 139(3):313–26. doi: 10.1016/j.pharmthera.2013.04.013
167. Gutmann DH, Kettenmann H. Microglia/brain Macrophages as Central Drivers of Brain Tumor Pathobiology. *Neuron* (2019) 104(3):442–9. doi: 10.1016/j.neuron.2019.08.028
168. Sayour EJ, McLendon P, McLendon R, De Leon G, Reynolds R, Kresak J, et al. Increased Proportion of FoxP3+ Regulatory T Cells in Tumor Infiltrating Lymphocytes is Associated With Tumor Recurrence and Reduced Survival in Patients With Glioblastoma. *Cancer Immunol Immunother* (2015) 64(4):419–27. doi: 10.1007/s00262-014-1651-7
169. Patterson JD, Henson JC, Breese RO, Bielamowicz KJ, Rodriguez A. CAR T Cell Therapy for Pediatric Brain Tumors. *Front Oncol* (2020) 10:1582. doi: 10.3389/fonc.2020.01582

Conflict of Interest: The authors declare that the research was conducted in the absence of any commercial or financial relationships that could be construed as a potential conflict of interest.

frontiers | Frontiers in Immunology

REVIEW
published: 13 April 2022
doi: 10.3389/fimmu.2022.866892

Immunovirotherapy for Pediatric Solid Tumors: A Promising Treatment That is Becoming a Reality

Daniel de la Nava[1,2,3], *Kadir Mert Selvi*[1,2,3] *and Marta M. Alonso*[1,2,3]*

[1] Health Research Institute of Navarra (IdiSNA), Pamplona, Spain, [2] Programs in Solid Tumors and Neuroscience, Foundation for the Applied Medical Research, Pamplona, Spain, [3] Department of Pediatrics, Clínica Universidad de Navarra, Pamplona, Spain

Immunotherapy has seen tremendous strides in the last decade, acquiring a prominent position at the forefront of cancer treatment since it has been proven to be efficacious for a wide variety of tumors. Nevertheless, while immunotherapy has changed the paradigm of adult tumor treatment, this progress has not yet been translated to the pediatric solid tumor population. For this reason, alternative curative therapies are urgently needed for the most aggressive pediatric tumors. In recent years, oncolytic virotherapy has consolidated as a feasible strategy for cancer treatment, not only for its tumor-specific effects and safety profile but also for its capacity to trigger an antitumor immune response. This review will summarize the current status of immunovirotherapy to treat cancer, focusing on pediatric solid malignancies. We will revisit previous basic, translational, and clinical research and discuss advances in overcoming the existing barriers and limitations to translate this promising therapeutic as an every-day cancer treatment for the pediatric and young adult populations.

Keywords: oncolytic viruses, pediatric solid tumors, pediatric brain tumors, sarcomas, neuroblastoma, clinical trials

OPEN ACCESS

Edited by:
Orazio Vittorio, University of New South Wales, Australia

Reviewed by:
Paul G. Schlegel, University Children's Hospital Würzburg, Germany
Vincenzo Cerullo, University of Helsinki, Finland

***Correspondence:**
Marta M. Alonso
mmalonso@unav.es

Specialty section:
This article was submitted to Cancer Immunity and Immunotherapy, a section of the journal Frontiers in Immunology

Received: *31 January 2022*
Accepted: *23 March 2022*
Published: *13 April 2022*

Citation:
de la Nava D, Selvi KM and Alonso MM (2022) Immunovirotherapy for Pediatric Solid Tumors: A Promising Treatment That is Becoming a Reality. Front. Immunol. 13:866892. doi: 10.3389/fimmu.2022.866892

INTRODUCTION OF PEDIATRIC CANCER

Pediatric cancer includes all malignancies that occur in children and adolescents between birth and 19 years of age, and it is estimated that every year approximately 400,000 cases are diagnosed worldwide (1, 2). Recent advances in cancer research have resulted in a marked increase in the cure rates of both adult and pediatric cancers. However, cancer remains a significant cause of death for children and adolescents (3). Among the factors that explain the improvement in survival rates are the optimization of supportive care, advances in biological and clinical tumor characterization and the development of new risk-adapted therapies are the most remarkable (4, 5).

Unfortunately, this improvement has not always been accompanied by improved quality of life because of side effects and long-term health complications in survivors of childhood cancers as they reach older age (6). These data underscore the necessity to develop safe and efficacious treatments that overcome the current limitations in the field of pediatric cancer.

In recent years, cancer therapy has experienced a remarkable transformation due to the advent of new classes of immunotherapies, including immune checkpoint inhibitors, bispecific T cell engagers (BiTEs) and CAR-T cells. In fact, CAR-T cells have provided a new paradigm for treatment, especially for liquid tumors (7, 8). Another approach that has gained popularity is the use of oncolytic viruses (OVs). These viruses combine their cytotoxic capacity with the ability to trigger an immune response, rendering them interesting therapeutic tools. The notion of viruses as anticancer agents came from anecdotic observations where tumors regressed spontaneously after the patients naturally acquired viral infections (9–11). These reports were mainly from the early 1900s, and it was not until the late 1980s that OVs were evaluated in depth, in part due to the development of research tools such as cell lines and animal models that have facilitated the evaluation of these agents (12). Since then, multiple investigations have been carried out, and the first OV has been approved for clinical use in the USA. The use of Talimogene Laherparepvec in clinical practice for recurrent melanoma represents a before-and-after picture for OVs, indicating the possibility of developing new, functional and perfectly designed tools for tumor treatment (13).

In this review, we discuss the role of OVs as a therapy for pediatric solid malignancies. We review the different types of viruses and their mechanism of action. We recapitulate the basic, translational and clinical research using virotherapy, alone or in combination with other therapies, to treat pediatric solid tumors, and we conclude with our thoughts regarding the potential future and hurdles for the development of this field to achieve its full therapeutic potential.

ONCOLYTIC VIRUSES

Oncolytic viral therapy is a promising therapeutic method that employs naturally occurring or genetically modified OVs that selectively proliferate in and kill tumor cells while causing no harm to healthy cells (14). OVs can be classified as DNA or RNA viruses on the basis of their genome. Furthermore, they differ in their viral envelope based on host cell membranes and viral glycoproteins. According to these criteria, these viruses can be classified as enveloped DNA OVs (herpesvirus, poxvirus), unenveloped DNA OVs (adenovirus, parvovirus), enveloped RNA OVs (paramyxovirus, rhabdovirus, togavirus, orthomyxovirus), or unenveloped RNA OVs (reovirus, picornavirus) (**Figure 1**).

OVs elicit antitumor responses mainly through two mechanisms: selective killing of tumor cells and stimulation of systemic antitumor immunity (15). Cancer cells provide an ideal setting for the selective replication of various OVs that take advantage of physiological changes in these cells. Several signaling pathways engaged in viral elimination, including interferon, Toll-like receptor (TLR) or Janus kinase-signal transducer and activator of transcription (JAK-STAT) pathways, may be defective or inhibited, enabling OVs to spread in tumor cells. Regarding

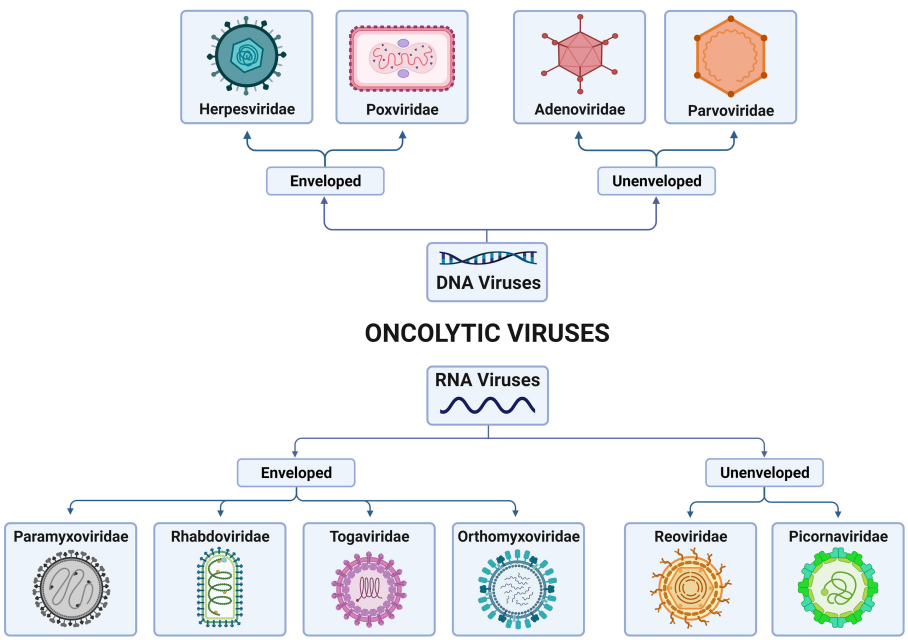

FIGURE 1 | Classification of families of oncolytic viruses (OVs) according to the genome and presence/absence of the viral envelope. OVs can be differentiated into DNA viruses and RNA viruses, depending on their genomic nature. In addition, both types can present, or not present, virus envelopes. Thus, DNA-enveloped viruses include those of the Herpesviridae and Poxviridae families; non-DNA-enveloped viruses include those of the Adenoviridae and Paroviridae families; RNA-enveloped viruses include those of the Paramyxoviridae, Rhabdoviridae, Togaviridae and Orthoyxoviridae families; and non-RNA-enveloped viruses include those of the Reoviridae and Picornaviridae families. Created with BioRender.com.

infectivity, cancer cells may also overexpress different surface receptors, such as CD46, ICAM-1, CD55, CD155 or integrins, allowing OVs to infect cancer cells (16). In addition to directly killing infected tumor cells *via* several oncolytic mechanisms, OVs have the ability to turn tumors from immunologically 'cold' to 'hot' by inducing proinflammatory conditions within the tumor microenvironment (TME) (15). Oncolytic cell death and subsequent release of tumor-associated antigens can induce innate and adaptive immune responses, resulting in therapeutic responses in both locally injected tumors and tumor metastases (15, 17, 18) (**Figure 2**).

With their multimodal antitumor activity, oncolytic virotherapies are now a key subject of study in cancer treatment research, and many clinical trials are currently being conducted for the utilization of OVs as therapeutic agents for different types of advanced malignancies (19, 20). OVs for different types of malignancies are chosen based on a variety of factors. Some of them may have intrinsic tropism and a preference for selective replication in cancer cells, whereas others can be genetically modified to elicit selective targeting of cancer cells (21, 22). Generally, OVs infect tumor cells *via* specific receptors on the cell surface. Once inside, the virus particles migrate through the cytoskeleton and start replication, being internalized or not into the nucleus. The viral seizure of the cellular machinery allows the generation of new virions, which then facilitate lysis of the infected cell and spread to infect new cells (23). New advances in oncolytic virotherapies are being achieved with genetic deletions and genetic engineering to improve tumor-selective replication and oncolytic capability while lowering viral pathogenicity for patient safety (21, 22, 24). Additionally, OVs can be designed to express novel therapeutic genes to enhance the antitumor action, generation of immunological responses, and suppression of tumor angiogenesis, along with other mechanisms (21, 25). Reoviruses, parvovirus H-1 and Newcastle disease virus (NDV) are examples of OVs that are naturally inclined to replicate in cancer cells (20). On the other hand, other OVs have been genetically modified for oncoselectivity, including adenoviruses, vaccinia virus (VV), vesicular stomatitis virus (VSV) and herpes simplex virus (HSV) (26, 27).

PRECLINICAL STUDIES USING VIROTHERAPY IN PEDIATRIC SOLID TUMORS

Adenovirus

Adenoviruses are among the most commonly used OVs in research (28). Among the different pediatric solid tumors, those of the central nervous system (CNS) are the most common malignancies among children aged 0 to 14 years, even more so than leukemias, and are among the most prevalent and deadly within the adolescent group (5–24) and young adults (25-39 years) (29). There are more than 100 types of brain tumors (30–32), each with its own characteristics. However, for the purpose of this review, we will focus on those with poor prognosis.

One adenovirus that has been extensively characterized in pediatric and adult brain tumors is Delta-24-RGD. This adenovirus, serotype 5, was specifically designed to destroy tumor cells (33, 34). It contains two genetic modifications: a 24-base pair deletion in E1A, which restricts virus replication in tumor cells, and the addition of the RGD-4C binding motif, which improves the infectivity, allowing the virus to target tumor cells *via* avβ3 and avβ5 integrins, which are overexpressed in a wide range of tumors. Delta-24-RGD showed a robust antiglioma effect in preclinical and clinical studies in adult patients with recurrent gliomas (34–36). Moreover, the virus displayed the capacity to trigger immune-mediated responses with an increased number of immune populations inside the tumors (37, 38). Our group has

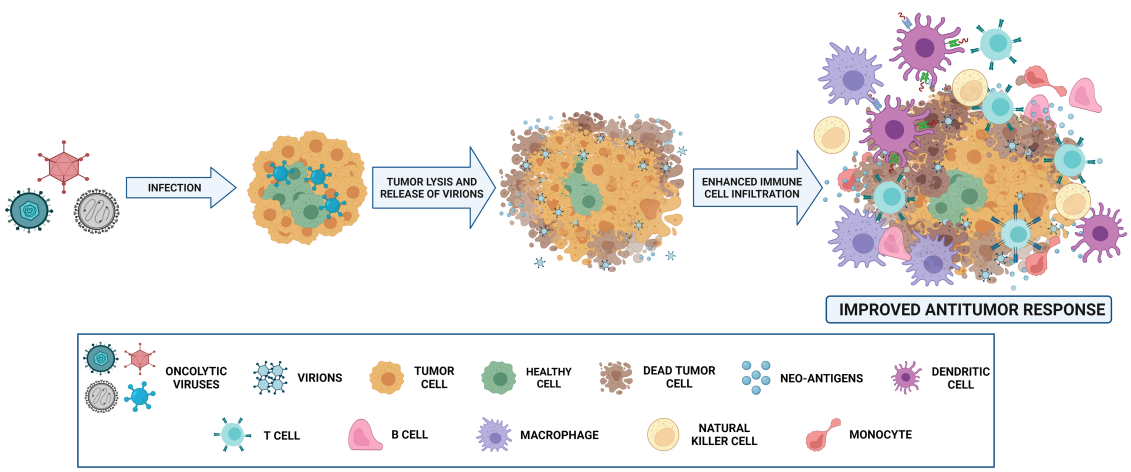

FIGURE 2 | Mechanism of action of oncolytic viruses (OVs). OVs, administered intravenously or intratumorally, infect normal and tumor cells. Nevertheless, they replicate only in malignant cells, and virion release then occurs. The infection and destruction of tumor cells lead to the release of antigens that cause proinflammatory recruitment of different immune cells, such as T and B cells, macrophages, NK cells, monocytes and dendritic cells. Thus, antitumoral effect is mediated not only by oncolytic capability, but also by immune microenvironment reshaping. Created with BioRender.com.

evaluated this virus in the context of high-risk pediatric brain tumors. We observed that treatment with Delta-24-RGD resulted in increased survival in human xenograft and syngeneic mouse models of pediatric high-grade gliomas (pHGGs) and diffuse midline gliomas (DMGs) (39). In immunocompetent mice, virus treatment led to robust recruitment of lymphocyte populations (including CD4+ and CD8+). Delta-24-RGD combined with radiotherapy exerted an improved antitumor effect in this type of tumors (40). Furthermore, we evaluated this virus in models of atypical teratoid/rhabdoid tumors (AT/RTs) and CNS-primitive neuroectodermal tumors (CNS-PNETs), rare pediatric embryonal tumors with a survival time of 6-12 months (41, 42). The adenovirus replicated efficiently in AT/RT and CNS-PNET cell lines, leading to a robust cytotoxic effect. *In vivo*, Delta-24-RGD expanded the overall survival in several animal models, leading, in some cases, to a long-term survival rate of 70%. The interrogation of the immune response triggered by Delta-24-RGD in humanized immunocompetent mouse models revealed an increase in CD8+ T cell infiltration and a general remodeling of the TME toward a proinflammatory phenotype (43). In this line of thinking, another adenovirus, VCN-01, armed with hyaluronidase, which allows the degradation of the extracellular matrix (44), also significantly extended the overall survival of mice bearing orthotopic PNET (45). Mesenchymal stem cells (MSCs), as OV carriers, have also been studied in treating DMGs. Chastkofsky and colleagues encapsulated the adenovirus CRAd.S.pK7 into MSCs to facilitate its delivery to the brainstem and to avoid potential fast clearance by the immune system (46). Although the virus replicated *in vitro*, the experiments performed in animal models did not show clinical benefit, and it was necessary to add radiotherapy to extend the overall survival.

Another strategy used to enhance the efficacy of oncolytic adenoviruses has been combination with gene therapy. In this sense, Arnone et al. explored the idea of treating a pediatric high-grade glioma with the OV Delta-24 in combination with a replication incompetent adenovirus encoding a BiTE which targets human hepatocellular carcinoma A2 receptor (EphA2), a protein that is correlated with tumor aggressiveness and poor patient outcome. The authors showed that the combination treatment was more efficient than either treatment alone in improving tumor burden and overall survival (47).

Neuroblastoma is a rare neuroendocrine childhood cancer that arises in any neural crest element from the developing sympathetic nervous system (48). It is the most common extracranial solid tumor in childhood and the most common malignancy diagnosed during the first year of life (49). Although outcomes in these patients have improved in recent decades, this improvement is attributable mainly to better cure rates among patients with low-risk neuroblastoma (49), whereas children bearing the more aggressive form of the disease have shown a modest advance (50). In this context, the adenoviruses OBP-301 and OBP-702, the tumor specificity of which is driven by the hTERT promoter, have been evaluated. The authors showed that treatment with either of these viruses produced an antitumor response in cell lines with high hTERT expression and reduced growth in a subcutaneous neuroblastoma model (51). Other approaches have employed cellular carriers to deliver the virus such as Celyvir; autologous MSCs loaded with Icovir-5 (an adenovirus dependent on an aberrant RB pathway). Mice bearing neuroblastomas and treated intravenously with Celyvir displayed a reduced tumor volume, recruitment of immune cells and a weaker protumoral and stronger inflammatory profile in the TME (52). This strategy is currently being evaluated in the clinic and is discussed below.

Pediatric sarcomas, which account for 10% of solid tumors in children, are a group of mesenchymal tumors originating from bone or soft tissue precursors (53). Although current treatment regimens based on chemotherapy, surgery and radiation have improved the 5-year OSR to 60-70%, patients with metastatic disease or recurrence have a poor prognosis, with a 5-year OSR of 30% or less (54, 55). The lack of efficacy of emergent therapies such as immunotherapy (56) has prompted the emergence of OVs as an alternative solution.

Our group has evaluated the antisarcoma effect of the RB pathway-based viruses Delta-24-RGD (57) and VCN-01 (58). Both adenoviruses were able to control tumor volume, and specifically for Delta-24-RGD, the use of cisplatin as a combinatorial treatment improved the antitumor virus response, showing that combination therapies are, in fact, a possible solution. In the quest to further improve the efficacy, our group engineered D24-ACT, which is based on the D24-RGD platform and armed with the immune costimulatory molecule 4-1BB ligand (4-1BBL), to improve the antitumor immune response. Local treatment with Delta-24-ACT in mice bearing orthotopic osteosarcoma murine tumors led to a reduction in both the primary tumor and metastases, and a significant increase in CD3+ and CD8+ T cells, among other immune populations, was found when comparing D24-ACT vs. D24-RGD (59). Our results suggest that potentiating the immune response could boost the efficacy in this type of tumor. In another study, a murine version of Celyvir (OAd-MSCs) was tested in combination with granulocyte-colony stimulating factor (G-CSF). The combination significantly reduced tumor growth *in vivo*, with tumors presenting higher infiltration of some immune cell populations (including CD4+ and CD8+ T cells) and reduced T cell exhaustion (60). OBP-502 has also been evaluated in osteosarcoma preclinical models. This adenovirus reduced the viability of cancer cells and induced immunogenic cell death *in vitro*, whereas intratumoral injection in combination with an anti-PD-1 antibody in subcutaneous models reduced tumor growth and enhanced tumor-infiltrating CD8+ T cells (61).

Herpes Simplex Virus

HSV is among the largest DNA viruses developed for gene transfer. It is nonintegrative, very potent as a lytic virus, highly replicative and with high cell tropism (62). HSV type I G207, which contains deletions in both copies of the neurovirulence gene $\gamma_1$34.5 and a disabling lacZ insertion within the ICP6 gene (63), has been proven to be safe when injected into the cerebellum (64) and developing mouse brains (65). In preclinical studies, HSV-1 G207 and M002 (encoding human

interleukin-12) demonstrated efficacy in pediatric high-grade glioma (66) and medulloblastoma (67). Another oncolytic herpes virus, HSV1716 (Seprehvir), showed efficacy in preclinical studies of high-grade gliomas and DMGs *via* changes in cytoskeletal dynamics and in molecular pathways related to cell polarity, migration, and movement (68). HSV-1 rRp450, which expresses the rat CYP2B1 enzyme and is able to activate the chemotherapeutic prodrug cyclophosphamide, prolonged overall survival in medulloblastoma and AT/RT, and its efficacy was further enhanced when cyclophosphamide was included in the treatment schedule (69).

In neuroblastoma models, HSV-1 M002 produced cell death in different neuroblastoma cell lines *in vitro* and reduced, alone and in combination with radiation, the tumor growth of this tumor *in vivo* (70). Similarly, a nestin-targeted oncolytic HSV also killed neuroblastoma tumor-initiating cells and prevented tumor formation in xenograft-bearing mice (71). FusOn-H2 (type 2 HSV), which specifically targets tumor cells with an aberrant Ras signaling pathway, exhibited efficacy in a syngeneic mouse model not only at the virus injection site but also at distant metastases (18).

In Ewing sarcoma, the second most common bone tumor in children and adolescents and a difficult to treat cancer (72), HSV-1 rRp450 was combined with macrophage reduction drugs. The combined treatment improved the efficacy of each agent alone and led to a reduction in M2-like macrophages in the tumor and spleen (73). HSV has also been tested in Rhabdomyosarcoma, the most common soft tissue sarcoma (74). Similar to other sarcomas, the chance of cure for metastatic and recurrent tumors is incredibly low (< 20%). In this context, HSV-1 M002 exhibited replication and oncolytic activity *via* apoptosis, reduced tumor growth and acted synergistically with radiation in subcutaneous mouse models (75). This virus has been additionally evaluated in serendipitous murine models of undifferentiated sarcoma, leading to an increase in effector CD4+ and CD8+ T cells, activated monocytes and a decrease in myeloid-derived suppressor cells (76).

Other Oncolytic Viruses

Parvovirus H-1 (H-1PV) is an apathogenic in humans and non-recombinant OV that occurs naturally in rats (77), and long-term survival was observed for adult high-grade gliomas mouse models after intratumoral, intravenous or intranasal virus application (78, 79). H-1PV showed efficacy in *in vitro* models of pediatric high-grade glioma (80), medulloblastoma (81) and Ewing sarcoma but failed to improve survival *in vivo* in this tumor (82).

Medulloblastoma and pleomorphic xanthoastrocytoma (a rare condition comprising <1% of all primary brain tumors) have been evaluated with PVSRIPO. PVSRIPO is an attenuated polio: rhinovirus chimera without neurovirulence and had been evaluated previously in adult recurrent glioblastoma patients with promising results (83). The authors observed that PVSRIPO could be used against these two malignancies *in vitro* (84). Other types of OVs have been used in preclinical models, such as a measles virus in AT/RT models (85) or the picornavirus Seneca Valley virus (SVV-001) in pediatric glioma (86), with an improvement observed in mice bearing tumor cells. Another study described the use of the oncolytic vesicular stomatitis virus $VSV^{\Delta M51}$ and oncolytic myxoma virus (87) as treatments *in vitro* and *in vivo* with good responses, although the models used were subcutaneous.

A specific Semliki Forest virus (SFV4miRT), an *Alphavirus* belonging to the *Togaviridae* family and modified to reduce neurovirulence through insertion of three microRNAs, prolonged survival in neuroblastoma and glioblastoma mouse models with low interferon-α/β secretion (88). Another OV belonging to this family, Sindbis virus (SINV), exhibited efficacy *in vitro via* apoptosis, reduced tumor growth and extended overall survival in subcutaneous neuroblastoma models (89). An attenuated, nonneurovirulent poliovirus was evaluated and exhibited replication in neuroblastoma cells and significant reduction in tumor growth in subcutaneous tumor-bearing mice (90). Additionally, in another study, MV-CEA (an engineered measles virus) produced neuroblastoma cell death *via* apoptosis *in vitro* and extended the overall survival in xenograft models after five doses were injected intratumorally (91). Interestingly, treatment with an OV that expresses a CXCR4 antagonist injected intravenously augmented the efficacy of DC vaccines (92). Another oncolytic Seneca Valley virus (NTX-010) proved effective in a subcutaneous neuroblastoma and Ewing sarcoma models (93). Zika virus has been evaluated as an OV. Mazar and colleagues showed that neuroblastoma cells are widely permissive to Zika infection and require CD24, although the efficacy in cell death has not been proven (94).

Measles OV decreased tumor growth of subcutaneous xenografts and prolonged survival with orthotopic and pulmonary metastatic osteosarcoma tumors (95). Also in osteosarcoma, other viruses such as the previously mentioned parvovirus H-1PV (96), oncolytic vesicular stomatitis virus $VSV^{\Delta M51}$ in combination with phosphoinositide 3-kinase inhibitor (97) and myxoma virus treated with immune checkpoint inhibitors (98) successfully demonstrated an antitumor effect. Interestingly, coculture of an Ewing sarcoma cell line with NK cells led to a better oncolytic effect of a measles OV (99).

The reovirus Reolysin exhibited efficacy in the treatment of osteosarcoma, Ewing sarcoma and rhabdomyosarcoma cell lines *in vitro* and in flank xenografts *in vivo*, in combination with radiotherapy or the chemotherapeutic cisplatin, injecting three doses every three weeks *via* tail vein administration (100). Phelps and collaborators developed a recombinant oncolytic myxoma virus engineered with CRIPSR/Cas9 gene editing capability targeting *NRAS* (Myx : NRAS). While nonmodified myxoma virus slightly improved the overall survival in rhabdomyosarcoma subcutaneous models, the clinical effect was improved greatly by using Myx : NRAS, and long-term survival was achieved (101). $VSV^{\Delta M51}$ has also been evaluated in rhabdomyosarcoma and synergized with the Smac mimetic compound LCL161 *in vitro* and *in vivo* in a syngeneic murine model (102). In another elegant work, Petrov and colleagues used canine adipose-derived MSCs as carriers of

vaccinia viruses as a "Trojan Horse" to circumvent an early immune attack to treat a canine soft tissue sarcoma (103).

ONCOLYTIC VIRUSES IN CLINICAL TRIALS

In this section, we recapitulate the latest updates from clinical trials using OVs as therapeutic agents in pediatric solid cancers. All clinical trials using OVs that have been conducted in pediatric populations are included in **Table 1**.

One of the first clinical approaches using an OV in the pediatric population was a case report published in 2006 (111). A 12-year-old boy with anaplastic astrocytoma who was subjected to conventional therapy (surgery, radiation and chemotherapy) and progressed was treated with MTH-68/H (attenuated strain of paramyxovirus NDV) as a compassionate use. MRI scans showed 30% tumor regression two months after viral infusion. However, the patient's condition began to decline 4 months after the first MTH-68/H treatment due to the growth of new tumor nodules, and additional surgery was required. The patient passed away after 41 months.

Since then, several formal clinical trials utilizing different OVs have been performed, all of them looking into safety and feasibility. For example, Seneca Valley virus (NTX-010) was used in advanced solid tumors with neuroendocrine features in a phase I trial that included adults and children (112). Patients with neuroblastoma, rhabdomyosarcoma, Wilms tumor, carcinoid tumor and adrenocorticocarcinoma were included in this trial, which included two arms: one with just the OV and another with the virus combined with cyclophosphamide. Dose-limiting toxicity was observed in the first arm but not in the second. Adverse events of grade ≤3, such as leukopenia, neutropenia, nausea, or anemia, were described. Unfortunately, no complete or partial responses were observed, and only stable disease was observed in 6 out of 12 patients in the first arm (neuroblastoma n = 4, carcinoid tumor n=1; and rhabdomyosarcoma n=1) and 4 out of 6 in the second arm (neuroblastoma n = 2; and Wilms tumor n = 2).

JX-594 (Pexa-Vec; a vaccinia virus) was evaluated in six patients with metastatic neuroblastoma, hepatocellular carcinoma and Ewing sarcoma. No severe toxicity was associated with virus administration. Regarding efficacy, 4 out of 6 patients presented stable disease and 2 progressive disease, and uninjected lesions progressed in all patients except one, whose lung nodules were stable (108).

TABLE 1 | Clinical trials, completed or active, using oncolytic viruses as treatment in pediatric solid tumors.

Family	Name	Phase/ Country	Modifications	Target Disease	Route	Identifier/ Reference
Adenovirus	Delta-24-RGD/ DNX-2401	I/Spain	24-base pair deletion in the Rb-binding region of the E1A gene, insertion of an integrin-binding motif RGD	DMG	intratumoral	NCT03178032 (104)
	VCN-01	I/Spain	24-base pair deletion in the Rb-binding region of the E1A gene, insertion of an integrin-binding motif RGD, human hyalurodinase gene insertion	Refractory retinoblastoma	intravitreal	NCT03284268
	Icovir-5 (Celyvir)[a]	I/Spain	24-base pair deletion in the Rb-binding region of the E1A gene, integrin-binding motif RGD insertion, E2F-1 promoter insertion	Metastatic/Refractory solid tumors	intravenously	NCT01844661 (105)
	Icovir-5 (AloCELYVIR)[b]	Ib/Spain		DMG/ Medullablastoma	intravenously	NCT04758533
Herpex Simples Virus Type 1	HSV1716/ Seprehvir	I/USA	Gene encoding ICP 34.5 protein (RL1) deletion	Non-CNS solid tumors	Intratumoral /intravenously	NCT00931931 (106)
	G207	I/USA	Deletion of the diploid γ134.5 gene, viral ribonucleotide reductase (UL39) disruption by lacZ insertion	Recurrent/ Refractory cerebellar brain tumors	intratumoral	NCT03911388
	G207	I/USA		Progressive/Recurrent supratentorial brain tumors	intratumoral	NCT02457845 (107)
	G207	I/USA		Recurrent/Progressive high-grade gliomas	intratumoral	NCT04482933
Vaccina Virus	JX-594	I/USA	Thymidine kinase gene (TK) disruption, human GM-CSF and β-galactosidase gene insertion	Refractory solid tumors	intratumoral	NCT01169584 (108)
Reovirus	Reolysin	II/USA	Unmodified	Metastatic sarcomas	intravenously	NCT00503295
	Reolysin	I/USA and Canada		Relapsed/Refractory Solid Tumors	intravenously	NCT01240538 (109)
Picornavirus	Seneca Valley Virus	I/USA	Naturally occurring	Advanced Solid Tumors with Neuroendocrine Features	intravenously	NCT01048892 (110)
Poliovirus/ rhinovirus chimera	PVSRIPO	Ib/USA	Poliovirus type I containing heterologous internal ribosomal entry site of human rhinovirus type 2	Recurrent malignant glioma (Grade III or IV)	intratumoral	NCT03043391

Updated Jan 2022. [a]Celyvir, Celyvir system consists on autologous MSCs carrying ICOVIR-5. [b]AloCELYVIR, AloCELYVIR system consists on allogenic MSCs carrying ICOVIR-5.

The oncolytic reovirus Reolysin was the drug chosen for another phase I clinical trial (109). Twenty-four children with relapsed or refractory extracranial solid tumors were administered Reolysin intravenously for 5 consecutive days every 28 days, alone or in combination with the chemotherapeutic cyclophosphamide. Adverse events of grade ≤4 and even grade 5 thromboembolism in one patient were described. Regarding efficacy, only three patients with stable disease received a second cycle, whereas two patients received a third cycle prior to progressive disease.

In a study published by Melen and collaborators, Celyvir was chosen for compassionate use for 13 patients with advanced refractory neuroblastoma. Children received weekly multidoses as a sole treatment. The only adverse effects found were mild and autolimited viral-related toxicities, and none of the patients experienced grade 3+ toxicities. Regarding clinical outcomes, progression was the most common (n=8), with stable disease (n=1), partial response (n=3) and complete response (n=1). The authors found that the nonresponder patients' MSCs showed lower levels of expression of adhesion molecules and migration capacities, and a higher number of T cell lymphocytes was found in responder patients (113).

Our group has finished a phase I, dose-escalation clinical trial using DNX-2401 followed by standard radiotherapy in naïve DMGs, in which 12 patients were enrolled (114). Correct infusion of viral particles was checked using gadolinium in all patients (104). The treatment regimen was well tolerated, with asthenia, headache, vomiting, pyrexia and neurological deterioration being the most commonly reported adverse events. The three serious adverse events reported were grade 3 abdominal pain, grade 3 lymphopenia and grade 3 clinical deterioration. Regarding efficacy, tumor reduction was observed in 9 out of 12 patients. The final report of this study is still pending. The preclinical studies mentioned above have allowed the transfer of HSV-1 G207 in a phase I clinical trial to treat pediatric high-grade gliomas, in which supratentorial tumors had, at recurrence, a median life expectancy of only 5.6 months. The injection was performed *via* catheterization, and dose-limiting toxicities in the 12 patients enrolled were classified as grade 1 and 2 (more common) and 3 (less common) related to HSV-1 G207. The median overall survival was 12.2 months, and 4 patients were still alive 18 months after HSV-1 G207 injection. Importantly, posttreatment tissues from patients showed a substantial increase in CD3+, CD4+ and CD8+ T cells (107).

The oncolytic herpes virus HSV1716, mentioned above in preclinical research, has been evaluated in a preclinical trial for the pediatric population (115). In this study, Streby et al. recruited nine patients with relapsed or refractory extracranial solid tumors (pediatric sarcomas, neuroblastoma and cholangiocarcinoma). No dose-limiting toxicities were observed, and all the adverse events were of grade ≤ 3. However, only two patients exhibited disease stabilization in response to the virus, and months later, the tumors started to progress (106).

PERSPECTIVE AND CONCLUDING REMARKS

As depicted along this review, OVs have exhibited potential applications in the treatment of pediatric solid tumors with encouraging results. However, OVs have been regularly evaluated in tumors whose survival has not improved much in recent decades (including pediatric cancers). Despite the great efforts and multitude of clinical trials carried out, these diseases continue to be devastating. This constitutes a double-edged sword for OVs. On the one hand, they offer an alternative for cancer patients for whom the currently available treatments do not lead to sufficient improvement, much less cure, of the pathology. On the other hand, all of these tumors are very aggressive, and there could be no room to obtain tangible improvement, at least with monotherapy. Notably, although OVs have shown marked antitumor effects in preclinical models, their clinical translation has not been so successful. Indeed, most of the clinical trials recapitulated the above recruitment of patients in their last stages of their diseases and therefore with modest results. Nevertheless, in recent years, combinations of OVs with several chemo- and immunotherapy regimens have been proposed, and preclinical research and clinical trials are currently being conducted that show benefit compared to OVs alone (116–119).

Another point in favor of OVs is their low toxicity and extremely safe profile with very few secondary effects. This makes them very attractive, especially in the pediatric population. Viral production is also not a problem, as these viruses are easy and affordable to manufacture.

We consider that the main disadvantage of OVs is the route of administration. In intravascular administration, OVs are recognized and inactivated by humoral components of the innate and adaptative immune system in the blood (120), so this route is frequently dismissed. Therefore, intratumoral delivery is the dominant route, which allows direct targeting of the tumor using simple clinical procedures. However, there are also some difficulties, such as the presence of tissue barriers that might prevent the spread of the virus or the existence of metastases which might compromise the oncolytic efficacy. For that reason, approaches that improve virus delivery are under investigation and will be key to the further development of the field. In that regard, the use of cellular carriers such as MSCs (as explained above) (46, 52, 60, 103, 113), protective coatings and genetic modifications of OVs are other strategies that are considered for delivery optimization (121).

Interpretation of virotherapy responses through imaging within the clinical trial is another cornerstone where numerous efforts are being allocated. It is imperative to understand better what the imaging is telling us and define parameters that allow us to identify responses and other biological parameters intrinsic to the treatment with OVs.

In closing, the establishment of OVs as a therapeutic option for the treatment of tumors with poor prognosis, including pediatric solid malignancies, is encouraging. In recent years, investigations using OVs as therapy have grown exponentially. The FDA approval of Talimogene Laherparepvec has demonstrated that OVs are actually being considered as therapeutic options. Although we still need to overcome some barriers regarding OV application, their feasibility and, on some occasions, efficacy in treatment have been demonstrated. Further efforts will be needed and, given that virotherapy is now in its adolescence, there is great room for optimization. In the short-middle term, we believe that OVs

will constitute a feasible therapeutic option to use alone or in combination with other strategies, for patients with pediatric solid tumors.

AUTHOR CONTRIBUTIONS

DN: Conceptualization, writing, review, editing and figure design. KS: Writing and figure design. MA: Conceptualization, supervision, writing, review and editing. All authors contributed to the article and approved the submitted version.

FUNDING

The performed work was supported through a Predoctoral Fellowship from Instituto de Salud Carlos III (FI20/00020 DN), Instituto de Salud Carlos III y Fondos Feder (PI19/01896 MA); Fundación La Caixa (MA); Fundación El sueño de Vicky, Asociación Pablo Ugarte-Fuerza Julen, Fundación ADEY, Fundación ACS, (MA); Department of Defense (DOD) Team Science Award undergrant (CA 160525 MA); ChadTough Defeat DIPG Foundation (MA) and AECC (PRYGN21937ALON MA). This project also received funding from the European Research Council (ERC) under the European Union´s Horizon 2020 Research and Innovation Programme (817884 ViroPedTher to MA).

ACKNOWLEDGMENTS

We want to thank the patients' and their family for their selfless contribution of the advancement of science. We apologize to all the colleagues that have not been cited due to the limited extension.

REFERENCES

1. Steliarova-Foucher E, Colombet M, Ries LAG, Moreno F, Dolya A, Bray F, et al. International Incidence of Childhood Cancer, 2001–10: A Population-Based Registry Study. *Lancet Oncol* (2017) 18:719–31. doi: 10.1016/S1470-2045(17)30186-9
2. World Health Organization. *CureAll Framework: WHO Global Initiative for Childhood Cancer: Increasing Access, Advancing Quality, Saving Lives*. Lyon (France): IARC Press (2021).
3. Steliarova-Foucher E, Stiller C, Kaatsch P, Berrino F, Coebergh JW, Lacour B, et al. Geographical Patterns and Time Trends of Cancer Incidence and Survival Among Children and Adolescents in Europe Since the 1970s (the ACCIS Project): An Epidemiological Study. *Lancet* (2004) 364:2097–105. doi: 10.1016/S0140-6736(04)17550-8
4. Hudson MM, Link MP, Simone JV. Milestones in the Curability of Pediatric Cancers. *J Clin Oncol* (2014) 32:2391–7. doi: 10.1200/JCO.2014.55.6571
5. Pritchard-Jones K, Pieters R, Reaman GH, Hjorth L, Downie P, Calaminus G, et al. Sustaining Innovation and Improvement in the Treatment of Childhood Cancer: Lessons From High-Income Countries. *Lancet Oncol* (2013) 14:e95–e103. doi: 10.1016/S1470-2045(13)70010-X
6. Kattner P, Strobel H, Khoshnevis N, Grunert M, Bartholomae S, Pruss M, et al. Compare and Contrast: Pediatric Cancer Versus Adult Malignancies. *Cancer Metastasis Rev* (2019) 38:673–82. doi: 10.1007/s10555-019-09836-y
7. June CH, O'Connor RS, Kawalekar OU, Ghassemi S, Milone MC. CAR T Cell Immunotherapy for Human Cancer. *Science* (2018) 359:1361–5. doi: 10.1126/science.aar6711
8. Larson RC, Maus MV. Recent Advances and Discoveries in the Mechanisms and Functions of CAR T Cells. *Nat Rev Cancer* (2021) 21:145–61. doi: 10.1038/s41568-020-00323-z
9. Dock G. The Influence of Compliting Disease Upon Leukaemia. *Am J Med Sci* (1904) 127:563–92. doi: 10.1097/00000441-190412740-00001
10. Pelner L, Fowler GA, Nauts HC. Effects of Concurrent Infections and Their Toxins on the Course of Leukemia. *Acta Med Scand Suppl* (1958) 338:1–47. doi: 10.1111/j.0954-6820.1958.tb17327.x
11. Bierman HR, Crile DM, Dod KS, Kelly KH, Petrakis NI, White LP, et al. Remissions in Leukemia of Childhood Following Acute Infectious Disease. Staphylococcus and Streptococcus, Varicella, and Feline Panleukopenias. *Cancer* (1953) 6:591–605. doi: 10.1002/1097-0142(195305)6:3<591::AID-NCR2820060317>3.0.CO;2-M
12. Kelly E, Russell SJ. History of Oncolytic Viruses: Genesis to Genetic Engineering. *Mol Ther* (2007) 15:651–9. doi: 10.1038/sj.mt.6300108
13. Sheridan C. First Oncolytic Virus Edges Towards Approval in Surprise Vote. *Nat Biotechnol* (2015) 33:569–70. doi: 10.1038/nbt0615-569
14. Chaurasiya S, Chen NG, Fong Y. Oncolytic Viruses and Immunity. *Curr Opin Immunol* (2018) 51:83–90. doi: 10.1016/j.coi.2018.03.008
15. Kaufman HL, Kohlhapp FJ, Zloza A. Oncolytic Viruses: A New Class of Immunotherapy Drugs. *Nat Rev Drug Discov* (2015) 14:642–62. doi: 10.1038/nrd4663
16. Shi T, Song X, Wang Y, Liu F, Wei J. Combining Oncolytic Viruses With Cancer Immunotherapy: Establishing a New Generation of Cancer Treatment. *Front Immunol* (2020) 11:683. doi: 10.3389/fimmu.2020.00683
17. Raja J, Ludwig JM, Gettinger SN, Schalper KA, Kim HS. Oncolytic Virus Immunotherapy: Future Prospects for Oncology. *J Immunother Cancer* (2018) 6:1–13. doi: 10.1186/s40425-018-0458-z
18. Li H, Dutuor A, Tao L, Fu X, Zhang X. Virotherapy With a Type 2 Herpes Simplex Virus-Derived Oncolytic Virus Induces Potent Antitumor Immunity Against Neuroblastoma. *Clin Cancer Res* (2007) 13:316–22. doi: 10.1158/1078-0432.CCR-06-1625
19. Marchini A, Daeffler L, Pozdeev VI, Angelova A, Rommelaere J. Immune Conversion of Tumor Microenvironment by Oncolytic Viruses: The Protoparvovirus H-1PV Case Study. *Front Immunol* (2019) 10:1848. doi: 10.3389/fimmu.2019.01848
20. Mondal M, Guo J, He P, Zhou D. Recent Advances of Oncolytic Virus in Cancer Therapy. *Hum Vaccines Immunother* (2020) 16:2389–402. doi: 10.1080/21645515.2020.1723363
21. Macedo N, Miller DM, Haq R, Kaufman HL. Clinical Landscape of Oncolytic Virus Research in 2020. *J Immunother Cancer* (2020) 8: e001486. doi: 10.1136/jitc-2020-001486
22. Peters C, Rabkin SD. Designing Herpes Viruses as Oncolytics. *Mol Ther - Oncol* (2015) 2:15010. doi: 10.1038/mto.2015.10
23. Parato KA, Senger D, Forsyth PAJ, Bell JC. Recent Progress in the Battle Between Oncolytic Viruses and Tumours. *Nat Rev Cancer* (2005) 5:965–76. doi: 10.1038/nrc1750
24. Wang G, Kang X, Chen KS, Jehng T, Jones L, Chen J, et al. An Engineered Oncolytic Virus Expressing PD-L1 Inhibitors Activates Tumor Neoantigen-Specific T Cell Responses. *Nat Commun* (2020) 11:1–14. doi: 10.1038/s41467-020-15229-5
25. El-Shemi AG, Ashshi AM, Na Y, Li Y, Basalamah M, Al-Allaf FA, et al. Combined Therapy With Oncolytic Adenoviruses Encoding TRAIL and IL-12 Genes Markedly Suppressed Human Hepatocellular Carcinoma Both *In Vitro* and in an Orthotopic Transplanted Mouse Model. *J Exp Clin Cancer Res* (2016) 35:1–16. doi: 10.1186/s13046-016-0353-8
26. Chiocca EA, Rabkin SD. Oncolytic Viruses and Their Application to Cancer Immunotherapy. *Cancer Immunol Res* (2014) 2:295–300. doi: 10.1158/2326-6066.CIR-14-0015
27. Hartley A, Kavishwar G, Salvato I, Marchini A. A Roadmap for the Success of Oncolytic Parvovirus-Based Anticancer Therapies. *Annu Rev Virol* (2020) 7:537–57. doi: 10.1146/annurev-virology-012220-023606
28. Harrington K, Freeman DJ, Kelly B, Harper J, Soria JC. Optimizing Oncolytic Virotherapy in Cancer Treatment. *Nat Rev Drug Discov* (2019) 18:689–706. doi: 10.1038/s41573-019-0029-0

29. Ostrom QT, Gittleman H, De Blank PM, Finlay JL, Gurney JG, McKean-Cowdin R, et al. American Brain Tumor Association Adolescent and Young Adult Primary Brain and Central Nervous System Tumors Diagnosed in the United States in 2008-2012. *Neuro Oncol* (2015) 18:i1–i50. doi: 10.1093/neuonc/nov297
30. World Health Organization Classification of Tumours Editorial Board. *World Health Organization Classification of Tumours of the Central Nervous System, 5th Edition*. Lyon (France): IARC Press (2022).
31. Louis DN, Perry A, Wesseling P, Brat DJ, Cree IA, Figarella-Branger D, et al. The 2021 WHO Classification of Tumors of the Central Nervous System: A Summary. *Neuro Oncol* (2021) 23:1231–51. doi: 10.1093/neuonc/noab106
32. Pfister SM, Reyes-Múgica M, Chan JKC, Hasle H, Lazar AJ, Rossi S, et al. A Summary of the Inaugural WHO Classification of Pediatric Tumors: Transitioning From the Optical Into the Molecular Era. *Cancer Discov* (2022) 12:331–55. doi: 10.1158/2159-8290.cd-21-1094
33. Suzuki K, Fueyo J, Krasnykh V, Reynolds PN, Curiel DT, Alemany R. A Conditionally Replicative Adenovirus With Enhanced Infectivity Shows Improved Oncolytic Potency. *Clin Cancer Res* (2001) 7:120–6.
34. Fueyo J, Alemany R, Gomez-Manzano C, Fuller GN, Khan A, Conrad CA, et al. Preclinical Characterization of the Antiglioma Activity of a Tropism-Enhanced Adenovirus Targeted to the Retinoblastoma Pathway. *J Natl Cancer Inst* (2003) 95:652–60. doi: 10.1093/jnci/95.9.652
35. Ene CI, Fueyo J, Lang FF. Delta-24 Adenoviral Therapy for Glioblastoma: Evolution From the Bench to Bedside and Future Considerations. *Neurosurg Focus* (2021) 50:1–6. doi: 10.3171/2020.11.FOCUS20853
36. Alonso MM, Jiang H, Yokoyama T, Xu J, Bekele NB, Lang FF, et al. Delta-24-RGD in Combination With RAD001 Induces Enhanced Anti-Glioma Effect *via* Autophagic Cell Death. *Mol Ther* (2008) 16:487–93. doi: 10.1038/sj.mt.6300400
37. Jiang H, Clise-Dwyer K, Ruisaard KE, Fan X, Tian W, Gumin J, et al. Delta-24-RGD Oncolytic Adenovirus Elicits Anti-Glioma Immunity in an Immunocompetent Mouse Model. *PloS One* (2014) 9:e97407. doi: 10.1371/journal.pone.0097407
38. Lang FF, Conrad C, Gomez-Manzano C, Alfred Yung WK, Sawaya R, Weinberg JS, et al. Phase I Study of DNX-2401 (Delta-24-RGD) Oncolytic Adenovirus: Replication and Immunotherapeutic Effects in Recurrent Malignant Glioma. *J Clin Oncol* (2018) 36:1419–27. doi: 10.1200/JCO.2017.75.8219
39. Martínez-Vélez N, Garcia-Moure M, Marigil M, González-Huarriz M, Puigdelloses M, Gallego Pérez-Larraya J, et al. The Oncolytic Virus Delta-24-RGD Elicits an Antitumor Effect in Pediatric Glioma and DIPG Mouse Models. *Nat Commun* (2019) 10:1–10. doi: 10.1038/s41467-019-10043-0
40. Martinez-Velez N, Marigil M, García-Moure M, Gonzalez-Huarriz M, Aristu JJ, Ramos-García LI, et al. Delta-24-RGD Combined With Radiotherapy Exerts a Potent Antitumor Effect in Diffuse Intrinsic Pontine Glioma and Pediatric High Grade Glioma Models. *Acta Neuropathol Commun* (2019) 7:1–12. doi: 10.1186/s40478-019-0714-6
41. Gajjar A, Bowers DC, Karajannis MA, Leary S, Witt H, Gottardo NG. Pediatric Brain Tumors: Innovative Genomic Information Is Transforming the Diagnostic and Clinical Landscape. *J Clin Oncol* (2015) 33:2986–98. doi: 10.1200/JCO.2014.59.9217
42. Ostrom QT, Chen Y, De Blank PM, Ondracek A, Farah P, Gittleman H, et al. The Descriptive Epidemiology of Atypical Teratoid/Rhabdoid Tumors in the United States, 2001-2010. *Neuro Oncol* (2014) 16:1392–9. doi: 10.1093/neuonc/nou090
43. Garcia-Moure M, Gonzalez-Huarriz M, Labiano S, Guruceaga E, Bandres E, Zalacain M, et al. Delta-24-RGD, an Oncolytic Adenovirus, Increases Survival and Promotes Proinflammatory Immune Landscape Remodeling in Models of AT/RT and CNS-PNET. *Clin Cancer Res* (2021) 27:1807–20. doi: 10.1158/1078-0432.CCR-20-3313
44. Rodríguez-García A, Giménez-Alejandre M, Rojas JJ, Moreno R, Bazan-Peregrino M, Cascalló M, et al. Safety and Efficacy of VCN-01, an Oncolytic Adenovirus Combining Fiber HSG-Binding Domain Replacement With RGD and Hyaluronidase Expression. *Clin Cancer Res* (2015) 21:1406–18. doi: 10.1158/1078-0432.CCR-14-2213
45. Garcia-Moure M, Martinez-Velez N, Gonzalez-Huarriz M, Marrodán L, Cascallo M, Alemany R, et al. The Oncolytic Adenovirus VCN-01 Promotes Anti-Tumor Effect in Primitive Neuroectodermal Tumor Models. *Sci Rep* (2019) 9:1–10. doi: 10.1038/s41598-019-51014-1
46. Chastkofsky MI, Pituch KC, Katagi H, Zannikou M, Ilut L, Xiao T, et al. Mesenchymal Stem Cells Successfully Deliver Oncolytic Virotherapy to Diffuse Intrinsic Pontine Glioma. *Clin Cancer Res* (2021) 27:1766–77. doi: 10.1158/1078-0432.CCR-20-1499
47. Arnone CM, Polito VA, Mastronuzzi A, Carai A, Diomedi FC, Antonucci L, et al. Oncolytic Adenovirus and Gene Therapy With EphA2-BiTE for the Treatment of Pediatric High-Grade Gliomas. *J Immunother Cancer* (2021) 9:e001930. doi: 10.1136/jitc-2020-001930
48. Matthay KK, Maris JM, Schleiermacher G, Nakagawara A, Mackall CL, Diller L, et al. Neuroblastoma. *Nat Rev Dis Prim* (2016) 2:16078. doi: 10.1038/nrdp.2016.78
49. Bowen KA, Chung DH. Recent Advances in Neuroblastoma. *Curr Opin Pediatr* (2009) 21:350–6. doi: 10.1097/MOP.0b013e32832b1240
50. Maris JM, Hogarty MD, Bagatell R, Cohn SL. Neuroblastoma. *Lancet* (2007) 369:2106–20. doi: 10.1016/S0140-6736(07)60983-0
51. Tanimoto T, Tazawa H, Ieda T, Nouso H, Tani M, Oyama T, et al. Elimination of MYCN-Amplified Neuroblastoma Cells by Telomerase-Targeted Oncolytic Virus *via* MYCN Suppression. *Mol Ther - Oncol* (2020) 18:14–23. doi: 10.1016/j.omto.2020.05.015
52. Franco-Luzón L, González-Murillo Á, Alcántara-Sánchez C, García-García L, Tabasi M, Huertas AL, et al. Systemic Oncolytic Adenovirus Delivered in Mesenchymal Carrier Cells Modulate Tumor Infiltrating Immune Cells and Tumor Microenvironment in Mice With Neuroblastoma. *Oncotarget* (2020) 11:347–61. doi: 10.18632/oncotarget.27401
53. Tejada FNH, Zamudio A, Marques-Piubelli ML, Cuglievan B, Harrison D. Advances in the Management of Pediatric Sarcomas. *Curr Oncol Rep* (2021) 23:1–9. doi: 10.21037/tau-20-480
54. Hingorani P, Janeway K, Crompton BD, Kadoch C, Mackall CL, Khan J, et al. Current State of Pediatric Sarcoma Biology and Opportunities for Future Discovery: A Report From the Sarcoma Translational Research Workshop. *Cancer Genet* (2016) 209:182–94. doi: 10.1016/j.cancergen.2016.03.004
55. Collins M, Wilhelm M, Conyers R, Herschtal A, Whelan J, Bielack S, et al. Benefits and Adverse Events in Younger Versus Older Patients Receiving Neoadjuvant Chemotherapy for Osteosarcoma: Findings From a Meta-Analysis. *J Clin Oncol* (2013) 31:2303–12. doi: 10.1200/JCO.2012.43.8598
56. Roberts SS, Chou AJ, Cheung NKV. Immunotherapy of Childhood Sarcomas. *Front Oncol* (2015) 5:181. doi: 10.3389/fonc.2015.00181
57. Martinez-Velez N, Xipell E, Jauregui P, Zalacain M, Marrodan L, Zandueta C, et al. The Oncolytic Adenovirus Δ24-RGD in Combination With Cisplatin Exerts a Potent Anti-Osteosarcoma Activity. *J Bone Miner Res* (2014) 29:2287–96. doi: 10.1002/jbmr.2253
58. Martínez-Vélez N, Xipell E, Vera B, de la Rocha AA, Zalacain M, Marrodan L, et al. The Oncolytic Adenovirus VCN-01 as Therapeutic Approach Against Pediatric Osteosarcoma. *Clin Cancer Res* (2016) 22:2217–25. doi: 10.1158/1078-0432.CCR-15-1899
59. Martínez-Vélez N, Laspidea V, Zalacain M, Labiano S, Garcia-Moure M, Puigdelloses M, et al. Local Treatment of a Pediatric Osteosarcoma Model With a 4-1BBL Armed Oncolytic Adenovirus Results in an Antitumor Effect and Leads to Immune Memory. *Mol Cancer Ther* (2021) 21(3):471–80. doi: 10.1158/1535-7163.mct-21-0565
60. Morales-Molina A, Gambera S, Leo A, García-Castro J. Combination Immunotherapy Using G-CSF and Oncolytic Virotherapy Reduces Tumor Growth in Osteosarcoma. *J Immunother Cancer* (2021) 9:1–13. doi: 10.1136/jitc-2020-001703
61. Mochizuki Y, Tazawa H, Demiya K, Kure M, Kondo H, Komatsubara T, et al. Telomerase-Specific Oncolytic Immunotherapy for Promoting Efficacy of PD-1 Blockade in Osteosarcoma. *Cancer Immunol Immunother* (2021) 70:1405–17. doi: 10.1007/s00262-020-02774-7
62. Cripe TP, Chen CY, Denton NL, Haworth KB, Hutzen B, Leddon JL, et al. Pediatric Cancer Gone Viral. Part I: Strategies for Utilizing Oncolytic Herpes Simplex Virus-1 in Children. *Mol Ther - Oncol* (2015) 2:15015. doi: 10.1038/mto.2015.15
63. Rabkin SD, Martuza RL, Manz HJ, Yazaki T. Treatment of Human Malignant Meningiomas by G207, a Replication-Competent Multimutated Herpes Simplex Virus 1. *Cancer Res* (1995) 55:4752–6.
64. Bernstock JD, Vicario N, Li R, Nan L, Totsch SK, Schlappi C, et al. Safety and Efficacy of Oncolytic HSV-1 G207 Inoculated Into the Cerebellum of Mice. *Cancer Gene Ther* (2020) 27:246–55. doi: 10.1038/s41417-019-0091-0

65. Radbill AE, Reddy AT, Markert JM, Wyss JM, Pike MM, Akella NS, et al. Effects of G207, a Conditionally Replication-Competent Oncolytic Herpes Simplex Virus, on the Developing Mammalian Brain. *J Neurovirol* (2007) 13:118–29. doi: 10.1080/13550280601187177
66. Friedman GK, Bernstock JD, Chen D, Nan L, Moore BP, Kelly VM, et al. Enhanced Sensitivity of Patient-Derived Pediatric High-Grade Brain Tumor Xenografts to Oncolytic HSV-1 Virotherapy Correlates With Nectin-1 Expression. *Sci Rep* (2018) 8:1–10. doi: 10.1038/s41598-018-32353-x
67. Friedman GK, Moore BP, Nan L, Kelly VM, Etminan T, Langford CP, et al. Pediatric Medulloblastoma Xenografts Including Molecular Subgroup 3 and CD133+ and CD15+ Cells are Sensitive to Killing by Oncolytic Herpes Simplex Viruses. *Neuro Oncol* (2016) 18:227–35. doi: 10.1093/neuonc/nov123
68. Cockle JV, Brüning-Richardson A, Scott KJ, Thompson J, Kottke T, Morrison E, et al. Oncolytic Herpes Simplex Virus Inhibits Pediatric Brain Tumor Migration and Invasion. *Mol Ther - Oncol* (2017) 5:75–86. doi: 10.1016/j.omto.2017.04.002
69. Studebaker AW, Hutzen BJ, Pierson CR, Haworth KB, Cripe TP, Jackson EM, et al. Oncolytic Herpes Virus Rrp450 Shows Efficacy in Orthotopic Xenograft Group 3/4 Medulloblastomas and Atypical Teratoid/Rhabdoid Tumors. *Mol Ther - Oncol* (2017) 6:22–30. doi: 10.1016/j.omto.2017.05.005
70. Gillory LA, Megison ML, Stewart JE, Mroczek-Musulman E, Nabers HC, Waters AM, et al. Preclinical Evaluation of Engineered Oncolytic Herpes Simplex Virus for the Treatment of Neuroblastoma. *PloS One* (2013) 8:1–19. doi: 10.1371/journal.pone.0077753
71. Mahller YY, Williams JP, Baird WH, Mitton B, Grossheim J, Saeki Y, et al. Neuroblastoma Cell Lines Contain Pluripotent Tumor Initiating Cells That Are Susceptible to a Targeted Oncolytic Virus. *PloS One* (2009) 4:e4235. doi: 10.1371/journal.pone.0004235
72. Balamuth NJ, Womer RB. Ewing's Sarcoma. *Lancet Oncol* (2010) 11:184–92. doi: 10.1016/S1470-2045(09)70286-4
73. Denton NL, Chen CY, Hutzen B, Currier MA, Scott T, Nartker B, et al. Myelolytic Treatments Enhance Oncolytic Herpes Virotherapy in Models of Ewing Sarcoma by Modulating the Immune Microenvironment. *Mol Ther - Oncol* (2018) 11:62–74. doi: 10.1016/j.omto.2018.10.001
74. Skapek SX, Ferrari A, Gupta AA, Lupo PJ, Butler E, Shipley J, et al. Rhabdomyosarcoma. *Nat Rev Dis Prim* (2019) 5:14–6. doi: 10.1038/s41572-018-0051-2
75. Waters AM, Stafman LL, Garner EF, Mruthyunjayappa S, Stewart JE, Friedman GK, et al. Effect of Repeat Dosing of Engineered Oncolytic Herpes Simplex Virus on Preclinical Models of Rhabdomyosarcoma. *Transl Oncol* (2016) 9:419–30. doi: 10.1016/j.tranon.2016.07.008
76. Ring EK, Li R, Moore BP, Nan L, Kelly VM, Han X, et al. Newly Characterized Murine Undifferentiated Sarcoma Models Sensitive to Virotherapy With Oncolytic HSV-1 M002. *Mol Ther - Oncol* (2017) 7:27–36. doi: 10.1016/j.omto.2017.09.003
77. Rommelaere J, Geletneky K, Angelova AL, Daeffler L, Dinsart C, Kiprianova I, et al. Oncolytic Parvoviruses as Cancer Therapeutics. *Cytokine Growth Factor Rev* (2010) 21:185–95. doi: 10.1016/j.cytogfr.2010.02.011
78. Geletneky K, Kiprianova I, Ayache A, Koch R, Herrero M, Deleu L, et al. Regression of Advanced Rat and Human Gliomas by Local or Systemic Treatment With Oncolytic Parvovirus H-1 in Rat Models. *Neuro Oncol* (2010) 12:804–14. doi: 10.1093/neuonc/noq023
79. Kiprianova I, Thomas N, Ayache A, Fischer M, Leuchs B, Klein M, et al. Regression of Glioma in Rat Models by Intranasal Application of Parvovirus H-1. *Clin Cancer Res* (2011) 17:5333–42. doi: 10.1158/1078-0432.CCR-10-3124
80. Josupeit R, Bender S, Kern S, Leuchs B, Hielscher T, Herold-Mende C, et al. Pediatric and Adult High-Grade Glioma Stem Cell Culture Models Are Permissive to Lytic Infection With Parvovirus H-1. *Viruses* (2016) 8:138. doi: 10.3390/v8050138
81. Lacroix J, Schlund F, Leuchs B, Adolph K, Sturm D, Bender S, et al. Oncolytic Effects of Parvovirus H-1 in Medulloblastoma Are Associated With Repression of Master Regulators of Early Neurogenesis. *Int J Cancer* (2014) 134:703–16. doi: 10.1002/ijc.28386
82. Lacroix J, Kis Z, Josupeit R, Schlund F, Stroh-Dege A, Frank-Stöhr M, et al. Preclinical Testing of an Oncolytic Parvovirus in Ewing Sarcoma: Protoparvovirus H-1 Induces Apoptosis and Lytic Infection *In Vitro* But Fails to Improve Survival *In Vivo*. *Viruses* (2018) 10:1–15. doi: 10.3390/v10060302
83. Desjardins A, Gromeier M, Herndon JE, Beaubier N, Bolognesi DP, Friedman AH, et al. Recurrent Glioblastoma Treated With Recombinant Poliovirus. *N Engl J Med* (2018) 379:150–61. doi: 10.1056/nejmoa1716435
84. Thompson EM, Brown M, Dobrikova E, Ramaswamy V, Taylor MD, McLendon R, et al. Poliovirus Receptor (CD155) Expression in Pediatric Brain Tumors Mediates Oncolysis of Medulloblastoma and Pleomorphic Xanthoastrocytoma. *J Neuropathol Exp Neurol* (2018) 77:696–702. doi: 10.1093/jnen/nly045
85. Studebaker AW, Hutzen B, Pierson CR, Shaffer TA, Raffel C, Jackson EM. Oncolytic Measles Virus Efficacy in Murine Xenograft Models of Atypical Teratoid Rhabdoid Tumors. *Neuro Oncol* (2015) 17:1568–77. doi: 10.1093/neuonc/nov058
86. Liu Z, Zhao X, Mao H, Baxter PA, Huang Y, Yu L, et al. Intravenous Injection of Oncolytic Picornavirus SVV-001 Prolongs Animal Survival in a Panel of Primary Tumor-Based Orthotopic Xenograft Mouse Models of Pediatric Glioma. *Neuro Oncol* (2013) 15:1173–85. doi: 10.1093/neuonc/not065
87. Wu Y, Lun X, Zhou H, Wang L, Sun B, Bell JC, et al. Oncolytic Efficacy of Recombinant Vesicular Stomatitis Virus and Myxoma Virus in Experimental Models of Rhabdoid Tumors. *Clin Cancer Res* (2008) 14:1218–27. doi: 10.1158/1078-0432.CCR-07-1330
88. Ramachandran M, Yu D, Dyczynski M, Baskaran S, Zhang L, Lulla A, et al. Safe and Effective Treatment of Experimental Neuroblastoma and Glioblastoma Using Systemically Delivered Triple Microrna-Detargeted Oncolytic Semliki Forest Virus. *Clin Cancer Res* (2017) 23:1519–30. doi: 10.1158/1078-0432.CCR-16-0925
89. Takenouchi A, Saito K, Saito E, Saito T, Hishiki T, Matsunaga T, et al. Oncolytic Viral Therapy for Neuroblastoma Cells With Sindbis Virus AR339 Strain. *Pediatr Surg Int* (2015) 31:1151–9. doi: 10.1007/s00383-015-3784-y
90. Toyoda H, Yin J, Mueller S, Wimmer E, Cello J. Oncolytic Treatment and Cure of Neuroblastoma by a Novel Attenuated Poliovirus in a Novel Poliovirus-Susceptible Animal Model. *Cancer Res* (2007) 67:2857–64. doi: 10.1158/0008-5472.CAN-06-3713
91. Zhang SC, Cai WS, Zhang Y, Jiang KL, Zhang KR, Wang WL. Engineered Measles Virus Edmonston Strain Used as a Novel Oncolytic Viral System Against Human Neuroblastoma Through a CD46 and Nectin 4-Independent Pathway. *Cancer Lett* (2012) 325:227–37. doi: 10.1016/j.canlet.2012.07.008
92. Komorowski M, Tisonczyk J, Kolakowska A, Drozdz R, Kozbor D. Modulation of the Tumor Microenvironment by CXCR4 Antagonist-Armed Viral Oncotherapy Enhances the Antitumor Efficacy of Dendritic Cell Vaccines Against Neuroblastoma in Syngeneic Mice. *Viruses* (2018) 10:1–16. doi: 10.3390/v10090455
93. Morton CL, Houghton PJ, Kolb EA, Gorlick R, Reynolds CP, Kang MH, et al. Initial Testing of the Replication Competent Seneca Valley Virus (NTX-010) by the Pediatric Preclinical Testing Program. *Pediatr Blood Cancer* (2010) 55:295–303. doi: 10.1002/pbc.22535
94. Mazar J, Li Y, Rosado A, Phelan P, Kedarinath K, Parks GD, et al. Zika Virus as an Oncolytic Treatment of Human Neuroblastoma Cells Requires CD24. *PloS One* (2018) 13:1–21. doi: 10.1371/journal.pone.0200358
95. Domingo-Musibay E, Allen C, Kurokawa C, Hardcastle JJ, Aderca I, Msaouel P, et al. Measles Edmonston Vaccine Strain Derivatives Have Potent Oncolytic Activity Against Osteosarcoma. *Cancer Gene Ther* (2014) 21:483–90. doi: 10.1038/cgt.2014.54
96. Geiss C, Kis Z, Leuchs B, Frank-Stöhr M, Schlehofer JR, Rommelaere J, et al. Preclinical Testing of an Oncolytic Parvovirus: Standard Protoparvovirus H-1PV Efficiently Induces Osteosarcoma Cell Lysis *In Vitro*. *Viruses* (2017) 9:301. doi: 10.3390/v9100301
97. Jiang J, Wang W, Xiang W, Jiang L, Zhou Q. The Phosphoinositide 3-Kinase Inhibitor ZSTK474 Increases the Susceptibility of Osteosarcoma Cells to Oncolytic Vesicular Stomatitis Virus VSVΔ51 *via* Aggravating Endoplasmic Reticulum Stress. *Bioengineered* (2021) 12:11847–57. doi: 10.1080/21655979.2021.1999372
98. Christie JD, Appel N, Canter H, Achi JG, Elliott NM, de Matos AL, et al. Systemic Delivery of TNF-Armed Myxoma Virus Plus Immune Checkpoint Inhibitor Eliminates Lung Metastatic Mouse Osteosarcoma. *Mol Ther - Oncol* (2021) 22:539–54. doi: 10.1016/j.omto.2021.07.014
99. Klose C, Berchtold S, Schmidt M, Beil J, Smirnow I, Venturelli S, et al. Biological Treatment of Pediatric Sarcomas by Combined Virotherapy and

NK Cell Therapy. *BMC Cancer* (2019) 19:1–15. doi: 10.1186/s12885-019-6387-5
100. Hingorani P, Zhang W, Lin J, Liu L, Guha C, Kolb EA. Systemic Administration of Reovirus (Reolysin) Inhibits Growth of Human Sarcoma Xenografts. *Cancer* (2011) 117:1764–74. doi: 10.1002/cncr.25741
101. Phelps MP, Yang H, Patel S, Rahman MM, McFadden G, Chen E. Oncolytic Virus-Mediated RAS Targeting in Rhabdomyosarcoma. *Mol Ther - Oncol* (2018) 11:52–61. doi: 10.1016/j.omto.2018.09.001
102. Dobson CC, Naing T, Beug ST, Faye MD, Chabot J, St-Jean M, et al. Oncolytic Virus Synergizes With Smac Mimetic Compounds to Induce Rhabdomyosarcoma Cell Death in a Syngeneic Murine Model. *Oncotarget* (2017) 8:3495–508. doi: 10.18632/oncotarget.13849
103. Petrov I, Gentschev I, Vyalkova A, Elashry MI, Klymiuk MC, Arnhold S, et al. Canine Adipose-Derived Mesenchymal Stem Cells (Cadmscs) as a "Trojan Horse" in Vaccinia Virus Mediated Oncolytic Therapy Against Canine Soft Tissue Sarcomas. *Viruses* (2020) 12:750. doi: 10.3390/v12070750
104. Tejada S, Díez-Valle R, Domínguez PD, Patiño-García A, González-Huarriz M, Fueyo J, et al. DNX-2401, an Oncolytic Virus, for the Treatment of Newly Diagnosed Diffuse Intrinsic Pontine Gliomas: A Case Report. *Front Oncol* (2018) 8:61. doi: 10.3389/fonc.2018.00061
105. Ruano D, López-Martín JA, Moreno L, Lassaletta Á, Bautista F, Andión M, et al. First-In-Human, First-In-Child Trial of Autologous MSCs Carrying the Oncolytic Virus Icovir-5 in Patients With Advanced Tumors. *Mol Ther* (2020) 28:1033–42. doi: 10.1016/j.ymthe.2020.01.019
106. Streby KA, Geller JI, Currier MA, Warren PS, Racadio JM, Towbin AJ, et al. Intratumoral Injection of HSV1716, an Oncolytic Herpes Virus, is Safe and Shows Evidence of Immune Response and Viral Replication in Young Cancer Patients. *Clin Cancer Res* (2017) 23:3566–74. doi: 10.1158/1078-0432.CCR-16-2900
107. Friedman GK, Johnston JM, Bag AK, Bernstock JD, Li R, Aban I, et al. Oncolytic HSV-1 G207 Immunovirotherapy for Pediatric High-Grade Gliomas. *N Engl J Med* (2021) 384:1613–22. doi: 10.1056/nejmoa2024947
108. Cripe TP, Ngo MC, Geller JI, Louis CU, Currier MA, Racadio JM, et al. Phase 1 Study of Intratumoral Pexa-Vec (JX-594), an Oncolytic and Immunotherapeutic Vaccinia Virus, in Pediatric Cancer Patients. *Mol Ther* (2015) 23:602–8. doi: 10.1038/mt.2014.243
109. Kolb EA, Sampson V, Stabley D, Walter A, Sol-Church K, Cripe T, et al. A Phase I Trial and Viral Clearance Study of Reovirus (Reolysin) in Children With Relapsed or Refractory Extracranial Solid Tumors: A Children's Oncology Group Phase I Consortium Report. *Pediatr Blood Cancer* (2015) 62:751–8. doi: 10.1002/pbc.25464
110. Rudin CM, Poirier JT, Senzer NN, Stephenson J, Loesch D, Burroughs KD, et al. Phase I Clinical Study of Seneca Valley Virus (SVV-001), a Replication-Competent Picornavirus, in Advanced Solid Tumors With Neuroendocrine Features. *Clin Cancer Res* (2011) 17:888–95. doi: 10.1158/1078-0432.CCR-10-1706
111. Wagner S, Csatary CM, Gosztonyi G, Koch HC, Hartmann C, Peters O, et al. Combined Treatment of Pediatric High-Grade Glioma With the Oncolytic Viral Strain MTH-68/H and Oral Valproic Acid. *Apmis* (2006) 114:731–43. doi: 10.1111/j.1600-0463.2006.apm_516.x
112. Burke MJ, Ahern C, Weigel BJ, Poirier JT, Rudin CM, Chen Y, et al. Phase I Trial of Seneca Valley Virus (NTX-010) in Children With Relapsed/Refractory Solid Tumors: A Report of the Children's Oncology Group. *Pediatr Blood Cancer* (2015) 62:743–50. doi: 10.1002/pbc.25269
113. Melen GJ, Franco-Luzón L, Ruano D, González-Murillo Á, Alfranca A, Casco F, et al. Influence of Carrier Cells on the Clinical Outcome of Children With Neuroblastoma Treated With High Dose of Oncolytic Adenovirus Delivered in Mesenchymal Stem Cells. *Cancer Lett* (2016) 371:161–70. doi: 10.1016/j.canlet.2015.11.036
114. Tejada S, Alonso M, Patiño A, Fueyo J, Gomez-Manzano C, Diez-Valle R. Phase I Trial of DNX-2401 for Diffuse Intrinsic Pontine Glioma Newly Diagnosed in Pediatric Patients. *Clin Neurosurg* (2018) 83:1050–6. doi: 10.1093/neuros/nyx507
115. Streby KA, Currier MA, Triplet M, Ott K, Dishman DJ, Vaughan MR, et al. First-In-Human Intravenous Seprehvir in Young Cancer Patients: A Phase 1 Clinical Trial. *Mol Ther* (2019) 27:1930–8. doi: 10.1016/j.ymthe.2019.08.020
116. Hwang JK, Hong J, Yun CO. Oncolytic Viruses and Immune Checkpoint Inhibitors: Preclinical Developments to Clinical Trials. *Int J Mol Sci* (2020) 21:1–26. doi: 10.3390/ijms21228627
117. Ajina A, Maher J. Prospects for Combined Use of Oncolytic Viruses and CAR T-Cells. *J Immunother Cancer* (2017) 5:1–27. doi: 10.1186/s40425-017-0294-6
118. Bommareddy PK, Shettigar M, Kaufman HL. Integrating Oncolytic Viruses in Combination Cancer Immunotherapy. *Nat Rev Immunol* (2018) 18:498–513. doi: 10.1038/s41577-018-0014-6
119. Ottolino-Perry K, Diallo JS, Lichty BD, Bell JC, Andrea McCart J. Intelligent Design: Combination Therapy With Oncolytic Viruses. *Mol Ther* (2010) 18:251–63. doi: 10.1038/mt.2009.283
120. Ochsenbein AF, Fehr T, Lutz C, Suter M, Brombacher F, Hengartner H, et al. Control of Early Viral and Bacterial Distribution and Disease by Natural Antibodies. *Sci (80-)* (1999) 286:2156–9. doi: 10.1126/science.286.5447.2156
121. Shin DH, Nguyen T, Ozpolat B, Lang F, Alonso M, Gomez-Manzano C, et al. Current Strategies to Circumvent the Antiviral Immunity to Optimize Cancer Virotherapy. *J Immunother Cancer* (2021) 9:1–10. doi: 10.1136/jitc-2020-002086

Conflict of Interest: MA has a research grant from DNAtrix not related to this work.

The remaining authors declare that the research was conducted in the absence of any commercial or financial relationships that could be construed as a potential conflict of interest.

Publisher's Note: All claims expressed in this article are solely those of the authors and do not necessarily represent those of their affiliated organizations, or those of the publisher, the editors and the reviewers. Any product that may be evaluated in this article, or claim that may be made by its manufacturer, is not guaranteed or endorsed by the publisher.

frontiers | Frontiers in Oncology

ORIGINAL RESEARCH
published: 22 April 2022
doi: 10.3389/fonc.2022.847088

Adiponectin Deficiency Enhances Anti-Tumor Immunity of CD8$^+$ T Cells in Rhabdomyosarcoma Through Inhibiting STAT3 Activation

Jiao Peng[1,2†], Haifeng Huang[3,4†], Qiuchan Huan[2], Chenghui Liao[5], Zebin Guo[3], Die Hu[1], Xiangchun Shen[2] and Haitao Xiao[3]*

[1] Department of Pharmacy, Peking University Shenzhen Hospital, Shenzhen, China, [2] The High Efficacy Application of Natural Medicinal Resources Engineering Center of Guizhou Province, School of Pharmaceutical Sciences, Guizhou Medical University, Guiyang, China, [3] School of Pharmaceutical Sciences, Health Science Center, Shenzhen University, Shenzhen, China, [4] School of Pharmaceutical Science, Chongqing Medical University, Chongqing, China, [5] School of Pharmaceutical Science, Harbin Medical University, Heilongjiang, China

OPEN ACCESS

Edited by:
Pouya Faridi,
Monash University, Australia

Reviewed by:
Saptak Banerjee,
Chittaranjan National Cancer Institute, India
Sengottuvelan Murugan,
Rutgers, The State University of New Jersey, United States
Mingfeng Zhao,
Tianjin First Central Hospital, China

***Correspondence:**
Haitao Xiao
xhaitao@szu.edu.cn

[†]These authors have contributed equally to this work

Specialty section:
This article was submitted to Cancer Immunity and Immunotherapy, a section of the journal Frontiers in Oncology

Received: 01 January 2022
Accepted: 25 March 2022
Published: 22 April 2022

Citation:
Peng J, Huang H, Huan Q, Liao C, Guo Z, Hu D, Shen X and Xiao H (2022) Adiponectin Deficiency Enhances Anti-Tumor Immunity of CD8$^+$ T Cells in Rhabdomyosarcoma Through Inhibiting STAT3 Activation. Front. Oncol. 12:847088. doi: 10.3389/fonc.2022.847088

Restoring the tumor-killing function of CD8$^+$ T cells in the tumor microenvironment is an important strategy for cancer immunotherapy. Our previous study indicated that adiponectin (APN) deficiency reprogramed tumor-associated macrophages into an M1-like phenotype to inhibit rhabdomyosarcoma growth. However, whether APN can directly regulate the anti-tumor activity of CD8$^+$ T cells remains unknown. In the present study, our results showed that exogenous APN inhibited *in vitro* CD8$^+$ T cell migration as well as cytokines IFN-γ and TNF-α production. APN deficiency *in vivo* strengthened CD8$^+$ T cell activation and cytotoxicity to restrain rhabdomyosarcoma, evidenced by an increase in the expression of IFN-γ and perforin in CD8$^+$ T cells and the frequency of CD8$^+$IFN-γ$^+$ T cells in the spleen and lymph nodes, as well as increasing cytokine production of IFN-γ, perforin, TNF-α, and decreasing cytokine production of IL-10 in the serum. Mechanistically, STAT3 was identified as a target of APN in negatively regulating the anti-tumor activity of CD8$^+$ T cells. *In vivo*, a STAT3 inhibitor remarkably increased CD8$^+$ as well as CD8$^+$IFN-γ$^+$ T cells in the spleen and lymph nodes. Taken together, we substantiated that APN deficiency directly maintains the activation of CD8$^+$ T cells to inhibit rhabdomyosarcoma growth by suppressing STAT3 activation, indicating a promising APN-based therapy for the treatment of rhabdomyosarcoma.

Keywords: CD8$^+$ T cells, adiponectin, rhabdomyosarcoma, anti-tumor immunity, STAT3

INTRODUCTION

Rhabdomyosarcoma (RMS) is a high-grade malignant soft tissue sarcoma that includes embryonal rhabdomyosarcoma (ERMS) and alveolar rhabdomyosarcoma (ARMS) (1). It commonly occurs in children and teenagers, with an estimated incidence rate of 4.4 cases per 1 million in individuals under 20 years of age, accounting for 3% of pediatric cancers diagnosed annually (1, 2). Current clinical treatment of RMS is based on multimodal therapies, including surgery and chemotherapy,

with or without radiotherapy (3). During the last few decades, progressive advancements in RMS treatment have made the overall survival rate up to 60%, but the overall survival rate of metastatic and relapsed/refractory RMS is only 10% to 20% (4, 5). Therefore, there is a clear need to develop therapeutic strategies for RMS. Recent mechanistic advances in immunology have identified that the immunosuppressive tumor microenvironment is the basis for tumor growth and its malignant properties since the host fails to induce an effective immune response (6). Hence, a therapeutic strategy that can counteract the immunosuppressive tumor microenvironment may be an alternative option for RMS.

Adiponectin (APN), a well-known adipocyte-secreted cytokine, has been shown to possess multiple immunoregulatory effects in both innate and adaptive immune systems. APN is capable of inducing anti-inflammatory cytokines, such as IL-10, IL-1RA, and IL-4, and suppressing pro-inflammatory cytokines, such as IL-1β, IL-6, and TNF-α from monocytes, macrophages, and dendritic cells (7–14). APN suppresses the cellular maturation of dendritic cells (7, 15), inhibits pro-inflammatory cytokines (IL-1β, IL-2, IL-8, TNF-α, IFN-γ) from T cells (7, 16), and induces T cell apoptosis and expansion of Tregs (15, 16). In our previous study, we found that APN was highly expressed in infantile RMS, especially in ARMS, one malignant subtype of RMS (17). APN deficiency could inhibit the growth of rhabdomyosarcoma in mice by reprogramming tumor-associated macrophages into an M1-like phenotype *via* suppressing p38 MAPK phosphorylation (17). We also found an extensive infiltration of $CD8^+$ T cells in tumor tissues (17). However, whether APN can directly regulate the anti-tumor effect of $CD8^+$ T cells remains unknown. In this study, we investigated the role APN on $CD8^+$ T cells in the tumor microenvironment of rhabdomyosarcoma-bearing mice, and found that APN deficiency inhibited rhabdomyosarcoma growth, which was associated with enhancing the anti-tumor response of $CD8^+$ T cells that infiltrated rhabdomyosarcoma through the inhibition of STAT3 activation.

RESULTS

Exogenous APN Inhibits $CD8^+$ T Cell Activation and Migration

To study the effect of APN on $CD8^+$ T cells, we first detected the expressions of APN receptors, AdipoR1 and AdipoR2, in inactive and activated $CD8^+$ T cells. The results revealed that these two receptors were expressed in $CD8^+$ T cells, and their expression was upregulated after TCR activation (**Figure 1A**), which was consistent with a previous report (16). Subsequently, we stimulated purified $CD8^+$ T cells with a combination of plate-bound anti-CD3 mAb and anti-CD28 mAb in the presence or absence of APN. The production of IFN-γ and TNF-α from $CD8^+$ T cells significantly declined after APN treatment (5 μg/mL), but no obvious proliferative effect was observed (**Figures 1B, C**). The effect of APN on the migration of $CD8^+$ T cells was also investigated using a transwell migration assay, which showed that the number of transmigrated $CD8^+$ T cells obviously decreased after APN treatment (5 μg/mL) (**Figure 1D**). These

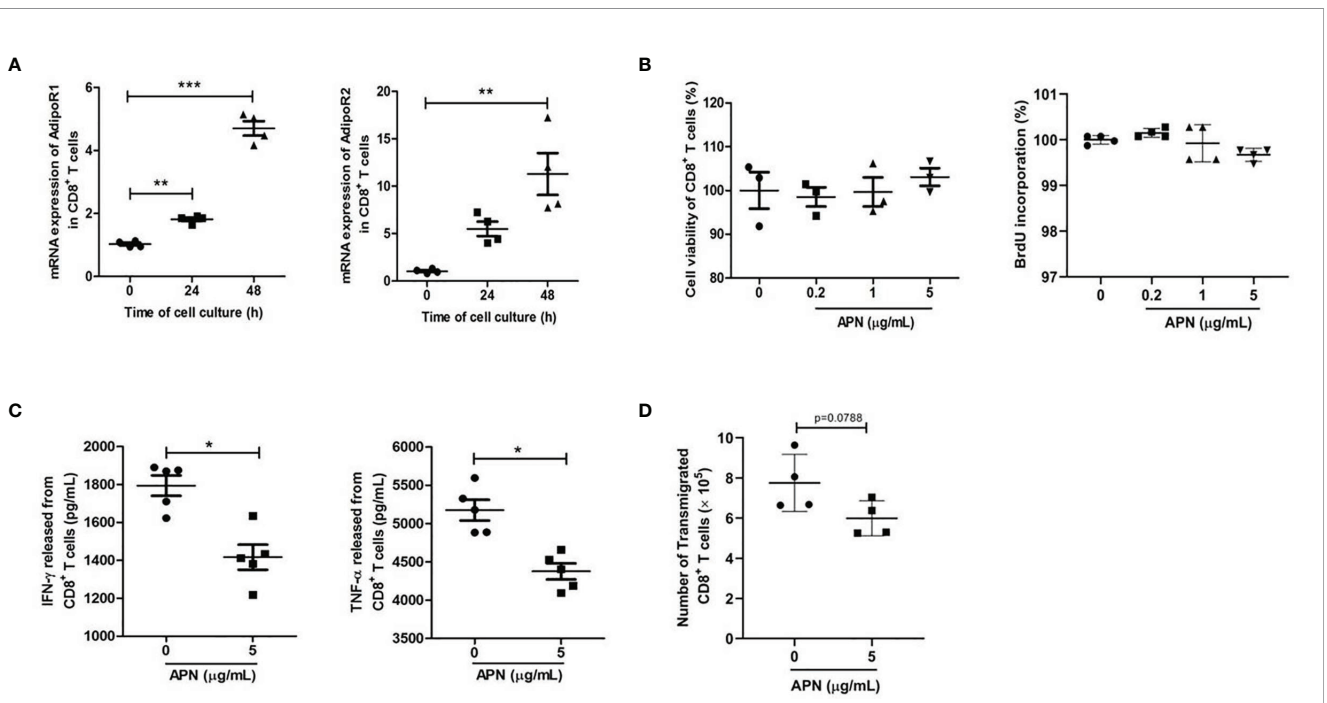

FIGURE 1 | Exogenous APN inhibits $CD8^+$ T cell activation and migration. **(A)** mRNA expression of AdipoR1 and AdipoR2 in inactive and activated $CD8^+$ T cells (n = 4). **(B)** The effect of APN on $CD8^+$ T cell proliferation (n =3-4). **(C)** The effect of APN on IFN-γ and TNF-α production from $CD8^+$ T cells (n =5). **(D)** The effect of APN on $CD8^+$ T cell migration (n=4). Data are expressed as the mean ± SEM from one of two or three separate experiments with same results. *p<.05, **p<.01 and ***p<.001.

data suggest that exogenous APN can inhibit $CD8^+$ T cell activation and migration.

APN Deficiency Inhibits Rhabdomyosarcoma Growth and Negatively Regulates the Anti-Tumor Effect of $CD8^+$ T Cells in Tumors

To investigate the role of APN in regulating the tumor-killing function of $CD8^+$ T cells in tumors, a rhabdomyosarcoma model was established in both $APN^{-/-}$ and wild-type mice by injecting the mice with MN/MCA1 cells. As expected, the tumor growth in $APN^{-/-}$ group was significantly reduced (**Figure 2A**), and massive $CD8^+$ T cell accumulation in the tumor mass, spleen, and lymph nodes was also observed in the $APN^{-/-}$ group (**Figures 2B, C**). Subsequently, we blocked $CD8^+$ T cells in tumor-bearing mice using CD8 mAb. As shown in **Figure 3**, the inhibitory effect of APN deletion on rhabdomyosarcoma growth was significantly abrogated after the blockade of CD8 mAb. These data suggest that APN deletion could negatively regulate the anti-tumor effect of $CD8^+$ T cells to directly suppress rhabdomyosarcoma growth.

APN Deficiency Enhances the Immune Response $CD8^+$ T Cells

We attempted to assess the immune status of $CD8^+$ T cells in $APN^{-/-}$ mice with rhabdomyosarcoma. The gene expression of IFN-γ, perforin, Gzma, and CXCR3 in $CD8^+$ T cells isolated from both rhabdomyosarcoma-bearing wild-type and $APN^{-/-}$ mice were quantified by RT-PCR. As shown in **Figure 4A**, $CD8^+$ T cells isolated from rhabdomyosarcoma-bearing $APN^{-/-}$ mice expressed relatively higher IFN-γ and perforin than those from rhabdomyosarcoma-bearing wild-type mice. Further, we detected $CD8^+IFN\text{-}\gamma^+$ T cells in the spleen and lymph nodes of both rhabdomyosarcoma-bearing wild-type and $APN^{-/-}$ mice using flow cytometry. Consistent with the results of the RT-PCR, $CD8^+IFN\text{-}\gamma^+T$ cells in the spleen and lymph nodes of rhabdomyosarcoma-bearing $APN^{-/-}$ mice were markedly boosted, compared with $CD8^+IFN\text{-}\gamma^+$ T cells from rhabdomyosarcoma-bearing wild-type mice (**Figure 4B**). Subsequently, we determined the protein levels of IFN-γ, perforin, TNF-α, and IL-10 in the serum of both rhabdomyosarcoma-bearing wild-type and $APN^{-/-}$ mice. As expected, compared to wild-type mice with rhabdomyosarcoma, the serum levels of IFN-γ, perforin and TNF-α of rhabdomyosarcoma-bearing $APN^{-/-}$ mice were much higher, whereas the level of IL-10 in serum was much lower (**Figure 4C**). These findings indicate that APN deletion significantly enhances $CD8^+$ T cell activation and cytotoxicity.

APN Deficiency Inhibits STAT3 Activation in $CD8^+$ T Cells

Since APN deletion greatly promotes $CD8^+$ T cell activation and enhances its cytotoxicity, we then explored the underlying mechanism. As described previously, STAT3 activation has been shown to inhibit the antitumor functions of $CD8^+$ T cells in

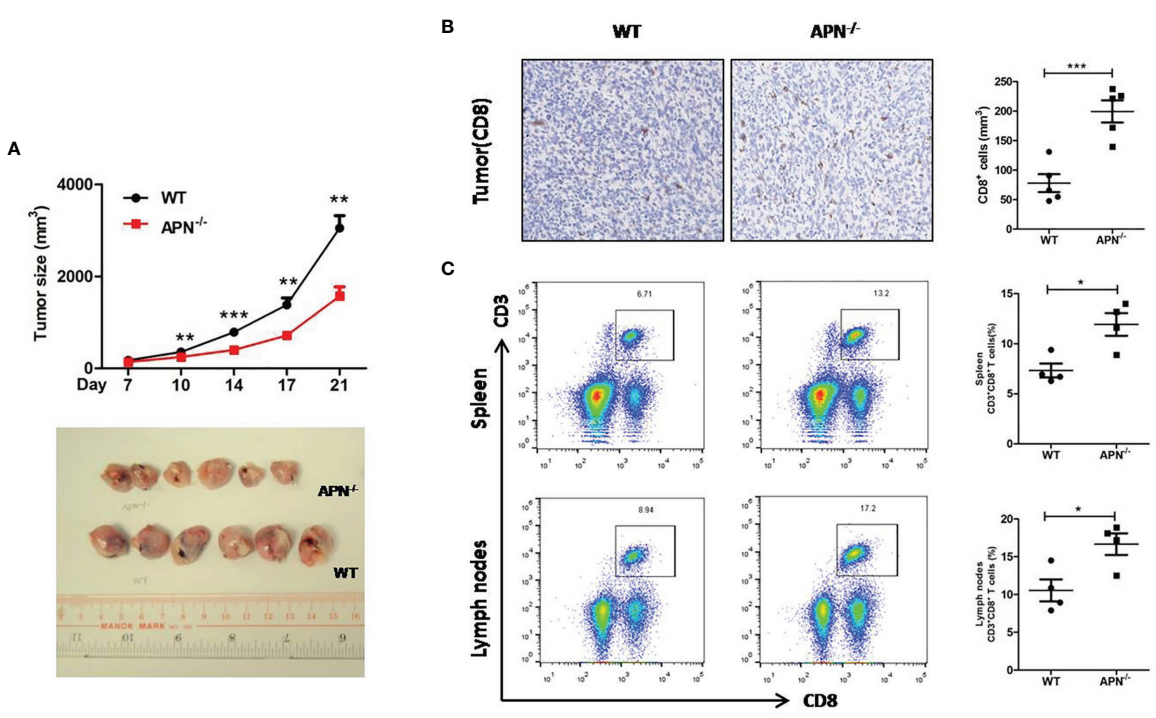

FIGURE 2 | APN deficiency inhibits rhabdomyosarcom growth and increases the accumulation of $CD8^+$ T cells in tumor mass, spleen and lymph nodes. **(A)** Tumor size of wild type (WT) and in APN deficiency ($APN^{-/-}$) mice (n=6 for each group). **(B)** CD8-positive cells in tumor mass (×200) (n=5 for each group). **(C)** The frequency $CD3^+CD8^+$ T cells in the spleen and lymph nodes (n=4 for each group). Data are expressed as the mean ± SEM. *p<0.05, **p<0.01 and ***p<0.001.

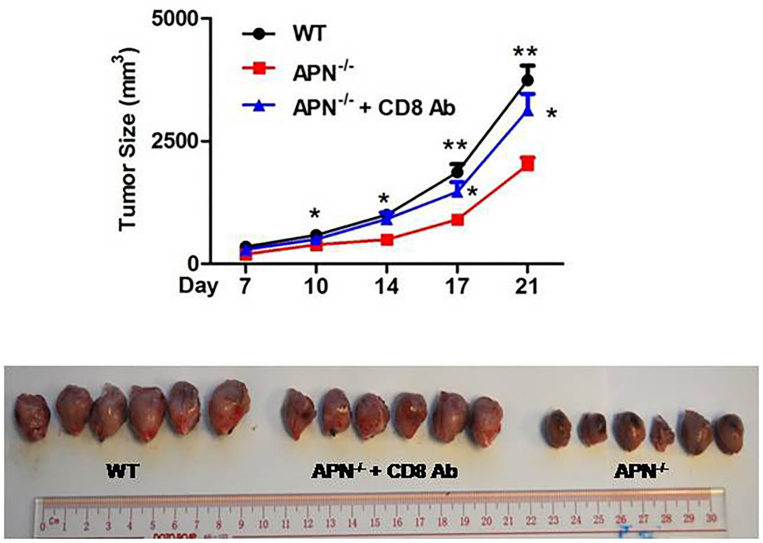

FIGURE 3 | Blockage of $CD8^+$ T cells impairs rhabdomyosarcom growth inhibition conferred by APN deficiency. MN/MCA1 cells were inoculated in $APN^{-/-}$ mice, the CD8 mAb (5 μg/mice) were injected intraperitoneally to the mice every two days. Data are expressed as the mean ± SEM (n=6 for each group). Compared to $APN^{-/-}$ mice, *p<.05 and **p<.01.

various cancers (18, 19). We detected the protein expression of STAT3 in $CD8^+$ T cells isolated from both rhabdomyosarcoma-bearing wild-type and $APN^{-/-}$ mice. As shown in **Figure 5**, the phosphorylation of STAT3 in $CD8^+$ T cells from $APN^{-/-}$ mice with rhabdomyosarcoma was significantly suppressed compared to that in rhabdomyosarcoma-bearing wild-type mice, suggesting that APN deficiency inhibited STAT3 activation in $CD8^+$ T cells. Subsequently, we administered the STAT3 inhibitor Stattic to rhabdomyosarcoma-bearing wild-type mice, and observed a remarkable tumor growth inhibition (**Figure 6A**), and the frequency of $CD8^+$ as well as $CD8^+$IFN-γ+ T cells in the spleen and lymph nodes were markedly upregulated (**Figures 6B, C**). These results all support the idea that APN deletion facilitates $CD8^+$ T cell activation *via* inhibiting STAT3.

DISCUSSION

Tumors have specific mechanisms that disrupt the T-cell response. $CD8^+$ T lymphocytes are central players in killing malignant cells in cancer immune responses. During tumor progression, $CD8^+$ T lymphocytes are usually functionally dysfunctional and exhausted in the tumor immunosuppressive microenvironment. Therefore, exploring an effective way to recover the anti-tumor function of $CD8^+$ T lymphocytes will contribute to the eradication of tumors. Our study clearly indicated that APN deficiency could enhance the immune response of $CD8^+$ T lymphocytes to inhibit rhabdomyosarcoma growth by suppressing STAT3 activation.

APN was initially found to effectively regulate the immune response of innate immune cells in tumors. Tan et al. reported that APN retarded the maturation of dendritic cells and subsequent blunt antitumor immunity (7). Our previous study showed that APN deletion could reprogram tumor-associated macrophages into an M1-like phenotype to inhibit the growth of rhabdomyosarcoma (17). In this study, we found *in vitro* evidence supporting APN suppression of $CD8^+$ T activation. APN deletion *in vivo* significantly promoted the accumulation of host $CD8^+$ T cells in rhabdomyosarcoma tumor masses as well as in spleen and lymph nodes, and this antitumor effect could be abrogated by a CD8 mAb blockade. These findings indicate that APN deletion could negatively regulate the tumor-killing function of $CD8^+$ T cells directly to suppress rhabdomyosarcoma. Notably, this is the first study to elucidate the regulatory effect of APN on $CD8^+$ T lymphocytes.

It is well known that $CD8^+$ T lymphocytes killing tumor cells are mediated by exocytosis using cytotoxic granules perforin and granzyme to directly destruct tumor cells, or by releasing cytokines, such as IFN-γ and TNF-α, to poison tumor cells indirectly (20). Our present study indicated that APN deficiency conferred a higher frequency of $CD8^+$IFN-γ^+ T cells in the spleen and lymph nodes, as well as higher levels of IFN-γ, perforin, and TNF-α and lower levels of IL-10 in the serum of rhabdomyosarcoma-bearing mice. These findings clearly indicate that APN deficiency greatly enhanced the capability of $CD8^+$ T cells to kill tumor cells.

However, the underlying mechanism of APN deficiency in promoting $CD8^+$ T cell activation and cytotoxicity remains to be explored. It has been reported that the expansion and cytolytic activity of $CD8^+$ T cells are closely related to STAT3 activation. Kujawski et al. found that engineered $STAT3^{-/-}$ $CD8^+$ T cells were effective in infiltrating tumors and inhibiting their growth (21). Yue et al. further revealed that silencing STAT3 in T cells allows CXCR3 (the receptor for CXCL10) to be expressed in $CD8^+$ T cells, leading to $CD8^+$ T cells effectively accumulating at tumor sites (19).

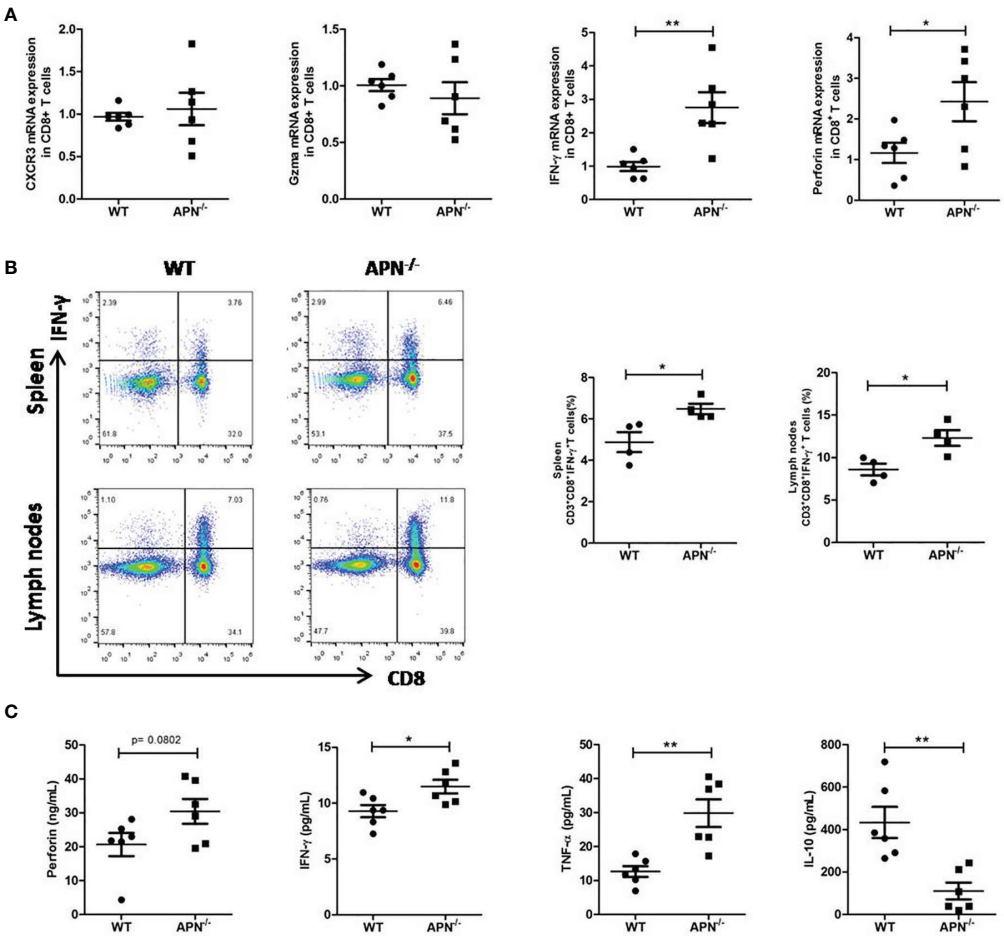

FIGURE 4 | APN deficiency enhances $CD8^+$ T cells immune response. **(A)** mRNA expression of IFN-γ, perforin, Gzma and CXCR3 in $CD8^+$ T cells isolated from rhabdomyosarcom-bearing wild-type and $APN^{-/-}$ mice (n=6 for each group). **(B)** The frequency $CD3^+CD8^+IFN\text{-}\gamma^+$ T cells in the spleen and lymph nodes of rhabdomyosarcom-bearing wild-type and $APN^{-/-}$ mice (n=4 for each group). **(C)** The levels of IFN-γ, perforin, TNF-α and IL-10 in the serum of rhabdomyosarcom-bearing wild-type and $APN^{-/-}$ mice (n=6 for each group). Data are expressed as the mean ± SEM. *p<.05 and **p<.01.

Moreover, Wang et al. reported that p-STAT3 was highly expressed on circulating $CD8^+$ T cells in peripheral blood from hepatocellular carcinoma (HCC) patients. Highly expressed p-STAT3 was positively correlated to high levels of IL-4, IL-6, and IL-10, and negatively correlated to low levels of IFN-γ in the serum, which may contribute to immune surveillance disability against tumor cells (22). In the present study, we observed a lower expression of p-STAT3 in $CD8^+$ T cells isolated from rhabdomyosarcoma-bearing $APN^{-/-}$ mice, which was also accompanied by higher IFN-γ and lower IL-10 in the serum. We also found that inhibition of STAT3 activation *in vivo* by STAT3 inhibitor greatly increased $CD8^+$ and $CD8^+IFN\text{-}\gamma^+$ T cells in the spleen and lymph nodes of rhabdomyosarcoma-bearing wild-type mice. These facts clearly indicate that the STAT3 signaling pathway may partly contribute to the effect of APN deficiency in promoting $CD8^+$ T cell activation and cytotoxicity.

In summary, this study demonstrated that APN deficiency could promote $CD8^+$ T cell activation and their cytotoxicity to kill tumors *via* inhibiting the STAT3 signaling pathway, and proved that targeting APN had potential in the treatment of rhabdomyosarcoma.

MATERIALS AND METHODS

Animals and Tumor Models

C57BL/6 wild-type mice were purchased from Beijing Vital River Laboratory Animal Technology Co., Ltd. (Beijing, China). APN knockout mice with a C57/BL6 background were a kind gift from Prof. AM Xu (The University of Hong Kong). The mice were housed and bred in a specific pathogen-free/SPF environment with a 12-h inverted light–dark cycle at a temperature of 23 ± 2°C. Six-to-eight-week-old male offspring of C57BL/6 wild-type mice and $APN^{-/-}$ mice were selected for the experiments. Soft tissue sarcoma was established as described in our previous study (17).

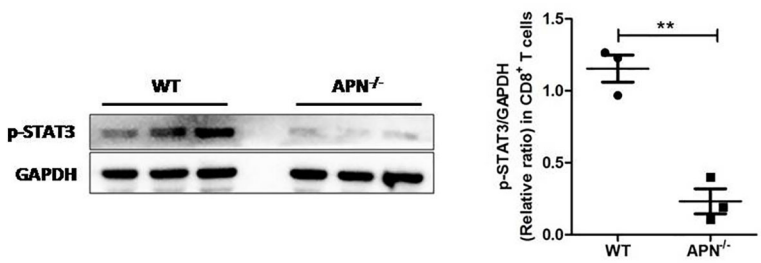

FIGURE 5 | APN deficiency inhibits STAT3 activation in $CD8^+$ T cells. MN/MCA1 cellswere inoculated in wild type (WT) and APN deficiency ($APN^{-/-}$) mice, the $CD8^+$ T cells were isolated from the spleen and lymph nodes after day 21. The expression of p-STAT3 was detected by western blot. Data are expressed as the mean ± SEM (n=3 independent mice for each group). $^{**}p<.01$.

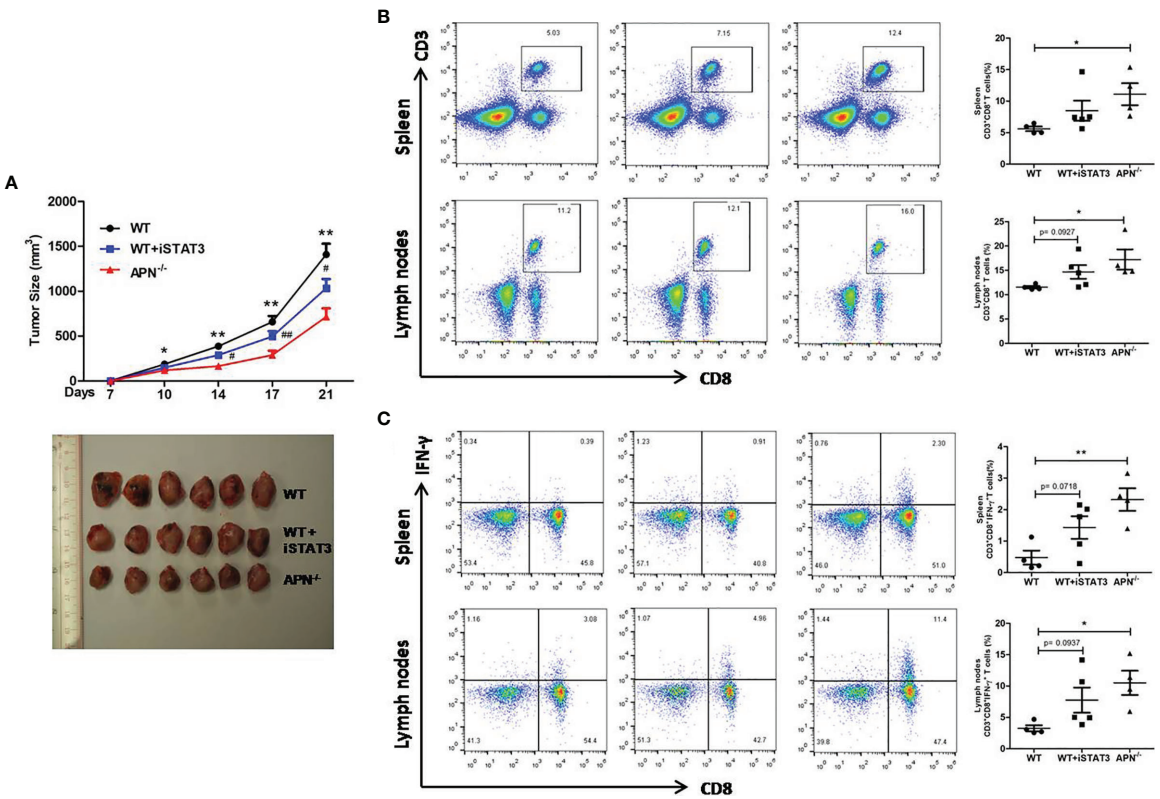

FIGURE 6 | STAT3 inhibition suppresses rhabdomyosarcom growth and increases the accumulation of $CD8^+$ and $CD8^+IFN\text{-}\gamma^+$ T cells in the spleen and lymph nodes. **(A)** Tumor size of wild type (WT), STAT3 inhibitor Stattic-treated WT (WT+iSTAT3) and APN deficiency ($APN^{-/-}$) mice (n=6 for each group); compared to $APN^{-/-}$ mice, $^*p < .05$ and $^{**}p < .01$; compared to WT mice, $^{\#}p < .05$ and $^{\#\#}p < .01$. **(B)** The frequency $CD3^+CD8^+$ T cells in the spleen and lymph nodes of WT, WT+iSTAT3 and $APN^{-/-}$ mice (n=4-5 for each group). **(C)** The frequency $CD3^+CD8^+IFN\text{-}\gamma+$ T cells in the spleen and lymph nodes of WT, WT+iSTAT3 and $APN^{-/-}$ mice (n=4-5 for each group). Data are expressed as the mean ± SEM. $^*p<.05$ and $^{**}p<.01$.

In brief, 1×10^5 MN/MCA1 cells were intramuscular injected into the caudal thigh muscle of mice. The tumor mass was measured, and the size was recorded twice a week. On day 21, the mice were sacrificed. The experimental protocol in this study was approved by the Animal Ethics Committees of Shenzhen University (Shenzhen, China) accordance to the National Institutes of Health guide for the Care and Use of Laboratory Animals (Registration No. 2018020).

Purification and Stimulation of $CD8^+$ T Cells

The $CD8^+$ T cells were purified from the spleens of wild-type and $APN^{-/-}$ mice after lysing red cells by positive selection using

immunomagnetic beads according to the manufacturer's instructions (CD8β [Ly-2] MicroBeads, Miltenyi). The purity of $CD8^+$ T cells was verified above 95% cutoff by FACS determination using FITC-conjugated anti-CD8β antibody (eBioscience). Purified $CD8^+$ T cells were stimulated with or without plate-bound anti-CD3 mAb (5 μg/mL) in combination with anti-CD28 mAb (1 μg/mL), in the presence or absence of APN (5μg/mL or a series of concentrations, as indicated).

Immunomodulatory Antibody and Static Treatments

To examine the role of $CD8^+$ T cells in APN deficiency-mediated inhibition of rhabdomyosarcoma growth, anti-mouse CD8α mAb (250 μg/mouse, BioXcell, West Lebanon, NH, USA) dissolved in 0.1 mL normal saline was intravenously injected into the tail of rhabdomyosarcoma-bearing $APN^{-/-}$ mice every two days from day 7 to day 21. In the control mice, 0.1 mL of normal saline was injected. To determine the effect of blocking STAT3 signaling, STAT3 inhibitor stattic (10 mg/Kg, MCE, New Jersey, USA) dissolved in 0.25 mL normal saline containing 40% PEG400 and 1% dimethyl sulfoxide was intraperitoneally injected into rhabdomyosarcoma-bearing wild-type mice every two days from day 7 to day 21, according to previous reports (23, 24). In the control mice, 0.25 mL of normal saline containing 40% PEG400 and 1% dimethyl sulfoxide was injected.

Cell Viability and Proliferation Assay

Purified $CD8^+$ T cells from the spleen of wild-type mice were cultured in 96- or 24-well plates with a combination of plate-bound anti-CD3 mAb (5 μg/mL) and anti-CD28 mAb (1 μg/mL), in the presence of indicated concentrations of APN (0, 0.2, 1, and 5 μg/mL). The cells were then incubated for 24 h at 37°C and 5% CO_2. Cell viability and proliferation were analyzed with a Cell Counting Kit-8 (CCK8, Beyotime, Shanghai, China) and a 5-bromo2-deoxyuridine (BrdU) proliferation ELISA kit (Beyotime, Shanghai, China), respectively, according to the manufacturer's protocols.

Transwell Migration Assay

The migration assay was performed using a transwell chamber (8 μm; Corning). Purified $CD8^+$ T cells (5×10^6/well) from the spleen of wild-type mice were suspended in 100 μL medium were placed into the top chamber, and 600 μL medium containing APN (5 μg/mL) was added to the bottom well. After 24 h of incubation, cells in the bottom well were collected and counted using a Countess automated cell counter (Thermo Fisher Scientific).

Immunohistochemistry Analysis

Immunohistochemistry was performed as previously described (17). In brief, paraffin sections of tumors were cut at 4 μm thickness and subjected to immunohistochemistry by heat-induced epitope retrieval with citrate buffer (0.01 M, pH 6.0). The samples were then treated with an endogenous peroxidase blocking solution (Dako Corp., Carpinteria, CA) and 10% goat serum to inhibit nonspecific binding. The tumor sections were incubated overnight with CD8 antibody at 4°C. The signals were detected using a VECTASTAIN Elite ABC Kit (Vector Laboratories, Burlingame, CA) according to the manufacturer's instructions.

Flow Cytometry Analysis

The spleens and lymph nodes were lightly ground between the frosted edges of two sterile glass slides, and the cell suspension was filtered through the 70-μm cell strainer. Immunosubsets from tumors, spleens, and lymph nodes were detected by flow cytometry (BD Biosciences, San Jose, CA). The frequency of $CD8^+IFN\text{-}\gamma^+$ T cells was assessed using intracellular cytokine staining. Purified cells were stimulated with PMA (10 ng/mL) and ionomycin (1 μg/mL) for 4 h and incubated for the last 1 h with brefeldin A (10 μg/mL). Cells were subjected to intracellular cytokine analysis using anti-IFN-γ antibody. The antibodies used for FACS included Pacific blue-conjugated anti-CD3, APC-conjugated anti-CD8, and PE-conjugated anti-IFN-γ (eBioscience). The data were analyzed using FlowJo software (TreeStar Inc., San Carlos, CA).

RNA Extraction and RT-PCR Analysis

The total RNA of the $CD8^+$ T cells was extracted using TRIzol® (Invitrogen) RNA extraction protocol. cDNA was synthesized using a Reverse Transcription Kit (Takara, Osaka, Japan), and quantitative real-time PCR was performed on an ABI 7500 Real-Time PCR (RT-PCR) system using a SYBR Green Master Mix (Applied Biosystems, Foster, CA, USA). Relative quantification of mRNA expression was normalized with β-actin and analyzed using the delta-delta Ct ($^{2\text{-}\Delta\Delta}$CT) method. Primer sequences (forward/reverse) were listed as follows: m-AdipoR1, forward 5′-ACG TTG GAG AGT CAT CCC GTA T-3′ and reverse 5′-CTC TGT GTG GAT GCG GAA GAT-3′; m-AdipoR2, forward 5′-GCC CAG CTT AGA GAC ACC TG-3′ and reverse 5′-GCC TTC CCA CAC CTT ACA AA-3′; m-IFN-γ, forward 5′- GCC ACG GCA CAG TCA TTG A-3′ and reverse 5′- TGC TGA TGG CCT GAT TGT CTT-3′; m-perforin, forward 5′- CAA GGT AGC CAA TTT TGC AGC-3′ and reverse 5′- GTA CAT GCG ACA CTC TAC TGT G-3′; m-CXCR3, forward 5′- TAC CTT GAG GTT AGT GAA CGT CA-3′ and reverse 5′- CGC TCT CGT TTT CCC CAT AAT C-3′; m-Gzma, forward 5′- TAC CTT GAG GTT AGT GAA CGT CA-3′ and reverse 5′-TGC TGCCCA CTG TAA CGT G-3′; m-β-actin, forward 5′-TGT CCA CCT TCC AGC AGA TGT-3′ and reverse 5′-AGC TCA GTA ACA GTC CGC CTA GA-3′.

ELISA and Western Blotting

The levels of IFN-γ, perforin, TNF-α, and IL-10 in the serum were measured by ELISA (BD Bioscience, San Jose, CA) according to the manufacturer's instructions. Western blotting was performed as previously described (23). Proteins were extracted from $CD8^+$ T cells in the presence of a cocktail of phosphatase inhibitors and phenylmethylsulfonyl fluoride (PMSF) (Roche Applied Science, Branford, CT, USA), resolved,separated by 8–10% SDS-PAGE, and transferred to PVDF membranes. The membranes were then probed with the primary antibodies against p-STAT3 and GAPDH (Cell Signaling Technology, Beverly, MA, USA). Following incubation with the corresponding horseradish peroxidase-conjugated secondary antibodies, the protein bands were visualized with enhanced chemiluminescence reagents (Thermo Scientific, Rockford, IL, USA), detected using the ECL system, and the band intensity was measured using ImageJ software (National Institutes of Health, Bethesda, Maryland, USA).

Statistical Analysis

GraphPad Prism 5.0 software (GraphPad Software Inc., San Diego, CA, USA) was used for all calculations. The results are expressed as the mean ± standard error of the mean (SEM). Comparisons between two groups were performed using a two-tailed Student's t-test, and comparisons between multiple groups were performed usingone-way ANOVA, followed by Duncan's multiple range tests. A $p < .05$ was considered statistically significant.

DATA AVAILABILITY STATEMENT

The original contributions presented in the study are included in the article/supplementary material. Further inquiries can be directed to the corresponding author.

ETHICS STATEMENT

The animal study was reviewed and approved by Animal Ethics Committees of Shenzhen University.

AUTHOR CONTRIBUTIONS

HX: Conceptualization, writing-original draft, and funding acquisition. JP: Investigation and funding acquisition. HH: Investigation and analyzed data. QH: Investigation. CL, ZG, DH: Data analysis, methodology and resources. XS: Conceptualization and edited the manuscript. All authors contributed to the article and approved the submitted version.

ACKNOWLEDGMENTS

This work was kindly funded by the National Natural Science Foundation of China (Project Nos. 81660479); Bethune Charitable Foundation of China (B-19-H-20200622), Medical Science and Technology Research Foundation of Guangdong province, China (A2020157 and A2020272). Also, we thank Instrument Analysis Center of Shenzhen University for the assistance with flow cytometry analysis.

REFERENCES

1. Skapek SX, Ferrari A, Gupta AA, Lupo PJ, Butler E, Shipley J, et al. Rhabdomyosarcoma. *Nat Rev Dis Primers* (2019) 5:1. doi: 10.1038/s41572-018-0051-2
2. Rogers TN, Dasgupta R. Management of Rhabdomyosarcoma in Pediatric Patients. *Surg Oncol Clin N Am* (2021) 30:339–53. doi: 10.1016/j.soc.2020.11.003
3. Nguyen TH, Barr FG. Therapeutic Approaches Targeting PAX3-FOXO1 and Its Regulatory and Transcriptional Pathways in Rhabdomyosarcoma. *Molecules* (2018) 23:2798. doi: 10.3390/molecules23112798
4. Meadors JL, Cui Y, Chen QR, Song YK, Khan J, Merlino G, et al. Murine Rhabdomyosarcoma is Immunogenic and Responsive to T-Cell-Based Immunotherapy. *Pediatr Blood Cancer* (2011) 57:921–9. doi: 10.1002/pbc.23048
5. Xiao W, Wang J, Wen X, Xu B, Que Y, Yu K, et al. Chimeric Antigen Receptor-Modified T-Cell Therapy for Platelet-Derived Growth Factor Receptor Alpha-Positive Rhabdomyosarcoma. *Cancer* (2020) 126(Suppl 9):2093–100. doi: 10.1002/cncr.32764
6. Yang J, Liu R, Deng Y, Qian J, Lu Z, Wang Y, et al. MiR-15a/16 Deficiency Enhances Anti-Tumor Immunity of Glioma-Infiltrating CD8+ T Cells Through Targeting mTOR. *Int J Cancer* (2017) 141:2082–92. doi: 10.1002/ijc.30912
7. Tan PH, Tyrrell HE, Gao L, Xu D, Quan J, Gill D, et al. Adiponectin Receptor Signaling on Dendritic Cells Blunts Antitumor Immunity. *Cancer Res* (2014) 74:5711–22. doi: 10.1158/0008-5472.CAN-13-1397
8. Wolf AM, Wolf D, Rumpold H, Enrich B, Tilg H. Adiponectin Induces the Anti-Inflammatory Cytokines IL-10 and IL-1RA in Human Leukocytes. *Biochem Biophys Res Commun* (2004) 323:630–5. doi: 10.1016/j.bbrc.2004.08.145
9. Kyriazi E, Tsiotra PC, Boutati E, Ikonomidis I, Fountoulaki K, Maratou E, et al. Effects of Adiponectin in TNF-Alpha, IL-6, and IL-10 Cytokine Production From Coronary Artery Disease Macrophages. *Horm Metab Res* (2011) 43:537–44. doi: 10.1055/s-0031-1277227
10. Wulster-Radcliffe MC, Ajuwon KM, Wang J, Christian JA, Spurlock ME. Adiponectin Differentially Regulates Cytokines in Porcine Macrophages. *Biochem Biophys Res Commun* (2004) 316:924–9. doi: 10.1016/j.bbrc.2004.02.130
11. Huang H, Park PH, McMullen MR, Nagy LE. Mechanisms for the Anti-Inflammatory Effects of Adiponectin in Macrophages. *J Gastroenterol Hepatol* (2008) 23(Suppl 1):S50–53. doi: 10.1111/j.1440-1746.2007.05284.x
12. Mandal P, Pratt BT, Barnes M, McMullen MR, Nagy LE. Molecular Mechanism for Adiponectin-Dependent M2 Macrophage Polarization: Link Between the Metabolic and Innate Immune Activity of Full-Length Adiponectin. *J Biol Chem* (2011) 286:13460–9. doi: 10.1074/jbc.M110.204644
13. Qi GM, Jia LX, Li YL, Li HH, Du J. Adiponectin Suppresses Angiotensin II-Induced Inflammation and Cardiac Fibrosis Through Activation of Macrophage Autophagy. *Endocrinology* (2014) 155:2254–65. doi: 10.1210/en.2013-2011
14. Yamauchi T, Kamon J, Waki H, Imai Y, Shimozawa N, Hioki K, et al. Globular Adiponectin Protected Ob/Ob Mice From Diabetes and ApoE-Deficient Mice From Atherosclerosis. *J Biol Chem* (2003) 278:2461–8. doi: 10.1074/jbc.M209033200
15. Tsang JY, Li D, Ho D, Peng J, Xu A, Lamb J, et al. Novel Immunomodulatory Effects of Adiponectin on Dendritic Cell Functions. *Int Immunopharmacol* (2011) 11:604–9. doi: 10.1016/j.intimp.2010.11.009
16. Wilk S, Scheibenbogen C, Bauer S, Jenke A, Rother M, Guerreiro M, et al. Adiponectin is a Negative Regulator of Antigen-Activated T Cells. *Eur J Immunol* (2011) 41:2323–32. doi: 10.1002/eji.201041349
17. Peng J, Tsang JY, Ho DH, Zhang R, Xiao H, Li D, et al. Modulatory Effects of Adiponectin on the Polarization of Tumor-Associated Macrophages. *Int J Cancer* (2015) 137:848–58. doi: 10.1002/ijc.29485
18. Zhang C, Yue C, Herrmann A, Song J, Egelston C, Wang T, et al. STAT3 Activation-Induced Fatty Acid Oxidation in CD8(+) T Effector Cells Is Critical for Obesity-Promoted Breast Tumor Growth. *Cell Metab* (2020) 31:148–161 e145. doi: 10.1016/j.cmet.2019.10.013
19. Yue C, Shen S, Deng J, Priceman SJ, Li W, Huang A, et al. STAT3 in CD8+ T Cells Inhibits Their Tumor Accumulation by Downregulating CXCR3/CXCL10 Axis. *Cancer Immunol Res* (2015) 3:864–70. doi: 10.1158/2326-6066.CIR-15-0014
20. Durgeau A, Virk Y, Corgnac S, Mami-Chouaib F. Recent Advances in Targeting CD8 T-Cell Immunity for More Effective Cancer Immunotherapy. *Front Immunol* (2018) 9:14. doi: 10.3389/fimmu.2018.00014
21. Kujawski M, Zhang C, Herrmann A, Reckamp K, Scuto A, Jensen M, et al. Targeting STAT3 in Adoptively Transferred T Cells Promotes Their *in vivo* expansion antitumor effects . *Cancer Res* (2010) 70:9599–610. doi: 10.1158/0008-5472.CAN-10-1293
22. Wang X, Xin W, Zhang H, Zhang F, Gao M, Yuan L, et al. Aberrant Expression of P-STAT3 in Peripheral Blood CD4+ and CD8+ T Cells Related to Hepatocellular Carcinoma Development. *Mol Med Rep* (2014) 10:2649–56. doi: 10.3892/mmr.2014.2510
23. Li Q, Zhang D, Chen X, He L, Li T, Xu X, et al. Nuclear PKM2 Contributes to Gefitinib Resistance *via* upregulation STAT3 activation colorectal cancer. *Sci Rep* (2015) 5:16082. doi: 10.1038/srep16082
24. Yokota T, Omachi K, Suico MA, Kamura M, Kojima H, Fukuda R, et al. STAT3 Inhibition Attenuates the Progressive Phenotypes of Alport Syndrome

Mouse Model. *Nephrol Dial Transplant* (2018) 33:214–23. doi: 10.1093/ndt/gfx246

Conflict of Interest: The authors declare that the research was conducted in the absence of any commercial or financial relationships that could be construed as a potential conflict of interest.

Publisher's Note: All claims expressed in this article are solely those of the authors and do not necessarily represent those of their affiliated organizations, or those of the publisher, the editors and the reviewers. Any product that may be evaluated in this article, or claim that may be made by its manufacturer, is not guaranteed or endorsed by the publisher.

frontiers | Frontiers in Immunology

ORIGINAL RESEARCH
published: 04 May 2022
doi: 10.3389/fimmu.2022.853904

Pediatric Pan-Central Nervous System Tumor Methylome Analyses Reveal Immune-Related LncRNAs

Yongsheng Li[1†], Sicong Xu[1†], Dahua Xu[1†], Tao Pan[1], Jing Guo[1], Shuo Gu[1], Qiuyu Lin[1], Xia Li[1,2], Kongning Li[1*] and Wei Xiang[1*]*

[1] College of Biomedical Information and Engineering, NHC Key Laboratory of Control of Tropical Diseases, Hainan Women and Children's Medical Center, Hainan Medical University, Haikou, China, [2] College of Bioinformatics Science and Technology, Harbin Medical University, Harbin, China

OPEN ACCESS

Edited by:
Riccardo Dolcetti,
Peter MacCallum Cancer Centre, Australia

Reviewed by:
Wenhao Ouyang,
Sun Yat-Sen Memorial Hospital, China
Swapna Mahurkar-Joshi,
University of California, Los Angeles, United States
Hongwei Wang,
Sun Yat-sen University, China

***Correspondence:**
Xia Li
lixia@hrbmu.edu.cn
Kongning Li
likongning@hainmc.edu.cn
Wei Xiang
xiangwei8@163.com

[†]These authors have contributed equally to this work

Specialty section:
This article was submitted to Cancer Immunity and Immunotherapy, a section of the journal Frontiers in Immunology

Received: 13 January 2022
Accepted: 11 April 2022
Published: 04 May 2022

Citation:
Li Y, Xu S, Xu D, Pan T, Guo J, Gu S, Lin Q, Li X, Li K and Xiang W (2022) Pediatric Pan-Central Nervous System Tumor Methylome Analyses Reveal Immune-Related LncRNAs. Front. Immunol. 13:853904. doi: 10.3389/fimmu.2022.853904

Pediatric central nervous system (CNS) tumors are the second most common cancer diagnosis among children. Long noncoding RNAs (lncRNAs) emerge as critical regulators of gene expression, and they play fundamental roles in immune regulation. However, knowledge on epigenetic changes in lncRNAs in diverse types of pediatric CNS tumors is lacking. Here, we integrated the DNA methylation profiles of 2,257 pediatric CNS tumors across 61 subtypes with lncRNA annotations and presented the epigenetically regulated landscape of lncRNAs. We revealed the prevalent lncRNA methylation heterogeneity across pediatric pan-CNS tumors. Based on lncRNA methylation profiles, we refined 14 lncRNA methylation clusters with distinct immune microenvironment patterns. Moreover, we found that lncRNA methylations were significantly correlated with immune cell infiltrations in diverse tumor subtypes. Immune-related lncRNAs were further identified by investigating their correlation with immune cell infiltrations and potentially regulated target genes. LncRNA with methylation perturbations potentially regulate the genes in immune-related pathways. We finally identified several candidate immune-related lncRNA biomarkers (i.e., SSTR5-AS1, CNTN4-AS1, and OSTM1-AS1) in pediatric cancer for further functional validation. In summary, our study represents a comprehensive repertoire of epigenetically regulated immune-related lncRNAs in pediatric pan-CNS tumors, and will facilitate the development of immunotherapeutic targets.

Keywords: pediatric tumors, immune pathways, cancer subtypes, long non-coding RNAs, DNA methylation

INTRODUCTION

Pediatric central nervous system (CNS) tumors are the second most common cancer among children (1), which form a heterogeneous group of tumors and are responsible for the highest number of cancer-related deaths in children (2). Genomic studies have revealed a number of genomic variants across new diagnoses as well as relapsed pediatric cancers (3, 4). It is now well established that high-throughput next-generation sequencing (NGS) approaches add significant value for cancer diagnoses and prognostic and therapeutic targets (5, 6). However, the discovery of pediatric cancer-associated alterations has primarily focused on genetic variants. Epigenome

alterations that contribute to deregulate transcription and promote oncogenic pathways in pediatric cancer are still largely unknown.

DNA methylation has a substantial impact on gene expression, affecting the development and progression of cancer (7). Emerging NGS technologies have increased our understanding of the DNA methylation in pediatric cancer biomarker identification, subtype classification, and prognostication (8). For example, the methylation age has been found to have potential as a prognostic biomarker in pediatric tumors (9). Genome-wide DNA methylation studies have identified hyper-methylated genes involved in tissue development in pediatric embryonic and alveolar rhabdomyosarcomas (10). DNA methylation profiles have been widely used to sub-classify CNS tumors, including pediatric cancer (11). These data highlight the important roles of DNA methylation in diverse pediatric CNS tumors. However, the majority of these studies focused on the DNA methylation perturbation in protein-coding genes, particularly the promoter regions.

Deep sequencing with new computational approaches for assembling transcriptome has identified tens of thousands of long noncoding RNAs (lncRNAs) across different tissues and cell types (12, 13). LncRNAs have been found to play important roles in diverse pediatric cancers. HOXD-AS1 was found to control the expression levels of clinically significant protein-coding genes involved in angiogenesis and inflammation in neuroblastomas (14). Linc-NeD125 can function independently of the hosted microRNA, by reducing cell proliferation and activating BCL-2 in neuroblastomas (15). Moreover, DNA methylation has been found to be a fundamental feature of epigenomes that can affect the expression of lncRNAs (16). Although several lncRNA methylation perturbations have been revealed in pediatric cancer, we still lack knowledge on the epigenetic landscapes of lncRNAs in diverse pediatric CNS tumors.

Moreover, immune therapy is an attractive alternative approach for targeting CNS tumors. Several studies have revealed the complex tumor immune microenvironment (TIME) in CNS tumors. For instance, tumor-associated macrophages make up a large proportion of immune cells in glioma patients and are associated with tumor grade (17). Activation of CD8 T cells can establish a neuron–immune–cancer axis, which was responsible for glioma growth (18). A recent study described the TIME of pediatric CNS tumors and identified tumor-specific immune clusters with phenotypic characteristics relevant to immunotherapy response (19). Furthermore, lncRNAs have been demonstrated to play important roles in cancer immunology (20–22). However, only a few immune-related lncRNAs have been identified in pediatric CNS tumors. Therefore, further studies on lncRNAs and their roles in immune regulation will be essential to identify immunotherapy targets in pediatric cancer.

To systematically analyze the epigenetically regulated lncRNAs across pediatric CNS tumors, we integrated the DNA methylation profiles of 2,257 pediatric CNS tumors across 61 subtypes. We revealed prevalent lncRNA methylation and further classified pediatric cancer into 14 lncRNA methylation clusters, which were characterized by distinct phenotypes. We also found that lncRNA methylations are significantly correlated with immune cell infiltrations and potentially regulate immune-related pathways. We show that analysis of lncRNA methylation can identify immune-related lncRNA biomarkers in pediatric cancers.

MATERIALS AND METHODS

DNA Methylation Across Pediatric Tumors

DNA methylation profiles across pediatric CNS tumors were collected from Gene Expression Omnibus (GEO) and ArrayExpress (**Table S1**). Here, an Illumina HumanMethylation 450 BeadChip was used for profiling the DNA methylation in pediatric cancers (19). In total, genome-wide DNA methylation profiles of 2,257 pediatric CNS tumors (age < 19 years old) across 61 World Health Organization (WHO) histopathological entities were extracted. To include the comprehensive pediatric cancer samples, we included all patients in our analysis. The raw ".idat" files were background-corrected, single-sample Noob and functional normalized (23) based on the "preprocessFunnorm" module in the minfi v.1.34.0 package (24).

LncRNA Annotations and Genomic Features

Genome-wide annotations of lncRNAs were downloaded from GENCODE (V34, GRCh38) (25). The numbers of exons for lncRNAs were calculated based on exon annotation of lncRNAs. The evolutionary conservation scores for lncRNAs were obtained using the phastCons100way.UCSC.hg38 (3.7.1) R package (26). The GC content and normalized CpG fraction (observed CpG/expected CpG) were calculated based on the sequences of lncRNAs, where the expected CpG was calculated as $(\text{GC content}/2)^2$ (27).

LncRNA Methylation

The genomic locations of DNA methylation probes were first transferred from GRCh37 to corresponding coordinates in GRCh38 through UCSC LiftOver (https://genome.ucsc.edu/cgi-bin/hgLiftOver). Next, the probes were filtered similar to one of the previous studies (11). First, the probes that were located on chromosomes X and Y were excluded. Next, the probes that included a single-nucleotide polymorphism (SNP) and those not mapping uniquely to the CRCh37 were excluded. In addition, we excluded probes that were not included in the Illumina EPIC array.

Next, we mapped the probes to the promoter regions of lncRNAs and protein-coding genes. Promoter regions were defined as the 4-kb regions centered at the transcriptional start sites (TSSs) of lncRNAs and genes (28, 29). In total, 56,072 and 156,664 probes were mapped to 9,389 and 17,762 protein-coding genes, respectively.

Classification of LncRNAs

The DNA methylation levels of lncRNAs were calculated as the average beta values of probes that mapped to the promoter

regions (30). Next, lncRNAs were classified into three categories: (i) hyper-methylated lncRNAs were defined as those with methylation levels > 0.7 in more than 80% samples; (ii) hypo-methylated lncRNAs were defined as those with methylation levels < 0.3 in more than 80% samples; and (iii) other lncRNAs not in the hyper- or hypo-methylated group were defined as inter-methylated lncRNAs.

The genomic differences (such as GC contents and normalized CpG fractions) among three lncRNAs groups were evaluated by Kolmogorov–Smirnov tests. Differences in conservation scores, number of CpGs, and exons were evaluated by Wilcoxon's rank sum tests.

Identification of Tumor Subtypes Based on LncRNA methylation

First, we selected the top 5% probes with high variation (S.D. > 0.267) that mapped to lncRNA promoters. The DNA methylation profiles of variable CpG sites were used for clustering the pediatric CNS tumor samples. The ConsensusClusterPlus package was used to identify the cancer subtypes (31), with 50 iterations and a resample rate of 0.8. The number of clusters ranged from $k = 2$ to 60. In addition, Pearson correlation coefficient was calculated for paired samples based on the DNA methylation profiles.

Likelihood Ratio Test

The Cox proportional hazards model was first constructed based on clinical features, including gender and age. Next, another two models that added WHO catalogs and lncRNA-based subtypes were used. Clinical clusters represent the Cox model constructed by gender and age. Original clusters represent the Cox model constructed by gender, age, and WHO category. LncRNA clusters represent the Cox model constructed by gender, age, WHO category, and lncRNA clusters. We estimated the likelihood ratio (LR) statistic of three regression models and the changes in LR were assessed by Chi-square test (32).

Immune Cell Infiltration in Pediatric Tumors

To estimate the immune cell infiltration in pediatric tumors, we first downloaded the signature matrix "StromalMatrix_V2" from MethyCIBERSORT (33). CpG signatures were provided for CD14+ (monocyte lineage), CD19+ (B-lymphocytes), effector lymphocytes (CD4_Eff), CD56+ (NK cells), CD8 (cytotoxic T-lymphocytes), endothelial cells, eosinophils (Eos), fibroblasts, neutrophils (Neu), and regulatory T lymphocytes (Treg). Next, the DNA methylation profiles were subjected into CIBERSORT with the DNA methylation signature (34). CIBERSORT was run based on 100 permutations without quantile normalization.

Immune Signatures

The immune signatures gene sets, including immune checkpoints, immune cytolytic activity (CYT), human leukocyte antigen (HLA), interferon (IFN) response, and tumor-infiltrating lymphocytes (TILs), were obtained from a previous study (35). In addition, 301 CpG probes that could predict the response to anti-PD-1 treatment in non-small cell lung cancer were collected (36). Another 67 immune cell type-specific gene–CpG pairs for 21 immune cell populations were collected from literature (37). The average methylation levels of related genes were used to estimate the DNA methylation activity of immune signatures. All CpG sites related to immune signatures are provided in **Table S2**.

Identification of Immune Cell Infiltration-Related LncRNAs

To identify immune cell infiltration-related lncRNAs, we calculated the Spearman correlation coefficient (SCC) between immune cell infiltration levels and lncRNA methylation in a specific pediatric CNS tumor subtype. LncRNAs with absolute SCC > 0.3 and p-adjusted < 0.05 were considered as immune cell infiltration-related lncRNAs.

Identification of LncRNAs Associated With Immune-Related Pathways

First, 1,811 protein coding genes involved in 17 immune-related pathways were obtained from one of our previous studies (20). Next, we identified the protein-coding gene within 10 kb for each immune cell infiltration-related lncRNA based on genomic locations. If the protein-coding gene within 10 kb was annotated in immune-related pathways, we considered this lncRNA to be involved in the regulation of immune-related pathways.

Differential Methylation and Survival Analysis

We compared the DNA methylation differences of lncRNAs based on t-test in a "one vs. rest" way. LncRNAs with an absolute value of methylation difference greater than 0.2 and a p-value less than 0.05 were considered to be differentially methylated.

Tumor samples were divided into two groups based on the DNA methylation level of lncRNAs. The cutoff was determined by the internal R function "survminer: surv_cutpoint". The difference in overall survival between two groups was assessed by the log-rank test.

RESULTS

Landscape of LncRNA Methylation in CNS Tumors

To investigate the methylation of lncRNAs, we obtained the genome-wide DNA methylation profiles for 2,257 pediatric tumor samples. In order to account for molecular or histological subtypes, these samples were further stratified into a total of 12 main classes, including 61 WHO-defined CNS tumor subtypes (**Figure 1A**), as previously defined (11). Next, we determine lncRNA methylation in cancers and classified lncRNAs into three categories according to the methylation profiles of pediatric tumors (**Figure 1B**). Approximately 30% of lncRNAs exhibited hyper-methylation and 40% of lncRNAs exhibited hypo-methylation across cancer subtypes (**Figure 1B**).

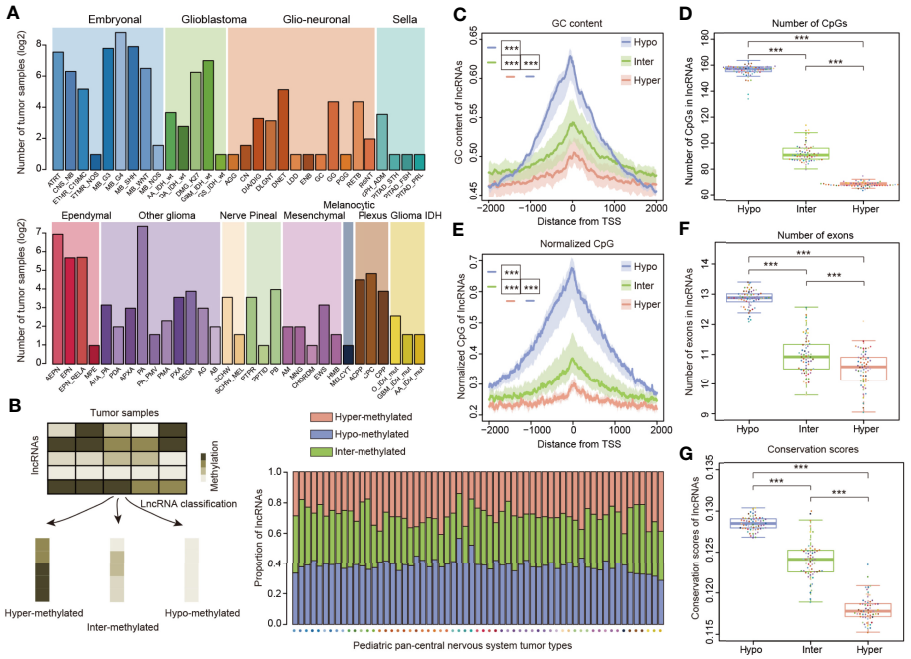

FIGURE 1 | LncRNA methylation patterns in pediatric pan-CNS tumors. **(A)** Number of tumor samples across different types of pediatric CNS tumors. The patients were classified into 12 major clusters with 61 sub-clusters. **(B)** Method to define the lncRNAs with different methylation patterns. The bar plots in the lower third show the proportion of lncRNAs with different methylation patterns across cancer types. **(C)** Distributions of GC content around the TSSs for lncRNAs with different methylation patterns. **(D)** Box plots showing the number of CpGs in lncRNA promoters with different methylation patterns. **(E)** Distributions of normalized CpG around the TSSs for lncRNAs with different methylation patterns. **(F)** Box plots showing the number of exons in lncRNAs for lncRNAs with different methylation patterns. **(G)** Box plots showing the average conservation scores in lncRNA promoters with different methylation patterns. *** indicates $p < 0.001$.

Since genes or lncRNAs with distinct methylation patterns exhibited different genomic characteristics (30, 38), we next compared the genomic and evolutional features of lncRNAs in three categories. We found that the enrichment of GC content and CpGs in all three types of lncRNAs is symmetric and peaks around the core lncRNA promoters (**Figures 1C, D**). In addition, hypo-methylated lncRNAs had significantly higher GC content and number of CpGs than the other two categories (**Figures 1C, D**, $p < 0.001$). As the number of CpGs might be affected by the length or GC content of lncRNAs, we thus calculated the normalized CpGs of lncRNAs. We found that hypo-methylated lncRNAs also had significantly higher normalized CpGs than the other two groups (**Figure 1E**, p-values < 0.001). These results were consistent with observations in protein-coding genes that high-CpG-content genes are hypo-methylated (27).

While lncRNAs exons are much less conserved than protein-coding genes (12), it is unknown whether the lncRNAs with different methylation patterns evolve in a distinct way. First, we compared the number of exons in lncRNAs and found that hypo-methylated lncRNAs had more exons than other lncRNAs (**Figure 1F**, p-values < 0.001). To quantify the evolutionary conservation of lncRNA promoters, we used phastCons scores of placental mammals (26). We compared the average conservation score of lncRNAs and found that hypo-methylated lncRNAs had significantly higher conservation scores (**Figure 1G**, p-values < 0.001). Similarly, we obtained the same results when we analyzed the pediatric cancer individually (**Figure S1**).

LncRNA Methylation Heterogeneity in CNS Tumors

Previous studies have reported substantial variability in the histopathological diagnosis of many CNS tumors (39). We next investigated the extent of the lncRNA methylation heterogeneity in pediatric CNS tumors. Consensus clustering of lncRNAs with variable DNA methylation identified 14 optimal subtypes that we refer to as C1–C7 and C9–C15 (**Figure 2A** and **Figure S2**, **Table S3**). Moreover, we visualized the Pearson correlation coefficient (PCC) of lncRNA methylations among tumor patients and found that patients clustered in the same clusters exhibited higher similarity in lncRNA methylation (**Figure 2B**). We next analyzed the compositions of cancer types in 14 lncRNA methylation clusters. Patients in several lncRNA clusters (i.e., C2, C3, C4, and C12) predominantly had an individual cancer type, while patients in C1, C5, C10 and C13 diverse types of pediatric cancer (**Figure 2C**). In particular, the patients in C1 were much heterogeneous, including 652 patients from 48 cancer types.

We next sought to characterize a more refined lncRNA methylation pattern in a single tumor type. We focused on medulloblastoma, which was classified into four subtypes (Group 3, Group 4, SHH, and WNT) in a previous study (40). We found

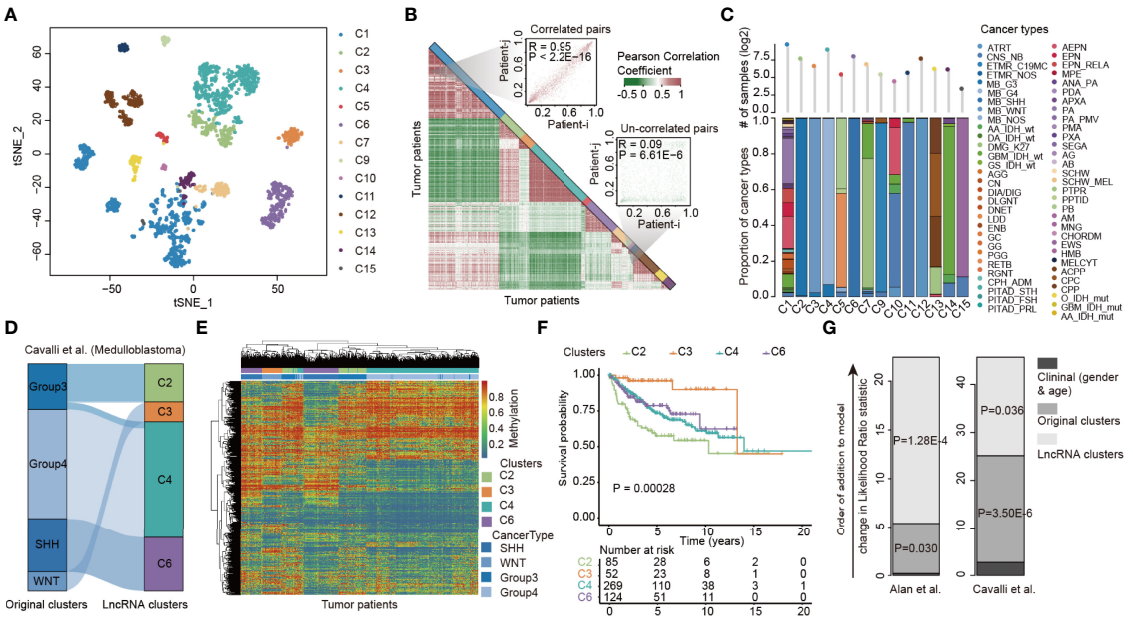

FIGURE 2 | LncRNA methylation heterogeneity in pediatric pan-CNS tumors. **(A)** Unsupervised clustering of tumor samples using tSNE dimensionality reduction. Individual samples are color-coded in the respective class color. **(B)** Heat maps showing the correlations of lncRNA methylation among tumor samples. Two representative examples were shown in the right side. **(C)** Bar plots showing the proportion of cancer types in each lncRNA methylation cluster. **(D)** Alluvial diagram of lncRNA methylation clusters in groups with different molecular subtypes. **(E)** Heat maps showing the methylation of lncRNAs in different clusters. **(F)** Kaplan–Meier curves of overall survival for patients with lncRNA methylation clusters. **(G)** The estimated log-likelihood ratio statistic of a Cox proportional hazards model. The change of LR statistic as features were added to the model was assessed for significance by Chi-square tests. Clinical clusters represent the Cox model constructed by gender and age. Original clusters represent the Cox model constructed by gender, age, and WHO category. LncRNA clusters represent the Cox model constructed by gender, age, WHO category, and lncRNA clusters.

that although the majority of patients in original clusters were classified into the same lncRNA methylation clusters, different lncRNA methylation characteristics were found in the patients of Group 3 (**Figure 2D**). The heat map corresponding to the lncRNA methylation clusters was generated, and we found that lncRNAs exhibited distinct methylation across clusters (**Figure 2E**).

To investigate whether the difference in lncRNA methylation pattern had clinical implications, we next performed Kaplan–Meier survival analysis. We found that the medulloblastoma patients in different lncRNA methylation clusters had significantly higher survival rates (**Figure 2F**, log-rank p = 0.00028). Moreover, we obtained similar results in another cancer type (**Figure S3**). However, it is not yet clear whether lncRNA methylation can provide additional prognostic power beyond original cancer types and clinical features. We thus performed a multivariate Cox proportional hazards analysis (32). In this model, we included age, sex, and original cancer types. As a result, we observed a large increase in the predictive fit by considering the lncRNA methylation (**Figure 2G**, p = 1.28E-4 and 0.036, Chi-square test), supporting the clinical value of lncRNA methylation patterns in cancer.

Immune Microenvironment Patterns of LncRNA CNS Subtypes

Detailed studies on the TIME are being conducted to uncover the underlying mechanisms of cancer (19). We next estimated the relative proportion of immune cells of patients by methylCIBERSORT (33). In general, we found that there were relatively high proportions of endothelial and fibroblast cells across all pediatric CNS tumors (**Figure 3A**). Moreover, individual lncRNA methylation subtypes varied significantly in the relative proportion of infiltrating cell types (**Figure 3B**). Moreover, we also investigated the immune signature scores and observed high variations among different lncRNA methylation clusters (**Figure 3B**).

For instance, a higher proportion of CD4_Eff was observed in C6 and C3 while limited CD4_Eff was infiltrated in C2 and C4 (**Figure 3C**). No CD4_Eff was infiltrated in C5, C12, and C15 clusters. These observations were consistent with the result that patients in C6 and C3 had better survival than those in C2 and C4 (**Figure 2F**). Although patients in the majority of clusters had a higher infiltration of fibroblast, C5, C9, C12, and C3 patients had a relatively limited infiltration of fibroblast (**Figure 3C**). In contrast, Treg cells were highly infiltrated in patients of C5 (**Figure 3B**) and the methylation of immune-related signatures was also relatively higher in C5. These observations suggested that regulatory T cells might oppose the recovery of nerve injury or psychological stress in CNS, which is consistent with the result of a recent study (41). Regulatory T cells have been demonstrated to counteract neuropathic pain through inhibition of the Th1 response at the site of peripheral nerve injury (42). Increased

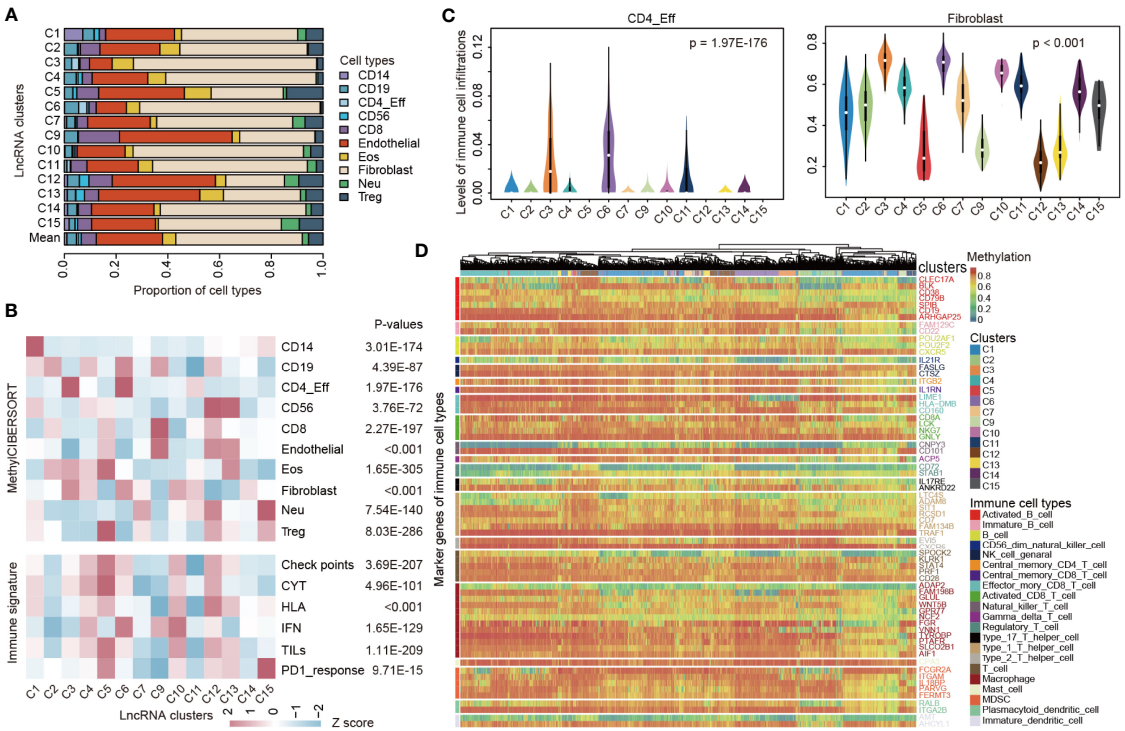

FIGURE 3 | TIME heterogeneity in pediatric pan-CNS tumors. **(A)** The proportions of immune cell-type infiltrations across lncRNA methylation clusters. **(B)** Heat maps showing the average immune cell infiltrations and immune signature scores across lncRNA methylation clusters. *p*-values were for ANOVA tests. **(C)** Violin plots showing the levels of immune cell infiltrations across lncRNA clusters. Left for CD4_Eff cells and right for fibroblast. **(D)** Heat maps showing the relative methylation of immune cell-type marker genes across patients in different lncRNA clusters. Genes were colored based on the immune cell types.

percentages of regulatory T cells have been associated with inflammatory and neuroendocrine responses to acute psychological stress (43).

We next investigated the DNA methylation of immune-related signatures and found that the marker genes exhibited diverse DNA methylation across clusters (**Figure 3D**). To systematically identify the pathways regulated by DNA methylation, we identified the quantitative differentially methylated regions (QDMRs) (44, 45). Functional enrichment analysis revealed that genes with differentially methylated patterns were significantly enriched in nervous system-related functions (**Figure S4**). For instance, genes in C7 clusters were enriched in "Fc gamma R-mediated phagocytosis" and "TNF signaling pathway". Genes in C4 were associated with gliogenesis (**Figure S4**). Together, these results suggested the diverse immune microenvironment patterns of lncRNA pediatric CNS subtypes.

LncRNA Methylation Associated With Immune Cell Infiltration

LncRNAs are emerging as critical regulators of gene expression and they play fundamental roles in immune regulation (20, 28). It is not clear to what extent lncRNA methylations were associated with immune cell infiltration, particularly in pediatric CNS tumors. We thus evaluated the correlation between lncRNA methylation and immune cell infiltrations in each cluster by Spearman correlation coefficient (SCC). In total, we identified 260 to 6,510 lncRNAs, whose methylations were correlated with immune cell infiltration, across 14 clusters (**Figure 4A**). The number of positively correlated lncRNAs was nearly the same as that of the negatively correlated ones. We next analyzed the correlation by immune cell types and found that lncRNA methylation correlated with immune cell infiltration and exhibited a complex pattern across clusters (**Figure 4B**). In general, we identified that lncRNA methylation correlated with diverse immune cell type infiltration in the majority of clusters. However, the majority of lncRNA methylation correlated with CD8 T-cell infiltration in C9 (**Figure 4B**). LncRNA methylation mainly correlated with CD56 and CD4_Eff in C10 and C11 (**Figure 4B**).

In total, we identified 6,901 lncRNAs in which methylation was correlated with at least two types of immune cells (**Figure 4C**). In particular, 32 lncRNAs were correlated with 10 immune cell infiltrations (**Figure 4D**). Interestingly, we found that methylations of these lncRNAs were almost positively correlated with CD8 and CD14 infiltration levels. Next, we further explored the methylation patterns of lncRNAs that were correlated with immune cell infiltrations. We found that hypo-methylated and hyper-methylated lncRNAs were more likely to be correlated with immune cell infiltrations in several

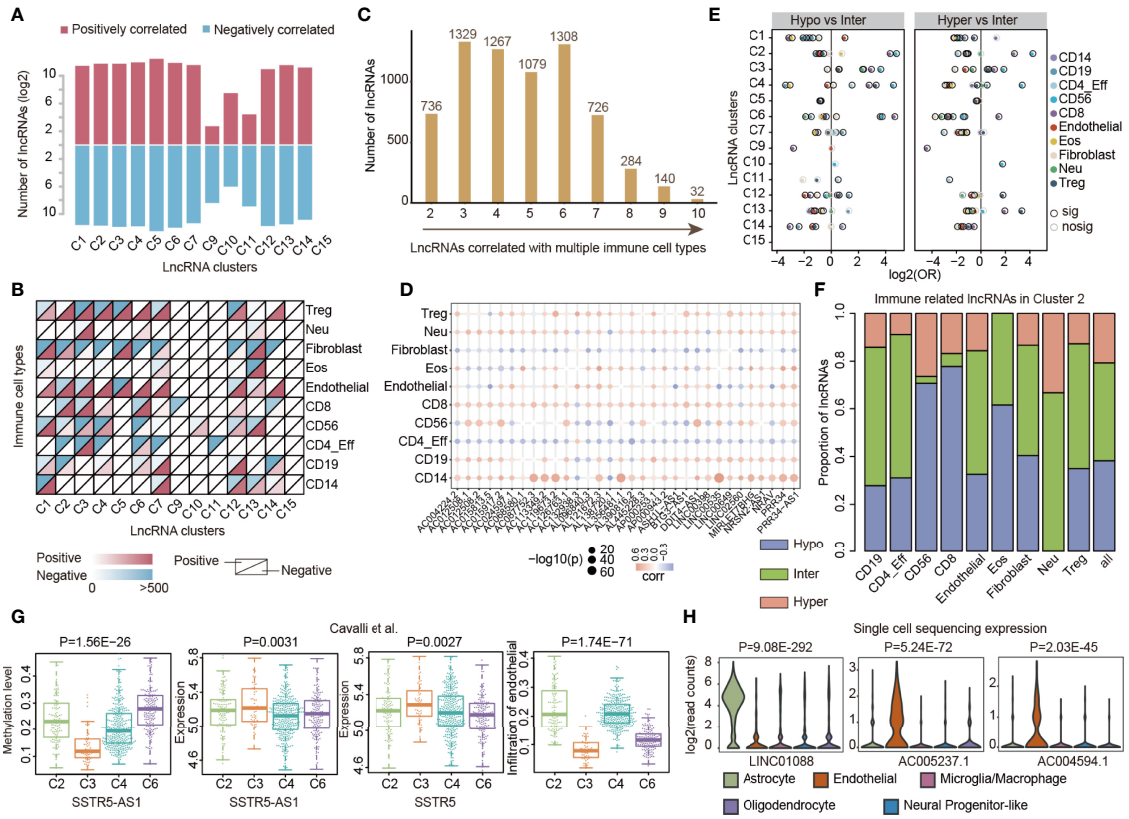

FIGURE 4 | LncRNA methylations correlated with immune cell infiltrations in cancer. **(A)** Bar plots showing the number of lncRNAs in which methylation correlated with immune cell infiltrations across lncRNA clusters. Red for positively correlated lncRNAs and blue for negatively correlated lncRNAs. **(B)** Heat maps showing the number of lncRNAs in which methylation correlated with different types of immune cell infiltrations across lncRNA clusters. **(C)** Number of lncRNAs that correlated with different numbers of immune cell types. **(D)** Balloon plots of correlation between lncRNA methylation and immune cell infiltration. The colors of the balls represent the correlations and sizes represent the –log10(*p*-values). **(E)** Balloon plots showing the enrichment of lncRNAs with different methylation patterns. Balls were colored according to the immune cell types and significant enrichments were colored by dark black margins. **(F)** The proportion of lncRNAs correlated with immune cell infiltrations with different methylation patterns. **(G)** Box plots showing the distribution of methylation, expression, and infiltration of endothelial cells in different lncRNA clusters. **(H)** Violin plots showing the expression of lncRNAs in different immune cells based on single-cell sequencing data.

clusters when compared with inter-methylated ones (**Figure 4E**), such as in C3 and C4. In particular, we found that hypo-methylated lncRNAs were more likely to be correlated with CD56 and CD8 infiltrations in C2 (**Figure 4F**, *p*-values < 0.05). Moreover, we explored the DNA methylation level of 32 lncRNAs in different clusters. We found that AL121672.3, MIRLET7BHG, PRR34, and PRR34-AS1 were hyper-methylated in C5 (**Figure S5**). LINC00398 was hyper-methylated in C7 and AC012508.1 and AC012508.2 were hyper-methylated in C9. The nearest protein-coding genes of the 32 lncRNAs were enriched in regulation of the muscle system process, negative regulation of the small-molecule metabolic process, and positive regulation of cell death (**Figure S5**).

To investigate the immune regulation of lncRNA methylation, we further analyzed the correlation in medulloblastoma. We identified that SSTR5-AS1 methylation was correlated with endothelial infiltration (**Figure S6**). By integrating DNA methylation and expression profiles, we found that SSTR5-AS1 was hypo-methylated and highly expressed in C3 (**Figure 4G**). Moreover, the potential target gene SSTR5 also exhibited significantly higher expression in patients of C3 (**Figure 4G**, $p = 0.0027$), which had relatively lower endothelial infiltration (**Figure 4G**, $p = 1.74E\text{-}71$). These observations suggested that lncRNA methylation might repress the expression of lncRNA first, further decrease the expression of the target gene, and finally repress the immune cell levels. Indeed, it has been demonstrated that SSTR5 can significantly reduce endothelial cell proliferation (46). Moreover, we also identified several lncRNAs that exhibited significantly lower (i.e., LINC01088) or higher (i.e., AC005237.1 and AC004594.1) expressions in endothelial cells based on single-cell data (**Figure 4H**) collected from one recent study (47). Taken together, these results suggest that prevalent lncRNA methylations were associated with immune cell infiltration, which plays important roles in TIME regulation in pediatric CNS tumors.

Immune-Related LncRNAs Associated With Cancer Subtypes

To gain insight into the function of lncRNA methylation in immune regulation, we next focused on 17 immunologically relevant gene sets representing distinct immune pathways derived from recent studies (20, 48). We used the protein-coding gene within 10 kb from lncRNAs that were correlated with immune cell infiltrations to predict their functions. We found that the lncRNAs potentially regulate a number of genes in immune-related pathways (**Figure 5A**). In particular, the majority of cytokines and cytokine receptors were regulated by lncRNAs. Next, we analyzed the methylation patterns of immune-related lncRNAs in 14 clusters. We found that there were high numbers of lncRNAs in C5 and C6 clusters, which were mainly hypo-methylated lncRNAs in C6 (**Figure 5B**).

Our previous study has demonstrated that if the lncRNAs can regulate more immune-related pathways, they are more likely to be involved in cancer (20). We next calculated the number of pathways regulated by immune cell infiltration-related lncRNAs. We found that the majority of lncRNAs potentially regulate one or two immune-related pathways and 9 lncRNAs can regulate more than three pathways (**Figure 5C**). In particular, we

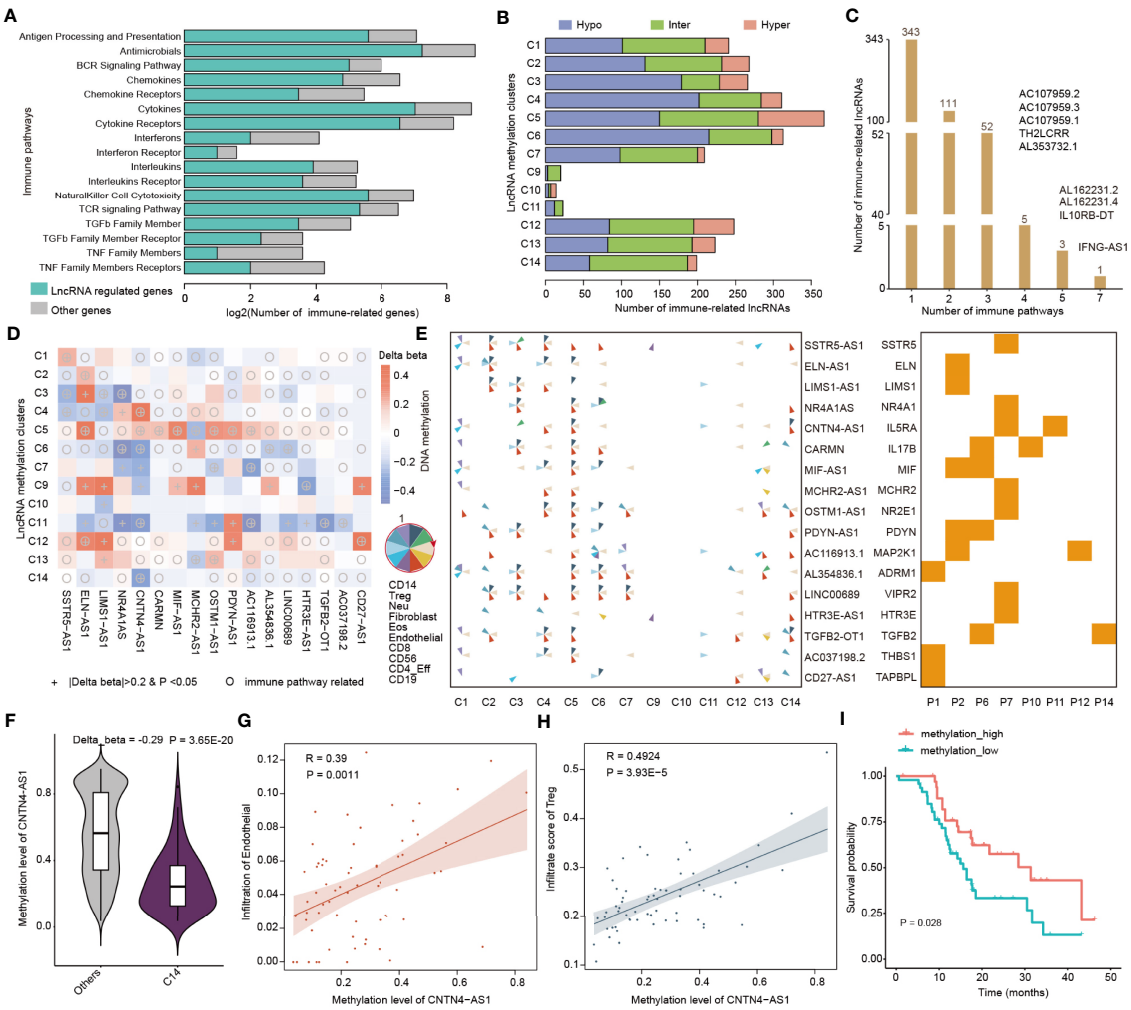

FIGURE 5 | LncRNA methylation involved in immune-related pathways. **(A)** Bar plots showing the number of genes regulated by lncRNAs in each immune-related pathway. The green bars are for lncRNA regulated genes and gray bars are for other genes. **(B)** Bar plots showing the number of immune-related lncRNAs identified in each lncRNA methylation cluster. Red for hyper-methylated lncRNAs, blue for hypo-methylated lncRNAs, and green for inter-methylated lncRNAs. **(C)** Number of lncRNAs that potentially regulate different numbers of immune-related pathways. **(D)** Heat maps showing the differential methylation of lncRNAs across different clusters. The colors represent the difference in DNA methylation levels and "+" indicates that $\beta > 0.2$ and $p < 0.05$, while the circles indicate that this lncRNA can potentially regulate immune-related pathways. **(E)** Pie charts showing the correlation of lncRNA methylation and immune cell infiltrations in different clusters. The order of the immune cells in the pie is shown in the left side. Right-side heat map showing whether the lncRNA can regulate the corresponding immune-related pathway. **(F)** Violin plots showing the methylation levels of CNTN4-AS1 in C14 and other clusters. **(G, H)** Scatter plots showing the correlation between methylation of CNTN4-AS1 and infiltration of immune cells. **(G)** for endothelial and **(H)** for Treg cells. **(I)** Kaplan–Meier curves of overall survival for patients with high or low CNTN4-AS1 methylation.

identified that IFNG-AS1 can regulate 7 immune-related pathways. The lncRNA IFNG-AS1 was found to strongly influence the responses to several pathogens by increasing interferon gamma (IFNγ) secretion (49). IFNG-AS1 is as an important regulator of IFNG expression, which was involved in dynamic and cell state-specific responses to infection (50). These results suggest that the immune-related lncRNAs play important roles in cancer.

Next, we used the "one vs. rest" method to identify the differentially methylated lncRNAs in each cluster. We identified 81 immune-related lncRNAs that were differentially methylated across 14 clusters (**Table S4**). In particular, we found that there were 17 immune-related lncRNAs reported in literature (**Figure 5D**). Moreover, we collected genome-wide DNA methylation from normal controls and compared the methylation level of hub lncRNAs between the CNS tumors and normal tissue. We found that SSTR5-AS1, LIMS1-AS1, MCHR2-AS1, AC116913.1, LINC00689, and TGFB2-OT1 exhibited significantly differential methylation in cancer (**Figure S7**, Wilcoxon's rank sum test p-values < 0.05). The methylations of these lncRNAs were correlated with diverse immune cell infiltrations across 14 clusters, and they can potentially regulate genes in immune-related pathways (**Figure 5E**). We also analyzed the methylation of the genes potentially regulated by lncRNAs and found that the methylation alterations of SSTR5, ELN, MCHR2, PDYN, and TAPBPL were consistent with lncRNAs (**Figure S8**). Next, we investigated to what extent the methylations of lncRNAs were associated with drug treatment response. We first obtained the DNA methylation of lncRNAs of brain tumors from the TCGA cohort. We found that the methylation levels of 12 hub lncRNAs were associated with the drug treatment response (**Figure S9**, Kruskal–Wallis test p-values < 0.05). These results suggest that these immune-related lncRNAs might be used for further functional investigation in pediatric CNS tumors.

In particular, we identified the lncRNA CNTN4-AS1, which was involved in neuronal differentiation and gliomagenesis (51). We found that CNTN4-AS1 exhibited significant hypo-methylation in C14 (**Figure 5F** and **Figure S10**, p = 3.65E-20), which was mainly formed by IDH wild-type glioma patients. The methylation of CNTN4-AS1 was correlated with endothelial and Treg infiltrations in the C14 cluster (**Figures 5G, H**). We also found that CNTN4-AS1 can regulate IL5RA (**Figure S10**), which plays important roles in the cytokine signaling pathway (52). In addition, we found that high methylation of CNTN4-AS1 was associated with better survival of pediatric glioma patients (**Figure 5I**, log-rank p = 0.028). These results suggest that CNTN4-AS1 methylation may be a potential biomarker for pediatric CNS tumor subtypes. We also identified several other biomarkers for pediatric tumor subtypes, such as OSTM1-AS1 and AC116913.1 (**Figures S10–S12**). The methylation level of OSTM-AS1 was correlated with immune cell infiltration in C1, C2, C4–C6, C7, and C12–C14 and altered in C5, C7, and C13 (**Figures S10 and S11**). OSTM-AS1 could potentially target NR2E1 and regulate the cytokine receptor pathway. The methylation level of AC116913.1 was correlated with immune cell infiltration in C2, C4–C7, C11, C13, and C14 and changed in C5, C7, and C11. AC116913.1 could potentially target MP5K1 and regulate the antimicrobials and natural killer cell cytotoxicity pathways (**Figure S8**). All the methylation levels of these lncRNAs were associated with the survival of pediatric gliomas (C7 and C14) (**Figures S10–S12**). We have also explored the DNA methylation level of these three lncRNAs by integrating the GBM and LGG cancer types from TCGA cohorts. We found that these lncRNAs were all hyper-methylated in adult CNS tumors, and the higher methylation level could predict a better overall survival (**Figure S13**).

DISCUSSION

Epigenetic factors tightly regulate the expression of lncRNAs, which play important roles in cancer development and progression (53). We have demonstrated that lncRNAs exhibited distinct methylation patterns (hyper-, hypo-, and inter-methylated lncRNAs) across pediatric CNS tumors. These lncRNAs had significant genomic features, including GC content, CpG content, number of exons, and conservation. In addition, we have performed lncRNA methylation-based pediatric pan-CNS tumor classification, which will be a valuable asset for clinical decision-making. In particular, we redefined four clusters of medulloblastomas that have different clinical implications. Integrating the lncRNA methylation information can provide additional power for clinical diagnosis.

Moreover, we estimated the TIME of pediatric pan-CNS tumors and found that patients in distinct lncRNA methylation clusters exhibited high heterogeneity in TIME. We demonstrated significant association with lncRNA methylation and immune cell infiltrations across lncRNA clusters. Our results are broadly in accordance with the small number of recent studies on immune infiltration in pediatric CNS tumors (54, 55). We also show that lncRNA clusters are clearly related to the expression of conventional immune targets, such as PDL1, CYT, and IFN. All these studies suggest the important differences in TIME across pediatric brain tumors.

We next explored the associations between lncRNA methylation and immune cell infiltrations. We found that lncRNA methylation was associated with diverse immune cell infiltrations across pediatric pan-CNS tumors. Emerging immune-related lncRNAs are identified in various cancers (22, 56); however, the underlying functions of lncRNAs are still unknown. Promotion or suppression of immune cells may be a major way for lncRNAs to function in cancer development and progression. For instance, MIR22HG has been demonstrated to promote CD8 T-cell infiltration and acts as a tumor suppressor in cancer (22). NKILA lncRNA can promote tumor immune evasion by sensitizing T cells to activation-induced cell death (57). Moreover, pan-adult cancer analysis also revealed that immune-related lncRNAs were likely to be correlated with immune cell infiltrations (20). In addition, we also revealed

that immune cell infiltration-related lncRNAs were potentially regulating genes in immune pathways. Identification of these lncRNAs provided a valuable resource for the functional characterization of lncRNA regulation in immunology through further experiments in cell lines or animal models.

Previous studies have revealed the critical roles of the N6-methyladenosine (m6A) modification of lncRNAs in various types of cancers (58, 59). We revealed that the numerous expressions of lncRNAs were associated with DNA methylation, such as PART1, RAMP2-AS1, DLGAP1-AS1, and DLEU1 (**Figure S14**). These lncRNAs have been demonstrated to be associated with brain tumors. For example, PART1 exerts tumor-suppressive functions in glioma *via* sponging miR-190a-3p and inactivation of the PTEN/AKT pathway (60). Knockdown of DLEU1 inhibits glioma progression and promotes temozolomide chemosensitivity by regulating autophagy (61). We next queried the immune-related lncRNAs in m6A-Atlas, which is a comprehensive knowledgebase for unraveling the m6A epitranscriptome (62). We found that several lncRNAs were correlated with m6A modification, such as SSTR5-AS1, MIF-AS1, and CARMN (**Table S5**). Collectively, these findings highlight the critical role of the DNA methylation and m6A modification in regulating lncRNAs, providing a new way to explore RNA epigenetic regulatory patterns in the future.

In conclusion, our study comprehensively analyzes the lncRNA methylation landscape across pediatric pan-CNS tumors and gives first indications of the potential of lncRNA methylation as an adjunct to tumor classification. The repertoire of epigenetically regulated immune-related lncRNAs will facilitate the development of immunotherapeutic targets in pediatric pan-CNS tumors.

DATA AVAILABILITY STATEMENT

The datasets presented in this study can be found in online repositories. The names of the repository/repositories and accession number(s) can be found in the article/**Supplementary Material**.

AUTHOR CONTRIBUTIONS

WX, XL, and KL designed the study. YL, SX, and DX analyzed and interpreted the data. TP, JG, and SX performed the immune analysis. SG and QL designed the figures. YL, XL, and WX wrote and edited manuscript. All authors contributed to the article and approved the submitted version.

FUNDING

This work was supported by the Hainan Province Science and Technology Special Fund (Nos. ZDYF2021SHFZ088, ZDYF2021SHFZ051 and ZDYF2020225), Major Science and Technology Program of Hainan Province (Nos. ZDKJ2019010 and hxk200020), the Hainan Provincial Natural Science Foundation of China (Nos. 820MS053 and 820RC637), project supported by Hainan Province Clinical Medical Center (QWYH202175), the National Key R&D Program of China (No. 2018YFC2000100), the Hainan Medical and Health Research Project (No. 2001032034A2004), the National Natural Science Foundation of China (Nos. 32160152, 31970646, 61873075, 32060152, 32070673, and 31871338), the Natural Science Foundation for Distinguished Young Scholars of Heilongjiang Province (No. JQ2019C004), and the Heilongjiang Touyan Innovation Team Program and Innovation Research Fund for Graduate Students (Nos. Hys2020-369, Qhys2021-348, Qhys2021-350, Qhys2021-351, Qhys2021-377, HYYB2021A01, and HYYS2021A31). We are grateful to the tremendous supports from Hainan Excellent Talent Team Project (Child health and early childhood development-The first 1000 days of life).

SUPPLEMENTARY MATERIAL

The Supplementary Material for this article can be found online at: https://www.frontiersin.org/articles/10.3389/fimmu.2022.853904/full#supplementary-material

REFERENCES

1. Linabery AM, Ross JA. Trends in Childhood Cancer Incidence in the U.S-2004). *Cancer* (2008) 112:416–32. doi: 10.1002/cncr.23169
2. Muskens IS, Zhang C, De Smith AJ, Biegel JA, Walsh KM, Wiemels JL. Germline Genetic Landscape of Pediatric Central Nervous System Tumors. *Neuro Oncol* (2019) 21:1376–88. doi: 10.1093/neuonc/noz108
3. Newman S, Nakitandwe J, Kesserwan CA, Azzato EM, Wheeler DA, Rusch M, et al. Genomes for Kids: The Scope of Pathogenic Mutations in Pediatric Cancer Revealed by Comprehensive DNA and RNA Sequencing. *Cancer Discov* (2021) 11(12):3008–27. doi: 10.1158/2159-8290.CD-20-1631
4. Schwartz JR, Ma J, Kamens J, Westover T, Walsh MP, Brady SW, et al. The Acquisition of Molecular Drivers in Pediatric Therapy-Related Myeloid Neoplasms. *Nat Commun* (2021) 12:985. doi: 10.1038/s41467-021-21255-8
5. Parsons DW, Roy A, Yang Y, Wang T, Scollon S, Bergstrom K, et al. Diagnostic Yield of Clinical Tumor and Germline Whole-Exome Sequencing for Children With Solid Tumors. *JAMA Oncol* (2016) 2:616–24. doi: 10.1001/jamaoncol.2015.5699
6. Surrey LF, Macfarland SP, Chang F, Cao K, Rathi KS, Akgumus GT, et al. Clinical Utility of Custom-Designed NGS Panel Testing in Pediatric Tumors. *Genome Med* (2019) 11:32. doi: 10.1186/s13073-019-0644-8
7. Wong M, Mayoh C, Lau LMS, Khuong-Quang DA, Pinese M, Kumar A, et al. Whole Genome, Transcriptome and Methylome Profiling Enhances Actionable Target Discovery in High-Risk Pediatric Cancer. *Nat Med* (2020) 26:1742–53. doi: 10.1038/s41591-020-1072-4
8. Nordlund J, Syvanen AC. Epigenetics in Pediatric Acute Lymphoblastic Leukemia. *Semin Cancer Biol* (2018) 51:129–38. doi: 10.1016/j.semcancer.2017.09.001
9. Kling T, Wenger A, Caren H. DNA Methylation-Based Age Estimation in Pediatric Healthy Tissues and Brain Tumors. *Aging (Albany NY)* (2020) 12:21037–56. doi: 10.18632/aging.202145
10. Mahoney SE, Yao Z, Keyes CC, Tapscott SJ, Diede SJ. Genome-Wide DNA Methylation Studies Suggest Distinct DNA Methylation Patterns in Pediatric Embryonal and Alveolar Rhabdomyosarcomas. *Epigenetics* (2012) 7:400–8. doi: 10.4161/epi.19463
11. Capper D, Jones DTW, Sill M, Hovestadt V, Schrimpf D, Sturm D, et al. DNA Methylation-Based Classification of Central Nervous System Tumours. *Nature* (2018) 555:469–74. doi: 10.1038/nature26000

12. Derrien T, Johnson R, Bussotti G, Tanzer A, Djebali S, Tilgner H, et al. The GENCODE V7 Catalog of Human Long Noncoding RNAs: Analysis of Their Gene Structure, Evolution, and Expression. *Genome Res* (2012) 22:1775–89. doi: 10.1101/gr.132159.111
13. Frankish A, Diekhans M, Jungreis I, Lagarde J, Loveland JE, Mudge JM, et al. Gencode 2021. *Nucleic Acids Res* (2021) 49:D916–23. doi: 10.1093/nar/gkaa1087
14. Yarmishyn AA, Batagov AO, Tan JZ, Sundaram GM, Sampath P, Kuznetsov VA, et al. HOXD-AS1 Is a Novel lncRNA Encoded in HOXD Cluster and a Marker of Neuroblastoma Progression Revealed *via* Integrative Analysis of Noncoding Transcriptome. *BMC Genomics* (2014) 15 Suppl 9:S7. doi: 10.1186/1471-2164-15-S9-S7
15. Bevilacqua V, Gioia U, Di Carlo V, Tortorelli AF, Colombo T, Bozzoni I, et al. Identification of Linc-NeD125, a Novel Long Non Coding RNA That Hosts miR-125b-1 and Negatively Controls Proliferation of Human Neuroblastoma Cells. *RNA Biol* (2015) 12:1323–37. doi: 10.1080/15476286.2015.1096488
16. Zhi H, Li X, Wang P, Gao Y, Gao B, Zhou D, et al. Lnc2Meth: A Manually Curated Database of Regulatory Relationships Between Long Non-Coding RNAs and DNA Methylation Associated With Human Disease. *Nucleic Acids Res* (2018) 46:D133–8. doi: 10.1093/nar/gkx985
17. Hambardzumyan D, Gutmann DH, Kettenmann H. The Role of Microglia and Macrophages in Glioma Maintenance and Progression. *Nat Neurosci* (2016) 19:20–7. doi: 10.1038/nn.4185
18. Guo X, Pan Y, Xiong M, Sanapala S, Anastasaki C, Cobb O, et al. Midkine Activation of CD8(+) T Cells Establishes a Neuron-Immune-Cancer Axis Responsible for Low-Grade Glioma Growth. *Nat Commun* (2020) 11:2177. doi: 10.1038/s41467-020-15770-3
19. Grabovska Y, Mackay A, O'hare P, Crosier S, Finetti M, Schwalbe EC, et al. Pediatric Pan-Central Nervous System Tumor Analysis of Immune-Cell Infiltration Identifies Correlates of Antitumor Immunity. *Nat Commun* (2020) 11:4324. doi: 10.1038/s41467-020-18070-y
20. Li Y, Jiang T, Zhou W, Li J, Li X, Wang Q, et al. Pan-Cancer Characterization of Immune-Related lncRNAs Identifies Potential Oncogenic Biomarkers. *Nat Commun* (2020) 11:1000. doi: 10.1038/s41467-020-14802-2
21. Lv D, Xu K, Jin X, Li J, Shi Y, Zhang M, et al. LncSpA: LncRNA Spatial Atlas of Expression Across Normal and Cancer Tissues. *Cancer Res* (2020) 80:2067–71. doi: 10.1158/0008-5472.CAN-19-2687
22. Xu J, Shao T, Song M, Xie Y, Zhou J, Yin J, et al. MIR22HG Acts as a Tumor Suppressor *via* TGFbeta/SMAD Signaling and Facilitates Immunotherapy in Colorectal Cancer. *Mol Cancer* (2020) 19:51. doi: 10.1186/s12943-020-01174-w
23. Fortin JP, Labbe A, Lemire M, Zanke BW, Hudson TJ, Fertig EJ, et al. Functional Normalization of 450k Methylation Array Data Improves Replication in Large Cancer Studies. *Genome Biol* (2014) 15:503. doi: 10.1186/s13059-014-0503-2
24. Aryee MJ, Jaffe AE, Corrada-Bravo H, Ladd-Acosta C, Feinberg AP, Hansen KD, et al. Minfi: A Flexible and Comprehensive Bioconductor Package for the Analysis of Infinium DNA Methylation Microarrays. *Bioinformatics* (2014) 30:1363–9. doi: 10.1093/bioinformatics/btu049
25. Frankish A, Diekhans M, Ferreira AM, Johnson R, Jungreis I, Loveland J, et al. GENCODE Reference Annotation for the Human and Mouse Genomes. *Nucleic Acids Res* (2019) 47:D766–73. doi: 10.1093/nar/gky955
26. Siepel A, Bejerano G, Pedersen JS, Hinrichs AS, Hou M, Rosenbloom K, et al. Evolutionarily Conserved Elements in Vertebrate, Insect, Worm, and Yeast Genomes. *Genome Res* (2005) 15:1034–50. doi: 10.1101/gr.3715005
27. Saxonov S, Berg P, Brutlag DL. A Genome-Wide Analysis of CpG Dinucleotides in the Human Genome Distinguishes Two Distinct Classes of Promoters. *Proc Natl Acad Sci USA* (2006) 103:1412–7. doi: 10.1073/pnas.0510310103
28. Li Y, Li L, Wang Z, Pan T, Sahni N, Jin X, et al. LncMAP: Pan-Cancer Atlas of Long Noncoding RNA-Mediated Transcriptional Network Perturbations. *Nucleic Acids Res* (2018) 46:1113–23. doi: 10.1093/nar/gkx1311
29. Wang Z, Yin J, Zhou W, Bai J, Xie Y, Xu K, et al. Complex Impact of DNA Methylation on Transcriptional Dysregulation Across 22 Human Cancer Types. *Nucleic Acids Res* (2020) 48:2287–302. doi: 10.1093/nar/gkaa041
30. Zhi H, Ning S, Li X, Li Y, Wu W, Li X. A Novel Reannotation Strategy for Dissecting DNA Methylation Patterns of Human Long Intergenic Non-Coding RNAs in Cancers. *Nucleic Acids Res* (2014) 42:8258–70. doi: 10.1093/nar/gku575
31. Wilkerson MD, Hayes DN. ConsensusClusterPlus: A Class Discovery Tool With Confidence Assessments and Item Tracking. *Bioinformatics* (2010) 26:1572–3. doi: 10.1093/bioinformatics/btq170
32. Zhang H, Deng Y, Zhang Y, Ping Y, Zhao H, Pang L, et al. Cooperative Genomic Alteration Network Reveals Molecular Classification Across 12 Major Cancer Types. *Nucleic Acids Res* (2017) 45:567–82. doi: 10.1093/nar/gkw1087
33. Chakravarthy A, Furness A, Joshi K, Ghorani E, Ford K, Ward MJ, et al. Pan-Cancer Deconvolution of Tumour Composition Using DNA Methylation. *Nat Commun* (2018) 9:3220. doi: 10.1038/s41467-018-05570-1
34. Chen B, Khodadoust MS, Liu CL, Newman AM, Alizadeh AA. Profiling Tumor Infiltrating Immune Cells With CIBERSORT. *Methods Mol Biol* (2018) 1711:243–59. doi: 10.1007/978-1-4939-7493-1_12
35. Ju M, Bi J, Wei Q, Jiang L, Guan Q, Zhang M, et al. Pan-Cancer Analysis of NLRP3 Inflammasome With Potential Implications in Prognosis and Immunotherapy in Human Cancer. *Brief Bioinform* (2021) 22. doi: 10.1093/bib/bbaa345
36. Duruisseaux M, Martinez-Cardus A, Calleja-Cervantes ME, Moran S, Castro De Moura M, Davalos V, et al. Epigenetic Prediction of Response to Anti-PD-1 Treatment in Non-Small-Cell Lung Cancer: A Multicentre, Retrospective Analysis. *Lancet Respir Med* (2018) 6:771–81. doi: 10.1016/S2213-2600(18)30284-4
37. Mitra S, Lauss M, Cabrita R, Choi J, Zhang T, Isaksson K, et al. Analysis of DNA Methylation Patterns in the Tumor Immune Microenvironment of Metastatic Melanoma. *Mol Oncol* (2020) 14:933–50. doi: 10.1002/1878-0261.12663
38. Li Y, Xu J, Chen H, Zhao Z, Li S, Bai J, et al. Characterizing Genes With Distinct Methylation Patterns in the Context of Protein-Protein Interaction Network: Application to Human Brain Tissues. *PloS One* (2013) 8:e65871. doi: 10.1371/journal.pone.0065871
39. Van Den Bent MJ. Interobserver Variation of the Histopathological Diagnosis in Clinical Trials on Glioma: A Clinician's Perspective. *Acta Neuropathol* (2010) 120:297–304. doi: 10.1007/s00401-010-0725-7
40. Cavalli FMG, Remke M, Rampasek L, Peacock J, Shih DJH, Luu B, et al. Intertumoral Heterogeneity Within Medulloblastoma Subgroups. *Cancer Cell* (2017) 31:737–754.e736. doi: 10.1016/j.ccell.2017.05.005
41. Rook GA, Lowry CA, Raison CL. Lymphocytes in Neuroprotection, Cognition and Emotion: Is Intolerance Really the Answer? *Brain Behav Immun* (2011) 25:591–601. doi: 10.1016/j.bbi.2010.12.005
42. Davoli-Ferreira M, De Lima KA, Fonseca MM, Guimaraes RM, Gomes FI, Cavallini MC, et al. Regulatory T Cells Counteract Neuropathic Pain Through Inhibition of the Th1 Response at the Site of Peripheral Nerve Injury. *Pain* (2020) 161:1730–43. doi: 10.1097/j.pain.0000000000001879
43. Ronaldson A, Gazali AM, Zalli A, Kaiser F, Thompson SJ, Henderson B, et al. Increased Percentages of Regulatory T Cells Are Associated With Inflammatory and Neuroendocrine Responses to Acute Psychological Stress and Poorer Health Status in Older Men and Women. *Psychopharmacol (Berl)* (2016) 233:1661–8. doi: 10.1007/s00213-015-3876-3
44. Zhang Y, Liu H, Lv J, Xiao X, Zhu J, Liu X, et al. QDMR: A Quantitative Method for Identification of Differentially Methylated Regions by Entropy. *Nucleic Acids Res* (2011) 39:e58. doi: 10.1093/nar/gkr053
45. Zhang S, Wang Y, Gu Y, Zhu J, Ci C, Guo Z, et al. Specific Breast Cancer Prognosis-Subtype Distinctions Based on DNA Methylation Patterns. *Mol Oncol* (2018) 12:1047–60. doi: 10.1002/1878-0261.12309
46. Yan S, Li M, Chai H, Yang H, Lin PH, Yao Q, et al. TNF-Alpha Decreases Expression of Somatostatin, Somatostatin Receptors, and Cortistatin in Human Coronary Endothelial Cells. *J Surg Res* (2005) 123:294–301. doi: 10.1016/j.jss.2004.07.244
47. Slyper M, Porter CBM, Ashenberg O, Waldman J, Drokhlyansky E, Wakiro I, et al. A Single-Cell and Single-Nucleus RNA-Seq Toolbox for Fresh and Frozen Human Tumors. *Nat Med* (2020) 26:792–802. doi: 10.1038/s41591-020-0844-1
48. Li Y, Burgman B, Mcgrail DJ, Sun M, Qi D, Shukla SA, et al. Integrated Genomic Characterization of the Human Immunome in Cancer. *Cancer Res* (2020) 80:4854–67. doi: 10.1158/0008-5472.CAN-20-0384

49. Stein N, Berhani O, Schmiedel D, Duev-Cohen A, Seidel E, Kol I, et al. IFNG-AS1 Enhances Interferon Gamma Production in Human Natural Killer Cells. *iScience* (2019) 11:466–73. doi: 10.1016/j.isci.2018.12.034
50. Petermann F, Pekowska A, Johnson CA, Jankovic D, Shih HY, Jiang K, et al. The Magnitude of IFN-Gamma Responses Is Fine-Tuned by DNA Architecture and the Non-Coding Transcript of Ifng-As1. *Mol Cell* (2019) 75:1229–1242.e1225. doi: 10.1016/j.molcel.2019.06.025
51. Wu X, Rauch TA, Zhong X, Bennett WP, Latif F, Krex D, et al. CpG Island Hypermethylation in Human Astrocytomas. *Cancer Res* (2010) 70:2718–27. doi: 10.1158/0008-5472.CAN-09-3631
52. Wilson TM, Maric I, Shukla J, Brown M, Santos C, Simakova O, et al. IL-5 Receptor Alpha Levels in Patients With Marked Eosinophilia or Mastocytosis. *J Allergy Clin Immunol* (2011) 128:1086–1092.e1081-1083. doi: 10.1016/j.jaci.2011.05.032
53. Guttman M, Amit I, Garber M, French C, Lin MF, Feldser D, et al. Chromatin Signature Reveals Over a Thousand Highly Conserved Large Non-Coding RNAs in Mammals. *Nature* (2009) 458:223–7. doi: 10.1038/nature07672
54. Vermeulen JF, Van Hecke W, Adriaansen EJM, Jansen MK, Bouma RG, Villacorta Hidalgo J, et al. Prognostic Relevance of Tumor-Infiltrating Lymphocytes and Immune Checkpoints in Pediatric Medulloblastoma. *Oncoimmunology* (2018) 7:e1398877. doi: 10.1080/2162402X.2017.1398877
55. Bockmayr M, Klauschen F, Maire CL, Rutkowski S, Westphal M, Lamszus K, et al. Immunologic Profiling of Mutational and Transcriptional Subgroups in Pediatric and Adult High-Grade Gliomas. *Cancer Immunol Res* (2019) 7:1401–11. doi: 10.1158/2326-6066.CIR-18-0939
56. Hong W, Liang L, Gu Y, Qi Z, Qiu H, Yang X, et al. Immune-Related lncRNA to Construct Novel Signature and Predict the Immune Landscape of Human Hepatocellular Carcinoma. *Mol Ther Nucleic Acids* (2020) 22:937–47. doi: 10.1016/j.omtn.2020.10.002
57. Huang D, Chen J, Yang L, Ouyang Q, Li J, Lao L, et al. NKILA lncRNA Promotes Tumor Immune Evasion by Sensitizing T Cells to Activation-Induced Cell Death. *Nat Immunol* (2018) 19:1112–25. doi: 10.1038/s41590-018-0207-y
58. Yi YC, Chen XY, Zhang J, Zhu JS. Novel Insights Into the Interplay Between M(6)A Modification and Noncoding RNAs in Cancer. *Mol Cancer* (2020) 19:121. doi: 10.1186/s12943-020-01233-2
59. Xu K, Cai Y, Zhang M, Zou H, Chang Z, Li D, et al. Pan-Cancer Characterization of Expression and Clinical Relevance of M(6)A-Related Tissue-Elevated Long non-Coding RNAs. *Mol Cancer* (2021) 20:31. doi: 10.1186/s12943-021-01324-8
60. Jin Z, Piao L, Sun G, Lv C, Jing Y, Jin R. Long Non-Coding RNA PART1 Exerts Tumor Suppressive Functions in Glioma *via* Sponging miR-190a-3p and Inactivation of PTEN/AKT Pathway. *Onco Targets Ther* (2020) 13:1073–86. doi: 10.2147/OTT.S232848
61. Lv QL, Wang LC, Li DC, Lin QX, Shen XL, Liu HY, et al. Knockdown lncRNA DLEU1 Inhibits Gliomas Progression and Promotes Temozolomide Chemosensitivity by Regulating Autophagy. *Front Pharmacol* (2020) 11:560543. doi: 10.3389/fphar.2020.560543
62. Tang Y, Chen K, Song B, Ma J, Wu X, Xu Q, et al. M6a-Atlas: A Comprehensive Knowledgebase for Unraveling the N6-Methyladenosine (M6a) Epitranscriptome. *Nucleic Acids Res* (2021) 49:D134–43. doi: 10.1093/nar/gkaa692

Conflict of Interest: The authors declare that the research was conducted in the absence of any commercial or financial relationships that could be construed as a potential conflict of interest.

Publisher's Note: All claims expressed in this article are solely those of the authors and do not necessarily represent those of their affiliated organizations, or those of the publisher, the editors and the reviewers. Any product that may be evaluated in this article, or claim that may be made by its manufacturer, is not guaranteed or endorsed by the publisher.

frontiers | Frontiers in Immunology

ORIGINAL RESEARCH
published: 06 May 2022
doi: 10.3389/fimmu.2022.879560

Hematological Prognostic Scoring System Can Predict Overall Survival and Can Indicate Response to Immunotherapy in Patients With Osteosarcoma

Longqing Li[1,2†], Yang Wang[1,2†], Xuanhong He[1,2], Zhuangzhuang Li[1,2], Minxun Lu[1,2], Taojun Gong[1,2], Qing Chang[1], Jingqi Lin[1], Chuang Liu[3], Yi Luo[1,2], Li Min[1,2], Yong Zhou[1,2] and Chongqi Tu[1,2*]*

[1] Department of Orthopedics, Orthopaedic Research Institute, West China Hospital, Sichuan University, Chengdu, China, [2] Bone and Joint 3D-Printing and Biomechanical Laboratory, Department of Orthopedics, West China Hospital, Sichuan University, Chengdu, China, [3] Institute of Jinan Yinfeng Medical Laboratory, Yinfeng Gene Technology Co Ltd, Jinan, China

Osteosarcoma is the most common primary malignant bone tumor with a high metastatic potential. Nowadays, there is a lack of new markers to identify prognosis of osteosarcoma patients with response to medical treatment. Recent studies have shown that hematological markers can reflect to some extent the microenvironment of an individual with the potential to predict patient prognosis. However, most of the previous studies have studied the prognostic value of a single hematological index, and it is difficult to comprehensively reflect the tumor microenvironment of patients. Here, we comprehensively collected 16 hematological markers and constructed a hematological prognostic scoring system (HPSS) using LASSO cox regression analysis. HPSS contains many indicators such as immunity, inflammation, coagulation and nutrition. Our results suggest that HPSS is an independent prognostic factor for overall survival in osteosarcoma patients and is an optimal addition to clinical characteristics and well suited to further identify high-risk patients from clinically low-risk patients. HPSS-based nomograms have good predictive ability. Finally, HPSS also has some hints for immunotherapy response in osteosarcoma patients.

Keywords: osteosarcoma, hematological, prognostic, inflammation, immunotherapy

OPEN ACCESS

Edited by:
Pouya Faridi,
Monash University, Australia

Reviewed by:
Huaiyuan Xu,
Sun Yat-sen University Cancer Center (SYSUCC), China
Lianghao Zhang,
First Affiliated Hospital of Zhengzhou University, China

***Correspondence:**
Yong Zhou
zhouyonggk@163.com
Chongqi Tu
tucq@scu.edu.cn

[†]These authors have contributed equally to this work

Specialty section:
This article was submitted to Cancer Immunity and Immunotherapy, a section of the journal Frontiers in Immunology

Received: *19 February 2022*
Accepted: *01 April 2022*
Published: *06 May 2022*

Citation:
Li L, Wang Y, He X, Li Z, Lu M, Gong T, Chang Q, Lin J, Liu C, Luo Y, Min L, Zhou Y and Tu C (2022) Hematological Prognostic Scoring System Can Predict Overall Survival and Can Indicate Response to Immunotherapy in Patients With Osteosarcoma. Front. Immunol. 13:879560. doi: 10.3389/fimmu.2022.879560

INTRODUCTION

Osteosarcoma is a rapidly progressive primary malignant bone tumor with high metastatic potential, accounting for 20% to 40% of all bone tumors (1, 2). Chemotherapy treatment, introduced in the 1970s, significantly improved the five-year survival rate of patients with non-metastatic osteosarcoma (3). However, approximately 15 – 20% of affected patients already have metastases at presentation and individuals with metastatic disease have low short- and long-term survival (4–6). In addition, tumor recurrence and chemoresistance are also recognized as important

prognostic factors (7, 8). These clinical features are important in distinguishing high-risk patients and guiding treatment (9). However, the progression of the disease may be distinct in patients with similar clinical features. Therefore, more factors need to be considered to facilitate precision treatment.

Immunotherapy has shown definite clinical benefit in some advanced solid tumors (10, 11). Osteosarcoma has relatively high programmed cell death 1 ligand-1 (PD-L1) expression and may therefore benefit from immunotherapy (12, 13). Unfortunately, several recent clinical trials have shown that immunotherapy does not achieve the desired efficacy in osteosarcoma (14, 15). Therefore, effective biomarkers may be needed to identify patients who may truly benefit from this therapy (16).

Recent studies have shown that preoperative hematological markers such as neutrophil to lymphocyte ratio (NLR), platelet to lymphocyte ratio (PLR), and lymphocyte to macrophage ratio (LMR) can reflect the individual's tumor microenvironment to some extent and can be used to predict the prognosis of cancer patients (17, 18). These hematological markers are readily available and cost-effective and are ideal prognostic markers. Many recent studies have confirmed the value of these markers in predicting survival and response to medical treatment in cancer patients, including osteosarcoma (19–21).However, single hematological markers have shortcomings such as insufficient prognostic power and instability. Therefore, overcoming these shortcomings will help to improve the value of hematological markers to promote their utilization.

In this study, we collected proven prognostic hematological marks and developed hematological prognostic scoring system (HPSS) by iterative least absolute contraction and selection operator (LASSO) COX proportional hazards regression analysis. Our study shows that HPSS overcomes the disadvantages such as insufficient predictive power and instability of a single hematological marker, and is an effective supplement to clinical features.

PATIENTS AND METHODS

Patients

With the approval of the Medical Ethics Committee, we reviewed the clinical data of osteosarcoma patients from January 2016 to January 2021 in the database of the Musculoskeletal Tumor Center of West China Hospital. During the review process, we included and excluded patients according to the following criteria: 1) patients with high grade osteosarcoma confirmed by histopathology; 2) patients have complete hematological test results before neoadjuvant chemotherapy; 3) patient received standard treatment at West China Hospital. The exclusion criteria:1) Patients with histopathologically confirmed low-grade osteosarcoma (intramedullary and bone surface) and periosteal osteosarcoma; 2) Patients who had received neoadjuvant chemotherapy before their first-time consultancy in our hospital; 3) patients with hematological diseases; 4) patients with other malignancies; 5) patients not received standard treatment (patients who are misdiagnosed and mistreated or fail to complete postoperative chemotherapy). Finally, 223 patients were included in our study after passing the inclusion and exclusion criteria. Each patient was followed up regularly until death or January 2022. The following follow-up principles were followed: reexamination every 3 months within 1 year after surgery; reexamination every 4 months 1-2 years after surgery; reexamination every 5 months 2-3 years after surgery; reexamination every 6 months 3-5 years after surgery; reexamination every year more than 5 years after surgery. All patients were randomly divided into a training set (n=156, 70%) and external validation set (n=67, 30%) using a random seed set in 2022.

In addition, 14 patients with metastatic advanced osteosarcoma treated with PD-L1 agents were included in the study. These patients were all tested for PD-L1 expression at a third-party testing facility (Institute of Ji'nan Yin Feng Medical Laboratory) and had a Tumor Proportion Score > = 1% (TPS) (22). TPS is defined as the proportion of tumor cells positive, i.e., number of tumor cells with positive PD-L1 membrane staining at any intensity/total number of tumor cells * 100%. The TPS of all patients was evaluated by two experienced pathologists. Recombinant Anti-PD-L1 Antibody 28-8(Abcam) was used in all patients; Patients lost operative indicatio and received standard chemotherapy before immunotherapy and had measurable lesions. All patients were administered with camrelizumab (Jiangsu Hengrui Medicine Co., Ltd. China) at a dose of 2 mg/kg every 21 days. All patients underwent a minimum of 2 cycles of immunotherapy. Patients were assessed for efficacy based on RECIST by two researchers not associated with this study.

Data Collection and Processing

Neutrophils count (Neut#), lymphocytes count (LYMPH#), monocytes count(MONO#), platelet count (PLT), hemoglobin (HB), red blood cell distribution width-coefficient of variation (RDW-CV), red blood cell distribution width-standard deviation (RDW-SD), albumin (A), lactate dehydrogenase (LDH), alkaline phosphatase (ALP), activated partial thromboplastin time (APTT), prothrombin time (PT), thrombin time (TT), fibrinogen (FIB) and international normalized ratio (INR) were extracted from the first blood routine, coagulation function tests and liver and kidney function of 223 patients before neoadjuvant chemotherapy. The formulas for calculating NLR, PLR, LMR, PNI, SII and SIRI are as follows: NLR = Neut#/LYMPH#, PLR = PLT/LYMPH#, LMR = LYMPH#/MONO#, PNI = A + 0.005* LYMPH#, SII = PLT*Neut#/LYMPH#, SIRI = Neut#* MONO#/LYMPH#. In addition, age, gender, tumor location, pathologic fracture status, and tumor metastasis status were abstracted from the patients' medical records. Overall survival (OS) was calculated from the date of tumor resection to the date of last follow-up or death. In the overall cohort, the optimal cutoff value for each hematological marker was calculated based on the "tdROC" package and converted into a binary variable according to the cutoff value. The 14 patients with osteosarcoma treated with camrelizumab had their hematological markers collected before the start of immunotherapy, and the haematological markers were divided into dichotomous variables following the same cutoff value as the overall cohort.

Development and Validation of the HPSS

First, univariate cox regression analysis was used to screen indicators of prognostic value in the overall cohort. Based on prognosis-related hematological markers, LASSO cox regression analysis was performed on the training set to determine the optimal hematological prognostic scoring system (HPSS). The LASSO model is an estimation method that enables the reduction of the set of indicators. LASSO regression has the advantages of ridge regression and subset selection at the same time, which makes it superior to other methods in terms of prediction accuracy and model interpretability for high-dimensional multicollinearity problems. The HPSS was calculated for each patient in the training and validation sets based on the coefficients assigned by the LASSO cox regression analysis. Receiver operating curves were used to compare HPSS to the individual hematology markers in both training and validation sets. In the training set, the optimal cutoff value was calculated for HPSS using the survivalROC "package, and the patients were divided into high-risk and low-risk groups based on the cutoff value. The same cutoff was used for the validation set. Kaplan-Meier survival curves were plotted to show the difference in OS between the two groups of patients. Whether HPSS is an independent prognostic factor for predicting OS in osteosarcoma patients was assessed using multivariate cox regression analysis. ROC curves for HPSS versus clinical variables were plotted and contrasted from 1 to 5 years in the training set and the validation set using the timeROC package.

Construction and Evaluation of the Nomogram

A nomogram was constructed combining HPSS with clinical features in the training set. The discrimination ability and accuracy of nomograms were evaluated by Harrell's Concordance Index and calibration curve, respectively. Decision curve analysis (DCA) was used to evaluate the clinical application of the nomogram. In addition, the constructed nomogram also predicted the overall survival of the validation cohort to assess the stability of the nomogram's predictive ability.

Exploration of the Relationship Between the HPSS and Clinical Characteristics

In all 223 patients, the relationship between the HPSS and traditional clinical features, such as tumor site, pathological fracture, tumor metastasis status, was further researched. At the same time, we divided the patients into four groups by tumor metastasis status, pathological fracture status combined with HPSS, respectively. Two-factor KM survival curves were drawn to show the differences in overall survival among the four groups of patients.

Assessing Immunotherapy Response Using HPSS

We calculated HPSS for 14 patients with advanced osteosarcoma treated with immunotherapy using the same coefficients as the training cohort. The immunotherapy efficacy of 14 patients was divided into disease control rate (DCR) and progressive disease (PD) based on RESICT. The fisher's exact test was used to assess the difference between DCR and PD between patients in the high-risk group and those in the low-risk group.

Statistical Analysis

Kolmogorov-Smirnov was used to assess whether continuous variables were normally distributed, and t-test or Mann-Whitney U test was used to assess differences between continuous variables according to the results. Categorical variables were evaluated using the chi-square test and the fisher's exact test based on the number of individuals in each group. All statistical analyses were conducted using R software, version 4.1.0 (Institute for Statistics and Mathematics, Vienna, Austria). P values < 0.05 were considered to indicate statistical significance.

RESULTS

Patient Characteristics

A total of 223 patients with osteosarcoma were included in the study, including 131 male and 92 female. The age of the patients ranged from 7 to 67 years with a mean age of 21 years. The majority of patients had tumors located in the extremities, and only 9 patients had tumors located in non-extremity sites. A total of 25 patients already had pathological fractures at presentation. In addition, 39 patients had already developed tumor metastasis at presentation. Two hundred twenty-three patients were randomly assigned to the training cohort versus the validation cohort. The demographic and clinical characteristics of the training cohort versus the validation cohort are shown in **Table 1**, with no significant differences between the two groups of cohorts. Optimal cutoff values for 16 hematological markers are provided with Supplementary **Table 1** (ALP, PLR, NLR, SII, FIB, SIRI, PT, HB, APTT, INR, PNI, LMR, RDW-CV, RDW-SD, LDH, TT). As shown in **Table 1**, the distributions of all variables in the training and validation sets are not significantly different.

Establishment and Validation of Hematological Risk Model for Osteosarcoma

First, we performed univariate cox regression analysis of hematologic markers in the overall cohort to determine the association between hematologic markers and OS in patients with osteosarcoma. As shown in **Figure 1**, univariate cox regression analysis showed that 9 hematological markers were statistically significant. As described above, a LASSO cox regression analysis was performed in the training set using 9 hematological indicators and the HPSS consisting of 7 hematological indicators was finally determined. The coefficients for each indicator in the HPSS are shown in **Table 1**, and the HPSS was calculated for each patient based on these coefficients. The results of ROC curves indicated that the predictive ability of HPSS was significantly higher than that of individual hematological markers both in the training and

TABLE 1 | Differences in the distribution of all variables between the training set and the validation set and the respective coefficients of the seven hematological indicators that make up the HPSS.

	Train (N = 156)	Test (N = 67)	P-value	Coefficient
OS.time				Not applicable
Mean (SD)	1020 (533)	996 (602)	0.787	
OS				Not applicable
Alive	101 (64.7%)	46 (68.7%)	0.681	
Died	55 (35.3%)	21 (31.3%)		
Gender				Not applicable
Male	89 (57.1%)	42 (62.7%)	0.525	
Female	67 (42.9%)	25 (37.3%)		
Age				Not applicable
Mean (SD)	21.8 (12.6)	21.4 (11.7)	0.823	
Metastasis.status				Not applicable
No	132 (84.6%)	52 (77.6%)	0.285	
Yes	24 (15.4%)	15 (22.4%)		
Tumor.site				Not applicable
Extremities	150 (96.2%)	64 (95.5%)	1	
Non-extremities	6 (3.8%)	3 (4.5%)		
Pathological.fracture				Not applicable
No	135 (86.5%)	63 (94.0%)	0.163	
Yes	21 (13.5%)	4 (6.0%)		
NLR				Excluded
High	60 (38.5%)	30 (44.8%)	0.464	
Low	96 (61.5%)	37 (55.2%)		
PLR				0.521
High	48 (30.8%)	19 (28.4%)	0.841	
Low	108 (69.2%)	48 (71.6%)		
LMR				Excluded
High	126 (80.8%)	58 (86.6%)	0.394	
Low	30 (19.2%)	9 (13.4%)		
PNI				-0.058
High	98 (62.8%)	44 (65.7%)	0.799	
Low	58 (37.2%)	23 (34.3%)		
SII				0.097
High	31 (19.9%)	17 (25.4%)	0.46	
Low	125 (80.1%)	50 (74.6%)		
SIRI				Excluded
High	37 (23.7%)	16 (23.9%)	1	
Low	119 (76.3%)	51 (76.1%)		
HB				Excluded
High	101 (64.7%)	47 (70.1%)	0.53	
Low	55 (35.3%)	20 (29.9%)		
RDW-SD				Excluded
High	58 (37.2%)	16 (23.9%)	0.0753	
Low	98 (62.8%)	51 (76.1%)		
RDW-CV				Excluded
High	86 (55.1%)	34 (50.7%)	0.649	
Low	70 (44.9%)	33 (49.3%)		
PT				0.051
High	37 (23.7%)	21 (31.3%)	0.306	
Low	119 (76.3%)	46 (68.7%)		
INR				Excluded
High	66 (42.3%)	29 (43.3%)	1	
Low	90 (57.7%)	38 (56.7%)		
APTT				Excluded
High	62 (39.7%)	23 (34.3%)	0.54	
Low	94 (60.3%)	44 (65.7%)		
TT				Excluded
High	84 (53.8%)	35 (52.2%)	0.941	
Low	72 (46.2%)	32 (47.8%)		
FIB				0.330
High	135 (86.5%)	58 (86.6%)	1	
Low	21 (13.5%)	9 (13.4%)		
ALP				0.785

(Continued)

TABLE 1 | Continued

	Train (N = 156)	Test (N = 67)	P-value	Coefficient
High	82 (52.6%)	40 (59.7%)	0.404	
Low	74 (47.4%)	27 (40.3%)		
LDH				0.186
High	103 (66.0%)	40 (59.7%)	0.453	
Low	53 (34.0%)	27 (40.3%)		

validation cohorts (0.817 vs 0.413-0.745; 0.827 vs 0.321-0.710, **Figures 1B, C**).

Optimal cutoff values were also calculated for HPSS. The training cohort was divided into two groups with the validation cohort according to the optimal cutoff value. As shown by **Figures 2A, B**, the overall survival of patients in the high HPSS risk group was low in both the training and validation cohorts ($P < 0.001$).

Subsequently, we also assessed whether HPSS was an independent prognostic factor for predicting overall survival in osteosarcoma patients. As shown in **Figures 3A–D**, the results of multivariate cox regression analysis showed that HPSS was an independent prognostic factor for overall survival in osteosarcoma patients in both the training and validation cohorts(training cohort: HR:6.796(2.521-18.317); validation cohort: HR:5.655(1.788-17.88)).

Finally, we plotted time-dependent ROC curves to contrast the predictive ability of HPSS with clinical features such as tumor metastatic status, and pathological fractures. As shown by **Figures 3E, F**, the predictive ability of the HPSS was similar in the change curves of the training and validation cohorts, that is, it was lowest in predicting 1-year mortality, but the predictive ability of the HPSS gradually increased with time. At 2 years and beyond, the predictive power of the HPSS was significantly higher than that of the clinical features.

Construction and Validation of HPSS-Based Nomograms

In order to promote the clinical application of HPSS, based on the training cohort, we constructed a nomogram combining HPSS with clinical characteristics. Cox proportional hazards regression assigned a score according to the hazard ratio for each covariate in the nomogram, and the sum of the scores for each covariate was the nomogram total score. The C-index of the constructed nomogram was 0.80, and the calibration curve indicated that the nomogram had good predictive accuracy in predicting 3-year and 5-year overall survival in the training cohort (**Figures 4A, B**). To further validate the stability of the nomogram, we tested the nomogram using the validation cohort. The C-index of the nomogram in the validation set was 0.77, and the calibration curve of the validation set showed that the nomogram still had good predictive ability in the validation cohort (**Figure 4C**). Finally, we explore the clinical benefits of nomograms through clinical decision analysis. Our results suggest that the nomogram added to the HPSS brings significant net benefits over models with only clinical features (**Figures 4D, E**).

Assessing the Stability of HPSS

In order to assess the stability of the HPSS and facilitate its precise application, we set up different subgroups according to

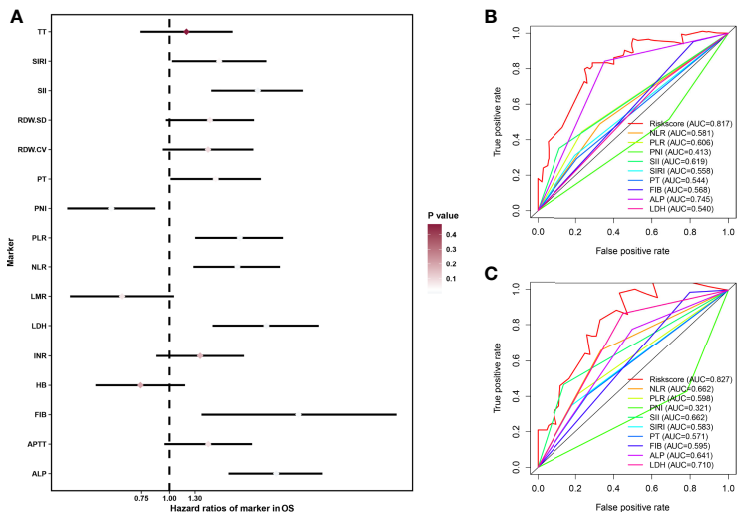

FIGURE 1 | Construction of HPSS and its comparison with individual hematological parameters. **(A)** Forest plot showing the results of univariate cox regression analysis of 16 hematological markers; **(B)** ROC curves showing the predictive power of HPSS in the training set versus a single hematology indicator; **(C)** ROC curves showing the predictive power of HPSS in the validation set versus a single hematology indicator.

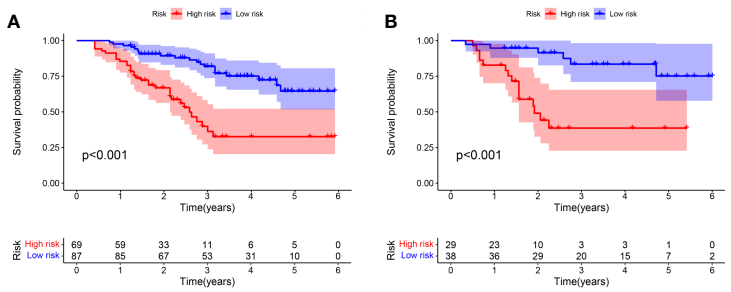

FIGURE 2 | There are significant differences between patients in HPSS risk groups. **(A)** High-risk patients in the training set had significantly lower overall survival than low-risk patients; **(B)** High-risk patients in the validation set had significantly lower overall survival than low-risk patients.

clinical characteristics to explore the application of the HPSS in each group. As shown in **Figure 5A**, patients were divided into 10 groups according to age, gender, tumor location, metastatic status and pathological fracture. The predictive ability of HPSS was limited in patients with metastatic group, and non-extremities group. Combined with the previously drawn time-dependent ROC curve, we believe that HPSS should be more used as a supplement to clinical features to further identify high-risk patients from patients in the low-risk group of clinical features.

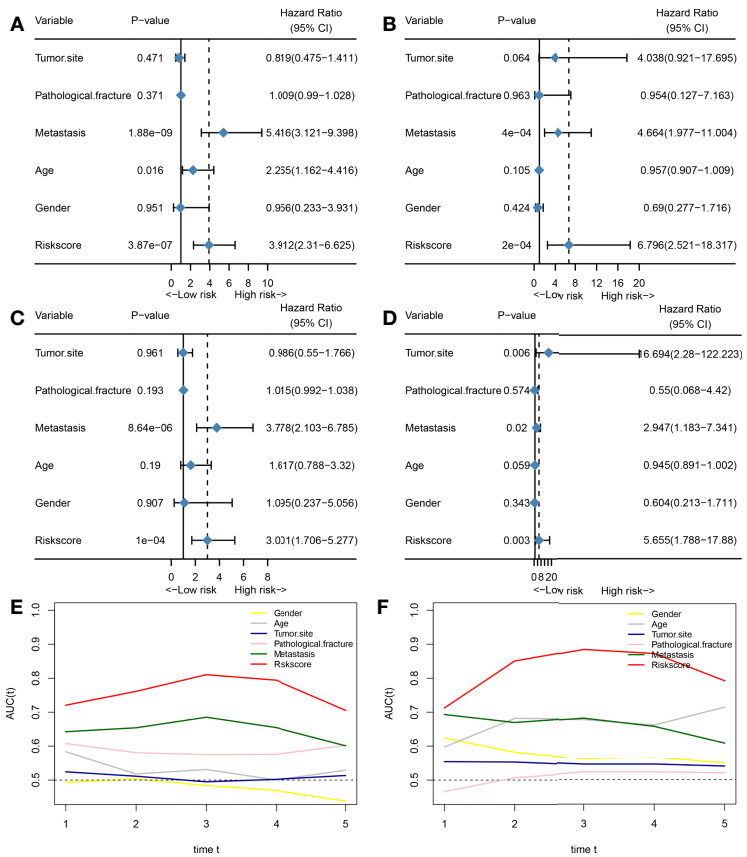

FIGURE 3 | HPSS is an independent prognostic factor for overall survival in patients with osteosarcoma and has certain advantages compared with clinical characteristics. **(A)** Forest plot showing the results of univariate COX regression analysis of HPSS and clinical characteristics in the training set; **(B)** Forest plot showing the results of multivariate COX regression analysis of HPSS and clinical characteristics in the training set; **(C)** Forest plot showing the results of univariate COX regression analysis of HPSS and clinical characteristics in the validation set; **(D)** Forest plot showing the results of multivariate COX regression analysis of HPSS and clinical characteristics in the validation set; **(E)** Time-dependent ROC curves showing the predictive power of HPSS and clinical features in the training set; **(F)** Time-dependent ROC curves showing the predictive power of HPSS and clinical features in the training set; It can be seen that the predictive power of each variable varies over time.

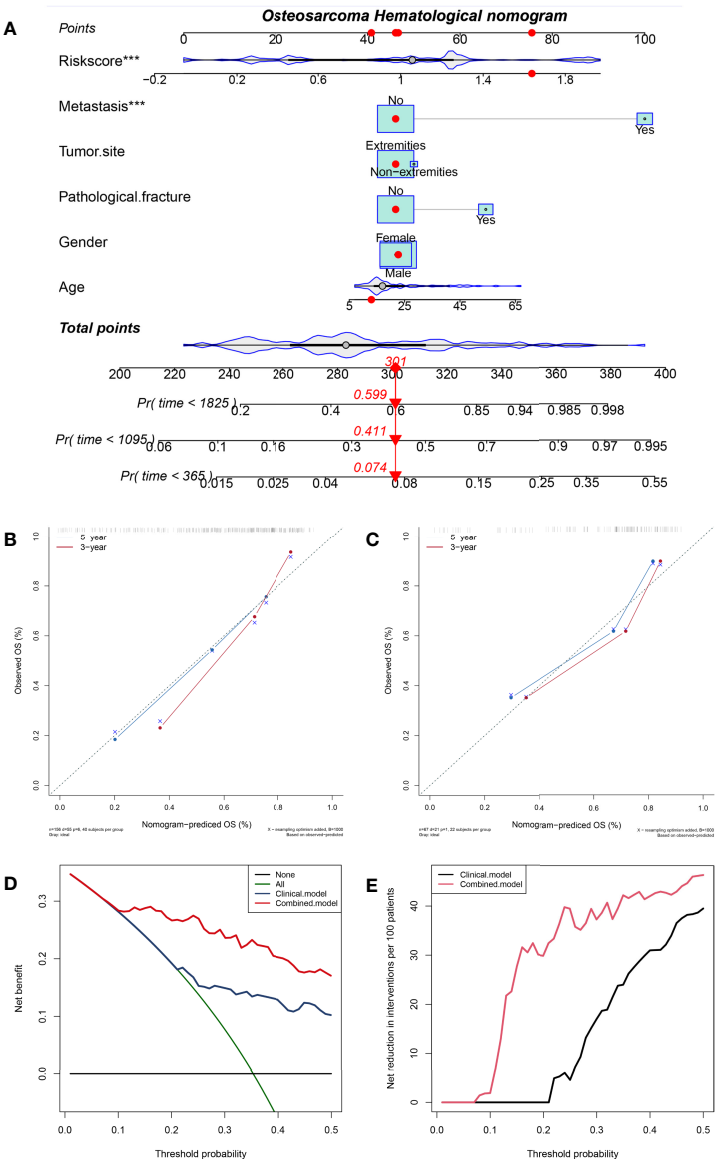

FIGURE 4 | A nomogram was constructed combining HPSS with clinical features and the predictive power of the nomogram was assessed. **(A)** The nomogram of the overall survival of patients with osteosarcoma shows that HPSS score and tumor metastasis status are the two most important variables; **(B)** Calibration curves for nomogram predicting 3-year and 5-year survival of patients in the training set; **(C)** Calibration curves for nomogram predicting 3-year and 5-year survival of patients in the validation set; **(D)** The clinical net benefit curve of the nomogram; **(E)** Clinical Net Reduction Curve for Nomogram. ***p < 0.001

Association Between HPSS and Clinical Features

Finally, we further assessed the relationship between HPSS and clinical characteristics. The results of the violin plot indicated that patients in the tumor metastasis group and pathological fracture group had higher HPSS scores (metastasis: P = 0.002; pathological fracture: P= 0.009). However, there was no significant difference in HPSS between patients with different gender, tumor location (**Figures 5B–E**).

As mentioned above, we believe that HPSS is the best complement to clinical features. Therefore, we combined HPSS with tumor metastasis status and divided patients into four groups to assess differences in patient survival. As shown, there was a significant difference in survival among the four groups. Among them, patients in the high HPSS risk group among patients in the non-metastatic group had significantly lower overall survival than those in the low HPSS risk group. Finally, we combined HPSS with pathological fracture status

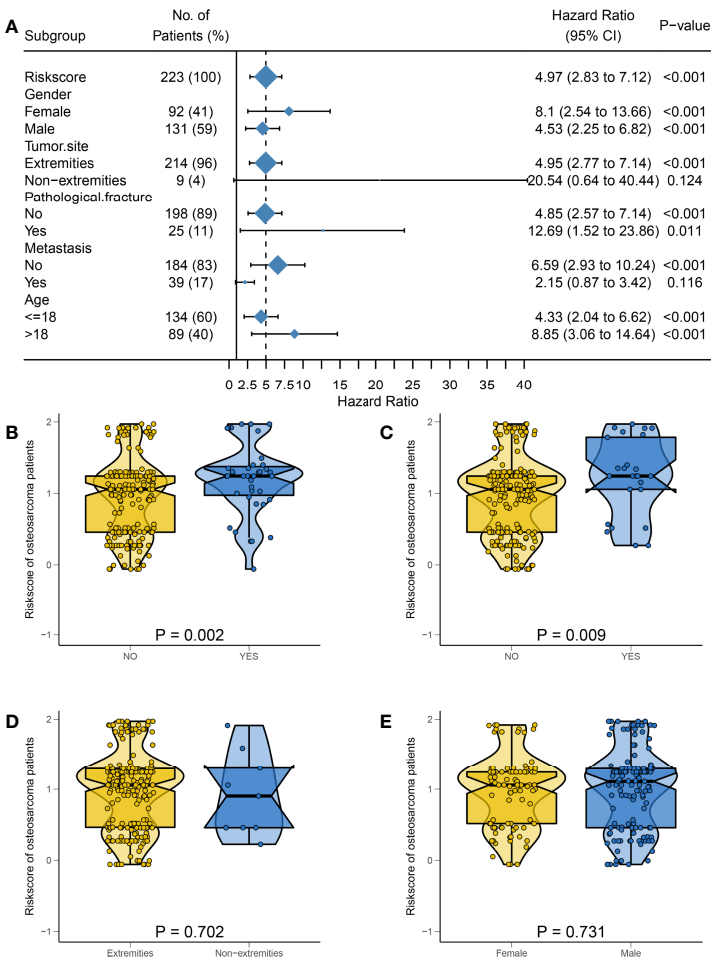

FIGURE 5 | The predictive power of HPSS in subgroups and the relationship between HPSS and clinical characteristics were assessed. **(A)** A forest plot showing the predictive power of HPSS in each subgroup, it can be seen that HPSS has limited predictive power in patients with tumor metastasis and non-extremity groups; **(B)** The relationship between HPSS and tumor metastasis status; **(C)** The relationship between HPSS and pathological fracture status; **(D)** The relationship between HPSS and tumor location; **(E)** The relationship between HPSS and gender.

with the same method to obtain similar conclusions (**Figures 6A, B**).

Assessing Immunotherapy Response Using HPSS

As described above, all patients had TPS ≥ 1%, however only 4 patients had TPS > 1%; these 4 patients had TPS of 8%, 5%, 3%, and 2%, respectively, and the remaining patients had TPS = 1%. **Figures 7A–D** presents the PD-L1 immunohistochemistry results of the 2 patients. According to RECIST, 9 of 14 patients developed PD and only 5 patients were assessed as DCR (**Figure 7E**). Based on HPSS, 7 patients were high risk and 7 patients were low risk. PD occurred in all patients in the high-risk group, and only 2 in the low-risk group. The results of Fisher's exact test suggest that HPSS can predict the response to immunotherapy to a certain extent (p = 0.0210, **Figure 7F**).

In addition, we evaluated the relationship between TPS and response to immunotherapy. DCR was achieved in 3 of 4 patients with TPS > 1% and in only 2 of 10 patients with TPS = 1%. Unfortunately, this difference did not reach statistical significance (p = 0.0949, **Figure 7G**). Finally, we also assessed the relationship between HPSS and TPS. Our results indicated no significant relationship between HPSS and TPS (p = 0.559, **Figure 7H**). **Figure 8** shows lung CT results before and after drug treatment in a PD patient and a DCR patient.

DISCUSSION

With the continuous development of surgical techniques and the continuous emergence of various novel treatments, the mortality rate of cancer patients is gradually decreasing. However, since the 1970s, the overall survival of osteosarcoma patients has reached a bottleneck period that has not been improved to date (1, 23, 24). With the continuous development of the concept of precision medicine, it is particularly important to develop personalized

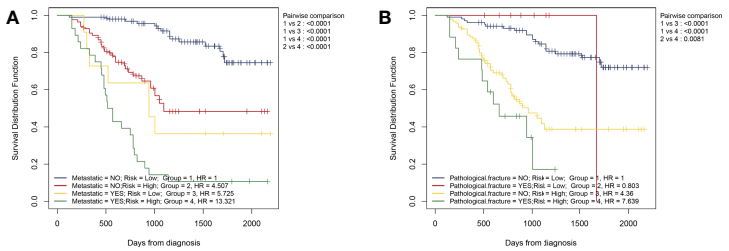

FIGURE 6 | Simple combination of HPSS and clinical features can better predict the prognosis of patients with osteosarcoma. **(A)** Patients with osteosarcoma can be divided into four groups according to tumor metastasis status and HPSS risk, and the KM survival curve shows the difference in survival among the four groups; **(B)** Patients with osteosarcoma can be divided into four groups according to pathological fracture status and HPSS risk, and the KM survival curve shows the difference in survival among the four groups.

treatment plans for cancer patients by grading management, and it is expected to improve the prognosis of cancer patients (25). More and more evidence shows that genetic changes and epigenetic modifications play an important role in the occurrence and progression of tumors. The use of genetic testing to assess the prognosis of patients especially the response to drug therapy has begun to be applied in the clinic. However, most of these tests rely on patient tissue and are expensive. Fortunately, recent studies have shown that many preoperative hematological markers can predict the prognosis of cancer patients (26–28). Unlike genetic testing, these hematological markers are inexpensive and readily available. In

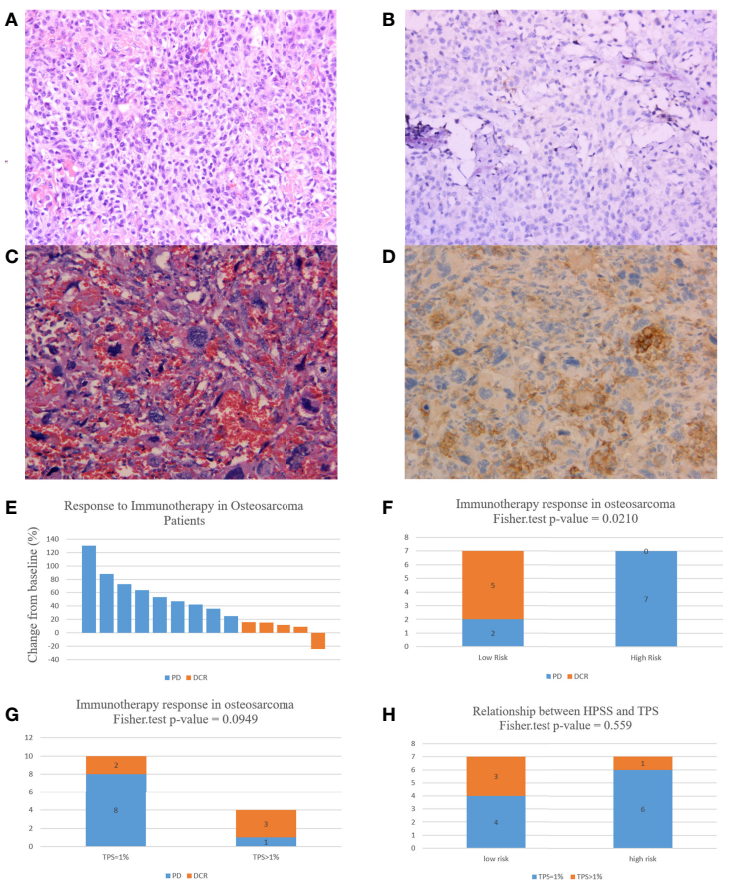

FIGURE 7 | HPSS can predict patient response to immunotherapy to a certain extent. **(A)** HE staining of a patient with 3% TPS expression; **(B)** PD-L1 expression in a patient with a TPS expression of 3; **(C)** HE staining of a patient with 8% TPS expression; **(D)** PD-L1 expression in a patient with a TPS expression of 8; **(E)** A waterfall plot of the response to immunotherapy in 14 osteosarcoma patients; **(F)** Histogram showing differences in immunotherapy status in HPSS risk groups; **(G)** Histogram showing differences in immunotherapy status in different TPS groups; **(H)** Differences in TPS values in different HPSS risk groups.

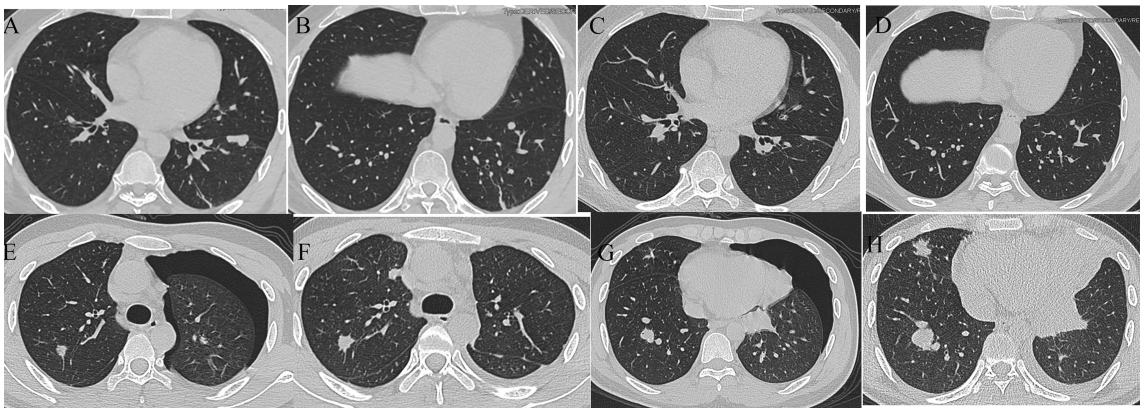

FIGURE 8 | Lung CT results of one PD and one DCR patient. **(A, B)** Lung CT results of a DCR patient before immunotherapy; **(C, D)** Lung CT results of a DCR patient after immunotherapy; **(E, F)** Lung CT results of a PD patient before immunotherapy; **(G, H)** Lung CT results of a PD patient after immunotherapy.

fact, most of them originate from the routine tests that every patient needs to perform on admission. Previous studies have mostly only demonstrated the prognostic value of a single hematological marker in cancer patients (29–31). However, given the complexity of the tumor microenvironment, it is difficult for a single hematological marker to fully reflect tumor characteristics and accurately predict tumor progression. In fact, although previous studies have shown that LMR has prognostic value in osteosarcoma patients, LMR has limited predictive power in our cohort (32–34). In this study, we extensively collected hematological markers that have been shown to be of prognostic value in osteosarcoma and constructed HPSS based on these markers. Compared with single hematological parameters, HPSS has more powerful predictive ability and is expected to overcome the disadvantage of unstable predictive ability of single hematological parameters. HPSS has a better predictive ability than clinical characteristics in predicting long-term patient survival. The nomogram based on HPSS has good predictive ability. The HPSS is a valid complement to clinical characteristics, and in combination with clinical characteristics enables further differentiation of patients in the clinically low-risk group. HPSS can predict the response to immunotherapy to some extent.

Tumor-associated inflammation has already been recognized as an important hallmark of cancer (35). Studies have shown that inflammatory processes promote cancer growth and transmission, as well as the activation of oncogenic signaling pathways, and are also potential mechanisms of immune resistance in cancer patients (36). And through dynamic and extensive interactions with cancer cells, immune cells also play an important role in the tumor microenvironment (37). Although the available evidence suggests a paradoxical role for neutrophils in preventing and promoting tumor progression, it is generally believed that in solid tumors, neutrophils expand in the tumor microenvironment and systemically, often associated with poor prognosis (38). In contrast, lymphocytes in the tumor microenvironment are thought to play an important role in antitumor immunity by producing cytokines and inducing tumor cell apoptosis (39). Platelets change the tumor microenvironment by secreting vascular growth factor is also considered to promote tumor cell growth and vascular proliferation, protect tumor cells from immune cell elimination, and promote tumor cell metastasis (40). As a classical inflammatory marker in cancer patients, the prognostic value of lactate dehydrogenase has been extensively studied (41). It is now generally accepted that elevated LDH levels are associated with poor prognosis in patients. In addition, some clinical trials have also demonstrated that elevated LDH correlates with response to immunotherapy, suggesting the potential value of monitoring LDH levels (42, 43). As the cornerstone of constituting the HPSS, the coefficients of SII, PLR and LDH were 0.096, 0.521 and 0.186, respectively, similarly indicating that higher SII, PLR and LDH is associated with poor prognosis in patients, further confirming previous results.

Almost all types of cancer are accompanied by a hypercoagulable state, even without thrombosis (44). Tumor cells create a hypercoagulable microenvironment by expressing coagulants, tissue factors, or inflammatory cytokines. There is a close link between the mechanism of tumor production and the system that controls blood coagulation from the early stages of the disease. The coagulation system is an important aspect of the unique vascular microenvironment for tumor proliferation and progression. The reason why tumors express substrates to induce a systemic hypercoagulable state is the discovery of circulating microparticles derived from tumor antigens or tissue factors, which are derived from the membranes of leukocytes, platelets, endothelial cells, and tumor cells after activation or apoptosis. PT test is a monitoring index of extrinsic coagulation system, which is related to fibrinogen deficiency, primary systemic and disseminated intravascular coagulation (DIC) (45). Recent studies have also shown that elevated PT is associated with poor prognosis in tumors such as liver cancer and colon cancer (46). As an important factor in the coagulation cascade and process, FIB has been shown to be associated with the invasive process of a variety of malignant tumors (29, 47). The FIB promotes angiogenesis and tumor growth by binding to

growth factors such as vascular endothelial growth factor and fibroblast growth factor-2 (48, 49). In our study, the coefficients of PT and FIB were 0.051 and 0.330, respectively, indicating that they were all associated with poor prognosis of patients.

PNI is a nutritional indicator that was originally developed to predict the risk of postoperative morbidity and mortality after gastrointestinal surgery (50). Because the original PNI is complex and difficult, and to facilitate routine use in clinical practice, Onodera et al. simplified the calculation method to make it based on serum albumin levels and peripheral blood lymphocyte counts (51). Serum albumin, a commonly used parameter of nutritional status, is inversely associated with prognosis in various cancers (52). Since PNI is a combination of lymphocytes and serum albumin, it is easy to understand the relationship between PNI and survival of cancer patients. Many studies have reported that poor tumor characteristics, such as poor differentiation, large size, and metastasis, are more likely to be observed in patients with tumors with lower PNI, suggesting that low PNI may promote tumor aggressiveness and thus worsen prognosis (53, 54). In our study, the coefficient of PNI was -0.058, which is consistent with previous conclusions.

Serum ALP levels are often positively correlated with osteoblast activity, and serum ALP is common in fractures, physiological growth and bone tumors. Studies on the prognostic value of serum ALP in osteosarcoma date back even before the era of chemotherapy (55). Now, it is generally believed that elevated serum ALP is associated with a worse prognosis in osteosarcoma patients (56). As an important part of constituting the HPSS, the coefficient of ALP was 0.940, indicating that elevated ALP is associated with poor patient prognosis. This is consistent with previous findings. We believe that the introduction of serum ALP makes HPSS more suitable for patients with bone tumors and enhances its predictive ability in patients with bone tumors.

Several recent clinical trials have shown very limited benefit from immune checkpoint inhibitor therapy in patients with advanced osteosarcoma (16, 57). Therefore, careful identification of patients who may benefit from this therapy is critical. It is generally accepted that patients with higher TPS are more likely to benefit from immunotherapy (58). The results of a recent clinical trial in patients with advanced non-small-cell lung cancer showed a positive survival benefit with immunotherapy in a population with TPS of 1% or higher (22). Unfortunately there is no uniform standard in osteosarcoma, therefore, our center referred to this result to only suggest that patients with TPS ≥ 1% try immunotherapy. Unexpectedly, our results show that TPS is not effective in predicting immunotherapy response in osteosarcoma patients. We speculate that it is mainly due to the following reasons. First, only 14 patients were included in the study and all were screened by TPS. In fact, there are more patients with osteosarcoma who are not recommended to try immunotherapy because of TPS < 1%. In addition, the TPS of patients with the highest TPS was only 8%. However, the cutoff value of TPS is generally considered to be 1% versus 50% (22). Recently, an increasing number of studies have focused on the use of hematological markers to assess the efficacy of immunotherapy in tumor patients. Studies have shown that using markers such as NLR, SII and LDH to identify patients with poor immunotherapy is a potential approach (59, 60). Therefore, we explored whether HPSS, which integrates multiple hematological markers, is equally valuable in predicting immunotherapy. It is gratifying that our results show that HPSS has such potential. However, since the study included only 14 patients and the response of immunotherapy in osteosarcoma was limited, the results of HPSS in predicting response to immunotherapy need to be interpreted with caution.

Overall, compared with a single hematological marker, HPSS has stronger predictive power. In our study, both the training and validation cohorts, HPSS showed a predictive potential superior to individual hematological markers. In studies reviewing previous single hematological parameters, we found that some hematological parameters differed in their prognostic value in different cohorts. This greatly affects the clinical application of hematological markers. We speculate that due to the poor predictive ability of a single hematological markers, it cannot comprehensively respond to the complex tumor microenvironment. Therefore, we extensively collected multiple hematological markers and constructed the HPSS to improve its predictive ability. We hope that HPSS with predictive ability can overcome the disadvantage of unstable predictive ability of a single hematological markers. Through further analysis of HPSS, we found that HPSS had a weak ability to predict early patient survival, but a strong ability to predict long-term patient survival. This is in contrast to clinical features such as tumor metastasis status and pathological fracture status. Therefore, we believe that HPSS is an effective complement to clinical features and is best suited for further identification of high-risk patients among patients at low risk for clinical features.

Finally, we have the following recommendations regarding the clinical application of HPSS. For patients with primary diagnosis of osteosarcoma, it is recommended to use the hematological parameters before chemotherapy to calculate HPSS. Because the results of these hematological parameters may be affected by chemotherapy and cannot truly reflect the patient's tumor microenvironment. However, for patients treated with immunotherapy, based on the consideration of clinical application, we believe that the calculation of HPSS should be adjusted to the detection time close to PD-L1; that is, the latest HPSS before immunotherapy should be calculated and synergized with TPS to predict the response to immunotherapy.

It must be acknowledged that our study has certain limitations. First, a retrospective study, which may lead to selection bias. Second, HPSS is composed of six hematological parameters, each of which has its own coefficient, and its calculation is more difficult than that of a single hematological marker. In addition, the hematologic markers included in this study were based on those previously shown to have prognostic value. Therefore, some markers that also have prognostic value for osteosarcoma patients may be overlooked. However, to the best of our knowledge, this is the first study to comprehensively assess the prognostic value of hematological markers in osteosarcoma, and therefore has some value. Further studies

are needed to validate our conclusions. In addition, we believe that further studies are needed to assess whether HPSS can guide the treatment of osteosarcoma patients. For example, increase the frequency of follow-up lung CT for patients with high HPSS who do not develop lung metastases, or increase the chemotherapy cycles for patients with high HPSS. At the same time, the HPSS score can be appropriately considered when screening patients for prior to the application of caritizumab.

CONCLUSION

Our study confirms the prognostic value of the comprehensive hematological score HPSS in patients with osteosarcoma. HPSS is an independent prognostic factor in patients with osteosarcoma. The nomogram constructed based on HPSS has good predictive ability. The HPSS is a valid addition to clinical characteristics and is suitable for further identification of high-risk patients from low clinical risk patients. HPSS has certain implications for the response to immunotherapy.

DATA AVAILABILITY STATEMENT

The raw data supporting the conclusions of this article will be made available by the authors, without undue reservation.

ETHICS STATEMENT

The studies involving human participants were reviewed and approved by Ethics Committee of West China Hospital of Sichuan University. Written informed consent to participate in this study was provided by the participants' legal guardian/next of kin.

AUTHOR CONTRIBUTIONS

'LL, YZ and CT designed the study and LL, XH, YW, ZL, CL, JL, QC jointly collected and managed the data. LL, TG co-drafted the manuscript. LM, YL, ML reviewed and corrected the manuscript. YZ and CT oversaw the entire research process. All authors contributed to the article and approved the submitted version.

FUNDING

The institution of one or more of the authors (ML, LM, YZ, CT) has received, during the study period, funding from the Science and Technology Research Program of Sichuan Province (2020YFS0036), the Chengdu Science and Technology Project (2017-CY02-00032-GX), 1·3·5 project for disciplines of excellence, West China Hospital, Sichuan University (ZYJC18036), the Fundamental Research Funds for the Central Universities (20826041E4071), Post-Docter Research Project, West China Hospital, Sichuan University (20HXBH136), and Project funded by China Postdoctoral Science Foundation (2021M702342).

ACKNOWLEDGMENTS

Thanks to the support of West China Hospital, Sichuan University for the research.

SUPPLEMENTARY MATERIAL

The Supplementary Material for this article can be found online at: https://www.frontiersin.org/articles/10.3389/fimmu.2022.879560/full#supplementary-material

REFERENCES

1. Isakoff MS, Bielack SS, Meltzer P, Gorlick R. Osteosarcoma: Current Treatment and a Collaborative Pathway to Success. *J Clin Oncol* (2015) 33 (27):3029–35. doi: 10.1200/jco.2014.59.4895
2. Valery PC, Laversanne M, Bray F. Bone Cancer Incidence by Morphological Subtype: A Global Assessment. *Cancer Causes Control: CCC* (2015) 26 (8):1127–39. doi: 10.1007/s10552-015-0607-3
3. Mirabello L, Troisi RJ, Savage SA. Osteosarcoma Incidence and Survival Rates From 1973 to 2004: Data From the Surveillance, Epidemiology, and End Results Program. *Cancer* (2009) 115(7):1531–43. doi: 10.1002/cncr.24121
4. Kempf-Bielack B, Bielack SS, Jürgens H, Branscheid D, Berdel WE, Exner GU, et al. Osteosarcoma Relapse After Combined Modality Therapy: An Analysis of Unselected Patients in the Cooperative Osteosarcoma Study Group (COSS). *J Clin Oncol* (2005) 23(3):559–68. doi: 10.1200/jco.2005.04.063
5. Aljubran AH, Griffin A, Pintilie M, Blackstein M. Osteosarcoma in Adolescents and Adults: Survival Analysis With and Without Lung Metastases. *Ann Oncol* (2009) 20(6):1136–41. doi: 10.1093/annonc/mdn731
6. Gorlick R, Janeway K, Lessnick S, Randall RL, Marina N. Children's Oncology Group's 2013 Blueprint for Research: Bone Tumors. *Pediatr Blood cancer* (2013) 60(6):1009–15. doi: 10.1002/pbc.24429
7. Saraf AJ, Fenger JM, Roberts RD. Osteosarcoma: Accelerating Progress Makes for a Hopeful Future. *Front Oncol* (2018) 8:4. doi: 10.3389/fonc.2018.00004
8. Meyers PA, Schwartz CL, Krailo M, Kleinerman ES, Betcher D, Bernstein ML, et al. Osteosarcoma: A Randomized, Prospective Trial of the Addition of Ifosfamide and/or Muramyl Tripeptide to Cisplatin, Doxorubicin, and High-Dose Methotrexate. *J Clin Oncol* (2005) 23(9):2004–11. doi: 10.1200/jco.2005.06.031
9. Whelan JS, Davis LE. Osteosarcoma, Chondrosarcoma, and Chordoma. *J Clin Oncol* (2018) 36(2):188–93. doi: 10.1200/jco.2017.75.1743
10. Hodi FS, O'Day SJ, McDermott DF, Weber RW, Sosman JA, Haanen JB, et al. Improved Survival With Ipilimumab in Patients With Metastatic Melanoma. *N Engl J Med* (2010) 363(8):711–23. doi: 10.1056/NEJMoa1003466
11. Garon EB, Rizvi NA, Hui R, Leighl N, Balmanoukian AS, Eder JP, et al. Pembrolizumab for the Treatment of Non-Small-Cell Lung Cancer. *N Engl J Med* (2015) 372(21):2018–28. doi: 10.1056/NEJMoa1501824
12. Sundara YT, Kostine M, Cleven AH, Bovée JV, Schilham MW, Cleton-Jansen AM. Increased PD-L1 and T-Cell Infiltration in the Presence of HLA Class I Expression in Metastatic High-Grade Osteosarcoma: A Rationale for T-Cell-Based Immunotherapy. *Cancer Immunol Immunother: CII* (2017) 66(1):119–28. doi: 10.1007/s00262-016-1925-3
13. Huang X, Zhang W, Zhang Z, Shi D, Wu F, Zhong B, et al. Prognostic Value of Programmed Cell Death 1 Ligand-1 (PD-L1) or PD-1 Expression in Patients With Osteosarcoma: A Meta-Analysis. *J Cancer* (2018) 9(14):2525–31. doi: 10.7150/jca.25011
14. D'Angelo SP, Mahoney MR, Van Tine BA, Atkins J, Milhem MM, Jahagirdar BN, et al. Nivolumab With or Without Ipilimumab Treatment for Metastatic

Sarcoma (Alliance A091401): Two Open-Label, Non-Comparative, Randomised, Phase 2 Trials. *Lancet Oncol* (2018) 19(3):416–26. doi: 10.1016/s1470-2045(18)30006-8
15. Tawbi HA, Burgess M, Bolejack V, Van Tine BA, Schuetze SM, Hu J, et al. Pembrolizumab in Advanced Soft-Tissue Sarcoma and Bone Sarcoma (SARC028): A Multicentre, Two-Cohort, Single-Arm, Open-Label, Phase 2 Trial. *Lancet Oncol* (2017) 18(11):1493–501. doi: 10.1016/s1470-2045(17)30624-1
16. Xie L, Xu J, Sun X, Guo W, Gu J, Liu K, et al. Apatinib Plus Camrelizumab (Anti-PD1 Therapy, SHR-1210) for Advanced Osteosarcoma (APFAO) Progressing After Chemotherapy: A Single-Arm, Open-Label, Phase 2 Trial. *J Immunother Cancer* (2020) 8(1):e000798. doi: 10.1136/jitc-2020-000798
17. Li LQ, Bai ZH, Zhang LH, Zhang Y, Lu XC, Zhang Y, et al. Meta-Analysis of Hematological Biomarkers as Reliable Indicators of Soft Tissue Sarcoma Prognosis. *Front Oncol* (2020) 10:30. doi: 10.3389/fonc.2020.00030
18. Zhang L, Li L, Liu J, Wang J, Fan Y, Dong B, et al. Meta-Analysis of Multiple Hematological Biomarkers as Prognostic Predictors of Survival in Bladder Cancer. *Med* (2020) 99(30):e20920. doi: 10.1097/md.0000000000020920
19. Suazo-Zepeda E, Bokern M, Vinke PC, Hiltermann TJN, de Bock GH, Sidorenkov G. Risk Factors for Adverse Events Induced by Immune Checkpoint Inhibitors in Patients With Non-Small-Cell Lung Cancer: A Systematic Review and Meta-Analysis. *Cancer Immunol Immunother: CII* (2021) 70(11):3069–80. doi: 10.1007/s00262-021-02996-3
20. Cupp MA, Cariolou M, Tzoulaki I, Aune D, Evangelou E, Berlanga-Taylor AJ. Neutrophil to Lymphocyte Ratio and Cancer Prognosis: An Umbrella Review of Systematic Reviews and Meta-Analyses of Observational Studies. *BMC Med* (2020) 18(1):360. doi: 10.1186/s12916-020-01817-1
21. Li YJ, Yao K, Lu MX, Zhang WB, Xiao C, Tu CQ. Prognostic Value of the C-Reactive Protein to Albumin Ratio: A Novel Inflammation-Based Prognostic Indicator in Osteosarcoma. *OncoTargets Ther* (2017) 10:5255–61. doi: 10.2147/ott.S140560
22. Mok TSK, Wu YL, Kudaba I, Kowalski DM, Cho BC, Turna HZ, et al. Pembrolizumab Versus Chemotherapy for Previously Untreated, PD-L1-Expressing, Locally Advanced or Metastatic Non-Small-Cell Lung Cancer (KEYNOTE-042): A Randomised, Open-Label, Controlled, Phase 3 Trial. *Lancet (Lond Engl)* (2019) 393(10183):1819–30. doi: 10.1016/s0140-6736(18)32409-7
23. Kager L, Tamamyan G, Bielack S. Novel Insights and Therapeutic Interventions for Pediatric Osteosarcoma. *Future Oncol (Lond Engl)* (2017) 13(4):357–68. doi: 10.2217/fon-2016-0261
24. Strauss SJ, Whelan JS. Current Questions in Bone Sarcomas. *Curr Opin Oncol* (2018) 30(4):252–9. doi: 10.1097/cco.0000000000000456
25. Forrest SJ, Geoerger B, Janeway KA. Precision Medicine in Pediatric Oncology. *Curr Opin Pediatr* (2018) 30(1):17–24. doi: 10.1097/mop.0000000000000570
26. Wang PF, Meng Z, Song HW, Yao K, Duan ZJ, Yu CJ, et al. Preoperative Changes in Hematological Markers and Predictors of Glioma Grade and Survival. *Front Pharmacol* (2018) 9:886. doi: 10.3389/fphar.2018.00886
27. Charrier M, Mezquita L, Lueza B, Dupraz L, Planchard D, Remon J, et al. Circulating Innate Immune Markers and Outcomes in Treatment-Naïve Advanced Non-Small Cell Lung Cancer Patients. *Eur J Cancer (Oxf Engl: 1990)* (2019) 108:88–96. doi: 10.1016/j.ejca.2018.12.017
28. Xu Z, Xu W, Cheng H, Shen W, Ying J, Cheng F, et al. The Prognostic Role of the Platelet-Lymphocytes Ratio in Gastric Cancer: A Meta-Analysis. *PloS One* (2016) 11(9):e0163719. doi: 10.1371/journal.pone.0163719
29. Liang YJ, Mei XY, Zeng B, Zhang SE, Yang L, Lao XM, et al. Prognostic Role of Preoperative D-Dimer, Fibrinogen and Platelet Levels in Patients With Oral Squamous Cell Carcinoma. *BMC Cancer* (2021) 21(1):122. doi: 10.1186/s12885-021-07841-5
30. Wang S, Ma L, Wang Z, He H, Chen H, Duan Z, et al. Lactate Dehydrogenase-A (LDH-A) Preserves Cancer Stemness and Recruitment of Tumor-Associated Macrophages to Promote Breast Cancer Progression. *Front Oncol* (2021) 11:654452. doi: 10.3389/fonc.2021.654452
31. Li X, Xu J, Zhu L, Yang S, Yu L, Lv W, et al. A Novel Nomogram With Preferable Capability in Predicting the Overall Survival of Patients After Radical Esophageal Cancer Resection Based on Accessible Clinical Indicators: A Comparison With AJCC Staging. *Cancer Med* (2021) 10(13):4228–39. doi: 10.1002/cam4.3878
32. Hu H, Deng X, Song Q, Lv H, Chen W, Xing X, et al. Prognostic Value of the Preoperative Lymphocyte-to-C-Reactive Protein Ratio and Albumin-to-Globulin Ratio in Patients With Osteosarcoma. *OncoTargets Ther* (2020) 13:12673–81. doi: 10.2147/ott.S287192
33. Liu B, Huang Y, Sun Y, Zhang J, Yao Y, Shen Z, et al. Prognostic Value of Inflammation-Based Scores in Patients With Osteosarcoma. *Sci Rep* (2016) 6:39862. doi: 10.1038/srep39862
34. Liu T, Fang XC, Ding Z, Sun ZG, Sun LM, Wang YL. Pre-Operative Lymphocyte-to-Monocyte Ratio as a Predictor of Overall Survival in Patients Suffering From Osteosarcoma. *FEBS Open bio* (2015) 5:682–7. doi: 10.1016/j.fob.2015.08.002
35. Hanahan D, Weinberg RA. Hallmarks of Cancer: The Next Generation. *Cell* (2011) 144(5):646–74. doi: 10.1016/j.cell.2011.02.013
36. Grivennikov SI, Greten FR, Karin M. Immunity, Inflammation, and Cancer. *Cell* (2010) 140(6):883–99. doi: 10.1016/j.cell.2010.01.025
37. Dunn GP, Old LJ, Schreiber RD. The Immunobiology of Cancer Immunosurveillance and Immunoediting. *Immun* (2004) 21(2):137–48. doi: 10.1016/j.immuni.2004.07.017
38. Powell DR, Huttenlocher A. Neutrophils in the Tumor Microenvironment. *Trends Immunol* (2016) 37(1):41–52. doi: 10.1016/j.it.2015.11.008
39. Galon J, Bruni D. Tumor Immunology and Tumor Evolution: Intertwined Histories. *Immun* (2020) 52(1):55–81. doi: 10.1016/j.immuni.2019.12.018
40. Gay LJ, Felding-Habermann B. Contribution of Platelets to Tumour Metastasis. *Nat Rev Cancer* (2011) 11(2):123–34. doi: 10.1038/nrc3004
41. Petrelli F, Cabiddu M, Coinu A, Borgonovo K, Ghilardi M, Lonati V, et al. Prognostic Role of Lactate Dehydrogenase in Solid Tumors: A Systematic Review and Meta-Analysis of 76 Studies. *Acta Oncol (Stockholm Sweden)* (2015) 54(7):961–70. doi: 10.3109/0284186x.2015.1043026
42. Inomata M, Hayashi R, Tanaka H, Shimokawa K, Tokui K, Taka C, et al. Elevated Levels of Plasma Lactate Dehydrogenase Is an Unfavorable Prognostic Factor in Patients With Epidermal Growth Factor Receptor Mutation-Positive Non-Small Cell Lung Cancer, Receiving Treatment With Gefitinib or Erlotinib. *Mol Clin Oncol* (2016) 4(5):774–8. doi: 10.3892/mco.2016.779
43. Diem S, Kasenda B, Spain L, Martin-Liberal J, Marconcini R, Gore M, et al. Serum Lactate Dehydrogenase as an Early Marker for Outcome in Patients Treated With Anti-PD-1 Therapy in Metastatic Melanoma. *Br J Cancer* (2016) 114(3):256–61. doi: 10.1038/bjc.2015.467
44. Lee AY. Cancer and Thromboembolic Disease: Pathogenic Mechanisms. *Cancer Treat Rev* (2002) 28(3):137–40. doi: 10.1016/s0305-7372(02)00044-0
45. Zhang L, Ye J, Luo Q, Kuang M, Mao M, Dai S, et al. Prediction of Poor Outcomes in Patients With Colorectal Cancer: Elevated Preoperative Prothrombin Time (PT) and Activated Partial Thromboplastin Time (APTT). *Cancer Manage Res* (2020) 12:5373–84. doi: 10.2147/cmar.S246695
46. Mao M, Wang X, Song Y, Sheng H, Han R, Lin W, et al. Novel Prognostic Scores Based on Plasma Prothrombin Time and Fibrinogen Levels in Patients With AFP-Negative Hepatocellular Carcinoma. *Cancer Control* (2020) 27(1):1073274820915520. doi: 10.1177/1073274820915520
47. Qiao Y, Ma M, Zhang H, Yu Z, Tang P. Prognostic Significance of the Combination of Fibrinogen and Tumor Marker Index in Esophageal Squamous Cell Carcinoma Patients. *OncoTargets Ther* (2021) 14:1101–11. doi: 10.2147/ott.S278831
48. Sahni A, Simpson-Haidaris PJ, Sahni SK, Vaday GG, Francis CW. Fibrinogen Synthesized by Cancer Cells Augments the Proliferative Effect of Fibroblast Growth Factor-2 (FGF-2). *J Thromb Haemostasis: JTH* (2008) 6(1):176–83. doi: 10.1111/j.1538-7836.2007.02808.x
49. Verheul HM, van Erp K, Homs MY, Yoon GS, van der Groep P, Rogers C, et al. The Relationship of Vascular Endothelial Growth Factor and Coagulation Factor (Fibrin and Fibrinogen) Expression in Clear Cell Renal Cell Carcinoma. *Urol* (2010) 75(3):608–14. doi: 10.1016/j.urology.2009.05.075
50. Smale BF, Mullen JL, Buzby GP, Rosato EF. The Efficacy of Nutritional Assessment and Support in Cancer Surgery. *Cancer* (1981) 47(10):2375–81. doi: 10.1002/1097-0142(19810515)47:10<2375::AID-CNCR2820471009>3.0.CO;2-I
51. Onodera T, Goseki N, Kosaki G. [Prognostic Nutritional Index in Gastrointestinal Surgery of Malnourished Cancer Patients]. *Nihon Geka Gakkai zasshi* (1984) 85(9):1001–5.
52. Miura K, Hamanaka K, Koizumi T, Kitaguchi Y, Terada Y, Nakamura D, et al. Clinical Significance of Preoperative Serum Albumin Level for Prognosis in

Surgically Resected Patients With Non-Small Cell Lung Cancer: Comparative Study of Normal Lung, Emphysema, and Pulmonary Fibrosis. *Lung Cancer (Amsterdam Netherl)* (2017) 111:88–95. doi: 10.1016/j.lungcan.2017.07.003
53. Mori S, Usami N, Fukumoto K, Mizuno T, Kuroda H, Sakakura N, et al. The Significance of the Prognostic Nutritional Index in Patients With Completely Resected Non-Small Cell Lung Cancer. *PloS One* (2015) 10(9):e0136897. doi: 10.1371/journal.pone.0136897
54. Chen P, Wang C, Cheng B, Nesa EU, Liu Y, Jia Y, et al. Plasma Fibrinogen and Serum Albumin Levels (FA Score) Act as a Promising Prognostic Indicator in Non-Small Cell Lung Cancer. *OncoTargets Ther* (2017) 10:3107–18. doi: 10.2147/ott.S138854
55. Bacci G, Longhi A, Fagioli F, Briccoli A, Versari M, Picci P. Adjuvant and Neoadjuvant Chemotherapy for Osteosarcoma of the Extremities: 27 Year Experience at Rizzoli Institute, Italy. *Eur J Cancer (Oxf Engl: 1990)* (2005) 41 (18):2836–45. doi: 10.1016/j.ejca.2005.08.026
56. Hao H, Chen L, Huang D, Ge J, Qiu Y, Hao L. Meta-Analysis of Alkaline Phosphatase and Prognosis for Osteosarcoma. *Eur J Cancer Care* (2017) 26(5). doi: 10.1111/ecc.12536
57. Boye K, Longhi A, Guren T, Lorenz S, Næss S, Pierini M, et al. Pembrolizumab in Advanced Osteosarcoma: Results of a Single-Arm, Open-Label, Phase 2 Trial. *Cancer Immunol Immunother: CII* (2021) 70(9):2617–24. doi: 10.1007/s00262-021-02876-w
58. Liu J, Li C, Seery S, Yu J, Meng X. Identifying Optimal First-Line Interventions for Advanced Non-Small Cell Lung Carcinoma According to PD-L1 Expression: A Systematic Review and Network Meta-Analysis. *Oncoimmunol* (2020) 9(1):1746112. doi: 10.1080/2162402x.2020.1746112
59. Sánchez-Gastaldo A, Muñoz-Fuentes MA, Molina-Pinelo S, Alonso-García M, Boyero L, Bernabé-Caro R. Correlation of Peripheral Blood Biomarkers With Clinical Outcomes in NSCLC Patients With High PD-L1 Expression Treated With Pembrolizumab. *Trans Lung Cancer Res* (2021) 10(6):2509–22. doi: 10.21037/tlcr-21-156
60. Fornarini G, Rebuzzi S, Banna G, Calabrò F, Scandurra G, De Giorgi U, et al. Immune-Inflammatory Biomarkers as Prognostic Factors for Immunotherapy in Pretreated Advanced Urinary Tract Cancer Patients: An Analysis of the Italian SAUL Cohort. *ESMO Open* (2021) 6(3):100118. doi: 10.1016/j.esmoop.2021.100118

Conflict of Interest: Author CL was employed by Yinfeng Gene Technology Co Ltd.

The remaining authors declare that the research was conducted in the absence of any commercial or financial relationships that could be construed as a potential conflict of interest.

Publisher's Note: All claims expressed in this article are solely those of the authors and do not necessarily represent those of their affiliated organizations, or those of the publisher, the editors and the reviewers. Any product that may be evaluated in this article, or claim that may be made by its manufacturer, is not guaranteed or endorsed by the publisher.

Advantages of publishing in Frontiers

OPEN ACCESS
Articles are free to read for greatest visibility and readership

FAST PUBLICATION
Around 90 days from submission to decision

HIGH QUALITY PEER-REVIEW
Rigorous, collaborative, and constructive peer-review

TRANSPARENT PEER-REVIEW
Editors and reviewers acknowledged by name on published articles

Frontiers
Avenue du Tribunal-Fédéral 34
1005 Lausanne | Switzerland

Visit us: www.frontiersin.org
Contact us: frontiersin.org/about/contact

REPRODUCIBILITY OF RESEARCH
Support open data and methods to enhance research reproducibility

DIGITAL PUBLISHING
Articles designed for optimal readership across devices

FOLLOW US
@frontiersin

IMPACT METRICS
Advanced article metrics track visibility across digital media

EXTENSIVE PROMOTION
Marketing and promotion of impactful research

LOOP RESEARCH NETWORK
Our network increases your article's readership